AD-A050 537 PRATT AND WHITNEY AIRCRAFT GROUP EAST HARTFORD CONN F/G 21/5
INVESTIGATION OF A HIGHLY LOADED TWO-STAGE FAN-DRIVE TURBINE. V--ETC(U)
JUN 70 H WELNA, D E DAHLBERG, W H HEISER F33615-68-C-1208
UNCLASSIFIED PWA-3967 AFAPL-TR-69-92-VOL-5 NL

1 OF 3
AD
AD 50537

~~CONFIDENTIAL~~ UNCLASSIFIED

AFAPL-TR-69-92
VOLUME V

(UNCLASSIFIED TITLE)
INVESTIGATION OF A HIGHLY LOADED TWO-STAGE FAN-DRIVE TURBINE

VOLUME V. Phase III, Boundary Layer Control Optimization and Off-Design Evaluation

H. Welna, D. E. Dahlberg and W. H. Heiser
Pratt & Whitney Aircraft
Division of United Aircraft Corporation

Technical Report
AFAPL-TR-69-92 Volume V
June, 1970

~~Downgraded at 3 Year Intervals;~~
~~Declassified after 12 Years;~~
~~DOD DIR. 5200.10.~~

~~SPECIAL HANDLING REQUIRED~~
~~NOT RELEASABLE TO FOREIGN NATIONALS~~
~~The information contained in this document will not be disclosed to foreign nationals or their representatives.~~

~~Release of this information affecting the national defense of the United States within the meaning of the Espionage Laws. Its transmission or the revelation of its contents to an unauthorized person is prohibited by law.~~

AIR FORCE AERO PROPULSION LABORATORY
AIR FORCE SYSTEMS COMMAND
WRIGHT-PATTERSON AIR FORCE BASE, OHIO

~~CONFIDENTIAL~~
UNCLASSIFIED

~~UNCLASSIFIED~~
~~CONFIDENTIAL~~

(UNCLASSIFIED TITLE)
INVESTIGATION OF A HIGHLY LOADED TWO-STAGE FAN-DRIVE TURBINE

VOLUME V. Phase III, Boundary Layer Control Optimization and Off-Design Evaluation

H. Welna, D. E. Dahlberg and W. H. Heiser
Pratt & Whitney Aircraft
Division of United Aircraft Corporation

FOREWORD

(U) This Interim Technical Status Report (Contractor's Reference No. PWA 3967) was prepared by Pratt & Whitney Aircraft, Division of United Aircraft Corporation, East Hartford, Connecticut, as the fifth Semiannual Report under United States Air Force Contract F33615-68-C-1208, Project No. 3066, Task No. 306606. This report was submitted by the Contractor on 30 June 1970, and covers the report period from 1 January 1970 to 30 June 1970.

(U) The findings and conclusions of this report are not deemed as final by the Contractor. They are subject to verification or revision in the Final Report to be published upon the completion of this Contract.

(U) The Air Force Program Monitor is Mr. Wayne Tall, APTC, Air Force Aero Propulsion Laboratory, Wright-Patterson Air Force Base, Ohio, 45433.

(U) This report contains no Classified information extracted from other Classified documents.

(U) Publication of this report does not constitute Air Force approval of the report's findings or conclusions. It is published only for the exchange and stimulation of ideas.

Wayne Tall
Project Engineer
Air Force Aero Propulsion Laboratory

UNCLASSIFIED ABSTRACT

(U) A comprehensive, four-phase, three-year program is in progress to investigate methods of improving the performance of fan-drive turbines. The goals of this program are to develop turbine design procedures and aerodynamic techniques for efficient, high work, low pressure turbines.

(U) The first phase effort of defining the preliminary turbine design has been completed and the results were reported (Reference 1). The second phase consisted of an experimental evaluation which included establishment of both two-dimensional loss levels and three-dimensional flow behavior for the baseline airfoils, and for airfoils utilizing various boundary layer control methods. The design of the baseline cascade packs was reported in Reference 2, and the annular cascade performance of the baseline airfoils was reported in Reference 3. The annular cascade results of the baseline airfoil boundary layer control methods were reported in Reference 4.

(U) The results of the plane-cascade, two-dimensional, baseline investigation, the decreased-solidity annular-cascade airfoil test results, and the Phase III boundary layer control optimization and off-design evaluation are presented in this report.

(The reverse of this page is blank)

TABLE OF CONTENTS

TABLE OF CONTENTS (Cont'd)

LIST OF ILLUSTRATIONS

LIST OF ILLUSTRATIONS (Cont'd)

LIST OF ILLUSTRATIONS (Cont'd)

LIST OF ILLUSTRATIONS (Cont'd)

LIST OF ILLUSTRATIONS (Cont'd)

LIST OF ILLUSTRATIONS (Cont'd)

LIST OF ILLUSTRATIONS (Cont'd)

LIST OF ILLUSTRATIONS (Cont'd)

LIST OF ILLUSTRATIONS (Cont'd)

LIST OF ILLUSTRATIONS (Cont'd)

LIST OF ILLUSTRATIONS (Cont'd)

LIST OF ILLUSTRATIONS (Cont'd)

LIST OF ILLUSTRATIONS (Cont'd)

LIST OF ILLUSTRATIONS (Cont'd)

LIST OF ILLUSTRATIONS (Cont'd)

LIST OF ILLUSTRATIONS (Cont'd)

LIST OF TABLES

LIST OF TABLES (Cont'd)

LIST OF SYMBOLS

A	- area, square inches
B	- axial chord, inches
C_L	- Zwiefel load coefficient
C_{L^*}	- load coefficient, $\Delta Cu/U$
E	- diffusion parameter
ΔH	- work, Btu per pound
M	- Mach number
P	- pressure, psia
ΔP	- pressure rise from minimum to exit value on suction surface
Q	- exit dynamic head
R_C	- radius of curvature, inches
T	- temperature, °R
u	- tangential velocity, feet per second
X	- axial distance, inches
Y	- tangential distance, inches
Z	- number of airfoils
α	- absolute gas angle, degrees
β	- relative gas angle degrees
τ	- gap, inches

Subscripts

0	inlet to first vane
1	inlet to first blade
2	exit from stage or airfoil section
G	gage point
S	static
T	total

(The reverse of this page is blank)

SECTION I

INTRODUCTION

(U) Future mission studies show that the bypass turbofan engine, which has seen increased use in military aircraft applications, will continue to be of primary interest. Characteristic of this type of engine is an increase in fuel economy with increased bypass ratio. In turn, high bypass ratio engines require higher fan power, which must be provided by the fan-drive or low-pressure turbine. This increased turbine power requirement must be met without a turbine efficiency penalty.

(U) Design analysis and optimization studies of aircraft jet engines involve a trade between component efficiencies and engine size and weight. The efficiency of a turbine is the result of optimization studies based on trade-offs between turbine diameter, rotational speed, number of stages and airfoil loading. The fan drive turbine design is constrained by further requirements. The rotational speed of the turbine must be limited in order that the fan tip Mach number does not exceed the limit for acceptable losses. At high by-pass ratios, where larger fan diameters are required, this problem is further aggravated. Applying conventional aerodynamics at fixed rotational speed, increased work can only be realized by further increases in the number of stages and/or the turbine diameter. Reduction of the turbine diameter or solidity results in a lighter turbine, but with a sacrifice in efficiency due to losses associated with increased loading. Considerable gains can be realized by an engine if the size and weight reduction can be made with no loss in efficiency. Therefore, current turbine technology must be improved in order to provide the desired level of performance for future turbofan engines.

(U) The objective of the work done under this contract is to analyze and test concepts which will increase the low pressure turbine loading while maintaining or increasing the turbine efficiency levels. The goals of this program are to develop turbine aerodynamic techniques and design procedures for efficient, high work, low-pressure turbines by means of analytical studies and cascade testing, and to demonstrate the effectiveness of the techniques by designing and testing a two-stage turbine that meets or exceeds the contract stage work and efficiency goals (See Section II).

(U) The total program is being conducted in four phases over a three year period, which commenced on 1 January 1968. Phase I defined the basic turbine design and an analysis of promising increased loading concepts was completed. The results of the Phase I study were reported in Reference 1. Phases II and III consisted of experimental testing to verify and extend the turbine aerodynamic techniques and design procedures for high loading levels. The design details of the baseline cascade test airfoils for both the annular segment and plane cascade rig were reported in Reference 2. The results of the annular cascade testing of the four baseline airfoils were reported in Reference 3. The annular cascade results of the baseline airfoil boundary layer control methods were reported in Reference 4. The results of the plane-cascade two-dimensional baseline investigation, the decreased-solidity annular cascade airfoil test results, and also the Phase III boundary layer control optimization and off-design evaluation are presented in this Report. Phase IV, consisting of the design and test of a two-stage demonstrator turbine, is currently in progress.

(U) Work on the Contract during this report period proceeded to the conclusion of Phase II, including plane cascade tests of the baseline airfoils and annular segment cascade test of medium solidity airfoils. Phase III testing of the boundary layer control optimization and their off-design evaluation was also completed.

SECTION II

BACKGROUND

(U) The High Stage Loading Low Pressure Turbine Contract consists of four phases. The testing and data analysis required in the first three phases of this Contract have been completed. Work on the Contract is currently proceeding in Phase IV.

(U) The results of the Phase I analysis are described in Reference 1. The objective of the Phase I study was to select a preliminary turbine design that is capable of meeting the performance requirements of this Contract (See Table I).

TABLE I

TURBINE DESIGN PARAMETERS

Number of Stages	2
Average Load Coefficient, C_{L^*}	2.2
First Blade Tip Wheel Speed	1000 fps
First Blade Inlet Hub-Tip Diameter Ratio	$\leq .8$
Exit Swirl Angle - Without Exit Guide Vanes	$\leq 20°$
Exit Swirl Angle - With Exit Guide Vanes	0°
Turbine Inlet Temperature	1450°F
Airflow	≥ 50 lbs/sec
Average Stage Efficiency	91%
Life	10,000 hrs

CONFIDENTIAL

(U) As part of Phase I, the analyses included the consideration of flowpath, reaction level, load coefficient level and variations in work distribution for which velocity triangles were generated. Furthermore, preliminary airfoil contours were defined for the same velocity triangles at three levels of reaction, and three levels of solidity for the resulting stages.

(U) Based on the Phase I study, and after additional airfoil refinement, the medium-reaction normal-solidity airfoil turbine design was selected for the Phase II and III evaluation. Phase II consisted of two- and three-dimensional experimental evaluation of the four baseline airfoils, investigation of promising end-wall boundary layer control techniques and evaluation of the baseline airfoils at a 15 percent higher Zweifel loading coefficient. The results of the two-dimensional evaluation are presented in this Report. The partial results of the medium solidity evaluation were presented in Reference 4, and are concluded in this Report. The results of the three-dimensional baseline airfoil evaluation were presented in Reference 3.

(U) The second vane was chosen for the end wall loss study by the process of elimination. The first stage vane and blade inside diameter and wall extensions indicated that separation occurred close enough to the test cascade to influence probe readings near this wall in future tests if it moved upstream. The short second stage blade chord could have made the fabrication of end wall boundary layer control techniques more difficult. The second vane, therefore, was the vehicle for four boundary layer control techniques, including the use of flow fence

and increased surface roughness, local airfoil recontouring, end wall contouring, and local airfoil recambering. The results of these evaluations (published in Reference 4) indicated that within the limited range of investigation of each technique, local recambering was the most effective.

(U) Local recambering was further pursued during Phase III evaluations, where three additional recambered designs were investigated. These were evaluated at both design and off-design conditions and the results of these tests are reported herein.

SECTION III

TWO-DIMENSIONAL DESIGN VERIFICATION (TASK IIa)

1. RFP OBJECTIVE

(U) Provide an experimental verification of two-dimensional design characteristics.

2. TASK OBJECTIVE

(U) The purpose of this Task was to conduct plane cascade tests in order to verify the aerodynamic concepts applied to the turbine design during the Phase I Program, and to establish the two-dimensional loss levels for the chosen turbine airfoil profiles at design conditions.

(U) The plane cascade tests served two equally important purposes. First, the measured profile losses were compared with those contained in the existing design procedures in order to verify their accuracy. Secondly, the total pressure and flow angle profiles at the exit plane indicated whether or not the surface boundary layer had separated. Each airfoil was designed so that such two-dimensional separation should not have occurred, and these tests constituted a verification of the entire airfoil section design procedure.

3. CASCADE PACK AND FACILITY DESIGN

(U) A summary of the pertinent design parameters for the airfoils tested in the plane cascade rig is shown in Table II. The six airfoil sections which were investigated are the mean section of each airfoil row and the second vane and second blade root sections. The cascade packs consisted of straight airfoils having the contours of their respective baseline airfoil designs. These airfoil sections were shown in Reference 2, Section III. In this same report, the airfoil coordinates, scale factors, and locations of airfoil static pressure taps were also presented. In addition, the method of assembly of the test packs and locations of the exit static taps on each test pack were also presented.

TABLE II

MEDIUM-REACTION NORMAL-SOLIDITY AIRFOIL SUMMARY

First Stage Vane	No. of Foils	Exit Mach No.	ΔP/Q Design	Max. Surface Mach No.
Root	62	0.949	0.313	1.150
¼ Root		0.891	0.244	1.036
Mean		0.852	0.213	0.966
¼ Tip		0.820	0.195	0.918
Tip		0.770	0.192	0.859
First Stage Blade				
Root	116	0.890	0.279	1.058
¼ Root		0.849	0.296	1.020
Mean		0.788	0.331	0.968
¼ Tip		0.738	0.294	0.883
Tip		0.730	0.236	0.840
Second Stage Vane				
Root	80	1.003	0.337	1.230
¼ Root		0.920	0.277	1.094
Mean		0.870	0.227	0.999
¼ Tip		0.821	0.196	0.928
Tip		0.765	0.203	0.865
Second Stage Blade				
Root	126	0.944	0.408	1.233
¼ Root		0.922	0.324	1.136
Mean		0.904	0.263	1.067
¼ Tip		0.897	0.236	1.040
Tip		0.892	0.224	1.025

UNCLASSIFIED

(U) The design of the plane cascade is shown schematically in Figure 1. The test section had a variable inlet and exit flow path in order that all six cascades could be evaluated using basically the same hardware. The variable geometry rig design permitted each cascade to be tested at its respective design incidence angle. One change was made to the rig (previously shown in Reference 2, Figure 15) after the initial rig checkout run was made. This included the addition of turning vanes in the inlet channel, since, as initially designed, there was a small flow distortion at the inlet to the test cascade pack. The problem was corrected by this change.

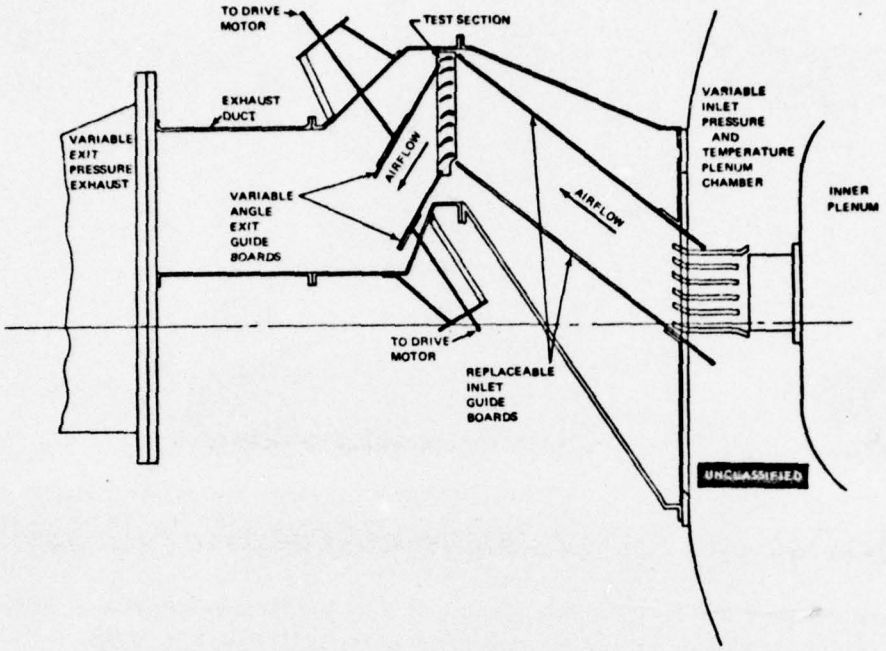

Figure 1 Schematic of Revised Plane Cascade Rig

(U) During the testing, both inlet and exit pressures were independently controlled, as well as the inlet temperature level, allowing the correct simulation of inlet and exit Mach numbers, and Reynolds number. The cascade pack total pressure and exit flow angle profiles were measured. Local and gapwise integrated loss coefficients were calculated for the test channels.

4. DISCUSSION

(U) A comparison of the loss coefficient data for the four plane cascade mean sections with the midspan values measured in the four normal solidity part annular cascade is presented in Table III. In addition, a comparison of these data with losses predicted by two different methods is shown. One of the predicted values was calculated using a modified Ainley and Mathieson correlation based on global airfoil design parameters. The other prediction was calculated using fully turbulent boundary layer characteristics computed by the Airfoil Boundary Layer Deck, which utilized the predicted airfoil surface static pressure distributions. The airfoil static pressure distributions were calculated by the Airfoil Pressure Distribution Program. It can be seen from this comparison (Table III) that the plane cascade loss levels are consistent with the midspan values from the annular segment cascade, and both are consistently below either of the predicted values for each airfoil. This is probably due to an extended region of laminar boundary resulting from low cascade inlet turbulence levels. The screen results upheld this judgement but may not yet reproduce the loss levels that will be obtained in the rotating machine.

TABLE III

MEASURED PLANE CASCADE LOSS COMPARISON WITH MEASURED MIDSPAN ANNULAR CASCADE LOSS AND PREDICTED LOSS AT DESIGN REYNOLDS NUMBERS

		Loss Coefficient Measured, $1-\phi^2$		Loss Coefficient Predicted, $1-\phi^2$	
Midspan Section	Exit Mach Number	Plane Cascade	Annular Cascade	Global Correlation	Fully Turbulent Boundary Layer
First Vane	0.852	0.025	0.017 0.023*	0.031	0.031
First Blade	0.788	0.025	0.027	0.036	0.049
Second Vane	0.870	0.024	0.021 0.028*	0.036	0.034
Second Blade	0.904	0.023	0.028	0.030	0.040

*With inlet turbulence screen.

(U) Table IV shows the measured loss levels for the four midspan sections as compared with the predicted loss levels using the Airfoil Boundary Layer Deck. In the boundary layer calculations previously mentioned (Table III), fully turbulent flow was assumed and transition was predicted internally by the program. For the values shown in Table IV, transition was fixed at the last minimum pressure. The excellent agreement shown here, in the three cases out of four that converged without separating, makes it appear that the selected transition point is correct. Additional proof is offered by the data.

TABLE IV

MEASURED PLANE CASCADE LOSSES COMPARED TO PREDICTED VALUES USING THE BOUNDARY LAYER DECK WITH TRANSITION ASSUMED AT THE SECOND MINIMUM PRESSURE

Midspan Section	Measured Loss Coefficient $1-\phi^2$	Predicted Loss Coefficient $1-\phi^2$
First Vane	0.025	0.025
First Blade	0.025	0.026
Second Vane	0.024	0.022
Second Blade	0.023	Separation Indicated

(U) The complete set of loss and measured exit flow angle data at various Reynolds numbers is presented as a function of Mach number in Figures 2 through 13. The lack of variation of the loss coefficient with Reynolds number at constant Mach number indicates that the transition point was stationary during the tests. The loss coefficient curves indicate a strong transonic drag rise on each airfoil section.

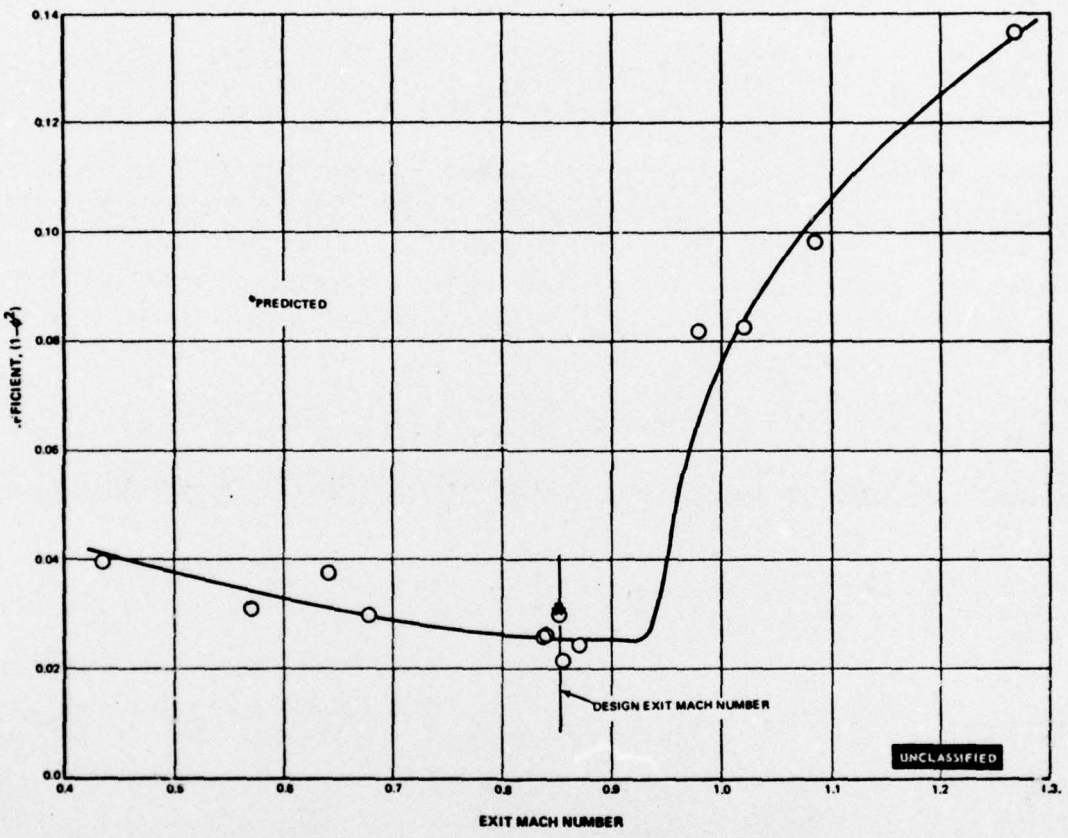

Figure 2 Variation of Loss Coefficient With Exit Mach Number - First Vane Mean Section

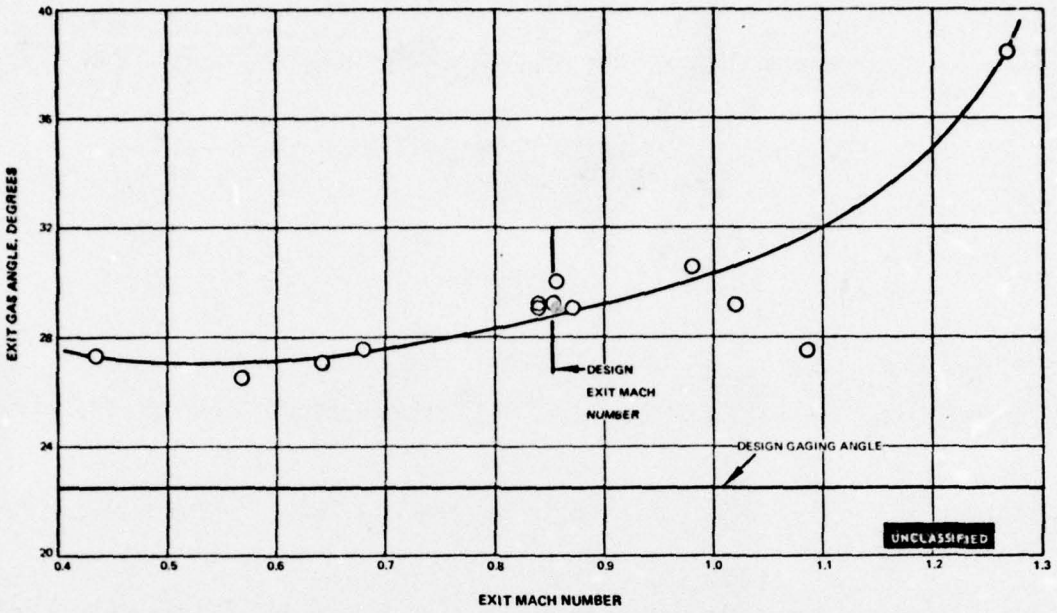

Figure 3 Variation of Exit Gas Angle with Exit Mach Number - First Vane Mean Section

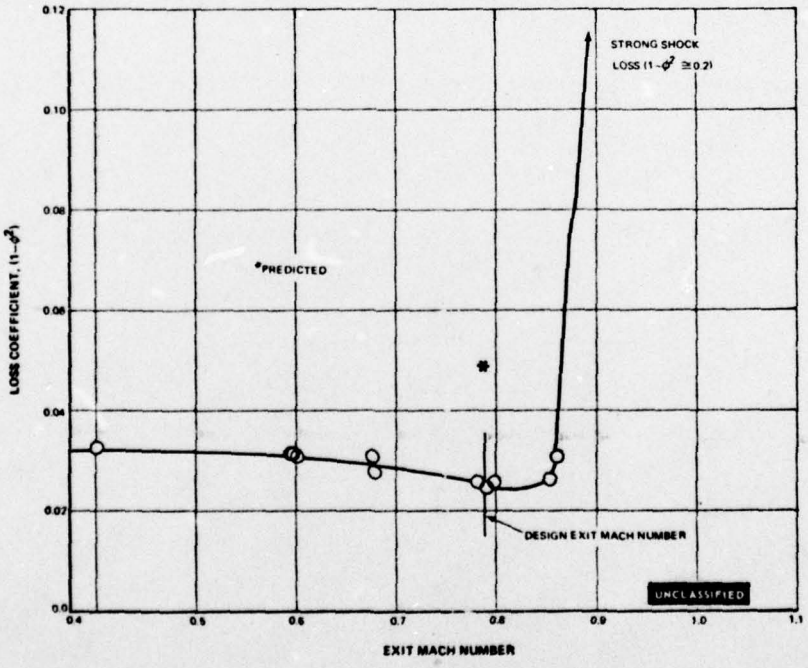

Figure 4 Variation of Loss Coefficient with Exit Mach Number - First Blade Mean Section

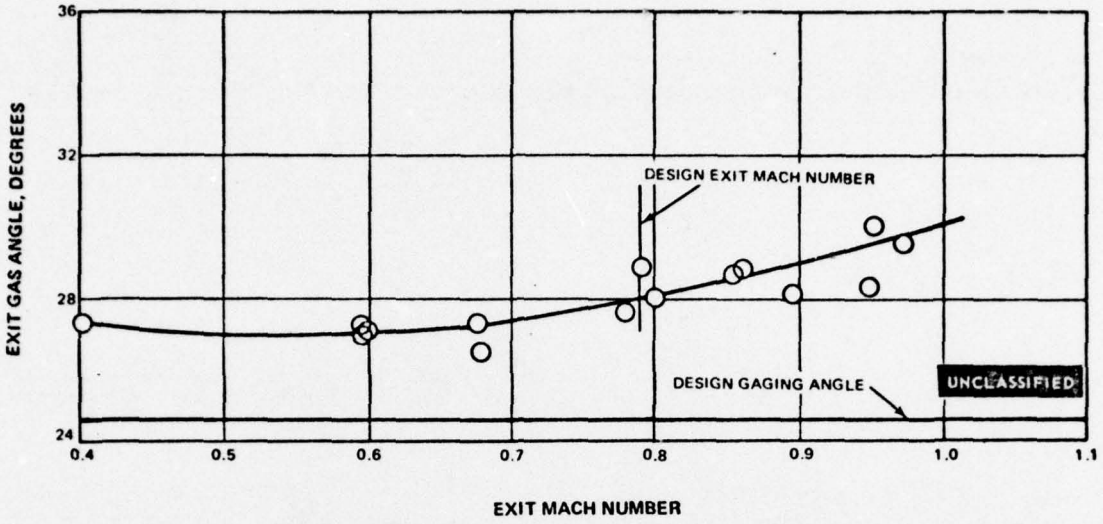

Figure 5 Variation of Exit Gas Angle with Exit Mach Number - First Blade Mean Section

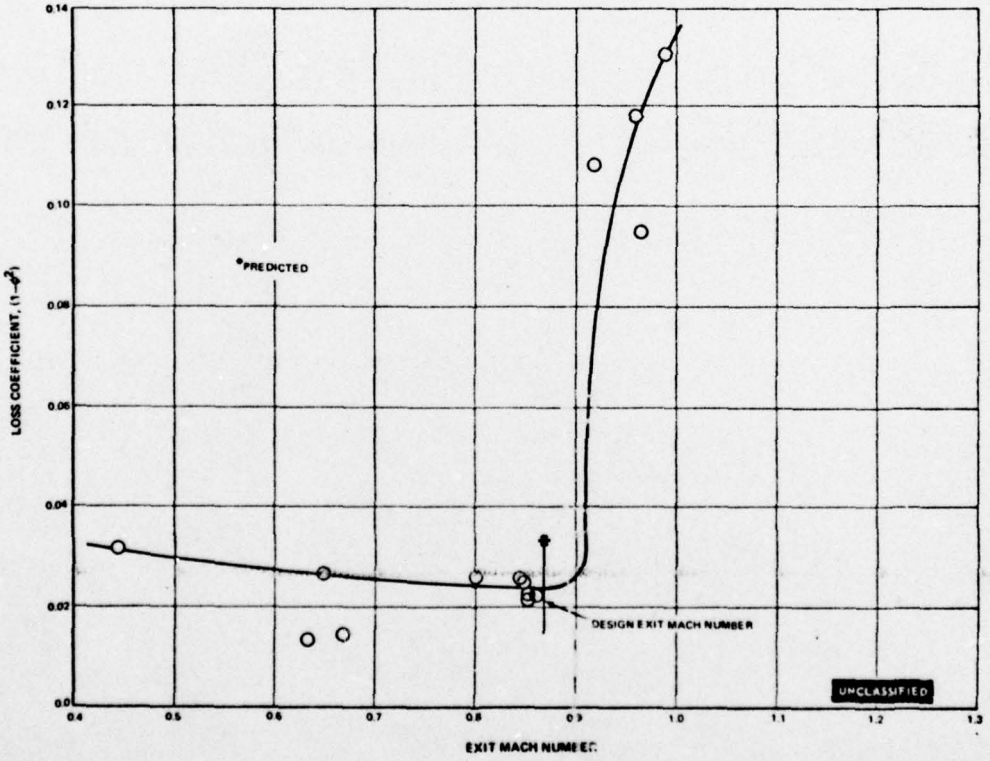

Figure 6 Variation of Loss Coefficient with Exit Mach Number - Second Vane Mean Section

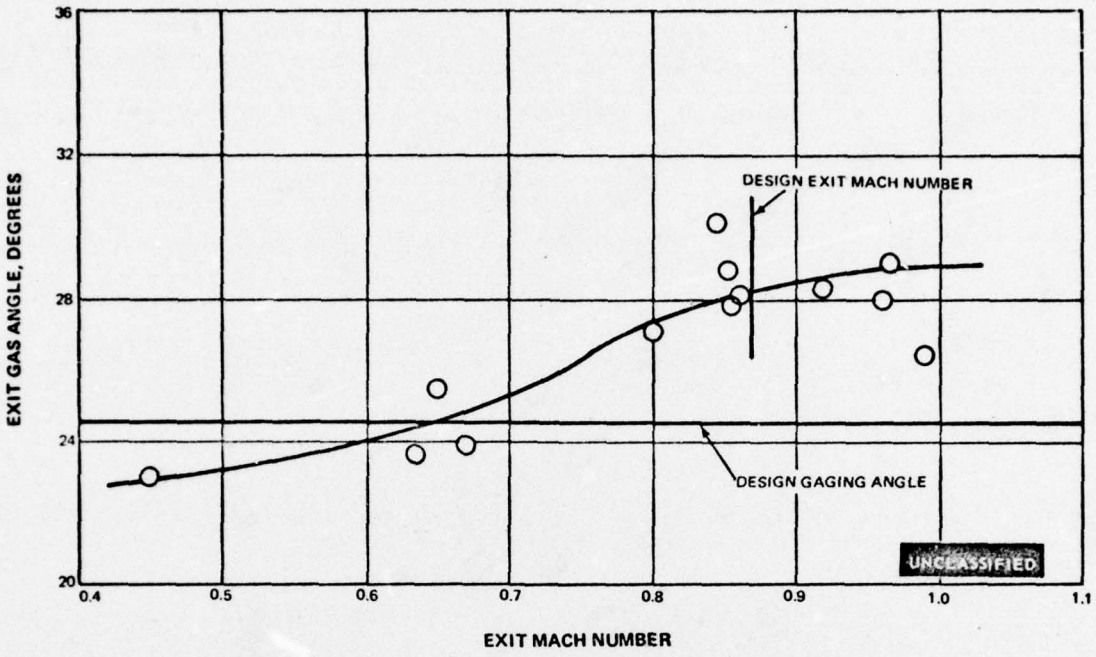

Figure 7 Variation of Exit Gas Angle with Exit Mach Number - Second Vane Mean Section

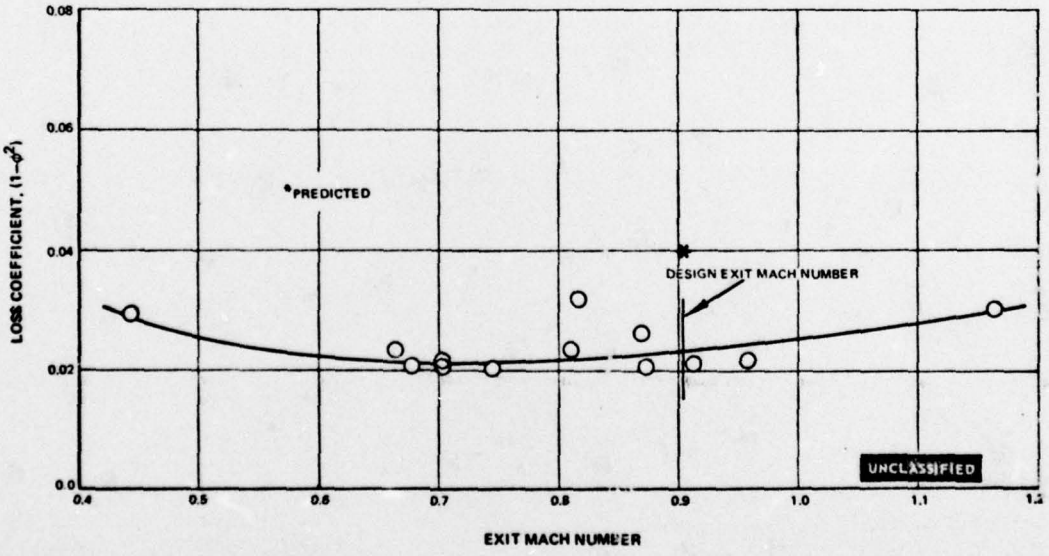

Figure 8 Variation of Loss Coefficient with Exit Mach Number - Second Blade Mean Section

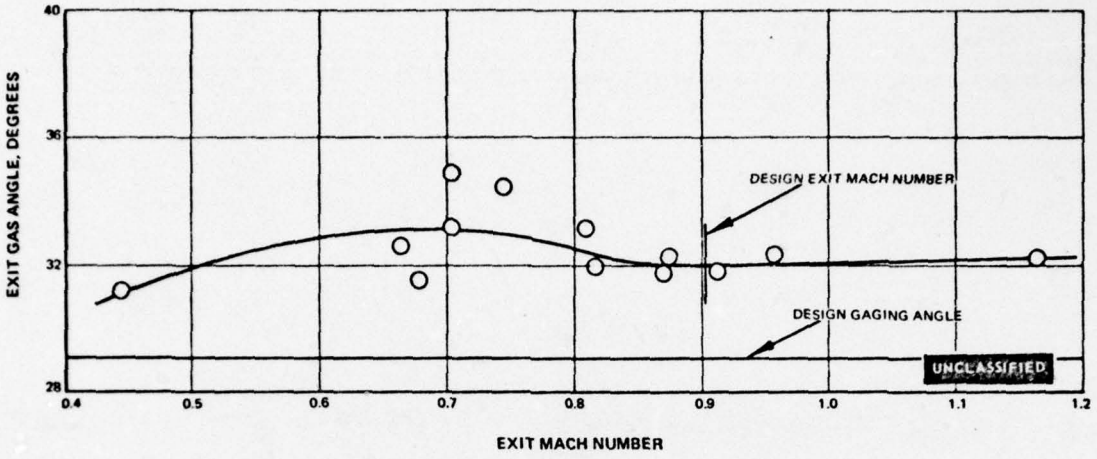

Figure 9 Variation of Exit Gas Angle with Exit Mach Number - Second Blade Mean Section

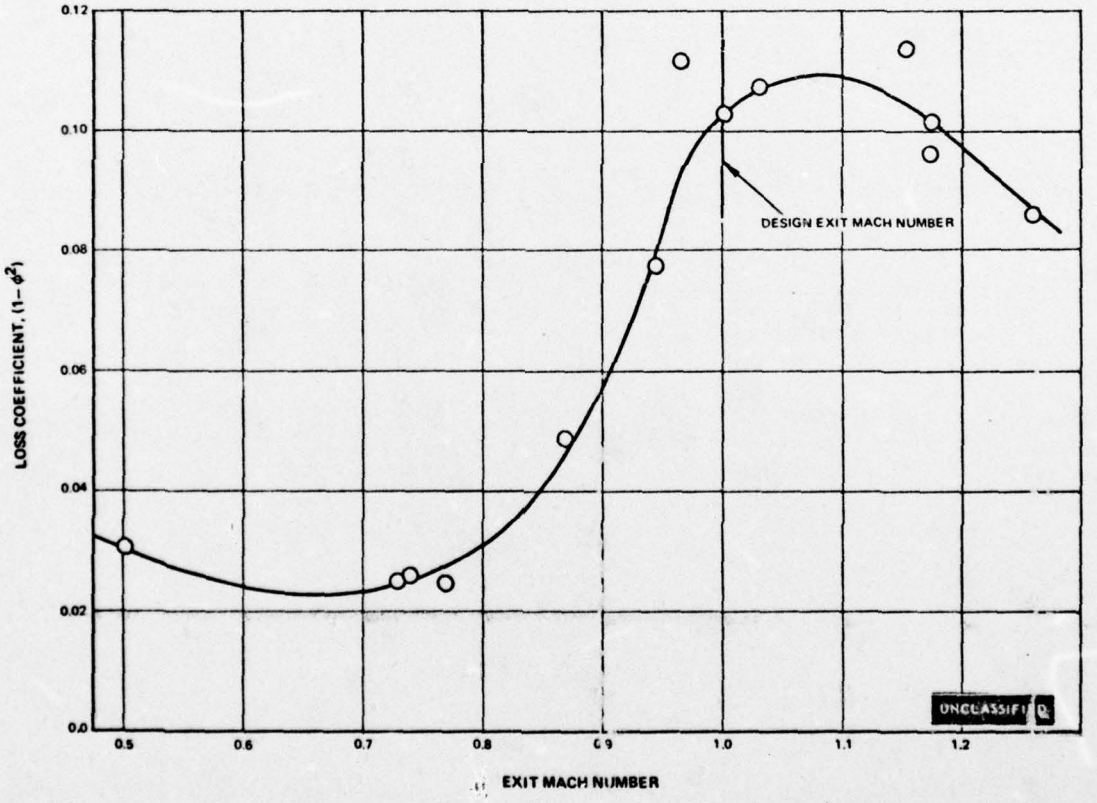

Figure 10 Variation of Loss Coefficient with Exit Mach Number - Second Vane Root Section

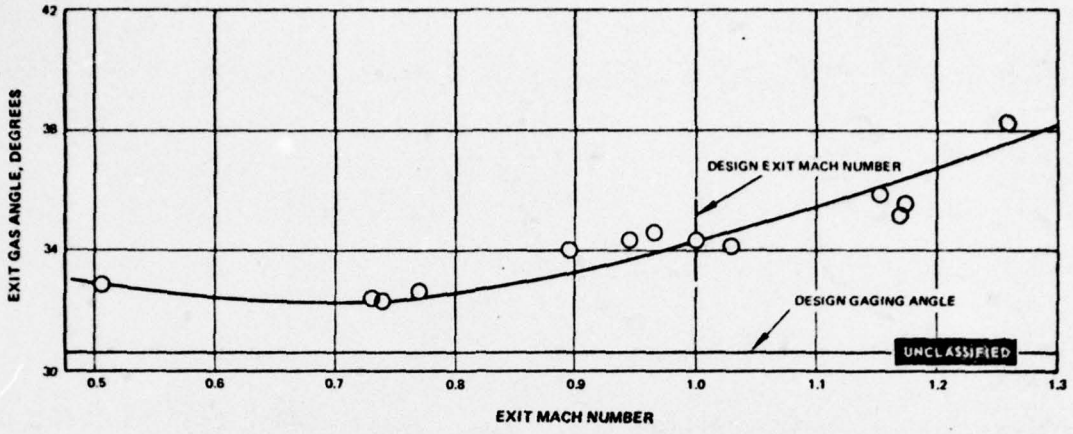

Figure 11 Variation of Exit Gas Angle with Exit Mach Number - Second Vane Root Section

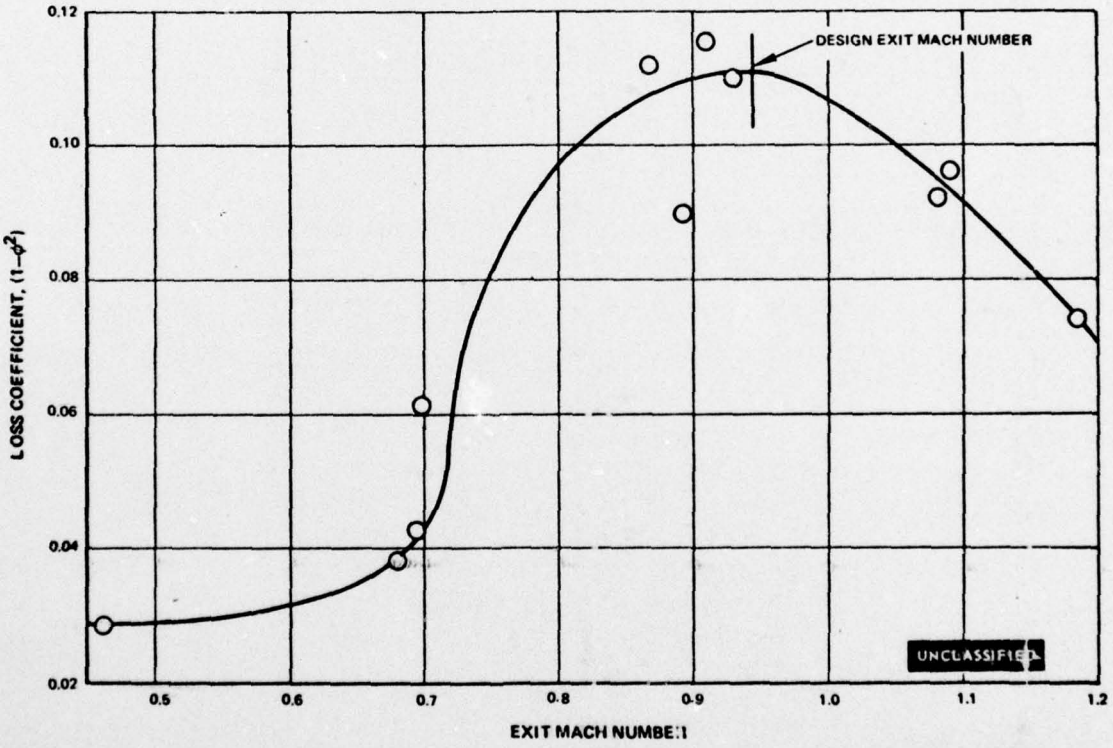

Figure 12 Variation of Loss Coefficient with Exit Mach Number - Second Blade Root Section

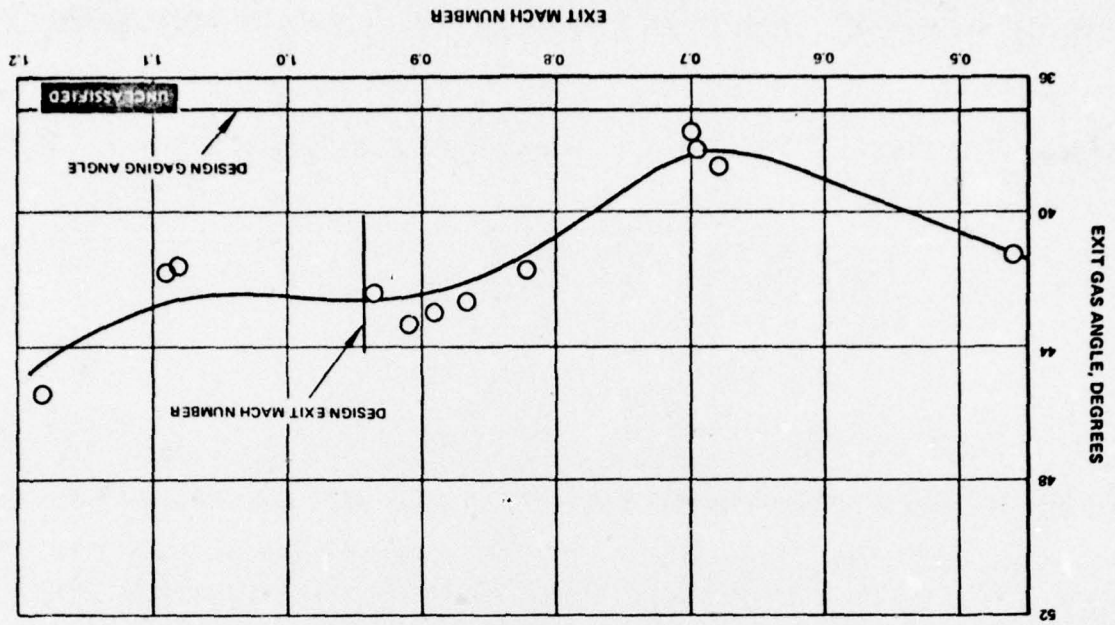

Figure 13 Variation of Exit Gas Angle with Exit Mach Number - Second Blade Root Section

(U) Figures 14 through 39 show the measured and predicted airfoil surface pressure distributions. The four midspan sections performed as expected in the vicinity of the design point. The two root sections, however, show a transonic drag rise before the design point is reached. In view of this, all of the six sections were reevaluated at their respective design points. The pressure distributions that would have been predicted using the new Transonic Pressure Distribution Deck, which is being used in the final contract turbine design, are shown for the six airfoils in Figures 16, 20, 24, 29, 34 and 37. In these figures, the pressure distributions predicted by the transonic pressure distribution deck and shown for the four mean sections, namely figures 16, 20, 24 and 29 are in good agreement with both the data and the original Airfoil Pressure Distribution Program. However, for the two root sections, there is a large disparity between the original and the new predictions; the latter being considerably closer to the data. The root sections have low reaction levels and high exit Mach numbers. The Transonic Pressure Distribution Program has been shown to be very effective when used to predict mixed-flow problems of this nature. The principal changes that the new program predicts are: less loading in the forward portion of the airfoil and higher loading (over-acceleration) in the rearward portion of the foil. The result of this is a shock, a condition necessary to get the over-accelerated flow up to the operating back-pressure, which stands off of the trailing edge of both airfoils. The measured pressure distributions indicate this by the very sharp pressure rises shown between 90 and 100 percent chord for both root sections. Using the Transonic Pressure Distribution Deck, then, airfoils may be designed to avoid this problem. The final design will utilize this advanced design technique.

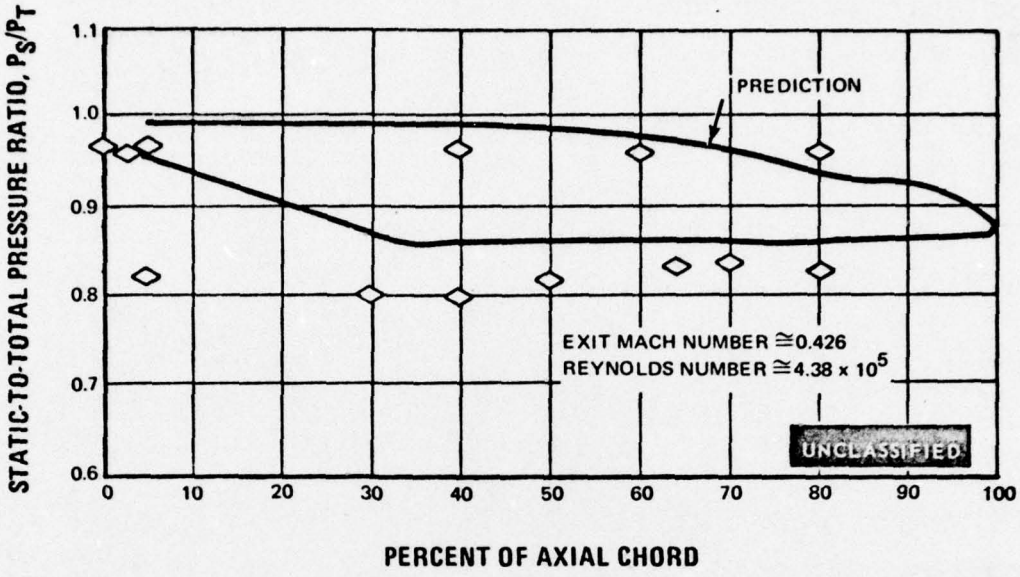

Figure 14 Static-to-Total Pressure Ratio Versus Percent of Axial Chord, First Vane Mean Section; Exit Mach Number = .426

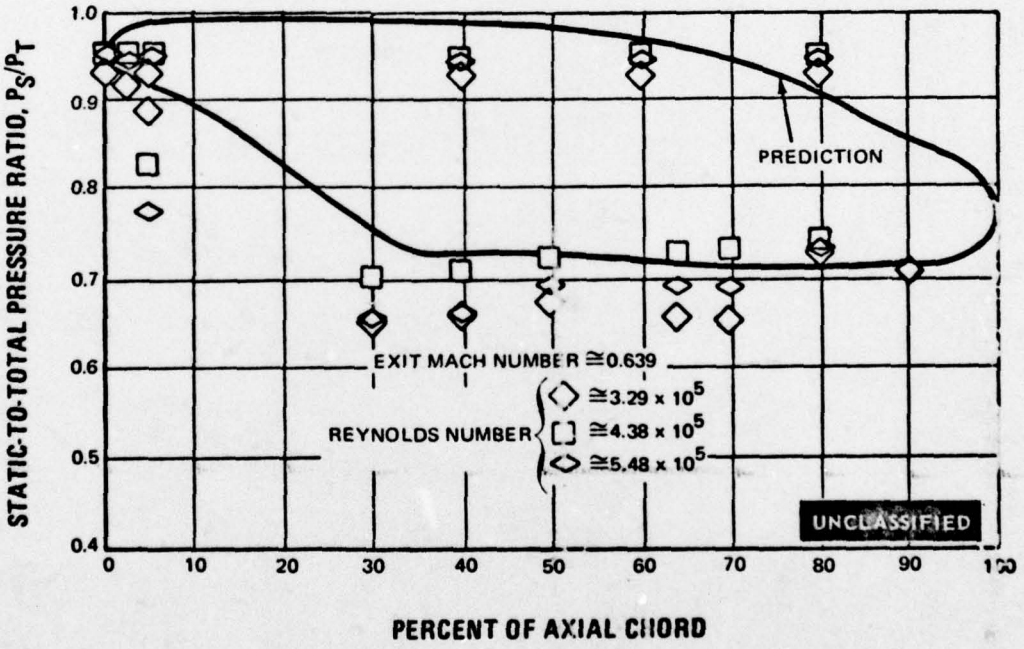

Figure 15 Static-to-Total Pressure Ratio Versus Percent of Axial Chord, First Vane Mean Section; Exit Mach Number = .639

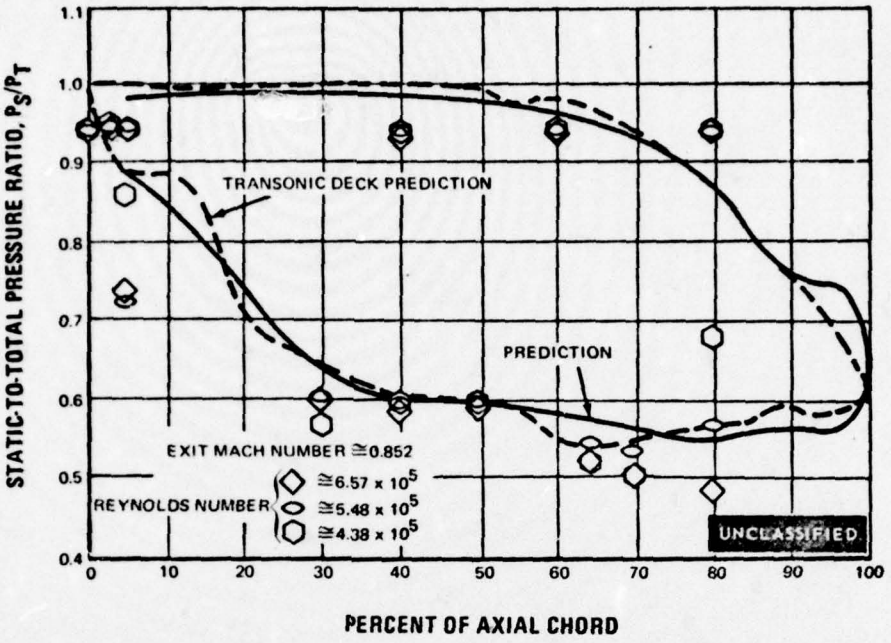

Figure 16 Static-to-Total Pressure Ratio Versus Percent of Axial Chord, First Vane Mean Section; Exit Mach Number = .852

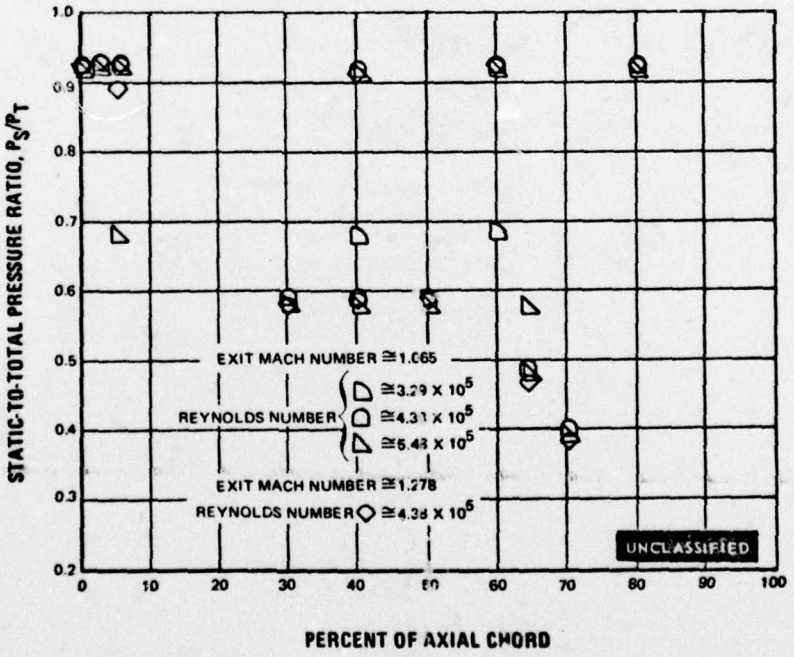

Figure 17 Static-to-Total Pressure Ratio Versus Percent of Axial Chord, First Vane Mean Section; Exit Mach Number = 1.065 and 1.278

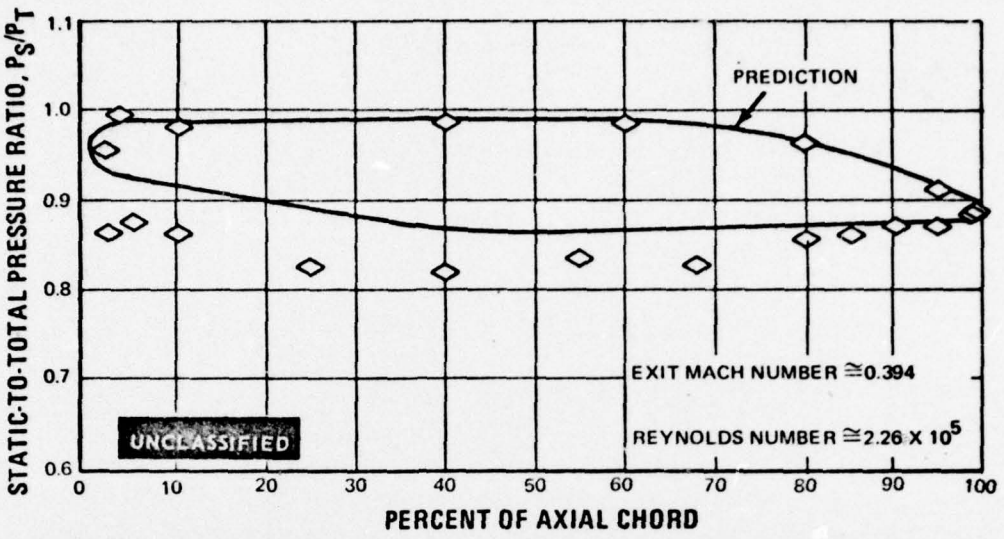

Figure 18 Static-to-Total Pressure Ratio Versus Percent of Axial Chord, First Blade Mean Section; Exit Mach Number = .394

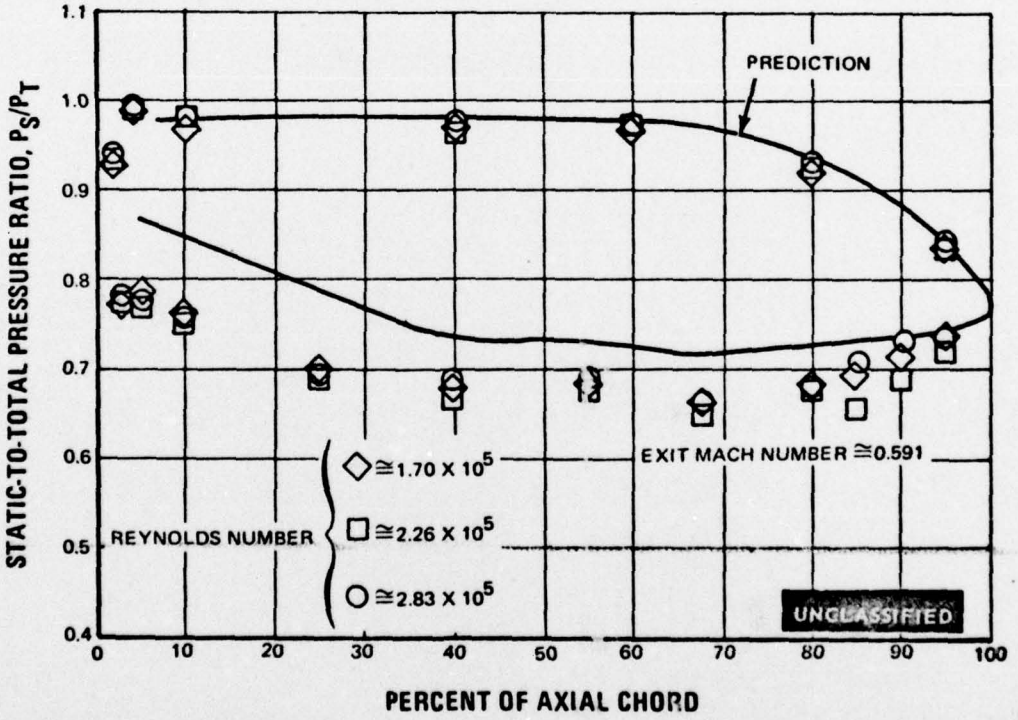

Figure 19 Static-to-Total Pressure Ratio Versus Percent of Axial Chord, First Blade Mean Section; Exit Mach Number = .591

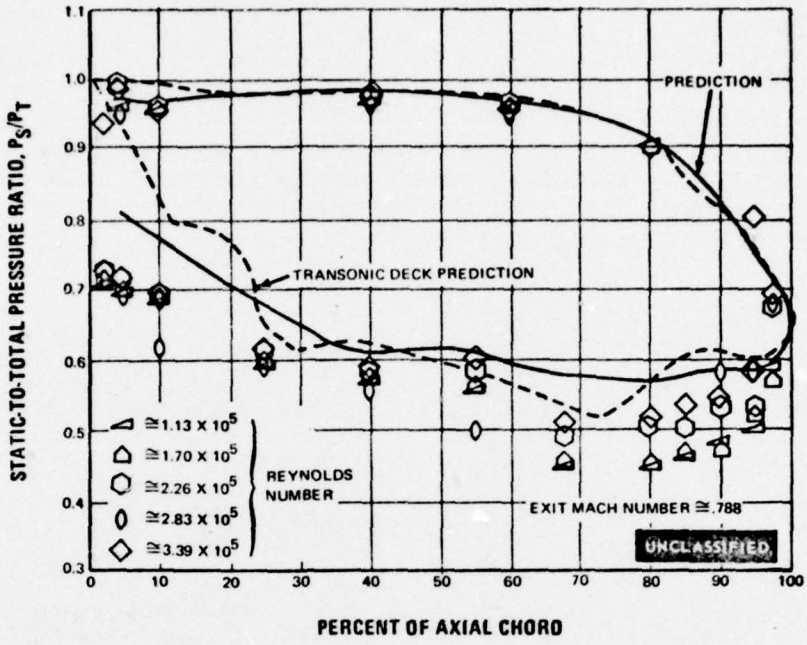

Figure 20 Static-to-Total Pressure Ratio Versus Percent of Axial Chord, First Blade Mean Section; Exit Mach Number = .788

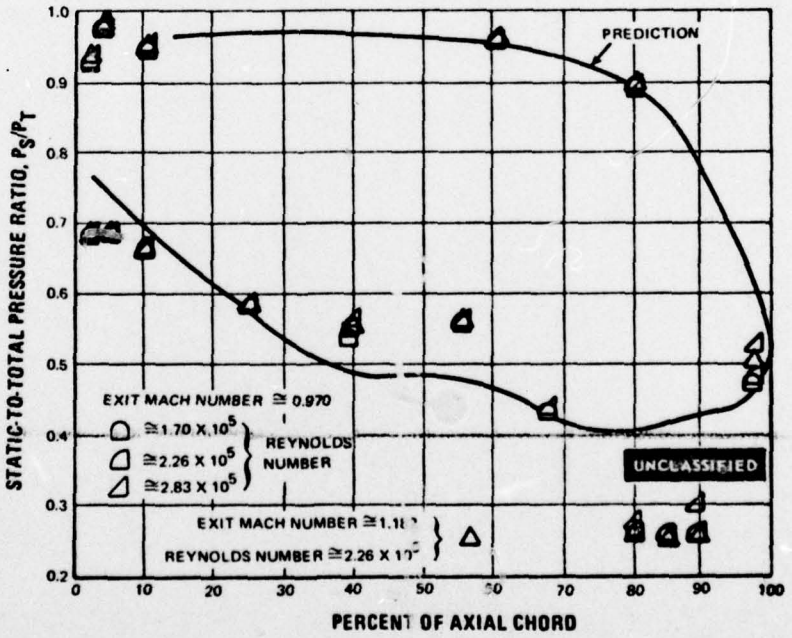

Figure 21 Static-to-Total Pressure Ratio Versus Percent of Axial Chord, First Blade Mean Section; Exit Mach Number = .970 and 1.182

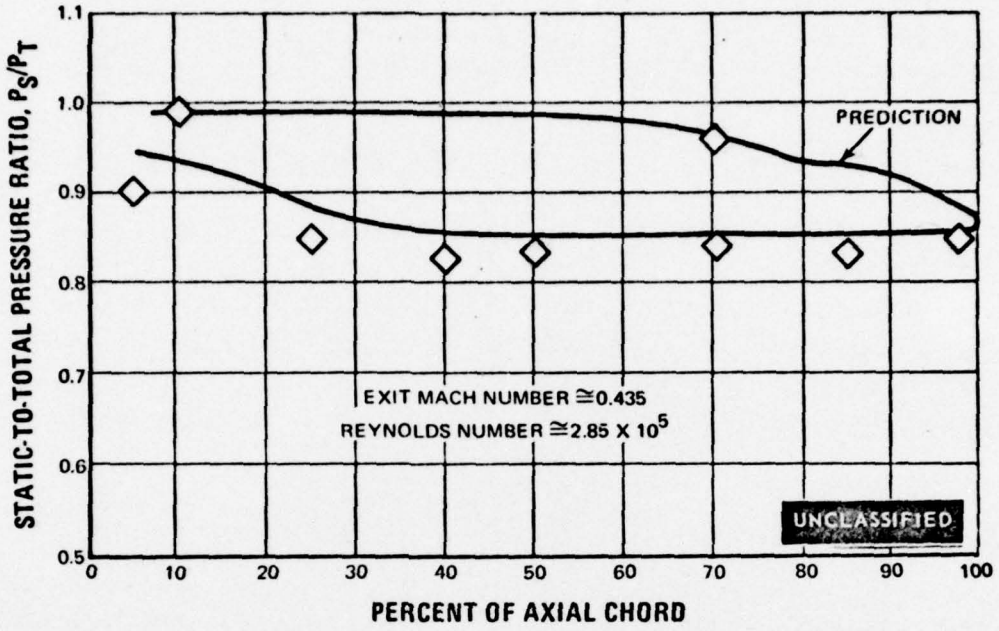

Figure 22 Static-to-Total Pressure Ratio Versus Percent of Axial Chord, Second Vane Mean Section; Exit Mach Number = .435

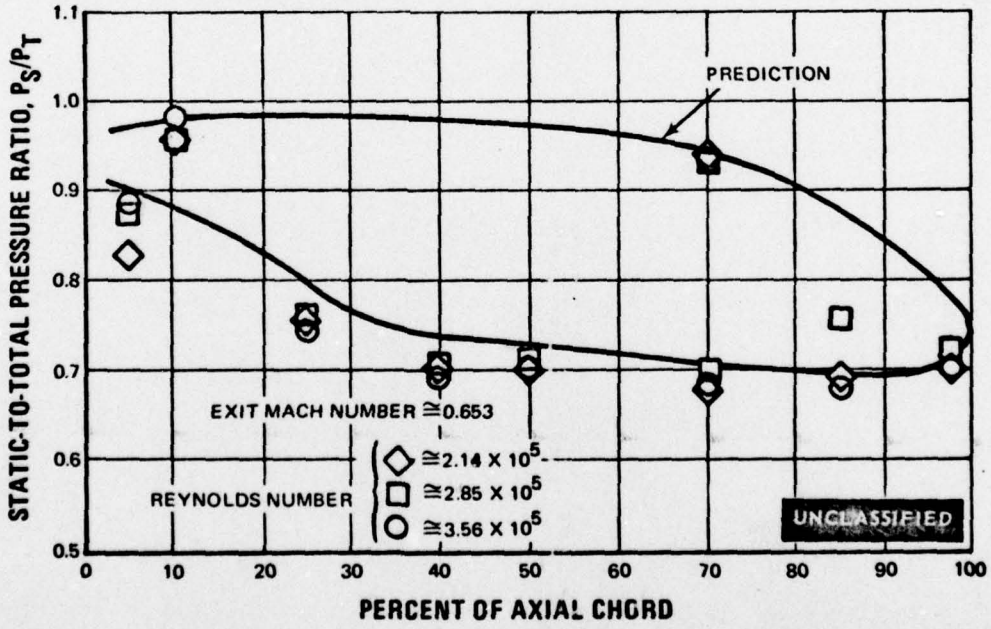

Figure 23 Static-to-Total Pressure Ratio Versus Percent of Axial Chord, Second Vane Mean Section; Exit Mach Number = .653

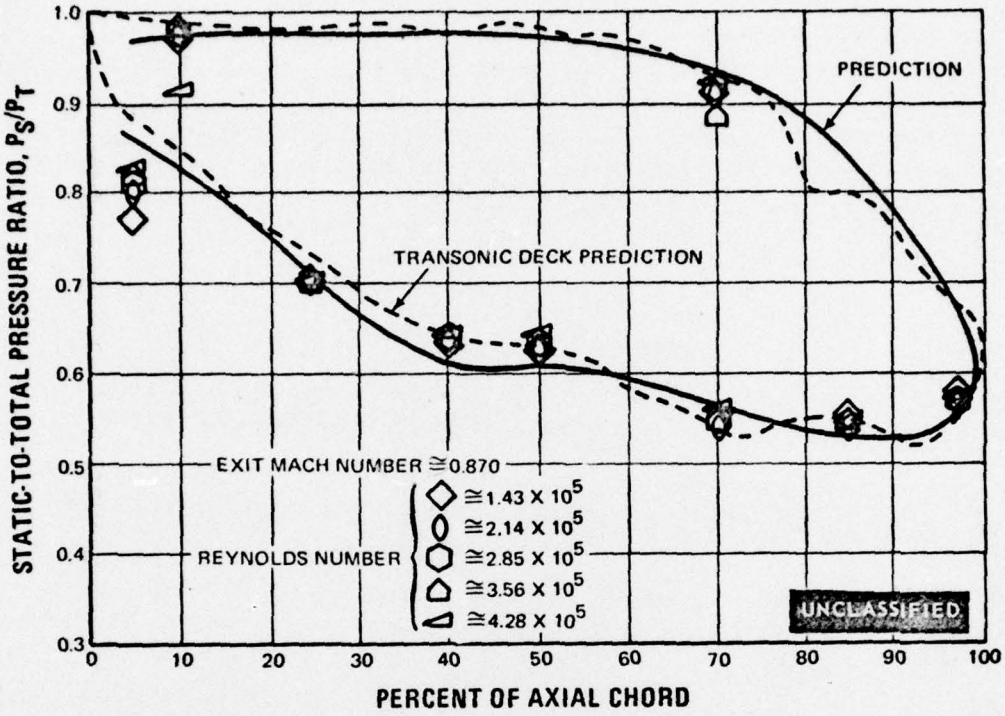

Figure 24 Static-to-Total Pressure Ratio Versus Percent of Axial Chord, Second Vane Mean Section; Exit Mach Number = .870

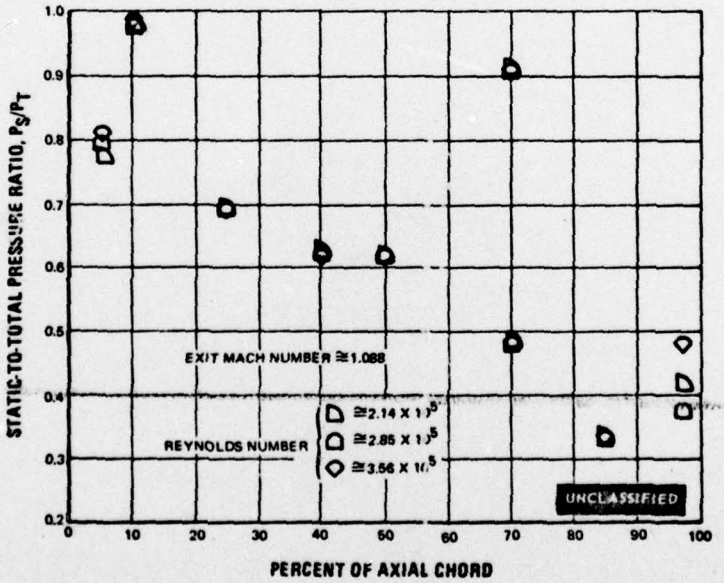

Figure 25 Static-to-Total Pressure Ratio Versus Percent of Axial Chord, Second Vane Mean Section; Exit Mach Number = 1.088

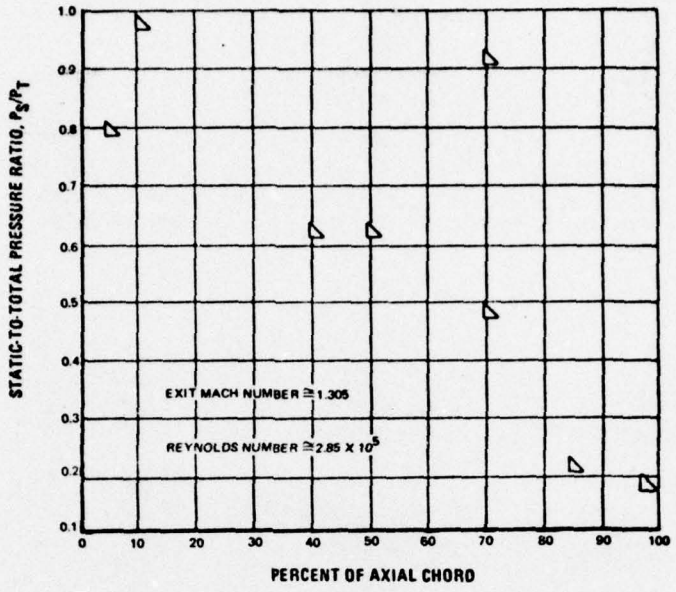

Figure 26 Static-to-Total Pressure Ratio Versus Percent of Axial Chord, Second Vane Mean Section; Exit Mach Number = 1.305

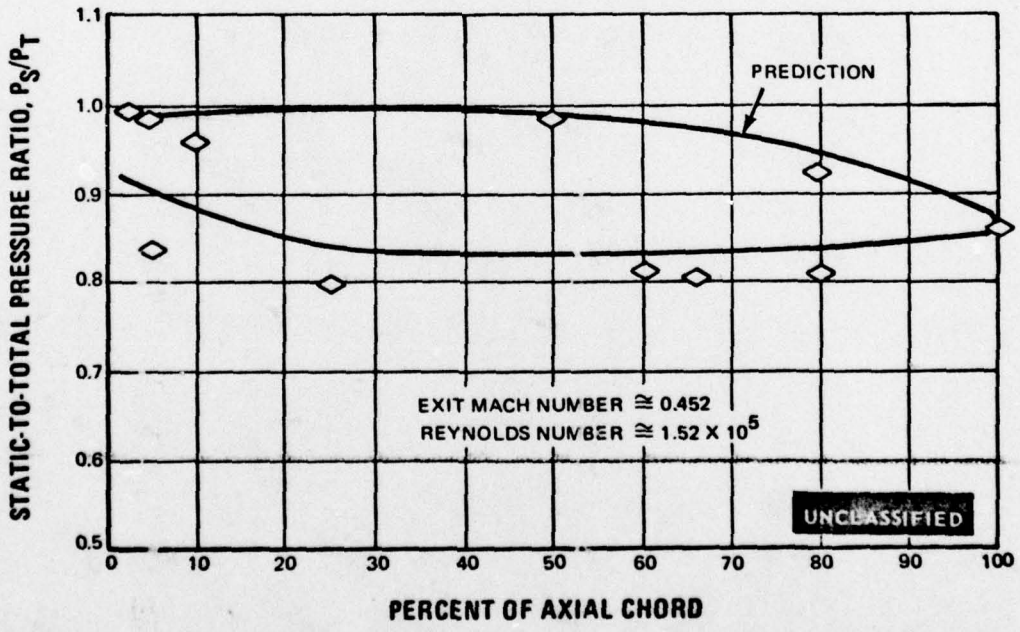

Figure 27 Static-to-Total Pressure Ratio Versus Percent of Axial Chord, Second Blade Mean Section; Exit Mach Number = .452

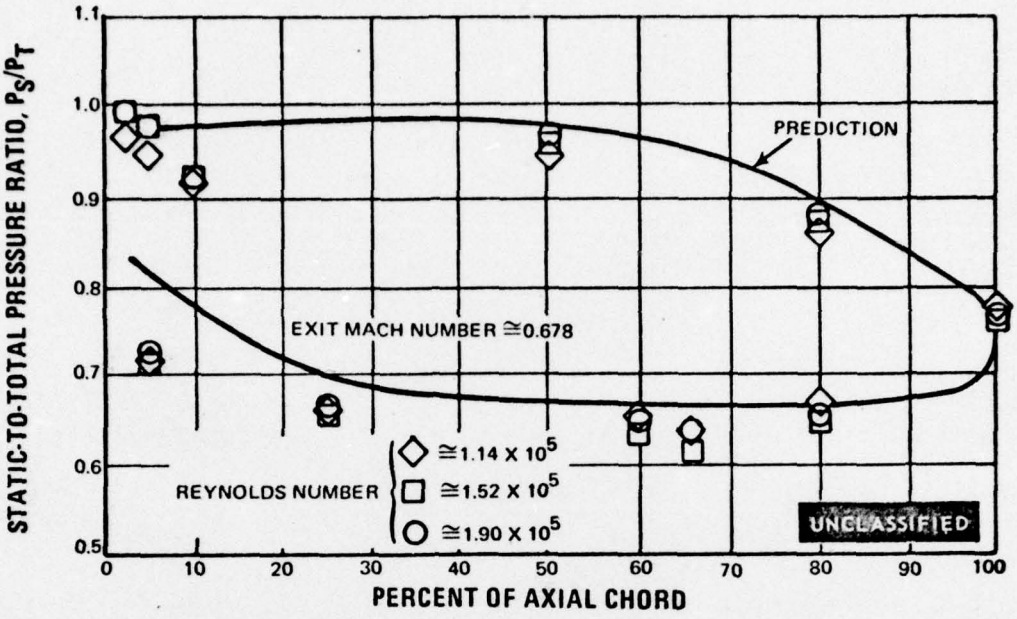

Figure 28 Static-to-Total Pressure Ratio Versus Percent of Axial Chord, Second Blade Mean Section; Exit Mach Number = .678

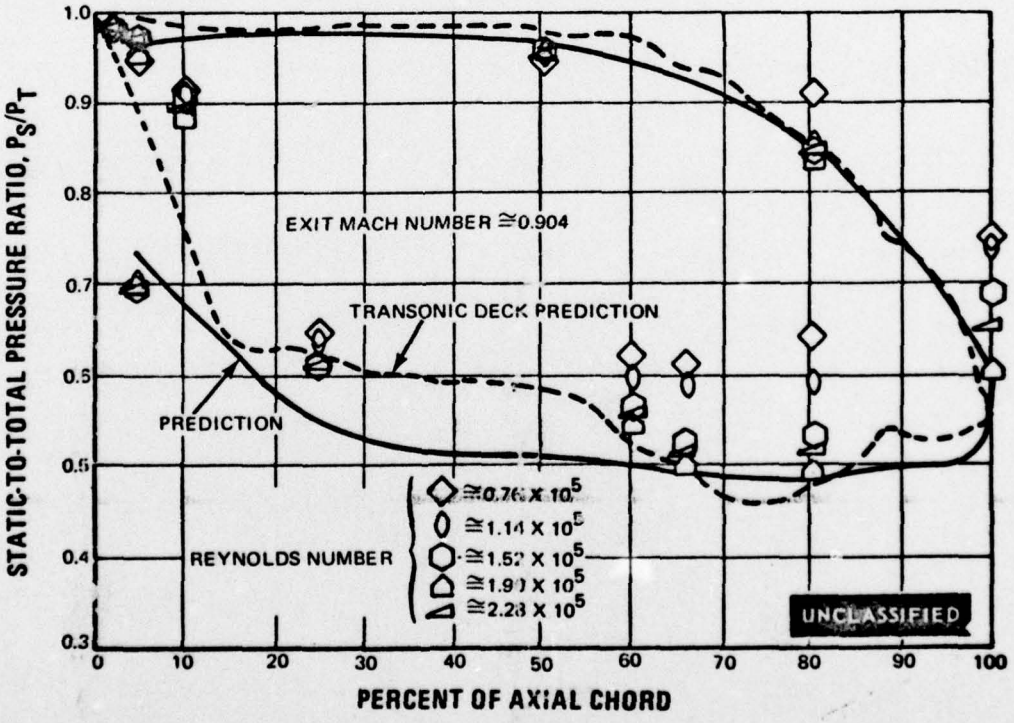

Figure 29 Static-to-Total Pressure Ratio Versus Percent of Axial Chord, Second Blade Mean Section; Exit Mach Number = .904

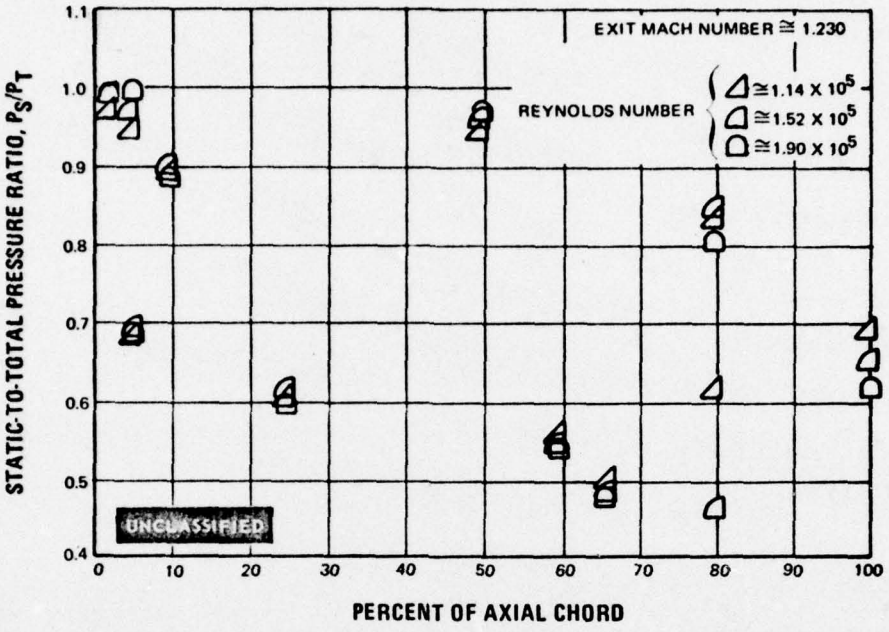

Figure 30 Static-to-Total Pressure Ratio Versus Percent of Axial Chord, Second Blade Mean Section; Exit Mach Number = 1.230

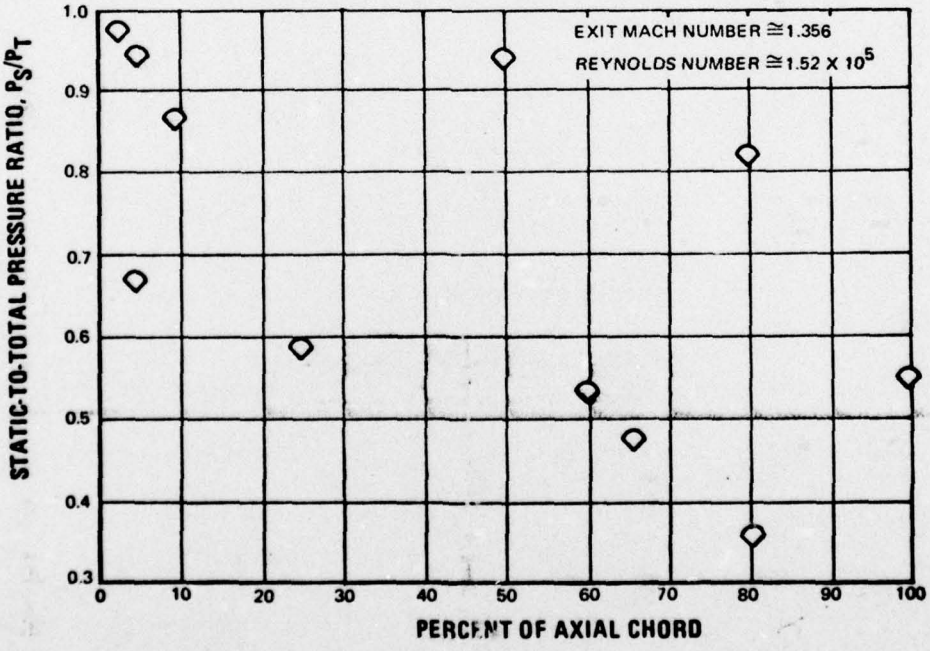

Figure 31 Static-to-Total Pressure Ratio Versus Percent of Axial Chord, Second Blade Mean Section; Exit Mach Number = 1.356

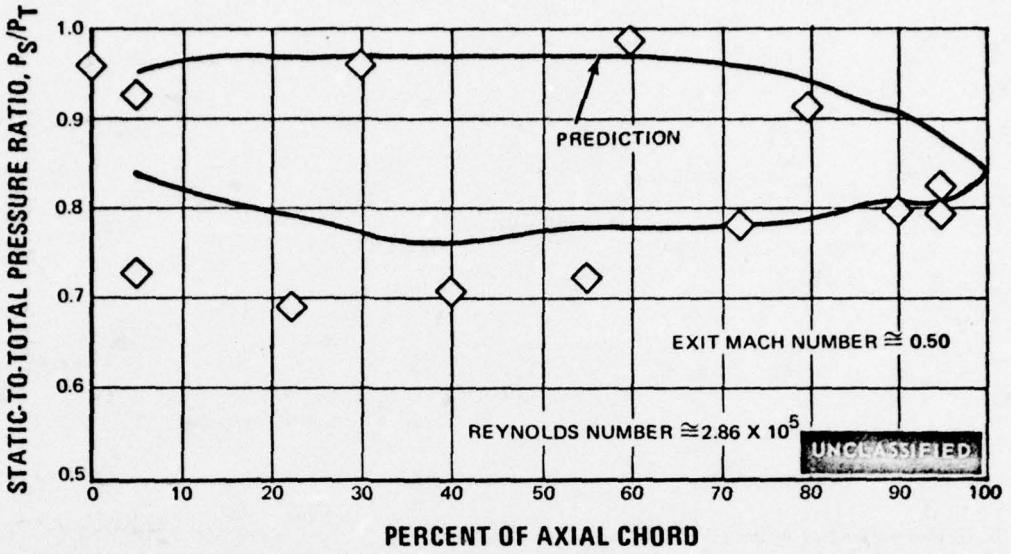

Figure 32 Static-to-Total Pressure Ratio Versus Percent of Axial Chord, Second Vane Root Section; Exit Mach Number = .50

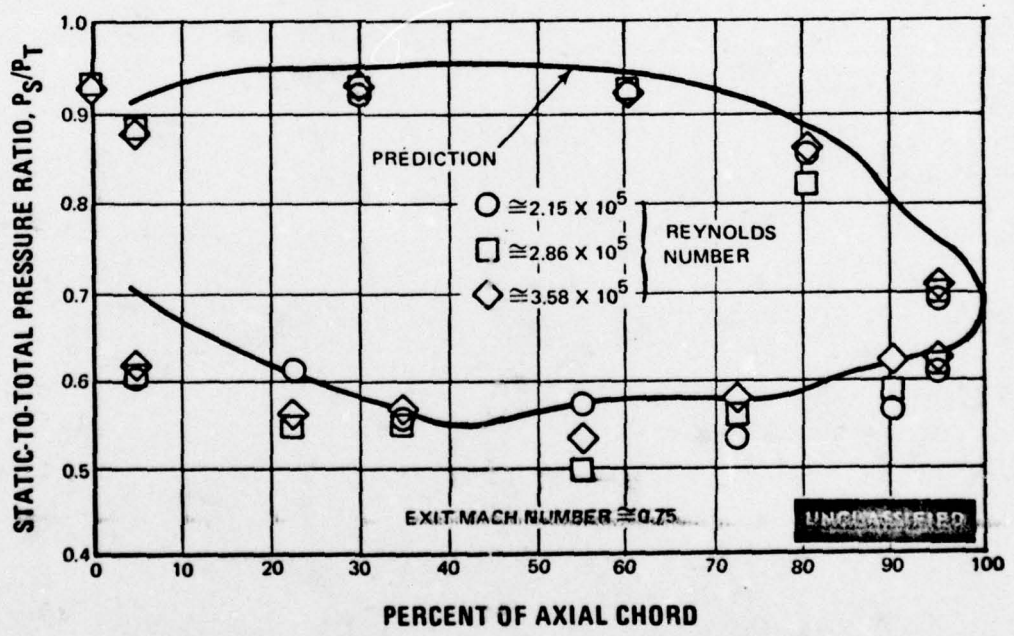

Figure 33 Static-to-Total Pressure Ratio Versus Percent of Axial Chord, Second Vane Root Section; Exit Mach Number = .75

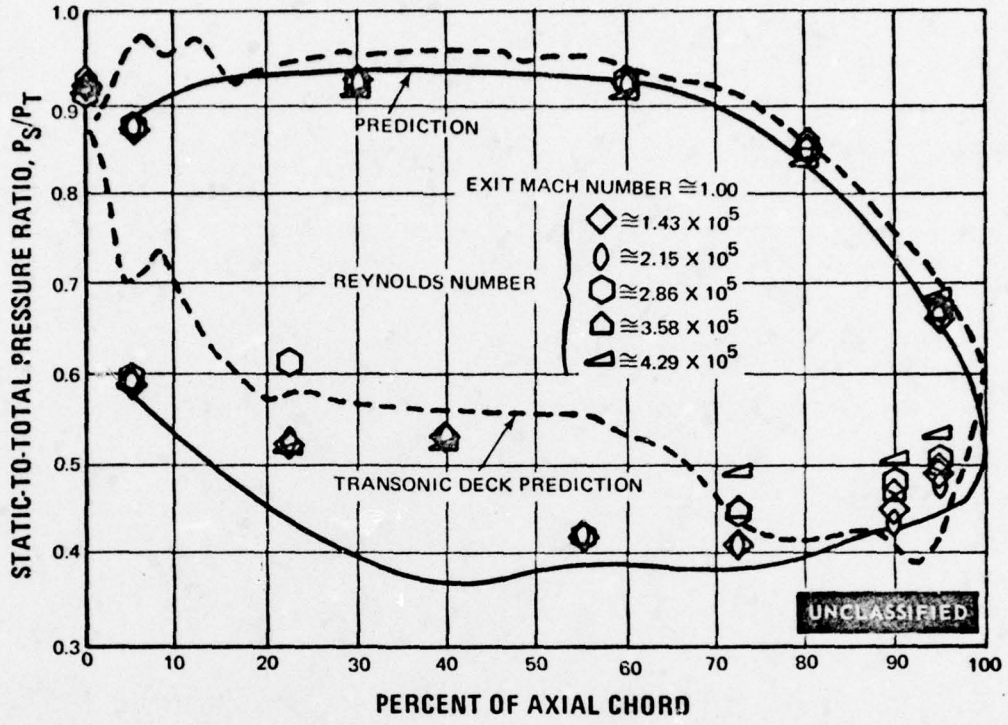

Figure 34 Static-to-Total Pressure Ratio Versus Percent of Axial Chord, Second Vane Root Section; Exit Mach Number = 1.00

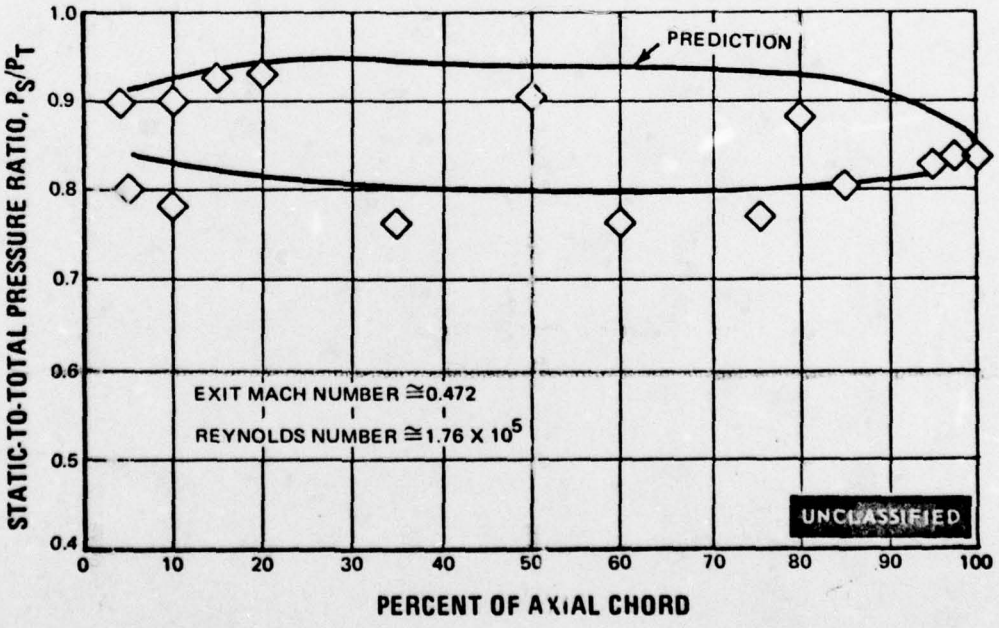

Figure 35 Static-to-Total Pressure Ratio Versus Percent of Axial Chord, Second Blade Root Section; Exit Mach Number = .472

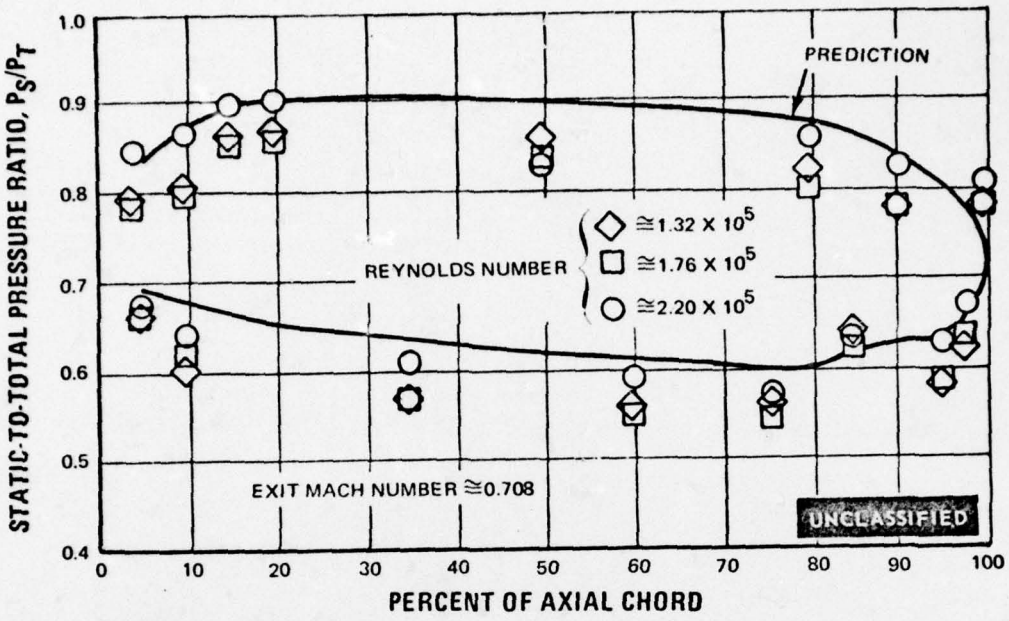

Figure 36 Static-to-Total Pressure Ratio Versus Percent of Axial Chord, Second Blade Root Section; Exit Mach Number = .708

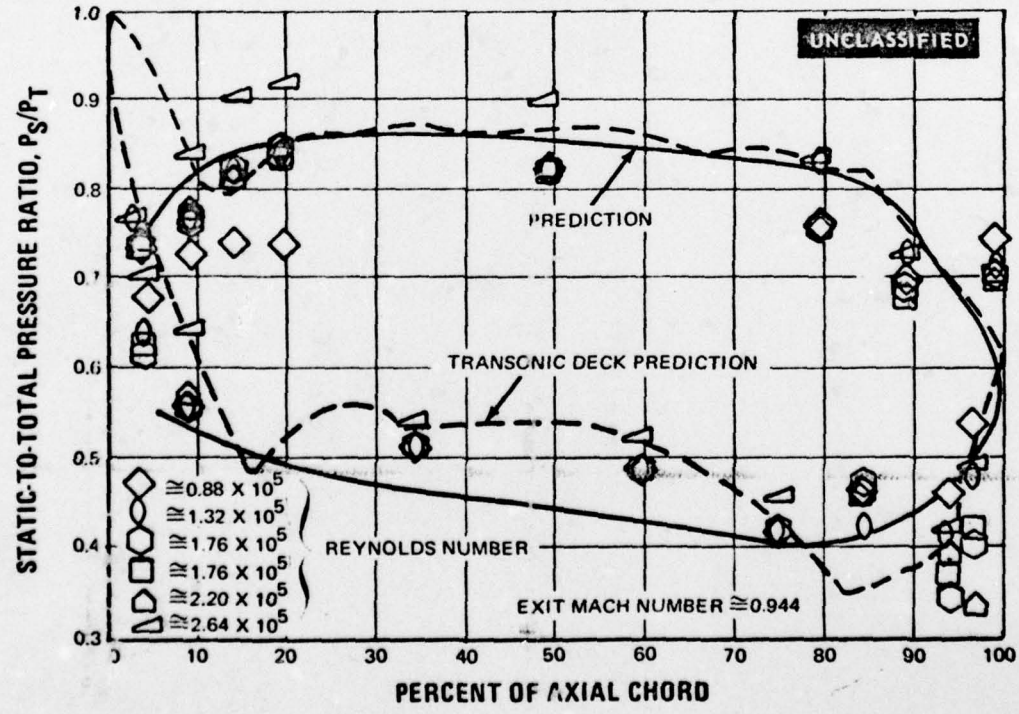

Figure 37 Static-to-Total Pressure Ratio Versus Percent of Axial Chord, Second Blade Root Section; Exit Mach Number = .944

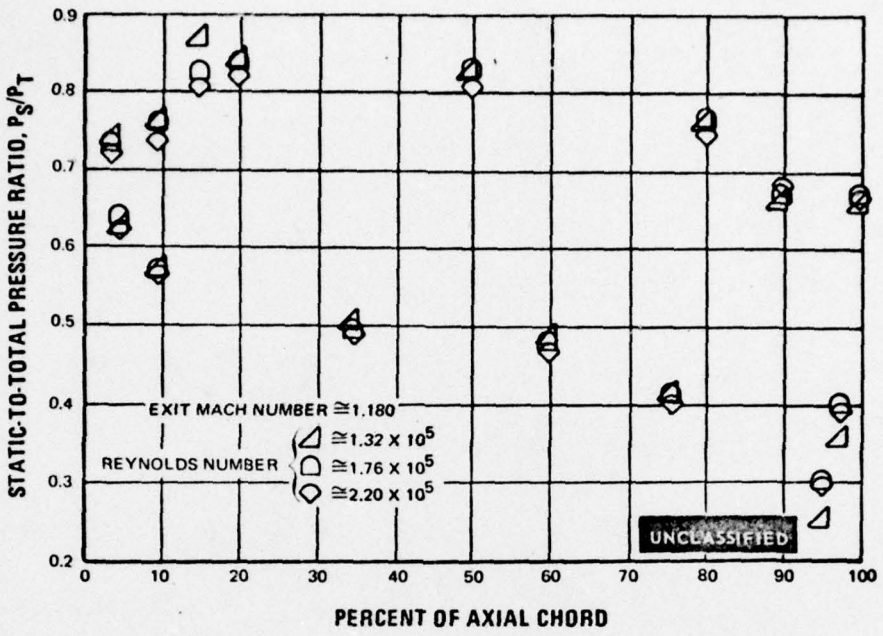

Figure 38 Static-to-Total Pressure Ratio Versus Percent of Axial Chord, Second Blade Root Section; Exit Mach Number = 1.180

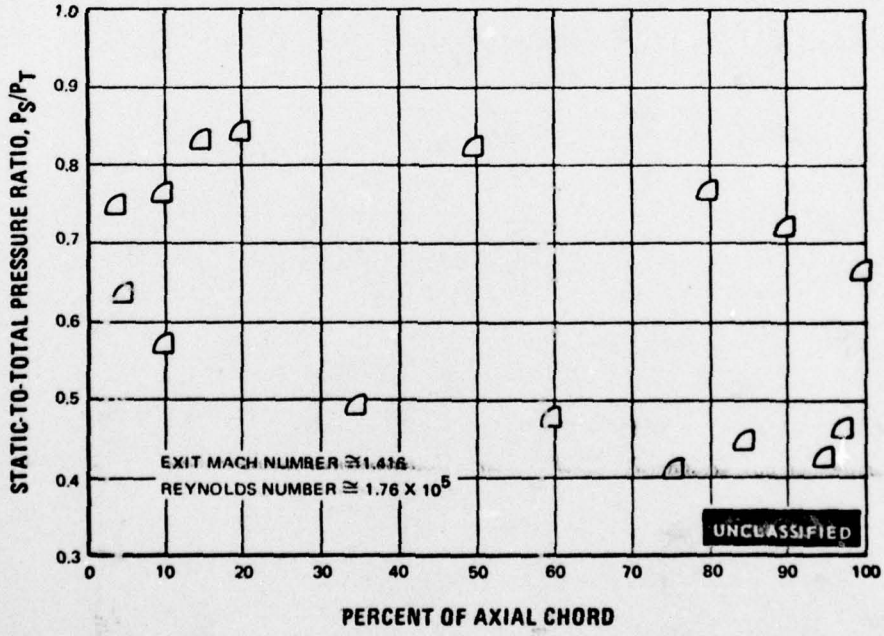

Figure 39 Static-to-Total Pressure Ratio Versus Percent of Axial Chord, Second Blade Root Section; Exit Mach Number = 1.416

(U) The second blade root section shows a higher profile loss than the combined profile and secondary loss in the blade root section of the part annular cascade test, but interaction between the complex mechanisms occurring in this area are sufficiently complicated that no firm conclusion may be drawn with respect to the result.

5. SUMMARY

(U) The midspan section loss coefficients for the first vane, first blade, second vane and second blade measured in the plane cascade were consistent with the mean values measured in the annular segment cascade.

(U) The airfoil root sections which will be designed for the demonstrator two-stage turbine will not have the shock problems exhibited by the tested preliminary airfoil root sections. The new Transonic Airfoil Pressure Distribution Program will be used to design the demonstrator turbine airfoils, which proved to be more accurate for predicting pressure distributions on transonic airfoils.

(U) The objectives of this task were met, since these test results verified the validity of the aerodynamic design procedures that were used to predict the airfoil surface pressure distributions and airfoil boundary layer characteristics.

6. TEST PROCEDURE

(U) The plane cascade tests of the medium-reaction normal-solidity airfoils were performed in the Willgoos Laboratory at East Hartford on X-213 stand. The six sections that were tested were the mean sections of the first vane, first blade, second vane, and second blade and the root sections of the second vane and second blade. These performance tests required the use of various combinations of compressors and exhausters, and utilized the heat of compression of the compressors to obtain various combinations of Mach numbers and Reynolds numbers at the cascade exit. Test conditions were always chosen so as to prevent the condensation of atmospheric water vapor.

(U) For each of the six plane sections a thirteen point test program was run. The test program was made to center about the design values of Mach number and Reynolds number, which are listed in Table V. The thirteen point test program is graphically portrayed in Figure 40. At each point the inlet wall, exit wall, and airfoil surface static pressure taps were read and a banjo-type probe was used to survey the exit plane for air angle and total pressure. The procedure listed below was used for these tests:

- The cascade pack was installed on the stand and all of the fixed instrumentation was connected
- The traversing probe was installed at the exit plane of the cascade pack and was correctly located with respect to the instrumented airfoil
- The total pressure transducers for the traversing probe and the data recording equipment were calibrated

- The laboratory compressors and exhausters which were required for the test were started and allowed to run until steady operating conditions were reached, which took about two hours

- Preceeding the test, the valves upstream of the cascade rig were closed and the exhausters were used to reduce the exit pressure to an arbitrary low value; in this manner any faulty static pressure taps were discovered

- In turn, each of the thirteen test points were set and a complete set of data was recorded

TABLE V

DESIGN MACH NUMBERS AND
REYNOLDS NUMBERS FOR THE SIX
PLANE CASCADE SECTIONS

Section	Mach Number	Reynolds number
First vane mean	0.852	4.38×10^5
First blade mean	0.788	2.26×10^5
Second vane root	1.003	2.86×10^5
Second vane mean	0.870	2.85×10^5
Second blade root	0.944	1.76×10^5
Second blade mean	0.904	1.52×10^5

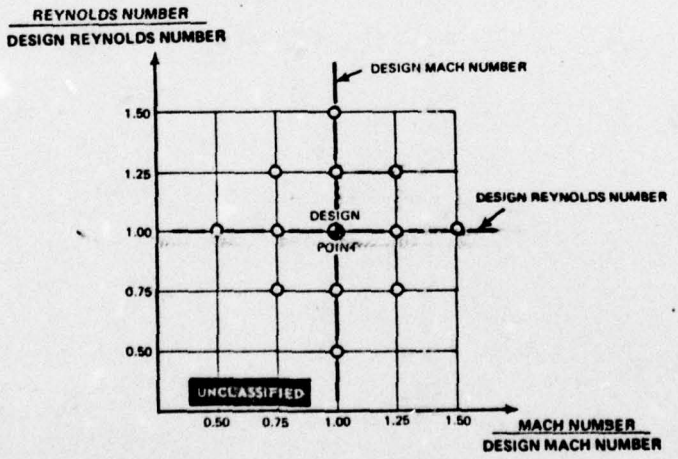

Figure 40 Plane Cascade Test Program

SECTION IV

MEDIUM SOLIDITY AIRFOIL EVALUATION (TASK IId)

1. OBJECTIVE

(U) The initial objective of Task IId was to investigate two additional boundary layer control methods, other than the two methods that were to be investigated under Task IIc, on two different airfoils. Since the performance of the four baseline airfoils was very similar (Reference 3), Task IIc was modified so that four boundary layer control methods were applied only to the second vane (Reference 4, Section IV), eliminating the need for Task IId as originally conceived. By mutual agreement between Pratt & Whitney Aircraft and the Air Force, the work substituted for the original Task IId was the evaluation of the performance of lower-solidity/higher-load-coefficient airfoils designed for the same velocity triangles as the baseline airfoils of Task IIb. The performance of the first vane and first blade lower-solidity airfoils was reported in Reference 4, and the second vane and second blade results, as well as a summary for all four airfoils investigated, are presented in this Section.

2. TASK OBJECTIVE

(U) Each of the four medium solidity airfoils were evaluated in an annular segment cascade exactly as in Task IIb (Reference 3). The data has been analyzed and the task objectives were met by the following steps:

- Measurement of all important aerodynamic properties at the cascade inlet and exit planes
- Reconstruction of the entire exit plane loss distribution
- Reconstruction of the entire exit plane flow pattern
- Measurement of the airfoil surface static pressure distributions at three radial locations
- Careful analysis of all data and visual clues

3. AIRFOIL SECTION AND FACILITY DESIGN

(U) The medium-reaction, medium-solidity airfoils were designed to the same turbine velocity diagrams as the normal solidity airfoils. These diagrams were presented in Reference 1. A summary of the pertinent design values, the airfoil elevations, gaging distribution, airfoil sections, predicted surface pressure distributions, and airfoil radius of curvature distributions for each of the four medium-solidity airfoils was presented at five spanwise locations in Reference 3. The four airfoils are the first and second vanes, and the first and second blades. The fabrication coordinates of each airfoil were also tabulated in Reference 3, including the airfoil angles, airfoil areas, axial chords and uncovered turnings.

(U) The details of the test section design, location of static pressure taps and the method of installation, details of the traversing probes and their calibration, location of the traversing planes, and probe corrections for pitch angle were presented in Reference 4. The axial location dimensions for the traversing planes and end wall static pressure taps were omitted in Reference 4. The following list gives the locations for planes M-M, N-N, O-O, and P-P shown in Reference 4, Figures 142 and 144.

- Plane M-M is located 1.00 inch axially upstream of the test vane tip section or test blade root section leading edge
- Plane N-N is located 0.788 inch axially downstream from plane M-M
- Plane O-O is located 0.185 inch axially downstream of the test airfoil trailing edge at the mean section C-C
- Plane P-P is located 0.625 inch axially downstream of the test airfoil trailing edge at the mean section C-C

4. DISCUSSION

(U) The partial results of this task have been reported in Reference 4, since at the time of publication of that report the performance of the medium solidity second vane and second blade had not been evaluated. This work has now been completed and will be reported herein. In addition, a comparison of the performance of the nominal and medium solidities will also be made.

(U) As previously reported (Reference 4) the inlet guide vanes for the second vane and second blade did not produce the correct inlet angle to their respective test airfoils. This deficiency was substantially improved by a reworking of these guide vanes and the new results are shown in Figures 41 and 42. The associated inlet total pressure spanwise pressure loss distributions are shown in Figures 43 and 44. The inlet total pressure loss contours from which these were obtained are shown in Figures 45 and 46.

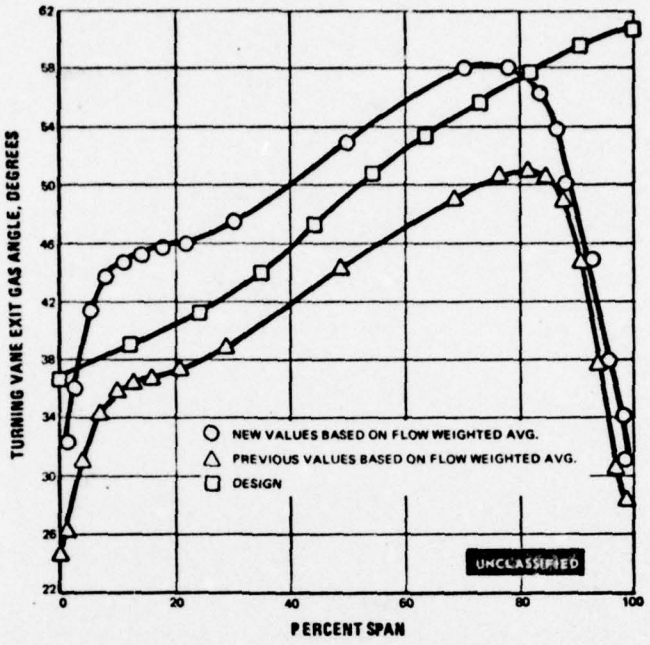

Figure 41 Inlet Guide Vane Spanwise Exit Angle Distribution, Second Vane, Medium Solidity Cascade - Midspan Exit Test Airfoil Mach No. = 0.820

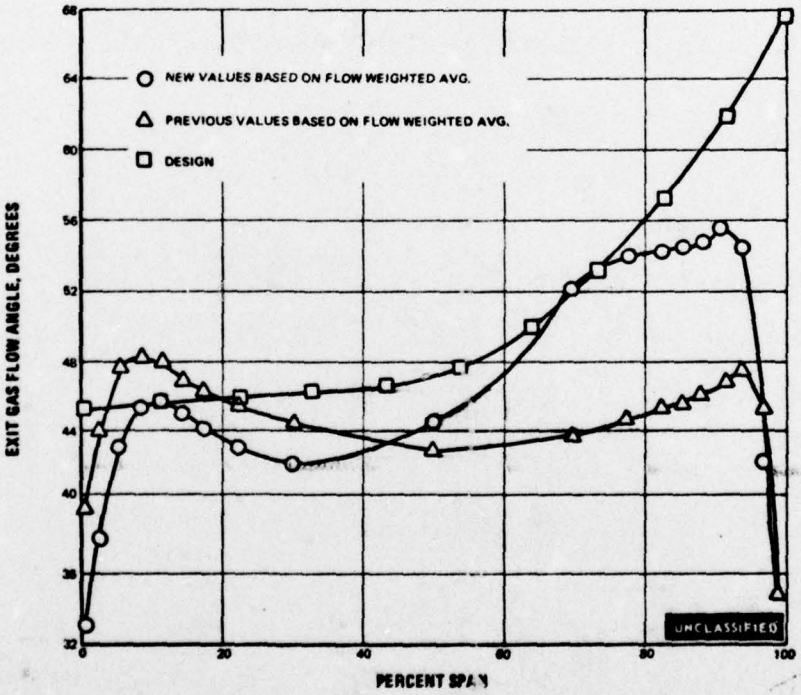

Figure 42 Inlet Guide Vane Spanwise Exit Angle Distribution, Second Blade, Medium Solidity Cascade - Midspan Exit Test Airfoil Mach No. = 0.940

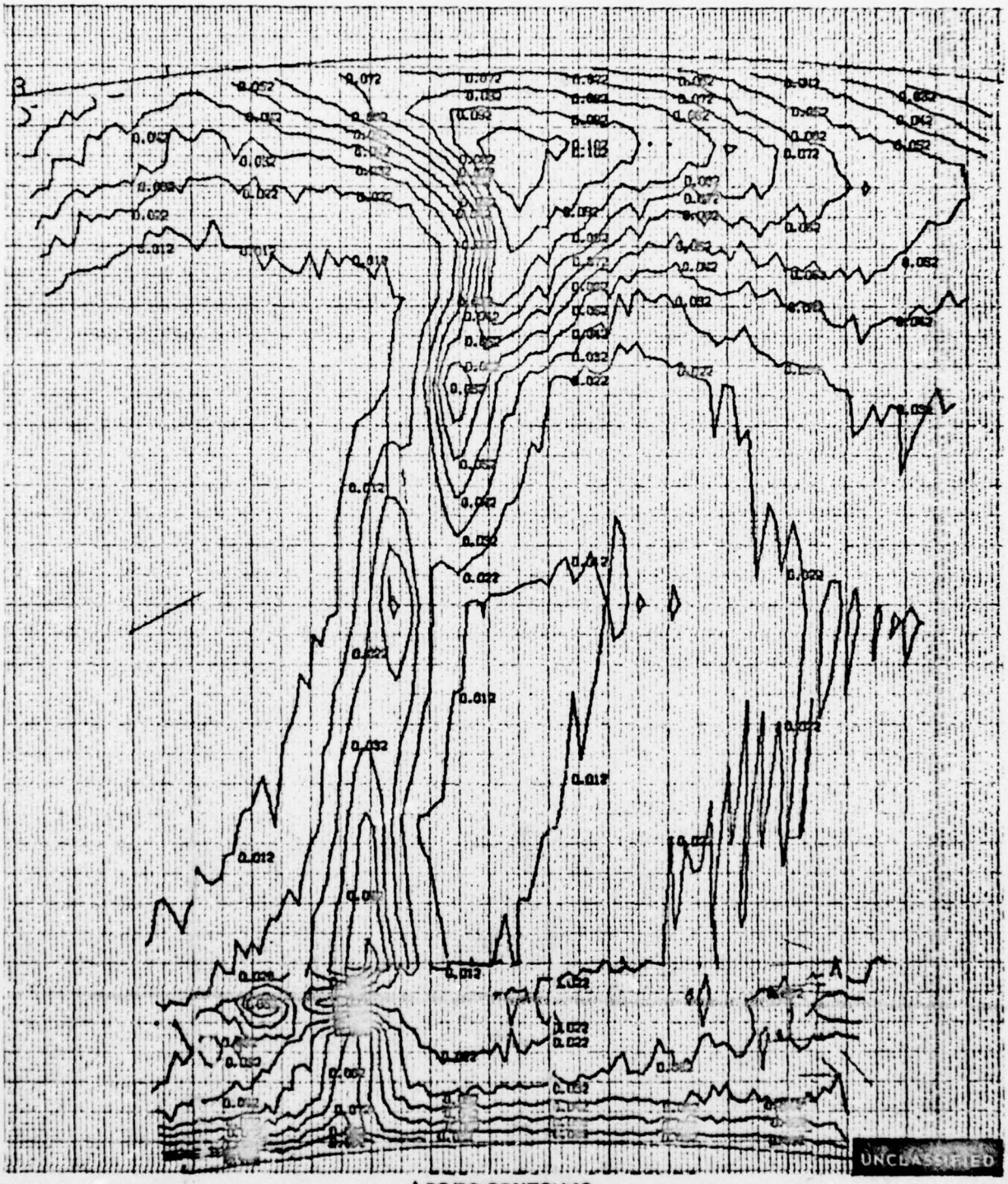

ΔPO/PO CONTOURS

Figure 43 Inlet Guide Vane Pressure Loss Contours, Second Vane, Medium Solidity Cascade - Midspan Exit Test Airfoil Mach No. = 0.820

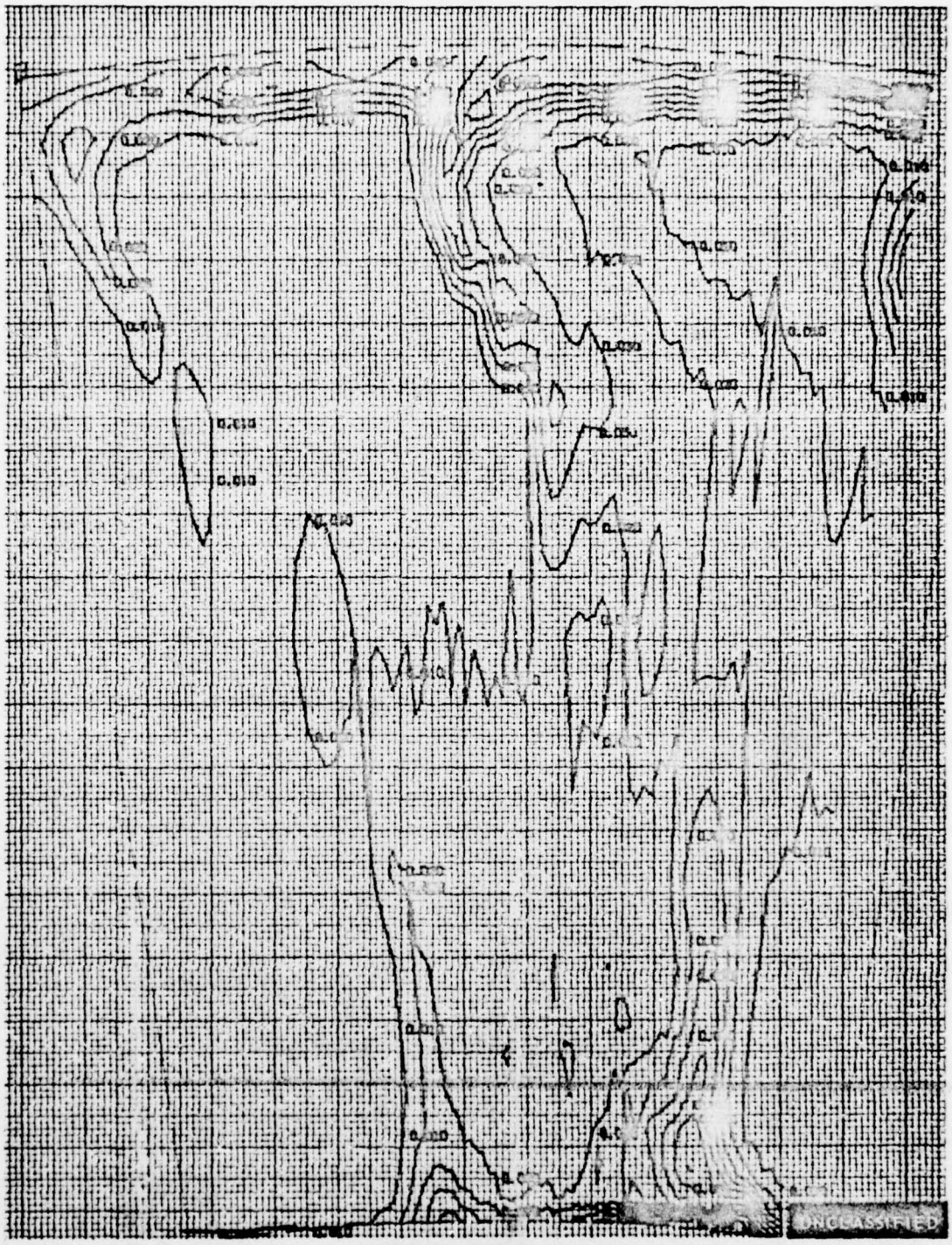

ΔPO/PO CONTOURS

Figure 44 Inlet Guide Vane Pressure Loss Contours, Second Blade, Medium Solidity Cascade, Midspan Exit Test Airfoil Mach No. = 0.940

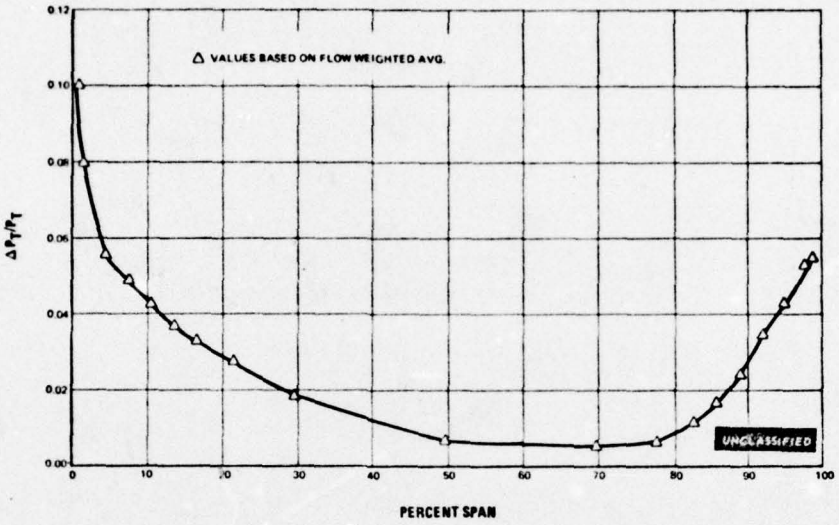

Figure 45 Inlet Guide Vane Spanwise Pressure Loss Distribution, Second Vane, Medium Solidity Cascade, Midspan Exit Test Airfoil Mach No. = 0.820

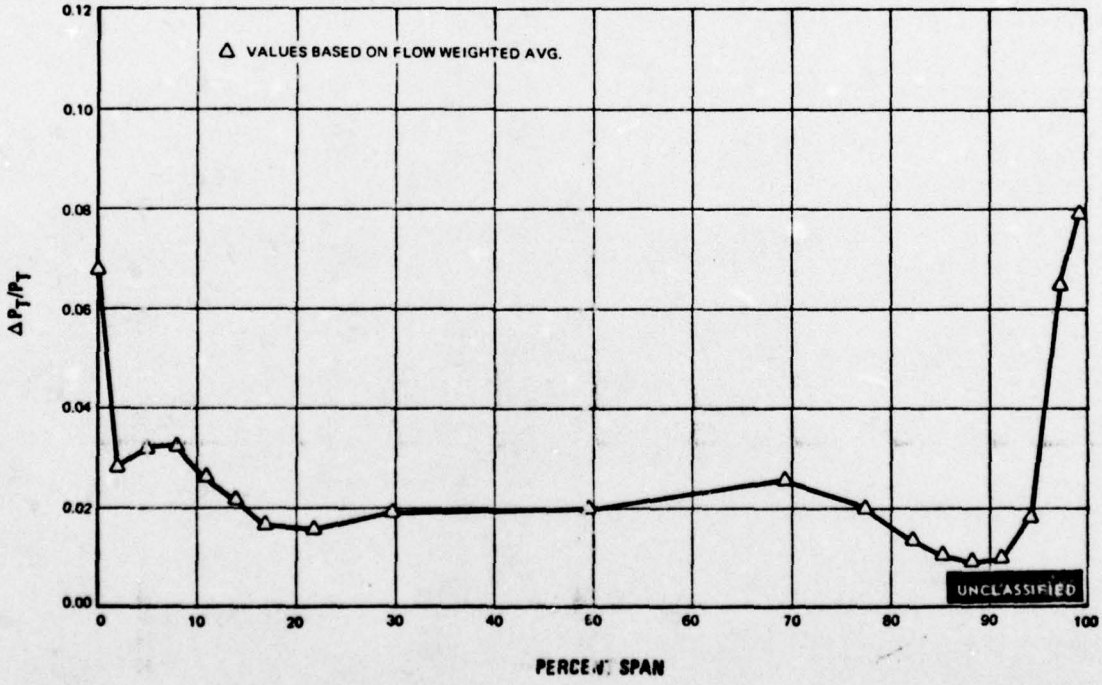

Figure 46 Inlet Guide Vane Spanwise Pressure Loss Distribution, Second Blade, Medium Solidity Cascade, Midspan Exit Test Airfoil Mach No. 0.940

(U) The second vane data indicates that the airfoils are separated over the majority of the span. The contour plot of loss $\left(\frac{\Delta Po}{Po}\right)$ (Figure 47) shows distinct wakes only near the root region and the spanwise flow-weighted average values of $\frac{\Delta Po}{Po}$ and $1-\phi^2$ shown in Figures 48 and 49 are very high over most of the span. The low $1-\phi^2$ values shown at the root and tip are partially due to the method of accounting for the spanwise inlet total pressure profile. The low total pressure fluid at the end walls of the inlet plane, assumed to remain at the same percent of the span, is actually convected radially inward to the quarter root and quarter tip regions of the exit plane. Therefore, a more meaningful average loss is found by flow-weighting the loss from the root-to-mean and mean-to-tip sections. These second vane averages are 0.085 and 0.234, respectively. The measured spanwise flow-weighted exit gas angle (Figure 50) and the exit gas angle contours (Figure 51) for the second vane show higher than predicted values particularly toward the tip section and the spanwise flow-weighted exit Mach number distribution shown in Figure 52 is lower than predicted. Both of these effects can be traced to airfoil boundary layer separation.

(U) The measured and predicted airfoil static pressure distributions are shown in Figures 53, 54 and 55 for the second vane root, mean and tip sections. The mean section test values show good agreement with predictions. The pressures in the throat-to-trailing-edge appear to be lower than predicted. This is likely due to the fact that the predictions of the Airfoil Pressure Distribution Program are inaccurate when extrapolated into the transonic flow regime. The tip section also shows good agreement except near the leading edge due to positive incidence at this section. The root is unloaded relative to the prediction due to the static pressure conditions at the exit plane. This situation was discussed in detail in Reference 3.

(U) The second blade data indicates that the airfoils are performing well from the root to the mean section and that the airfoils are separated from the mean to the tip section. The contour plot of $\Delta Po/Po$ in Figure 56, and the spanwise loss distribution in Figure 57 clearly show destinct wakes and low losses from the root to the mean section. The spanwise flow weighted values of $1-\phi^2$ shown in Figure 58 are also low from the root to the mean and increasingly higher from the mean to the tip section. The spanwise Mach number distributions (Figure 59) and calculated values of spanwise flow coefficient indicated that separation occurred in the tip region of this airfoil. The plots of exit gas angle contours (Figure 60) and spanwise flow-weighted exit gas angle (Figure 61) did not support the possibility of complete separation, however, implying perhaps that reattachment took place.

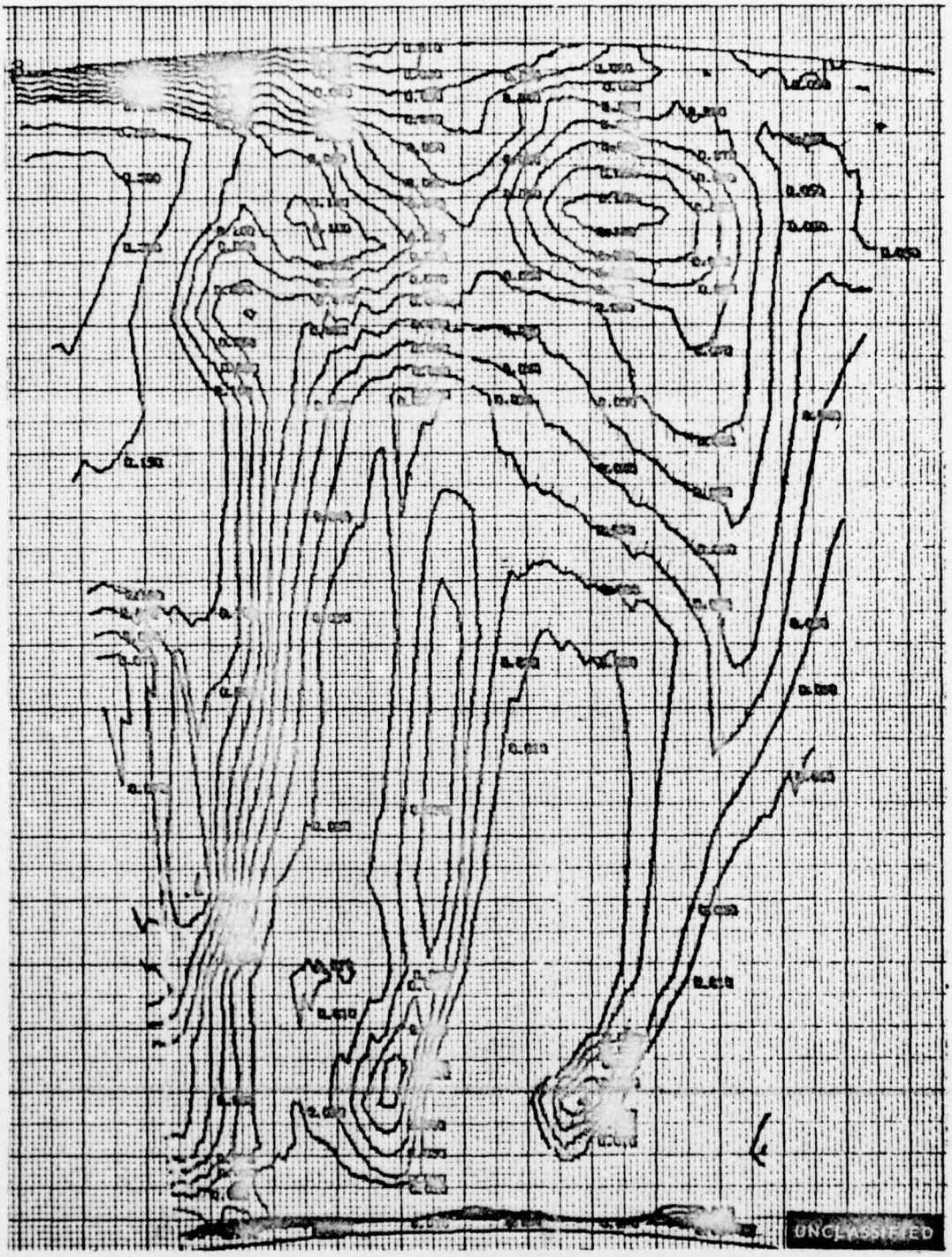

ΔPO/PO CONTOURS

Figure 47 Pressure Loss Contours, Second Vane, Medium Solidity, Three Flow Passages, Midspan Exit Mach No. = 0.820

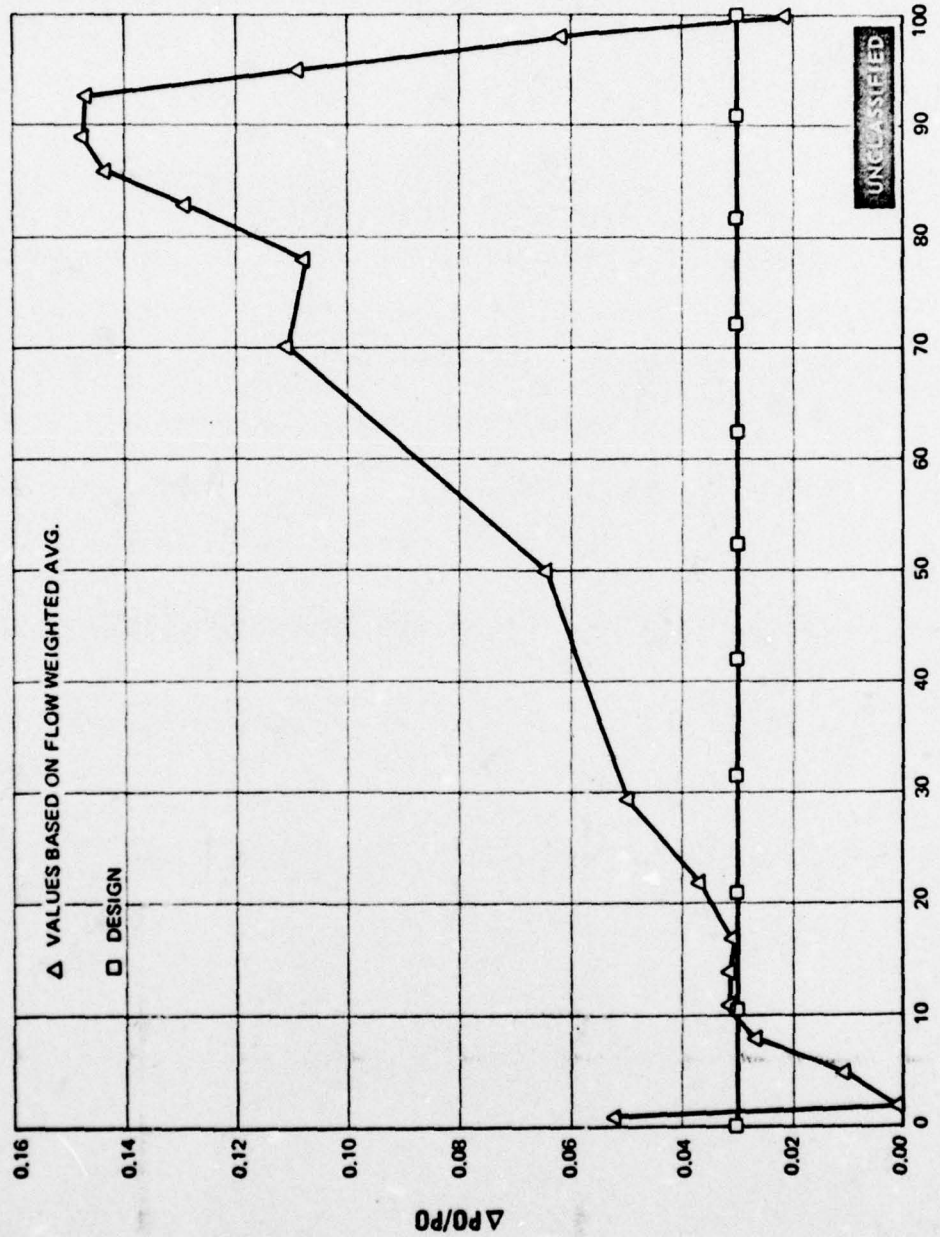

Figure 48 Spanwise Pressure Loss Distribution, Second Vane, Medium Solidity, Midspan Exit Mach No. = 0.820

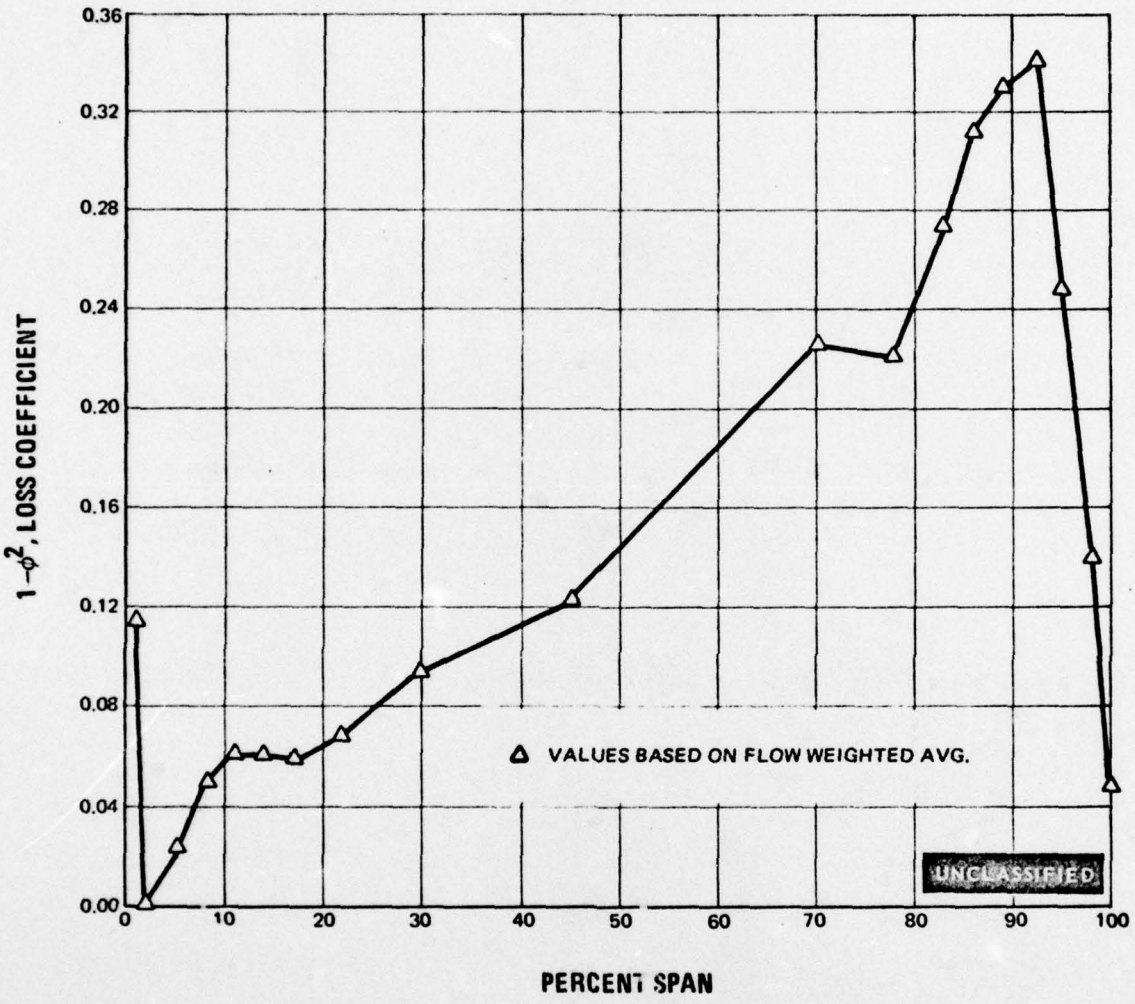

Figure 49 Spanwise Loss Coefficient Distribution, Second Vane, Medium Solidity, Mid-span Exit Mach No. = 0.820

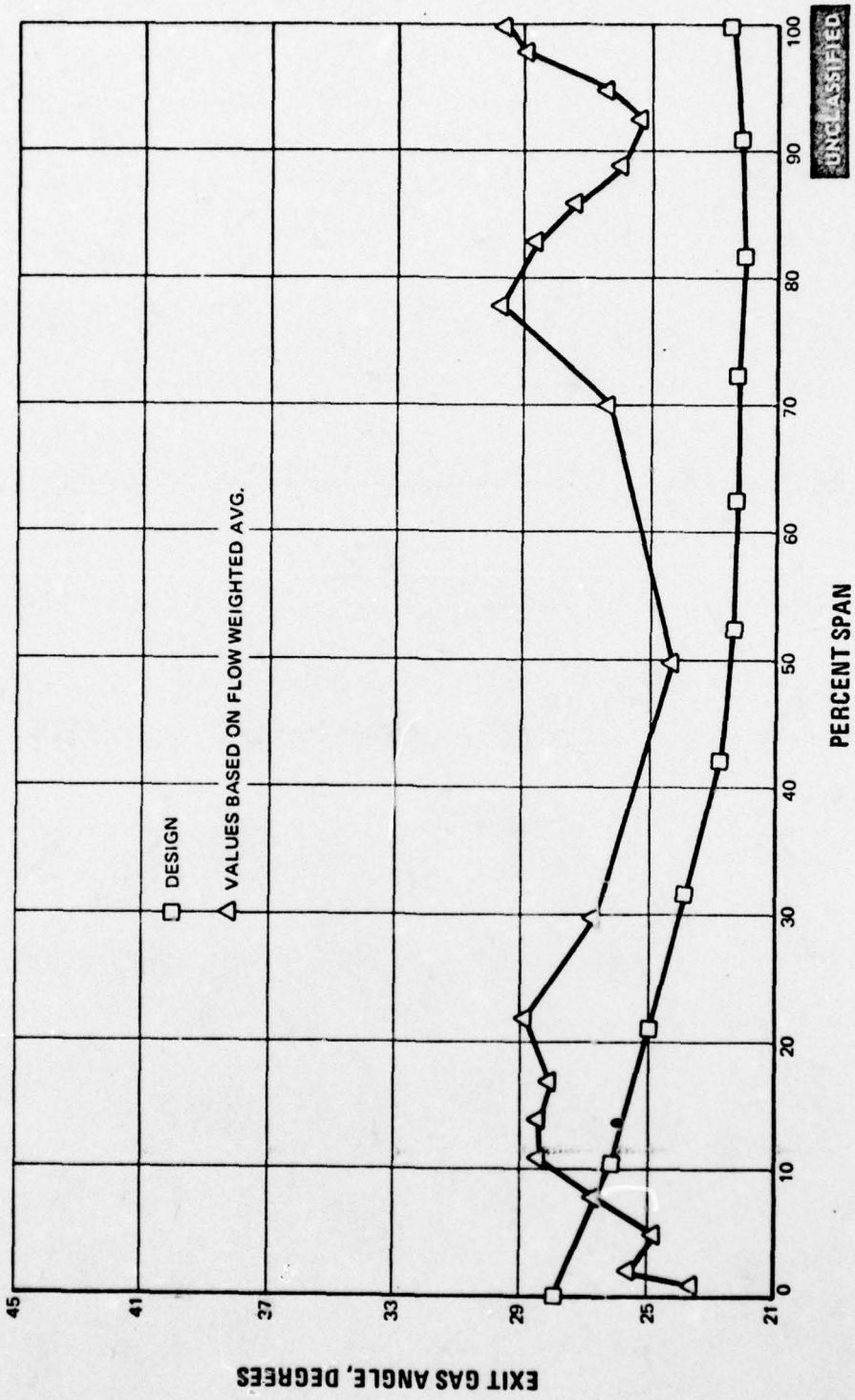

Figure 50 Spanwise Exit Gas Angle Distribution, Second Vane, Medium Solidity, Mid-span Exit Mach No. = 0.820

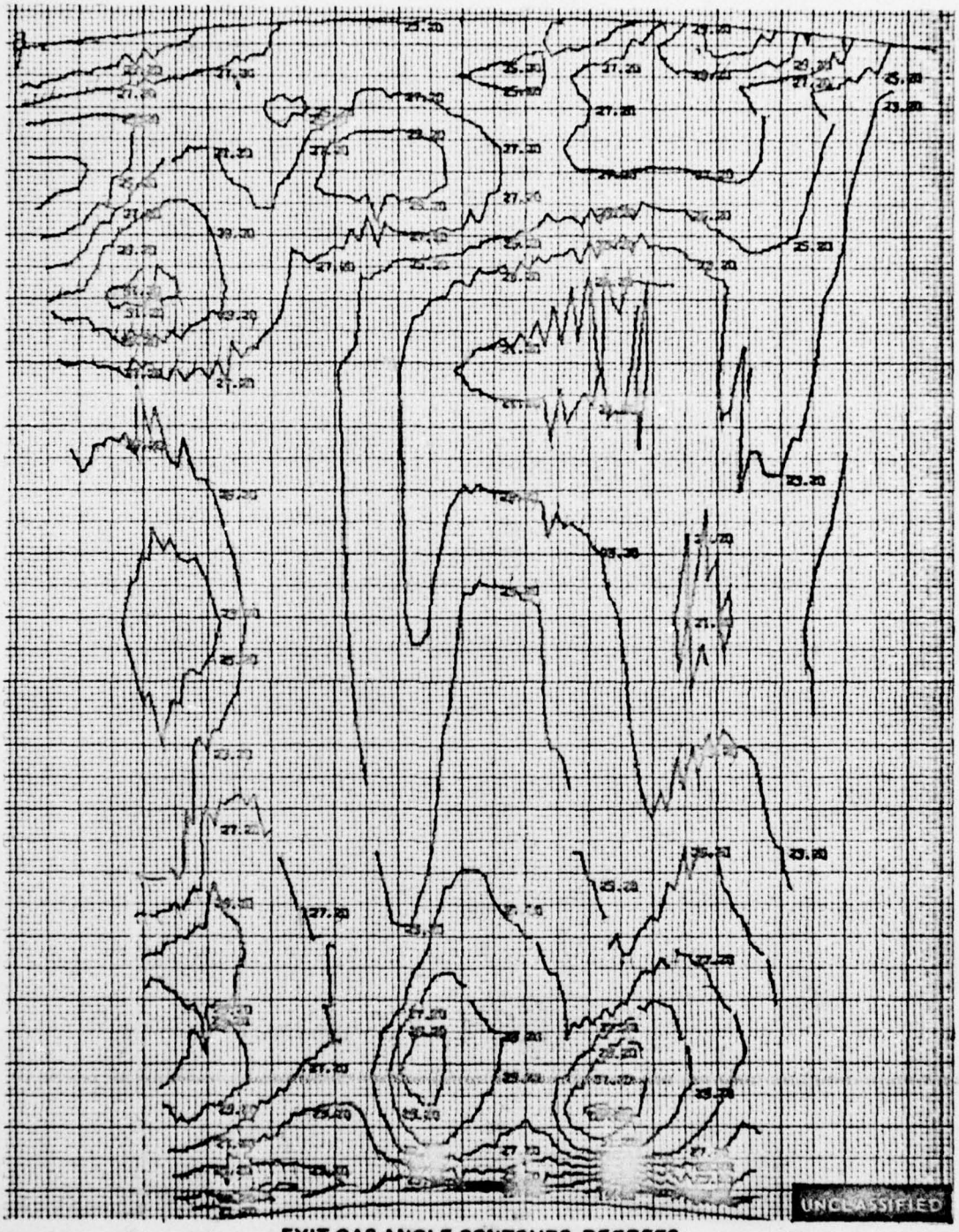

EXIT GAS ANGLE CONTOURS, DEGREES

Figure 51 Exit Gas Angle Contours, Second Vane, Medium Solidity, Three Flow Passages, Midspan Exit Mach No. = 0.820

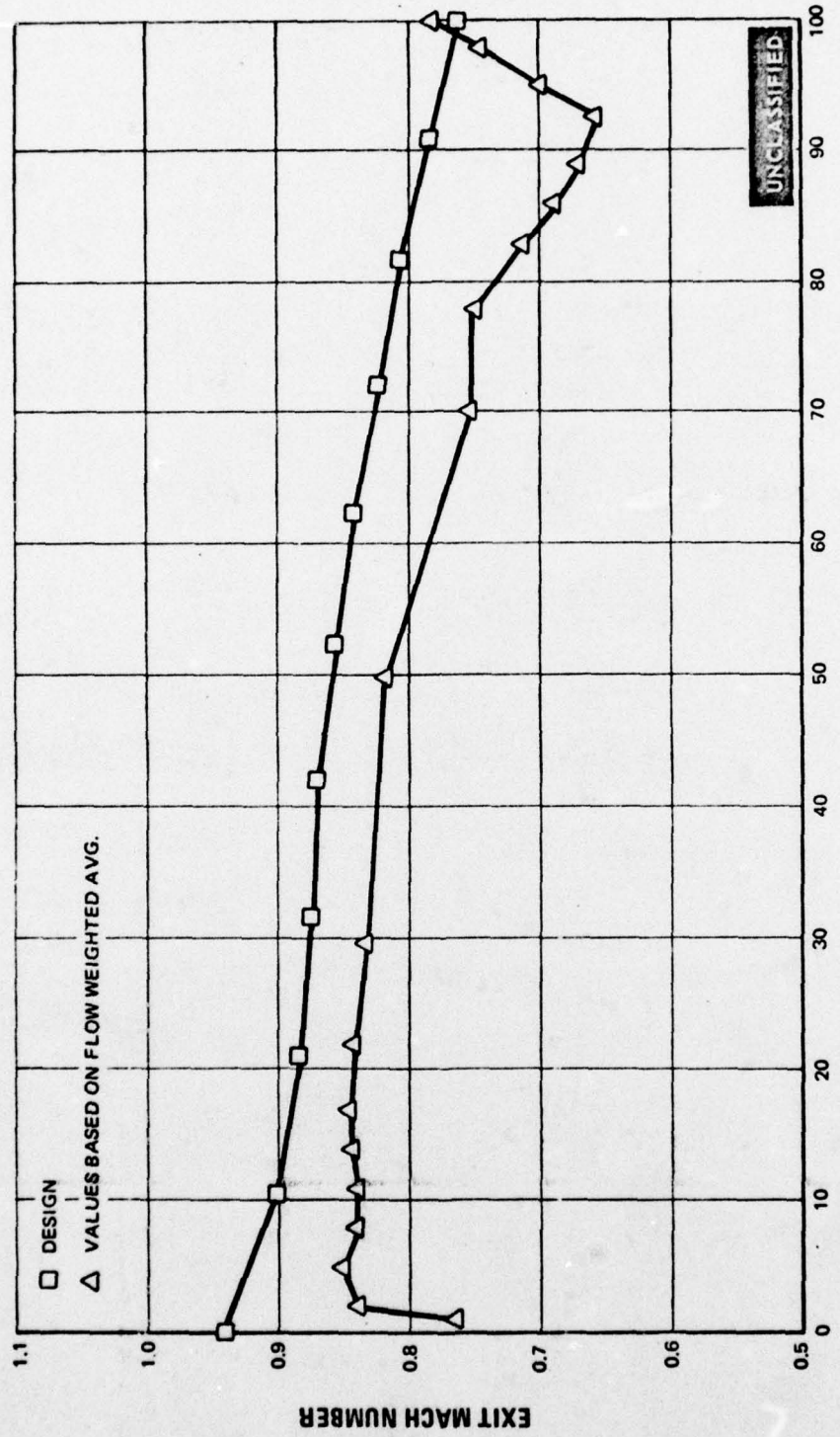

Figure 52 Spanwise Exit Mach Number Distribution, Second Vane, Medium Solidity, Midspan Exit Mach No. = 0.820

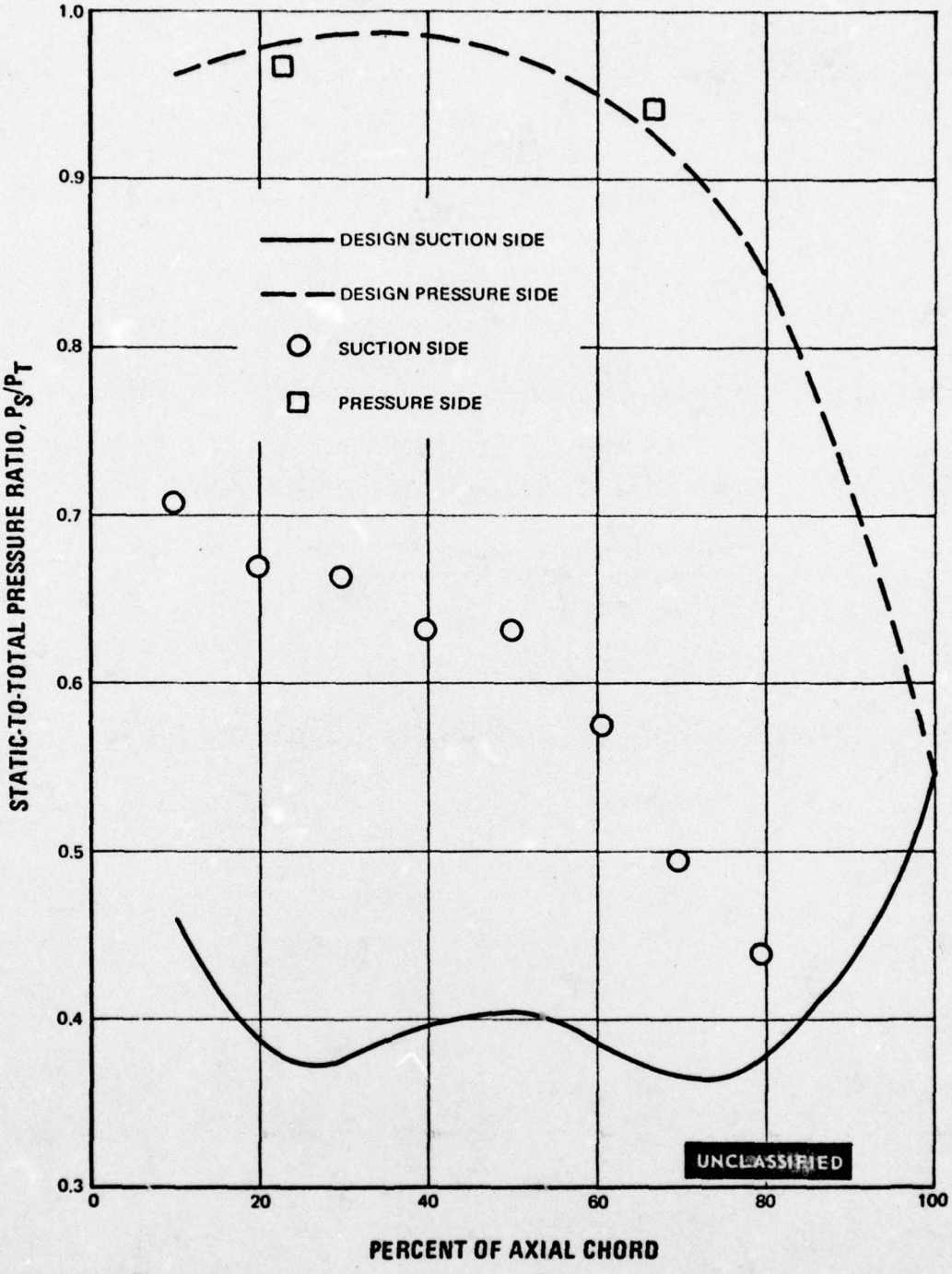

Figure 53 Static-to-Total Pressure Ratio Versus Percent Axial Chord, Second Vane, Medium Solidity, Root Section

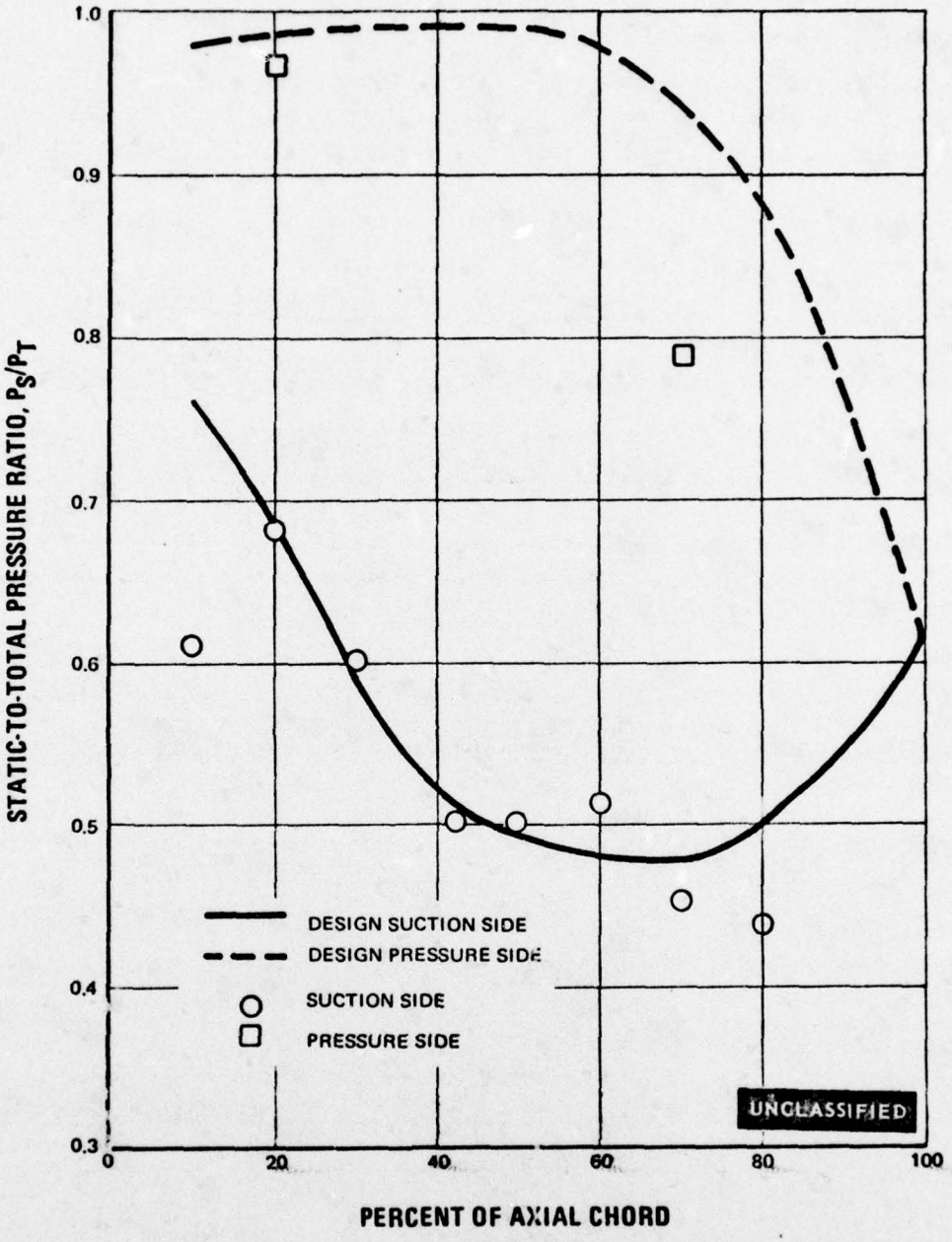

Figure 54 Static-to-Total Pressure Ratio Versus Percent Axial Chord, Second Vane, Medium Solidity, Mean Section

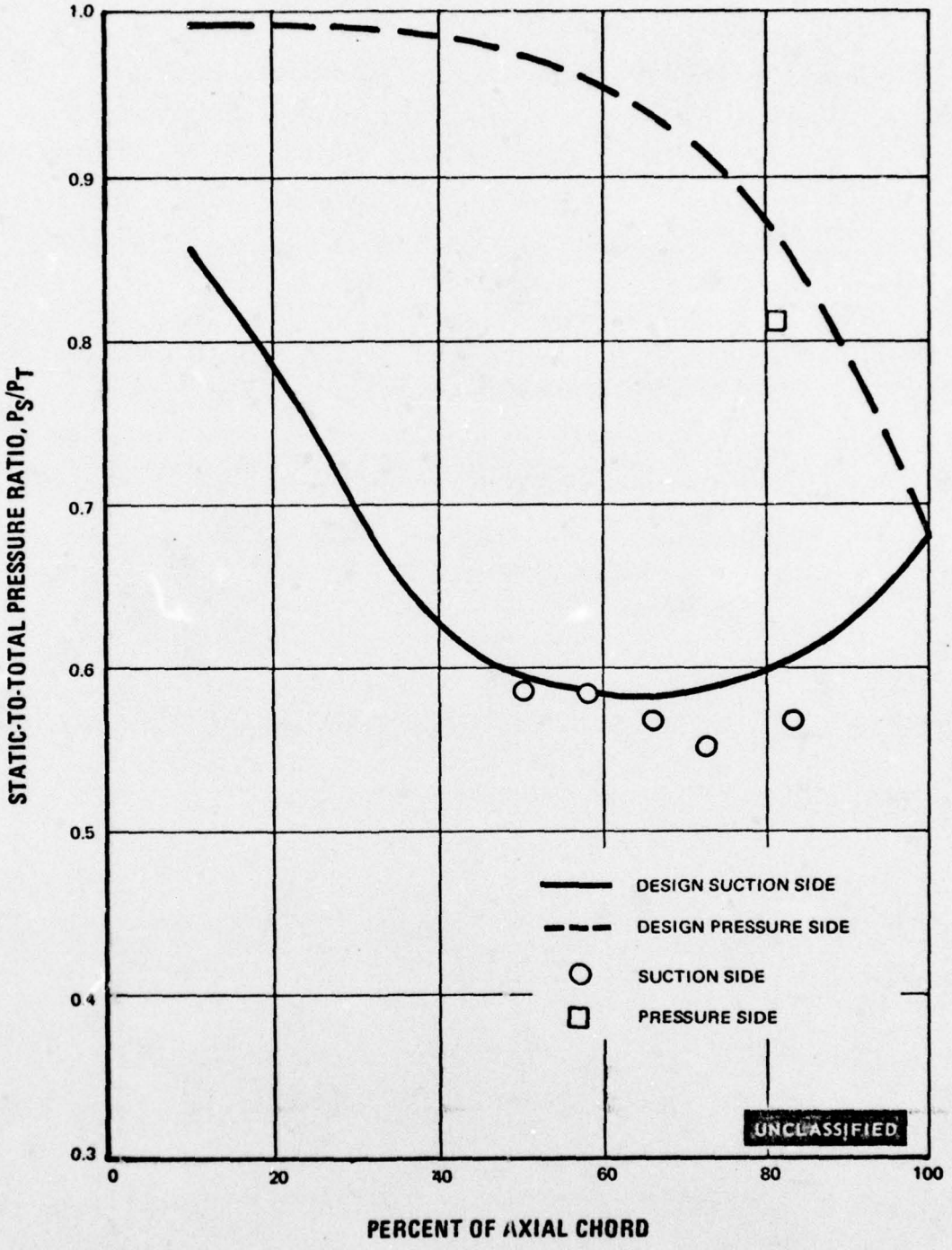

Figure 55 Static-to-Total Pressure Ratio Versus Percent Axial Chord, Second Vane, Medium Solidity, Tip Section

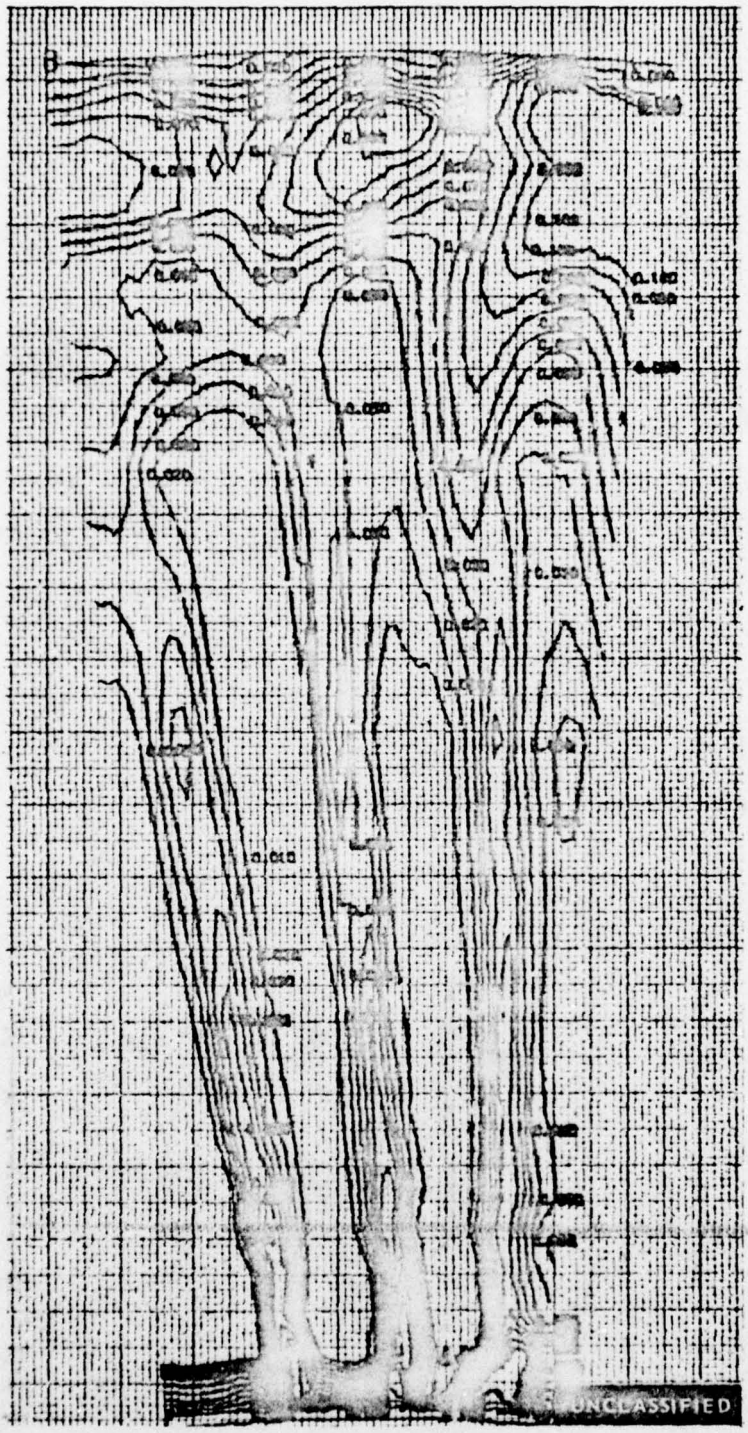

ΔPO/PO CONTOURS

Figure 56 Pressure Loss Contours, Second Blade Medium Solidity, Three Flow Passages, Midspan Exit Mach No. = 0.940

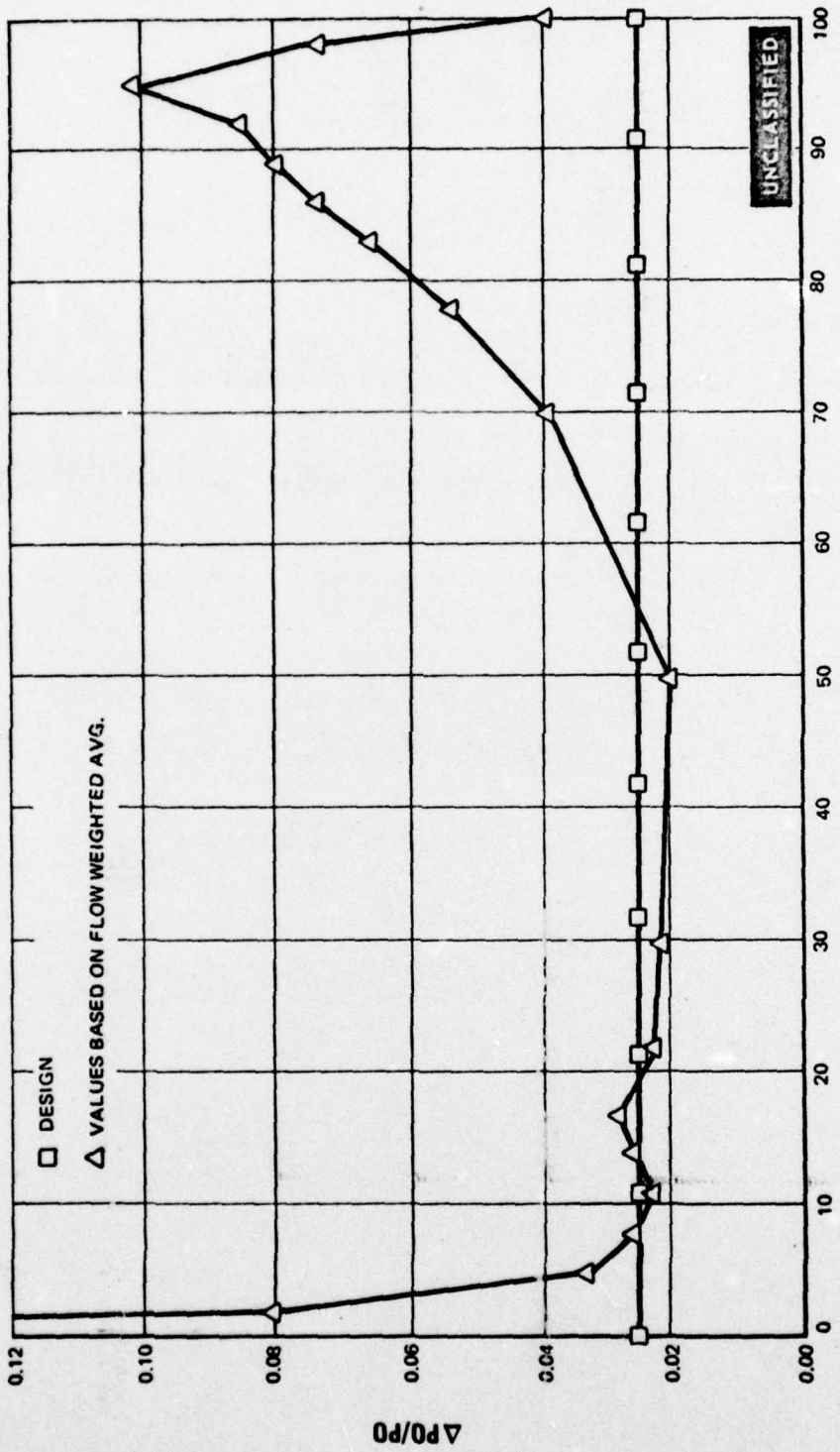

Figure 57 Spanwise Pressure Loss Distribution, Second Blade, Medium Solidity, Midspan Exit Mach No. = 0.940

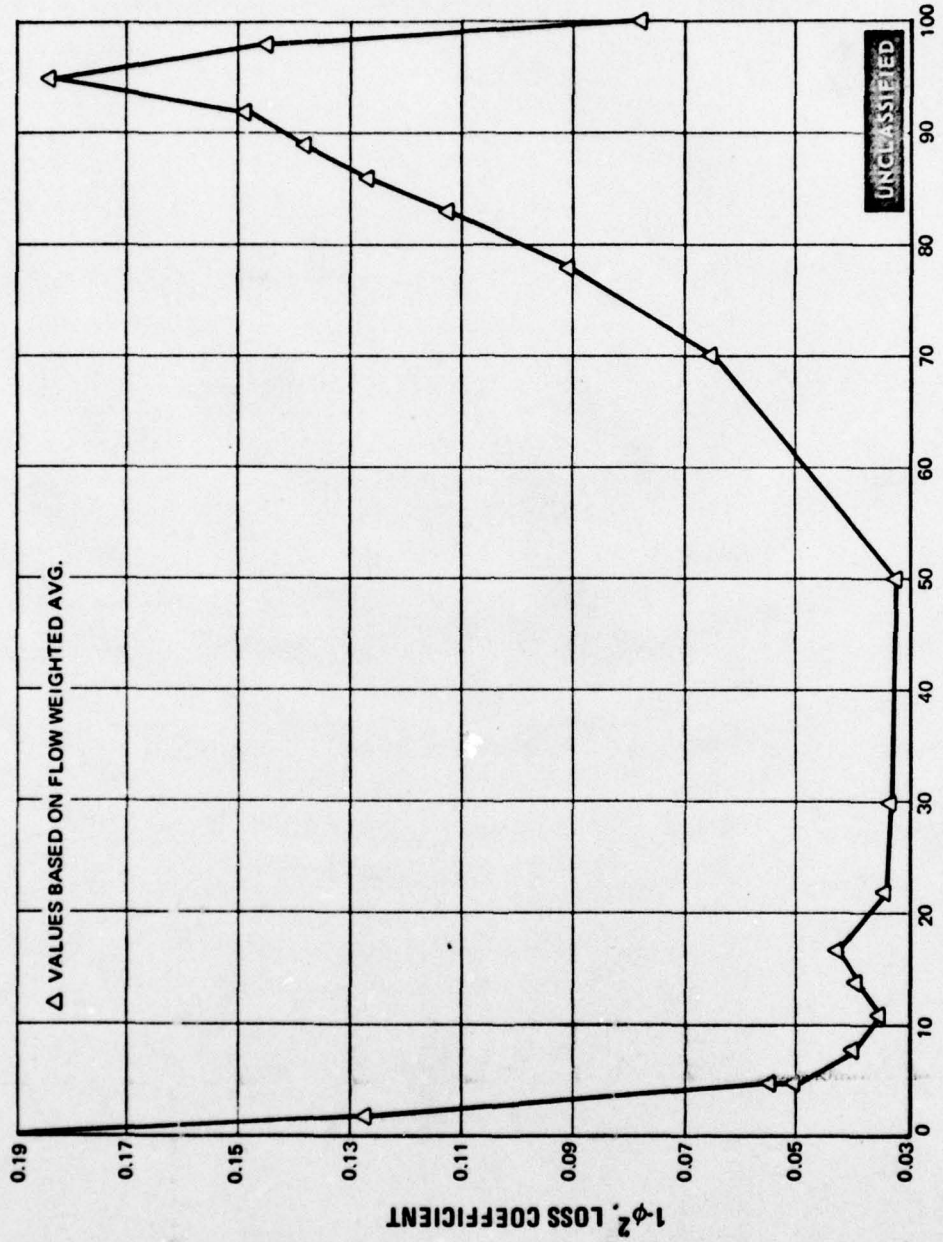

Figure 58 Spanwise Loss Coefficient Distribution, Second Blade, Medium Solidity, Midspan Exit Mach No. = 0.940

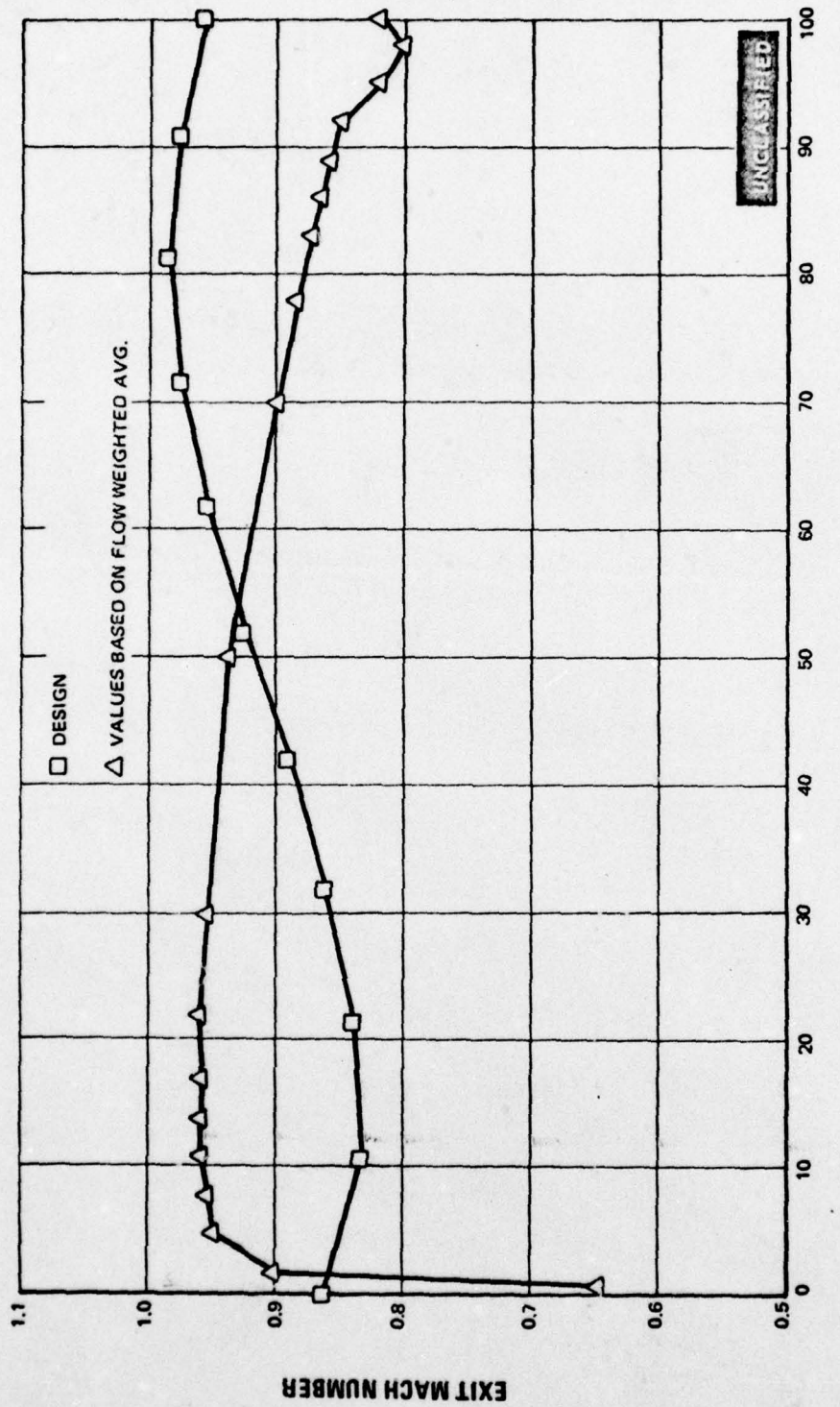

Figure 59 Spanwise Exit Mach Number Distribution, Second Blade, Medium Solidity, Midspan Exit Mach No. = 0.940

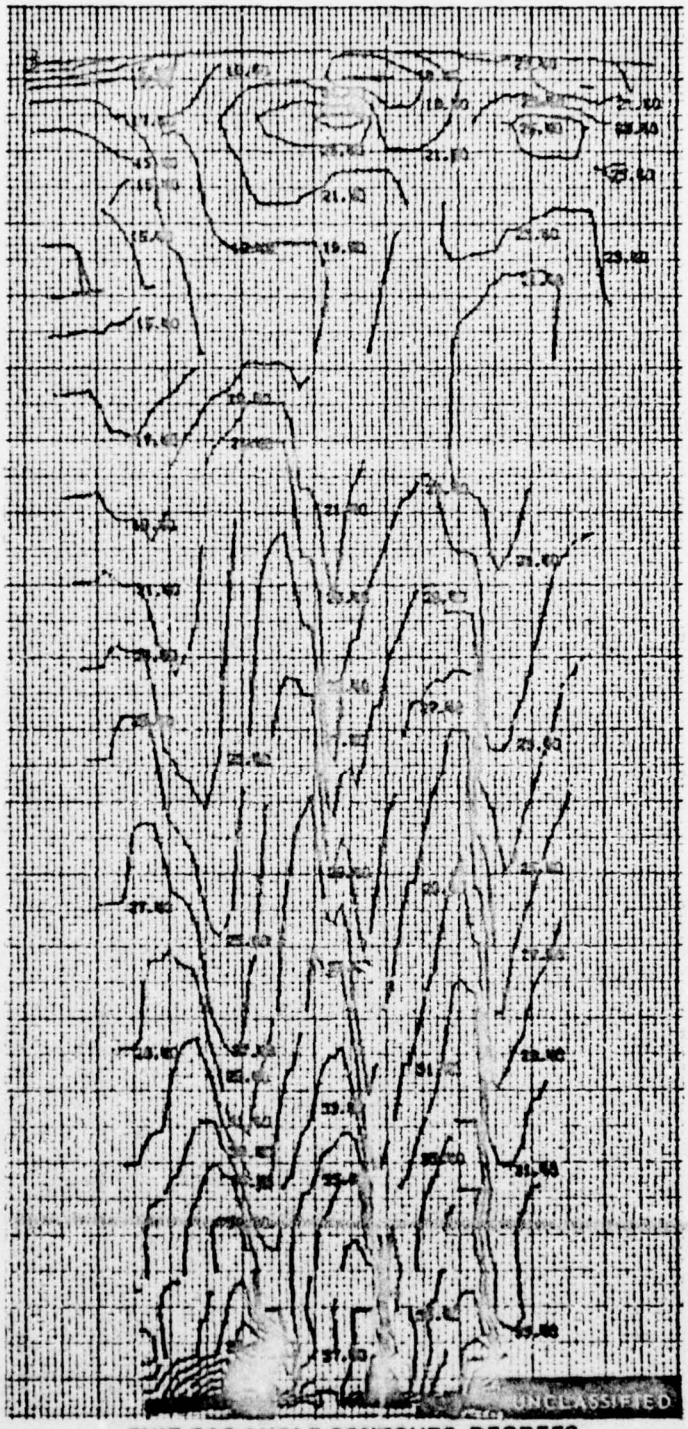

EXIT GAS ANGLE CONTOURS, DEGREES

Figure 60 Exit Gas Angle Contours, Second Blade, Medium Solidity, Three Flow Passages, Midspan Exit Mach No. = 0.940

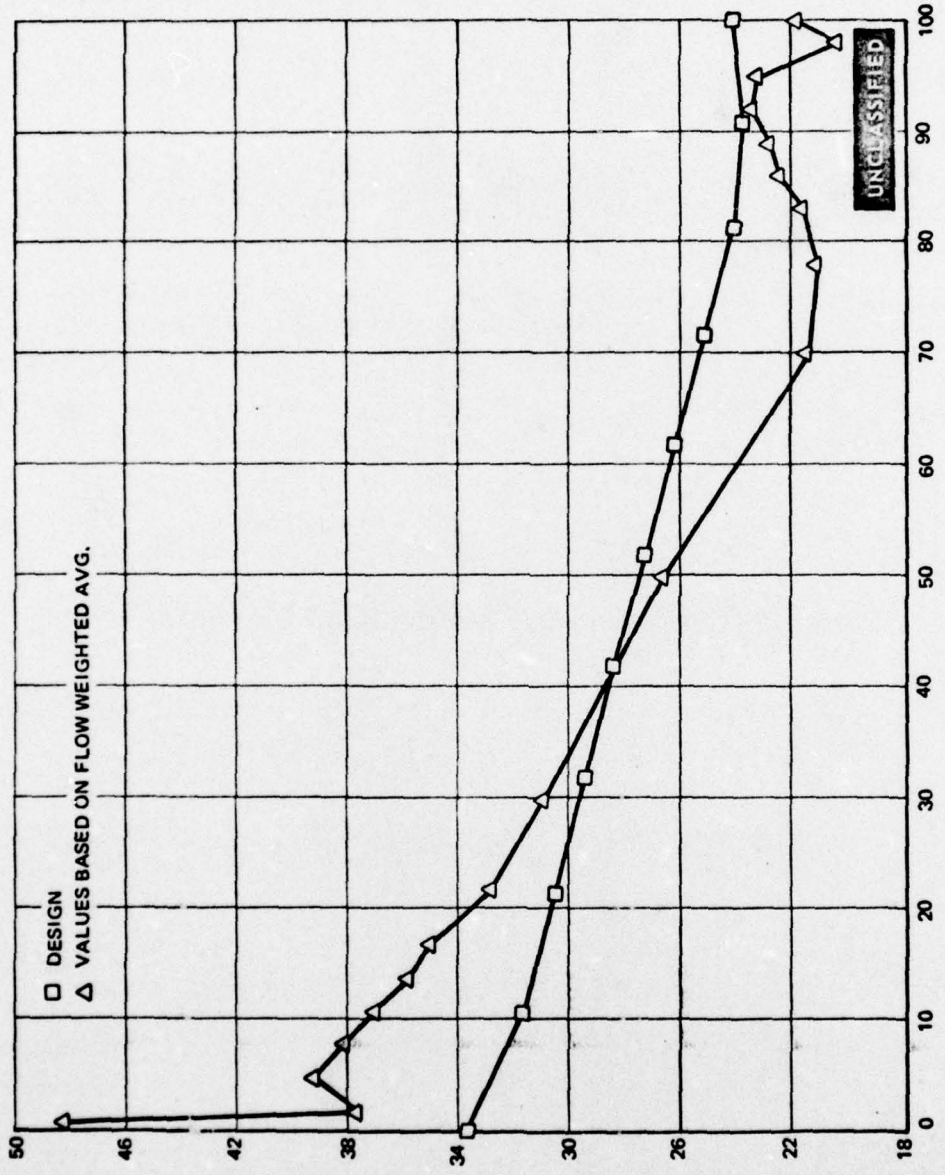

Figure 61 Spanwise Exit Gas Angle Distribution, Second Blade, Medium Solidity, Mid-span Exit Mach No. = 0.940

(U) The measured and predicted airfoil pressure distributions are shown in Figures 62, 63 and 64. From the data available it may be concluded that the mean section was performing as predicted. Although one data point agrees with prediction, the inlet angle profile gives evidence that the tip section was operating at positive incidence of at least 10 degrees and, therefore, the actual pressure distribution would show lower suction side values of P_s/P_t than predicted near the leading edge. The root section is unloaded relative to the prediction for the usual reasons.

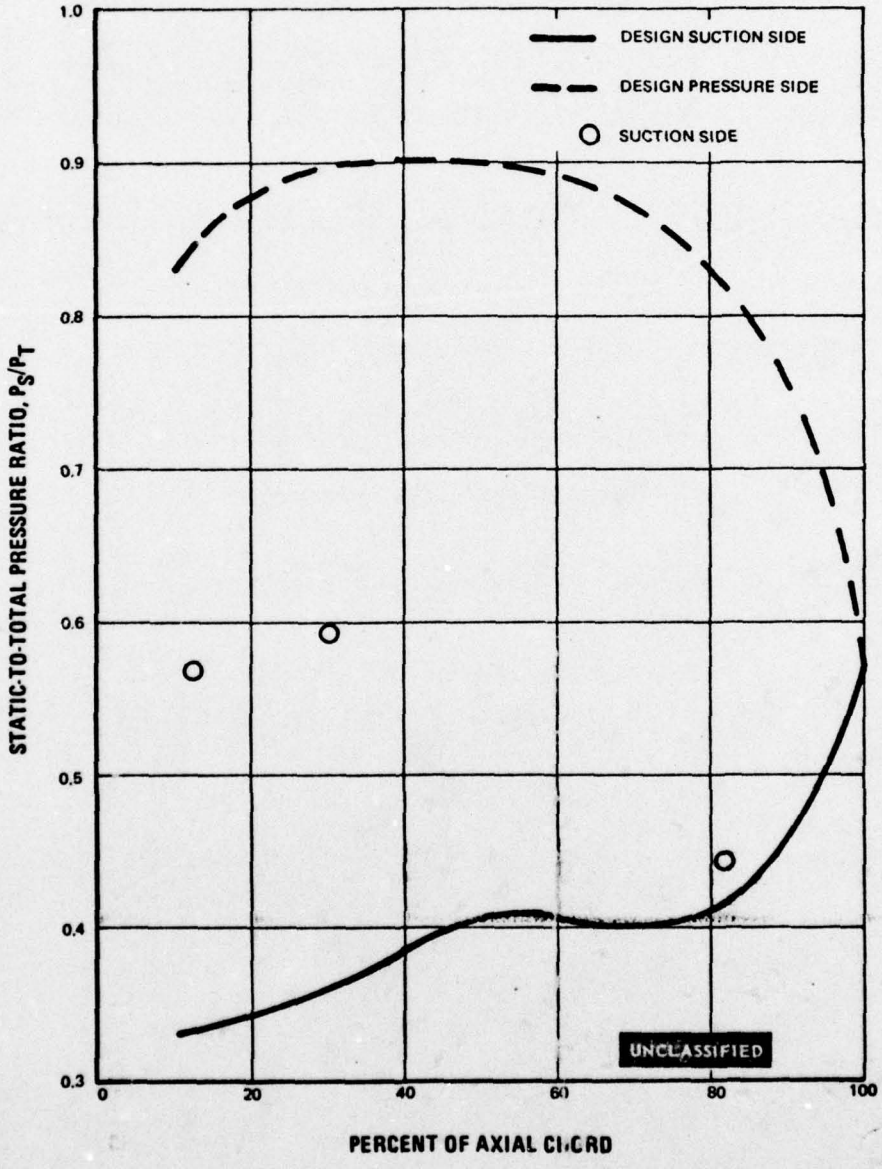

Figure 62 Static-to-Total Pressure Ratio Versus Percent Axial Chord, Second Blade, Medium Solidity, Root Section

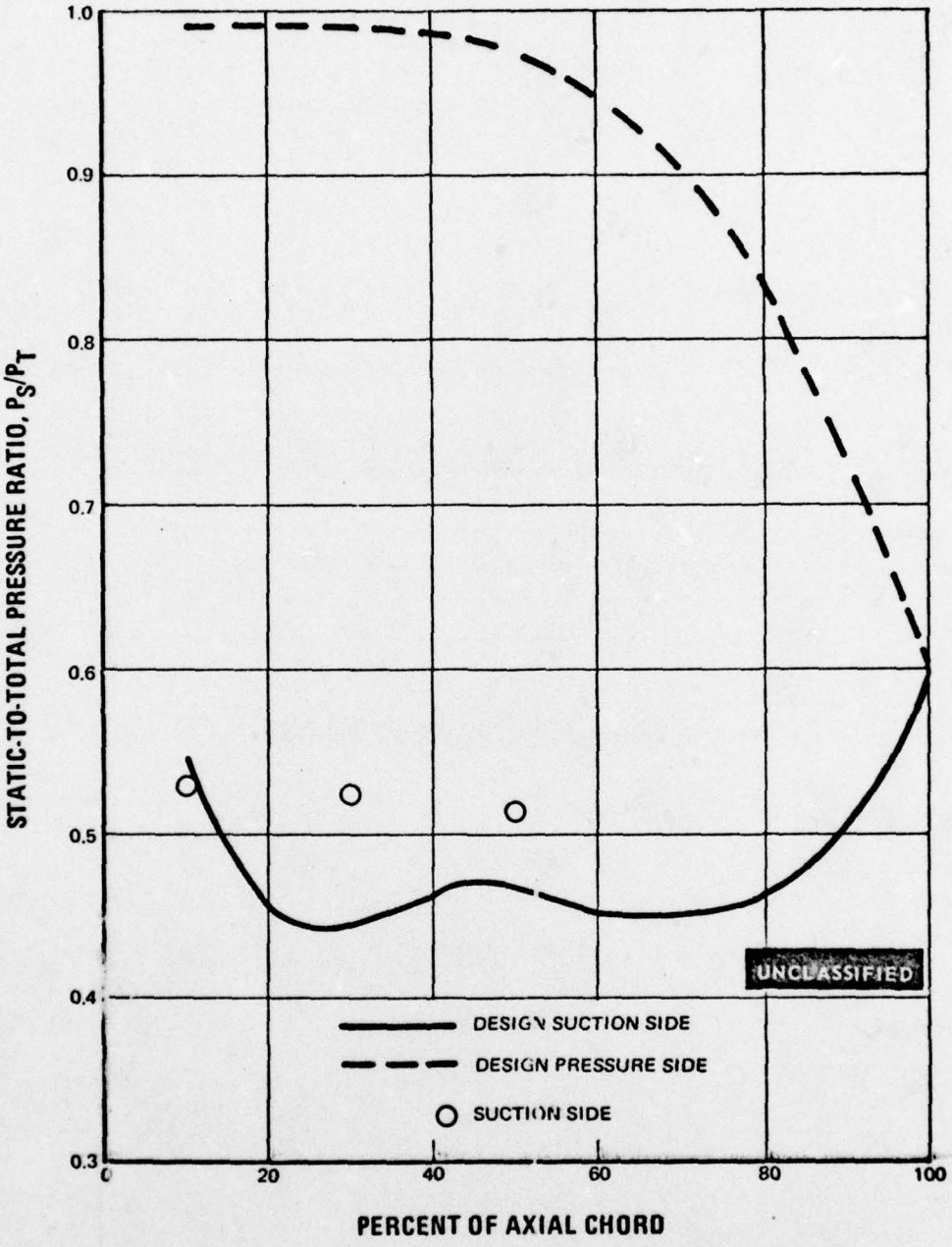

Figure 63 Static-to-Total Pressure Ratio Versus Percent Axial Chord, Second Blade, Medium Solidity, Mean Section

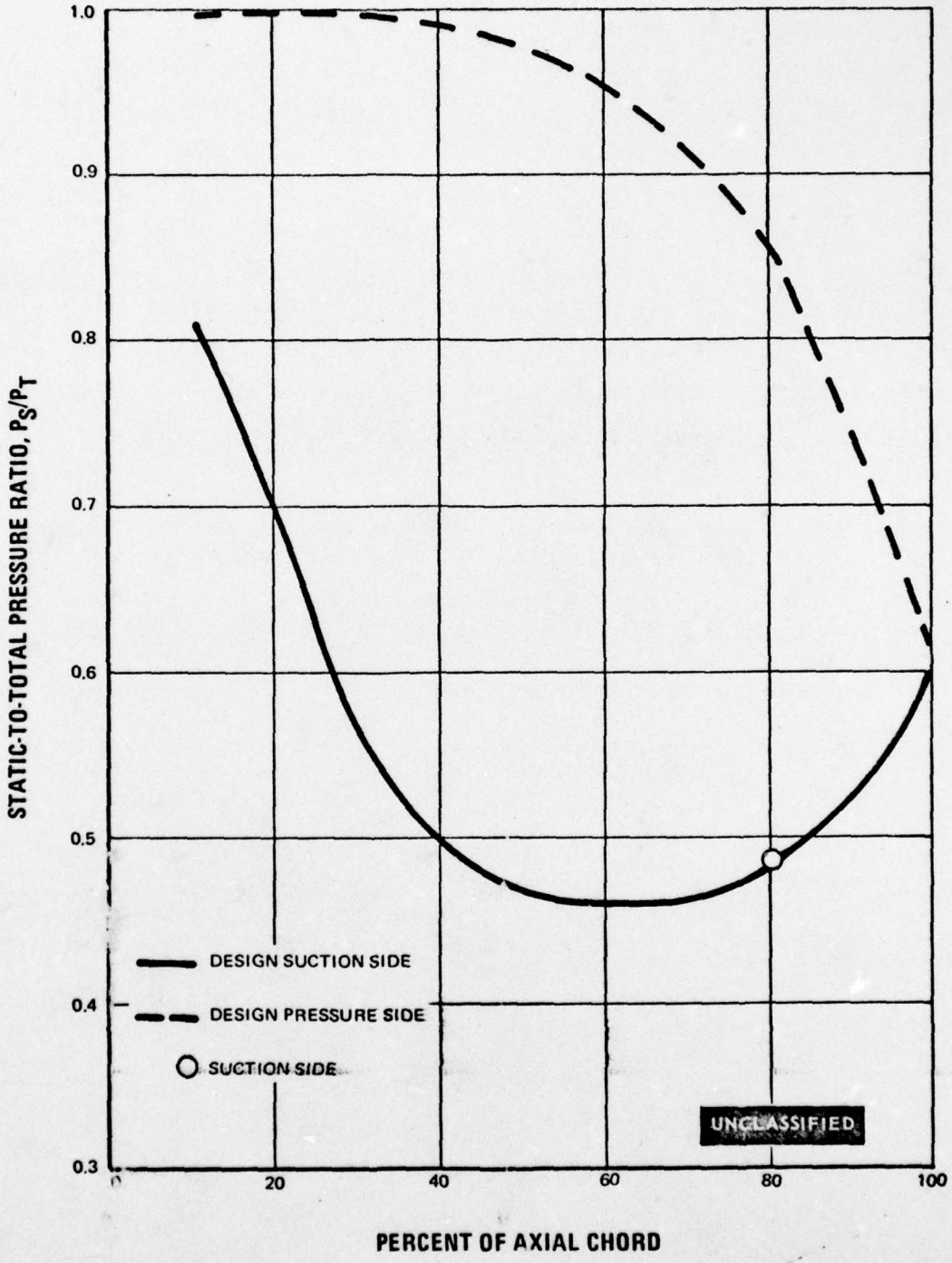

Figure 64 Static-to-Total Pressure Ratio Versus Percent Axial Chord, Second Blade, Medium Solidity, Tip Section

(U) A complete summary of the loss data taken on medium solidity airfoils for the various midspan Mach numbers and Reynolds numbers is shown in Table VI.

TABLE VI

SUMMARY OF TASK IId DATA - MEDIUM SOLIDITY AIRFOILS

Airfoil	Midspan Turbine Design M_2	Midspan Test M_2	Midspan Test Reynolds No. *Design	Midspan Test $1-\phi^2$	Flow Weighted Averages		
					Root To Mean Test $1-\phi^2$	Mean To Tip Test $1-\phi^2$	Overall Test $1-\phi^2$
First Vane	0.852	0.837	*4.38×10^5	0.031	0.051	0.050	0.051
		0.739	4.38×10^5	0.035	0.054	0.055	0.054
		0.941	4.38×10^5	0.031	0.040	0.044	0.042
		0.827	6.56×10^5	0.040	0.072	0.059	0.065
		0.814	2.19×10^5	0.047	0.079	0.068	0.073
		0.880	3.28×10^5	0.026	—	—	—
First Blade	0.788	0.774	*2.26×10^5	0.114	0.200	0.125	0.159
		0.671	2.26×10^5	0.120	0.191	0.145	0.167
		0.867	2.26×10^5	0.091	0.148	0.114	0.129
Second Vane	0.870	0.818	*2.95×10^5	0.123	0.085	0.214	0.157
		0.732	2.95×10^5	0.136	0.078	0.210	0.152
		0.915	2.95×10^5	0.121	0.86	0.202	0.150
Second Blade	0.904	0.935	*1.52×10^5	0.033	0.042	0.092	0.070
		0.839	1.52×10^5	0.033	0.037	0.103	0.075
		1.000	1.52×10^5	0.046	0.058	0.093	0.078

5. SUMMARY

(U) A comparison of the performance of the normal and medium solidity airfoils is included in this Section.

(U) The basic objective of Task IId was to evaluate the performance of cascades of lower solidity and higher load coefficient designed for similar aerodynamic inlet and exit conditions as the baseline normal solidity airfoils. With the completion of the medium solidity performance evaluation, a comparison of the performance of these two designs can be made. A summary of the measured and predicted loss coefficients for the normal and medium solidity designs at the turbine design point Mach number and Reynolds number is shown in Table VII. Based on this loss data and on the exit gas angle distributions reported previously, it can be concluded that the normal solidity designs are sufficiently superior to the medium solidity designs when compared under annular segment cascade conditions to justify their choice in the final turbine design.

TABLE VII

SUMMARY OF DESIGN POINT 1-ϕ^2 LOSS COEFFICIENTS FOR NORMAL AND MEDIUM SOLIDITY AIRFOILS

	Turbine Design Midspan Exit Mach No.	Midspan		Root To Mean Average	Mean To Tip Average	Overall Average
		Test	Predicted For Fully Turbulent Boundary Layer	Test	Test	Test
Normal Solidity First Vane	0.854	0.017 0.023*	0.031	0.029	0.035	0.034 0.032*
Medium Solidity First Vane	0.854	0.031	0.035	0.051	0.050	0.051
Normal Solidity First Blade	0.780	0.0266	0.049	0.0368	0.0433	0.040
Medium Solidity First Blade	0.780	0.114	0.043	0.200	0.125	0.159
Normal Solidity Second Vane	0.869	0.021 0.028*	0.034	0.0275	0.0325	0.030 0.034*
Medium Solidity Second Vane	0.869	0.123	0.034	0.085	0.214	0.157
Normal Solidity Second Blade	0.904	0.028	0.040	0.0322	0.0438	0.038
Medium Solidity Second Blade	0.904	0.033	0.046	0.042	0.092	0.070

* Inlet-Screen Installed

UNCLASSIFIED

(U) However, due to the transitional nature of the airfoil, evidenced by the very low profile losses of the normal solidity airfoils and the apparent importance of the effective free stream turbulence level shown by the inlet screen tests, it is not possible to make a definite conclusion concerning the relative performance of these designs in a rotating turbine. If the effective free stream turbulence level in the rotating turbine is sufficiently high to move the boundary layer transition further toward the airfoil leading edge on the suction side, it is expected that the profile losses on the normal solidity airfoils will approach the higher fully turbulent boundary layer predictions. For the medium solidity airfoils, this change in boundary layer transition could actually improve the performance, since a more turbulent boundary layer would have greater resistance to separation.

(U) It is recommended that the tests of the medium solidity airfoils are repeated under conditions for which the boundary layer is certain to be turbulent. Experience shows that the surest way to achieve this goal is by use of a suction surface trip wire. Such tests would not only be especially informative for this specific program, but would be of interest to all aerodynamic programs.

(The reverse of this page is blank)

SECTION V
BOUNDARY LAYER CONTROL OPTIMIZATION (TASK III a)

1. OBJECTIVE

(U) Determine the optimum geometry for the selected boundary layer control method.

2. TASK OBJECTIVE

(U) Three geometrical variations of the selected boundary layer control scheme were evaluated in an annular segment cascade on the second vane baseline airfoil. The purpose of these tests was to further investigate techniques for reducing end-wall losses. The selected scheme was local airfoil recambering, since after an experimental evaluation of (1) local recontouring (2) local recambering (3) end-wall contouring and (4) use of flow fences and application of increased surface roughness (Reference 4, Section V), this method proved to be most promising to diminish the end-wall losses.

(U) Each airfoil design was separately tested at the design incidence angle and Reynolds number and three Mach numbers near the design point. Exit surveys were made over the entire central passage containing the test airfoil in order to obtain loss coefficients and exit angle deviations. During these tests, oil and graphite flow visualization techniques were used to observe flow patterns on the airfoils.

(U) The task objectives were met and the geometry for the locally recambered airfoil which had the lowest end-wall losses was determined by:

- Reconstruction of the entire exit plane loss distribution for each scheme
- Reconstruction of the entire exit plane flow pattern for each scheme

(U) Analysis of this exit plane data revealed the high and low loss regions in the passages and the merits of each scheme were determined.

3. CASCADE AIRFOIL DESIGN

(U) Three geometrical variations of local recambering were applied to the second vane baseline airfoil. The design exit angle distributions are shown in Figure 65 for the three variations referred to as A, B, and C. The total integrated spanwise work was maintained constant at the baseline value for each recambering design. Included for comparison (Figure 65) are the exit gas angle distributions for the original baseline airfoil and the first local recambering (Task II c). The airfoil elevations of recambering designs A, B and C are presented in Figures 66, 67 and 68. The airfoil sections are presented in Figures 69 through 91, and the corresponding predicted airfoil surface pressure distributions, convergence and radius of curvature are presented in Figures 92 through 106. The fabrication coordinates for each of the sections for these three airfoils are

tabulated in the Appendix. For recambering design A they appear in Tables VIII through XV, for recambering design B in Tables XVI through XXIII and for recambering design C in Tables XXIV through XXXI. Such additional airfoil information as airfoil angles, gaging distance, airfoil area, axial chord, and uncovered turning is also tabulated therein.

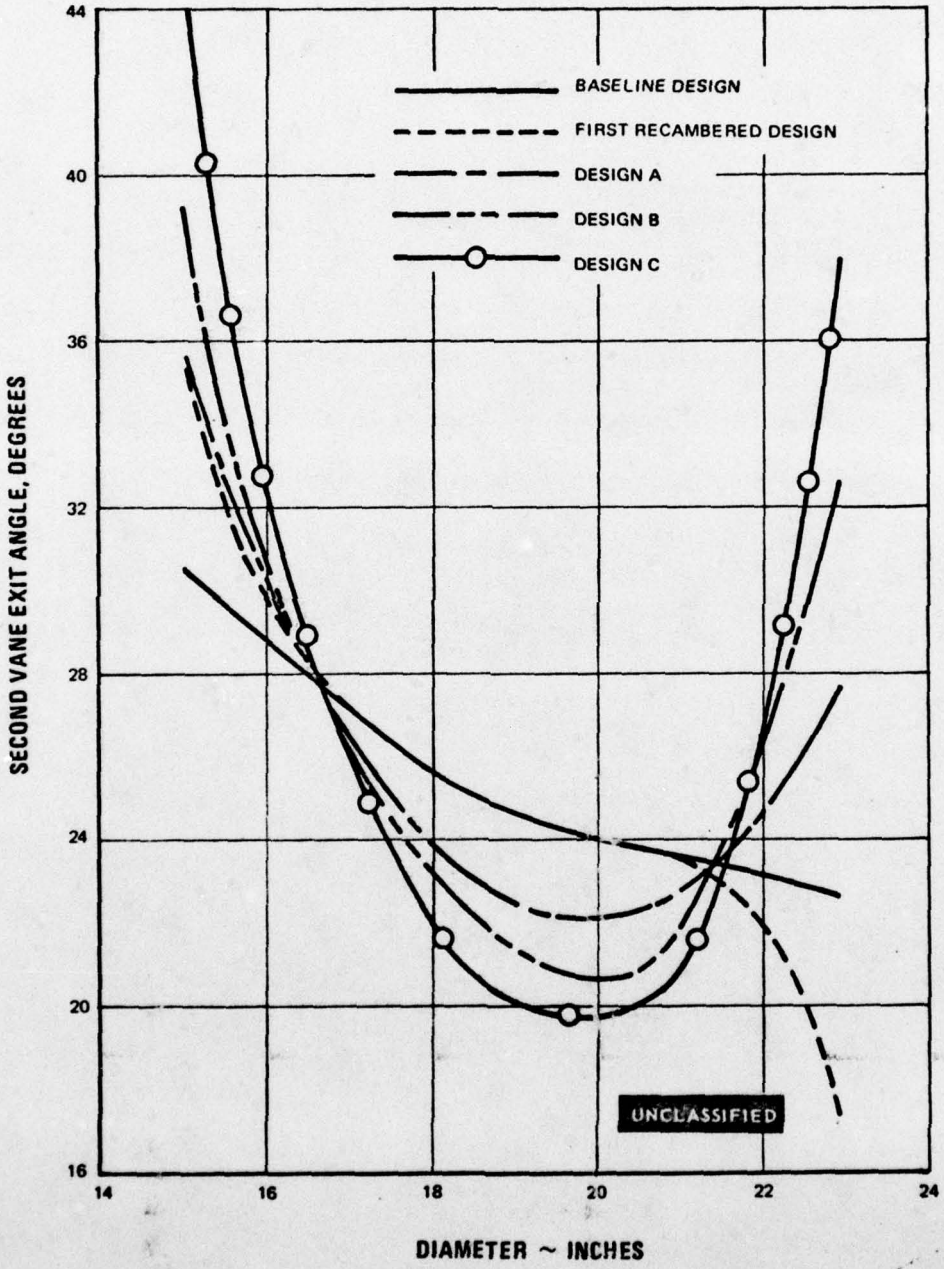

Figure 65 Second Vane Recambering Design Comparison

NOTE: ACTUAL AIRFOIL SHOULD BE EXTENDED TO R=11.945" (TIP EXTENDED SECTION, K–K) AND R=7.0" (ROOT EXTENDED SECTION, J–J). THE X AND Y DEFINING COORDINATES FOR THE TIP AND ROOT EXTENDED SECTIONS ARE THE SAME AS SECTIONS GG AND FF RESPECTIVELY.

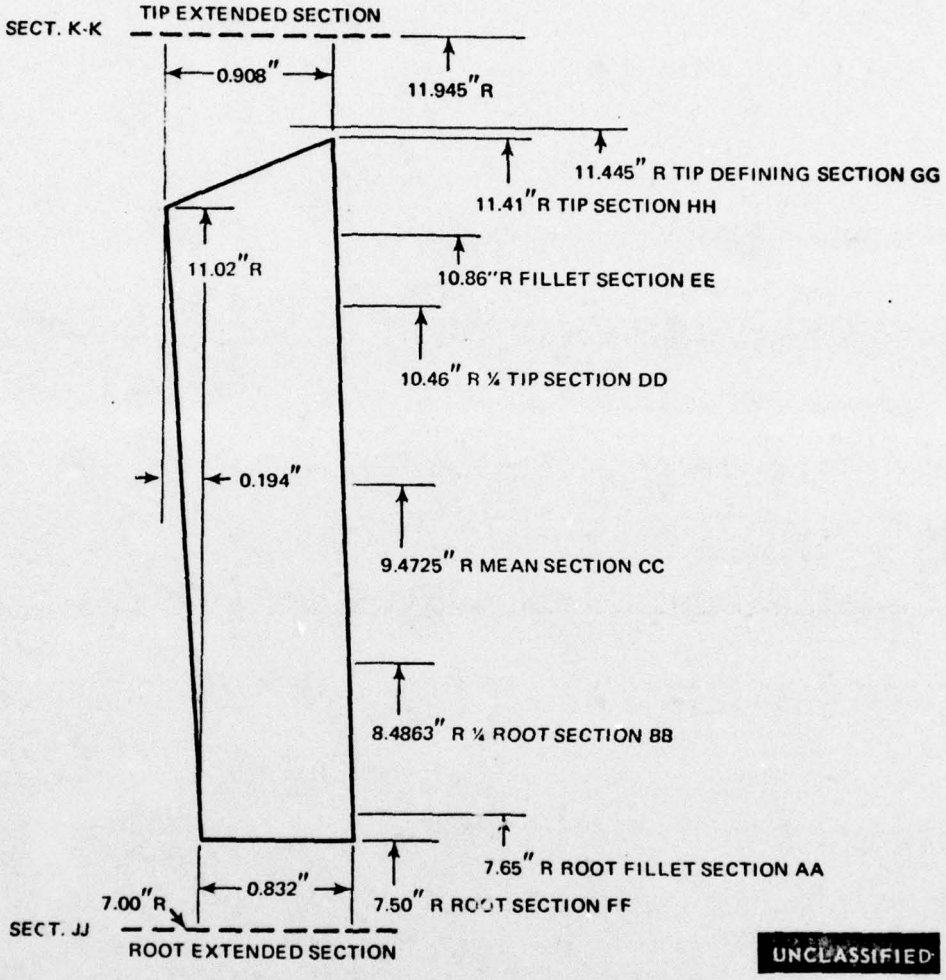

Figure 66 Elevation and Section Location of Second Vane, Recambering Design A

NOTE: CONSTANT SECTION EXISTS BETWEEN R=11.445 (TIP DEFINING SECTION) AND R=11.945 (TIP EXTENDED SECTION) CONSTANT SECTION EXISTS BETWEEN R=7.5 (ROOT SECTION) AND R=7.0 (ROOT EXTENDED SECTION).

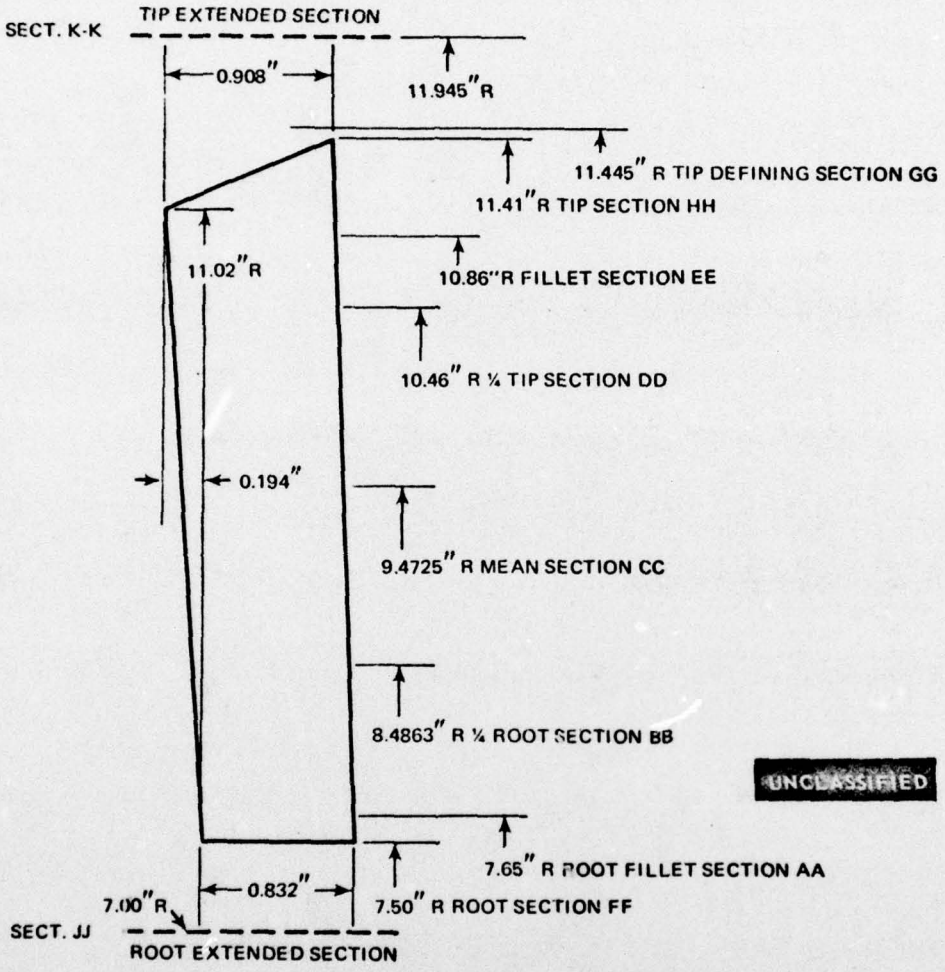

Figure 67 Elevation and Section Location of Second Vane, Recambering Design B

NOTE: CONSTANT SECTION EXISTS BETWEEN R=11.445 (TIP DEFINING SECTION) AND R=11.945 (TIP EXTENDED SECTION). CONSTANT SECTION EXISTS BETWEEN R=7.5 (ROOT SECTION) AND R=7.0 (ROOT EXTENDED SECTION).

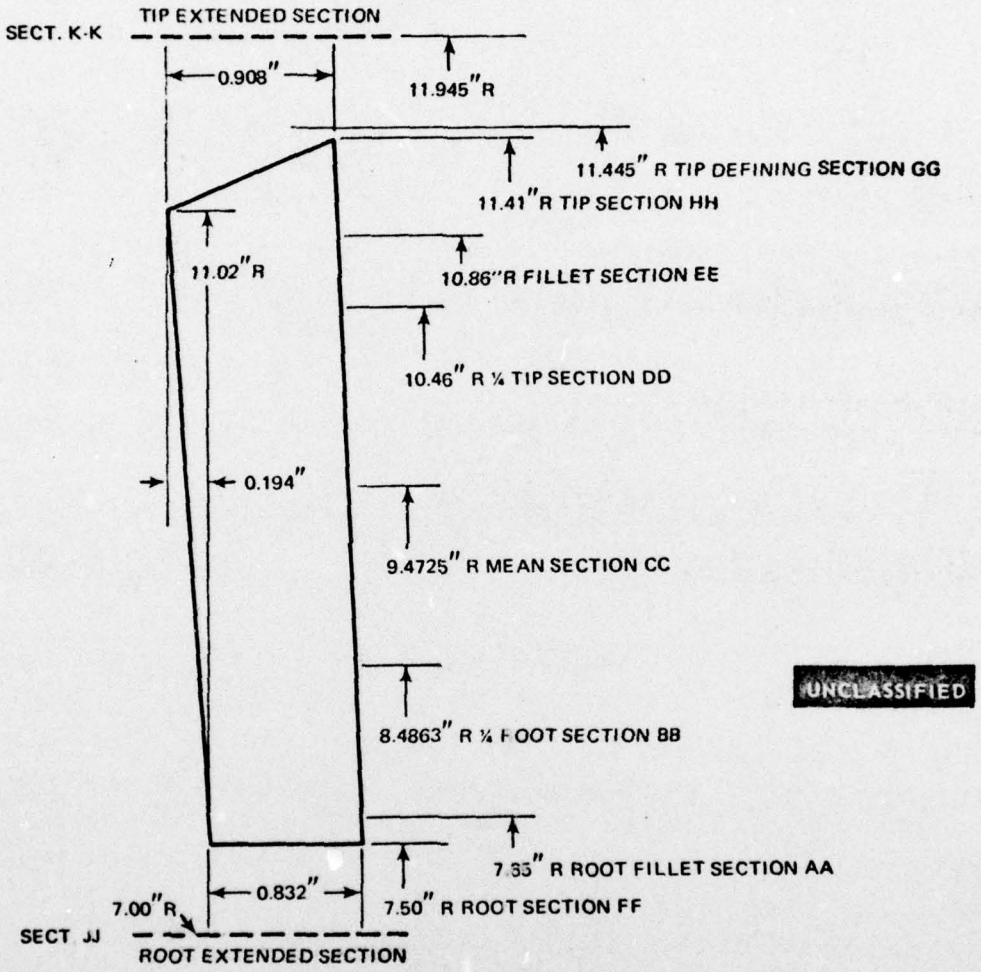

Figure 68 Elevation and Section Location of Second Vane, Recambering Design C

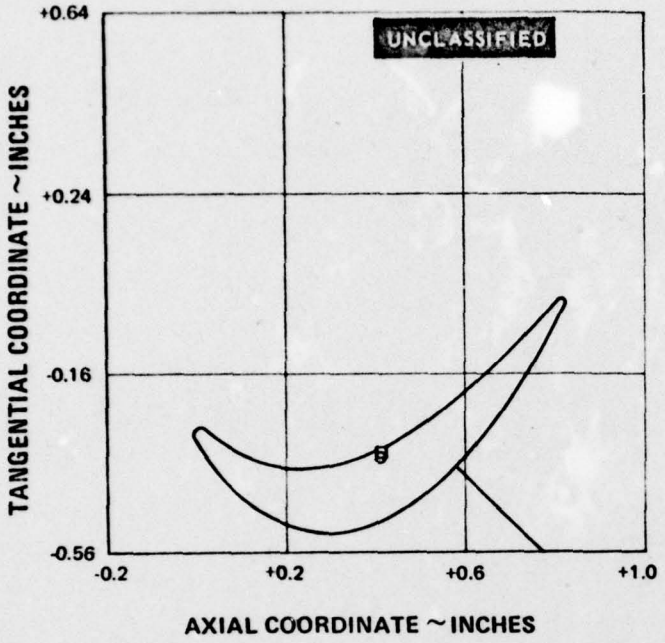

HOT DIMENSIONS

NUMBER OF FOILS	80.00	
DIAMETER	15.3000	IN.
GAGING	0.3240	IN.
PITCH	0.6008	IN.
AXIAL WIDTH	0.8357	IN.
BLADE INLET ANGLE	37.73	DEG.
GAS INLET ANGLE	38.00	DEG.
BLADE EXIT ANGLE	33.83	DEG.
GAS EXIT ANGLE	33.70	DEG.
GAGING ANGLE	32.63	DEG.
UNCOVERED TURNING	17.54	DEG.
PRINCIPAL AXIS	-24.29	DEG.
L. E. RADIUS	0.0179	IN.
T. E. RADIUS	0.0100	IN.
METAL AREA	0.1008	$IN.^2$

	X	Y
○ C.G.	0.4107	-0.3436
□ RADIAL REF. GAGE	0.4132 0.5788	-0.3347 -0.3650

Figure 69 Recambering Design A, Second Vane, Root Fillet Section (AA)

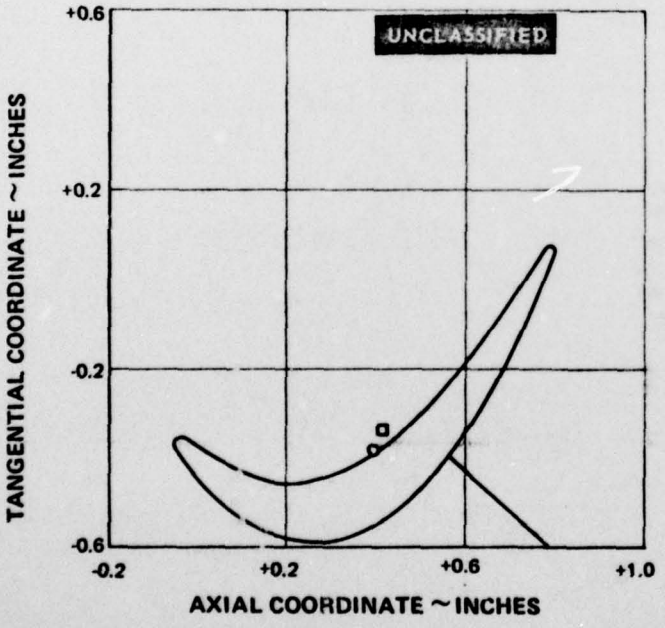

HOT DIMENSIONS

NUMBER OF FOILS	80.00	
DIAMETER	16.9726	IN.
GAGING	0.2969	IN.
PITCH	0.6665	IN.
AXIAL WIDTH	0.8565	IN.
BLADE INLET ANGLE	42.10	DEG
GAS INLET ANGLE	42.10	DEG
BLADE EXIT ANGLE	26.45	DEG
GAS EXIT ANGLE	26.45	DEG
GAGING ANGLE	26.45	DEG
UNCOVERED TURNING	18.49	DEG
PRINCIPAL AXIS	-32.60	DEG
L. E. RADIUS	0.0200	IN.
T. E. RADIUS	0.0100	IN.
METAL AREA	0.1073	$IN.^2$

	X	Y
○ C. G.	0.3939	-0.3812
□ RADIAL REF.	0.4132	-0.3347
GAGE	0.5531	-0.4044

Figure 70 Recambering Design A, Second Vane, 1/4 Root Section (BB)

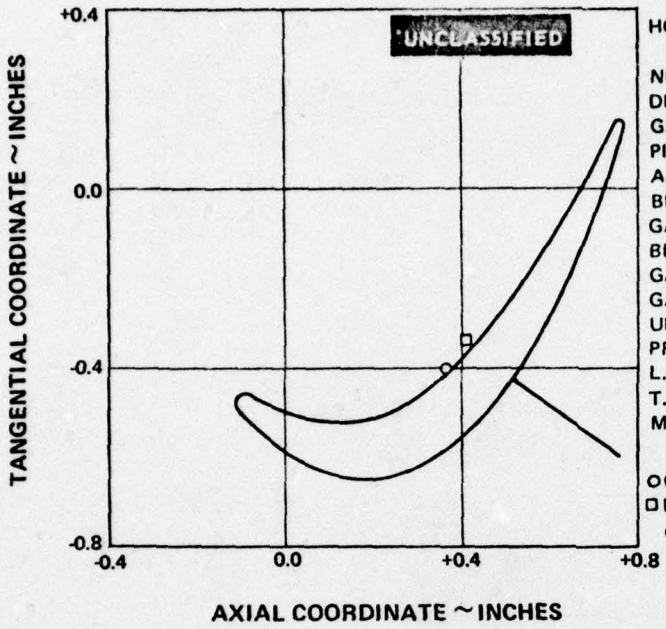

HOT DIMENSIONS		
NUMBER OF FOILS	80.00	
DIAMETER	18.9450	IN.
GAGING	0.2895	IN.
PITCH	0.7440	IN.
AXIAL WIDTH	0.8810	IN.
BLADE INLET ANGLE	50.50	DEG
GAS INLET ANGLE	50.50	DEG
BLADE EXIT ANGLE	22.50	DEG
GAS EXIT ANGLE	22.50	DEG
GAGING ANGLE	22.90	DEG
UNCOVERED TURNING	18.39	DEG
PRINCIPAL AXIS	-40.29	DEG
L. E. RADIUS	0.0225	IN.
T. E. RADIUS	0.0100	IN.
METAL AREA	0.1178	$IN.^2$
	X	Y
○ C. G.	0.3686	-0.3981
□ RADIAL REF.	0.4132	-0.3347
GAGE	0.5185	-0.4207

Figure 71 Recambering Design A, Second Vane, Mean Section (CC)

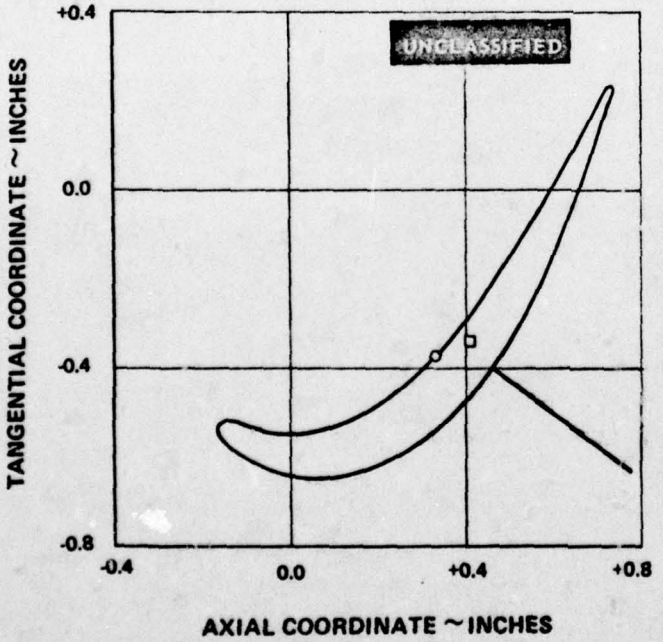

HOT DIMENSIONS		
NUMBER OF FOILS	80.00	
DIAMETER	20.9176	IN.
GAGING	0.8223	IN.
PITCH	0.8214	IN.
AXIAL WIDTH	0.9055	IN.
BLADE INLET ANGLE	57.40	DEG
GAS INLET ANGLE	57.40	DEG
BLADE EXIT ANGLE	22.75	DEG
GAS EXIT ANGLE	22.75	DEG
GAGING ANGLE	23.10	DEG
UNCOVERED TURNING	18.36	DEG
PRINICPAL AXIS	-44.14	DEG
L. E. RADIUS	0.0250	IN.
T. E. RADIUS	0.0100	IN.
METAL AREA	0.1190	$IN.^2$
	X	Y
○ C. G.	0.3340	-0.3648
□ RADIAL REF.	0.4132	-0.3347
GAGE	0.4646	-0.3958

Figure 72 Recambering Design A, Second Vane, 1/4 Tip Section (DD)

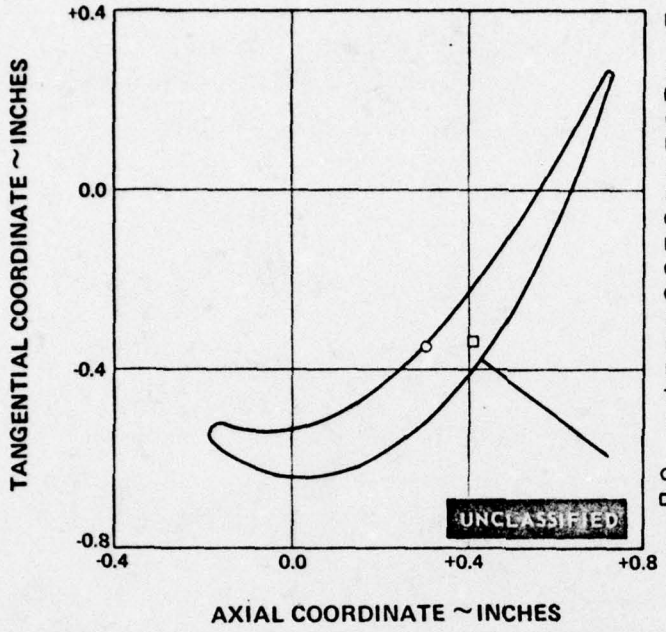

HOT DIMENSIONS

NUMBER OF FOILS	80.00	
DIAMETER	21.7200	IN.
GAGING	0.3519	IN.
PITCH	0.8529	IN.
AXIAL WIDTH	0.9155	IN.
BLADE INLET ANGLE	59.76	G
GAS INLET ANGLE	59.90	DEG
BLADE EXIT ANGLE	24.14	DEG
GAS EXIT ANGLE	24.05	DEG
GAGING ANGLE	24.37	DEG
UNCOVERED TURNING	17.22	DEG
PRINCIPAL AXIS	-44.92	DEG
L. E. RADIUS	0.0260	IN.
T. E. RADIUS	0.0100	IN.
METAL AREA	0.1220	$IN.^2$

	X	Y
○ C. G.	0.3059	-0.3455
□ RADIAL REF GAGE	0.4132	-0.3347
	0.4306	-0.3745

Figure 73 Recambering Design A, Second Vane, Fillet Section (EE)

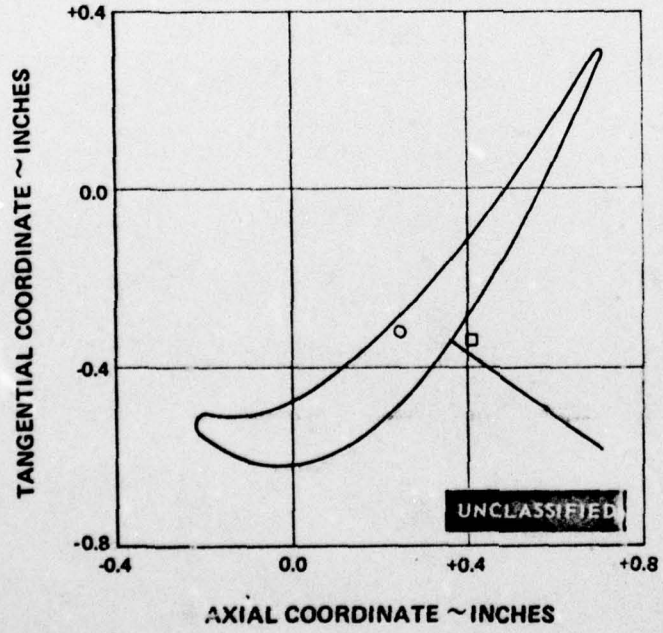

HOT DIMENSIONS

NUMBER OF FOILS	80.00	
DIAMETER	22.8200	IN.
GAGING	0.4060	IN.
PITCH	0.8961	IN.
AXIAL WIDTH	0.9291	IN.
BLADE INLET ANGLE	62.72	DEG
GAS INLET ANGLE	62.75	DEG
BLADE EXIT ANGLE	27.32	DEG
GAS EXIT ANGLE	27.30	DEG
GAGING ANGLE	26.94	DEG
UNCOVERED TURNING	12.84	DEG
PRINCIPAL AXIS	-45.64	DEG
L. E. RADIUS	0.0274	IN.
T. E. RADIUS	0.0100	IN.
METAL AREA	0.1311	$IN.^2$

	X	Y
○ C. G.	0.2515	-0.3179
□ RADIAL REF. GAGE	0.4132	-0.3347
	0.3681	-0.3444

Figure 74 Recambering Design A, Second Vane, Tip Section (HH)

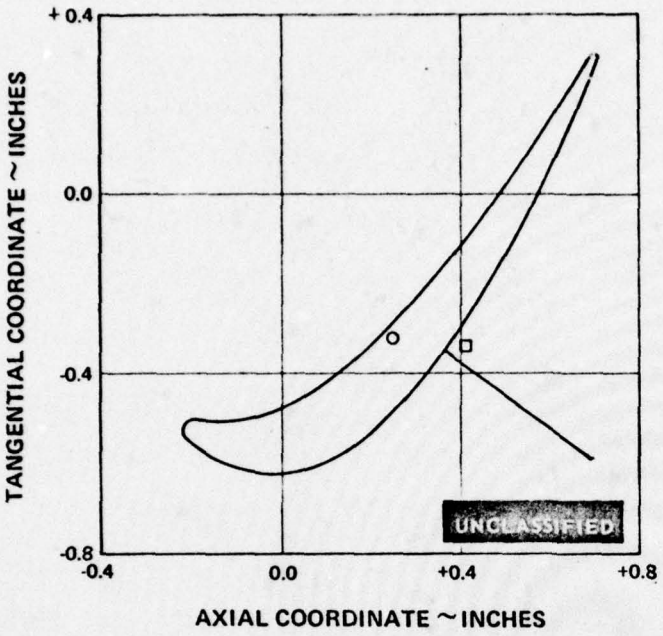

HOT DIMENSIONS

NUMBER OF FOILS	80.00	
DIAMETER	22.8900	IN.
GAGING	0.4098	IN.
PITCH	0.8989	IN.
AXIAL WIDTH	0.9300	IN.
BLADE INLET ANGLE	62.90	DEG
GAS INLET ANGLE	62.90	DEG
BLADE EXIT ANGLE	27.57	DEG
GAS EXIT ANGLE	27.57	DEG
GAGING ANGLE	27.12	DEG
UNCOVERED TURNING	12.47	DEG
PRINCIPAL AXIS	-45.68	DEG
L. E. RADIUS	0.0275	IN.
T. E. RADIUS	0.0100	IN.
METAL AREA	0.1319	$IN.^2$

	X	Y
○ C. G.	0.2475	-0.3161
□ RADIAL REF.	0.4132	-0.3347
GAGE	0.3633	-0.3431

Figure 75 Recambering Design A, Second Vane, Tip Defining Section (GG)

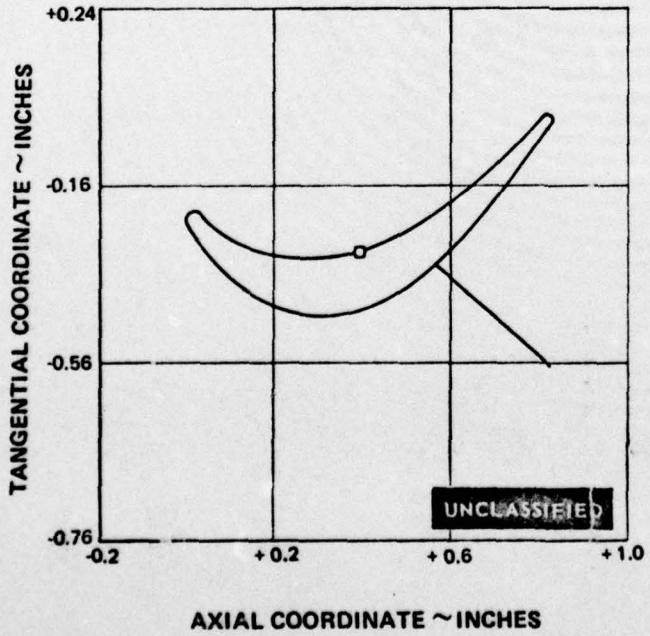

HOT DIMENSIONS

NUMBER OF FOILS	80.00	
DIAMETER	15.0000	IN.
GAGING	0.3552	IN.
PITCH	0.5890	IN.
AXIAL WIDTH	0.8320	IN.
BLADE INLET ANGLE	37.33	DEG
GAS INLET ANGLE	37.33	DEG
BLADE EXIT ANGLE	39.00	DEG
GAS EXIT ANGLE	39.00	DEG
GAGING ANGLE	37.08	DEG
UNCOVERED TURNING	10.65	DEG
PRINCIPAL AXIS	-17.11	DEG
L. E. RADIUS	0.0200	IN.
T. E. RADIUS	0.0100	IN.
METAL AREA	0.0817	$IN.^2$

	X	Y
○ C. G.	0.3924	-0.3113
□ RADIAL REF.	0.3924	-0.3113
GAGE	0.5738	-0.3312

Figure 76 Recambering Design B, Second Vane, Root Section (FF)

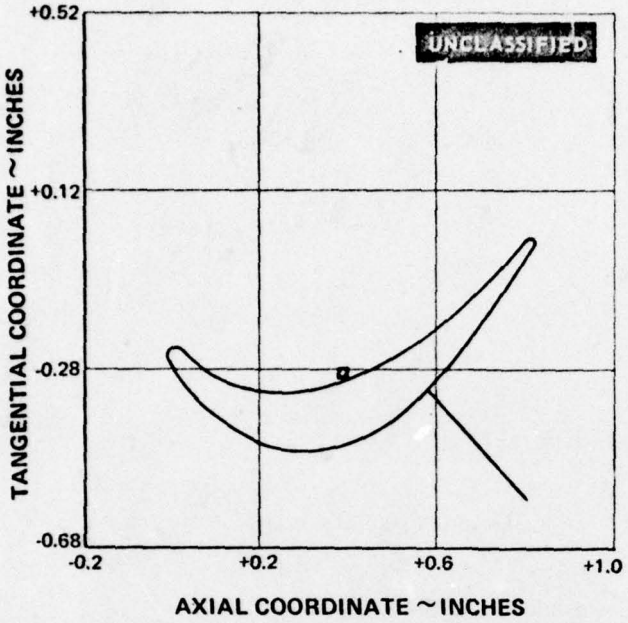

HOT DIMENSIONS

NUMBER OF FOILS	80.00	
DIAMETER	15.3000	IN.
GAGING	0.3432	IN.
PITCH	0.6008	IN.
AXIAL WIDTH	0.8357	IN.
BLADE INLET ANGLE	37.73	DEG
GAS INLET ANGLE	38.00	DEG
BLADE EXIT ANGLE	36.51	DEG
GAS EXIT ANGLE	35.60	DEG
GAGING ANGLE	34.83	DEG
UNCOVERED TURNING	12.02	DEG
PRINCIPAL AXIS	-19.37	DEG
L. E. RADIUS	0.0204	IN.
T. E. RADIUS	0.0100	IN.
METAL AREA	0.0880	$IN.^2$

	X	Y
○ C. G.	0.3938	-0.3225
□ RADIAL REF. GAGE	0.3924	-0.3113
	0.5720	-0.3448

Figure 77 Recambering Design B, Second Vane, Root Fillet Section (AA)

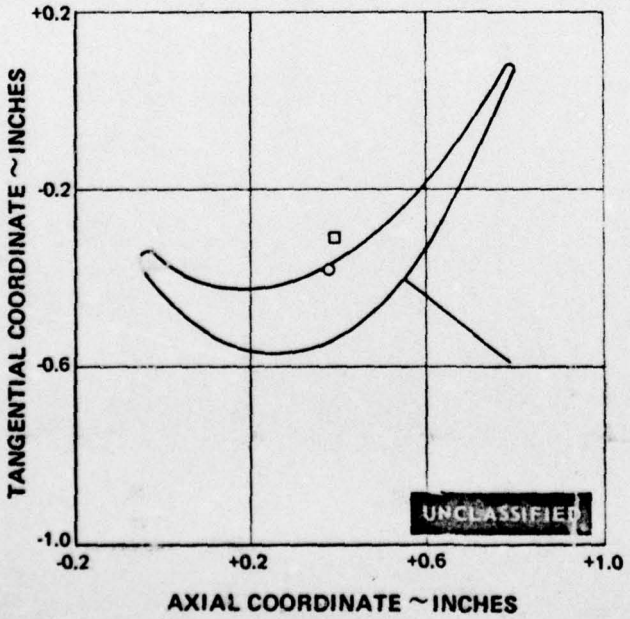

HOT DIMENSIONS

NUMBER OF FOILS	80.00	
DIAMETER	16.9726	IN.
GAGING	0.2953	IN.
PITCH	0.6665	IN.
AXIAL WIDTH	0.8565	IN.
BLADE INLET ANGLE	42.10	DEG
GAS INLET ANGLE	42.10	DEG
BLADE EXIT ANGLE	26.35	DEG
GAS EXIT ANGLE	26.35	DEG
GAGING ANGLE	26.30	DEG
UNCOVERED TURNING	15.10	DEG
PRINCIPAL AXIS	-30.14	DEG
L. E. RADIUS	0.0225	IN.
T. E. RADIUS	0.0100	IN.
METAL AREA	0.1100	$IN.^2$

	X	Y
○ C. G.	0.3802	-0.3847
□ RADIAL REF. GAGE	0.3924	-0.3113
	0.5532	-0.4068

Figure 78 Recambering Design B, Second Vane, 1/4 Root Section (BB)

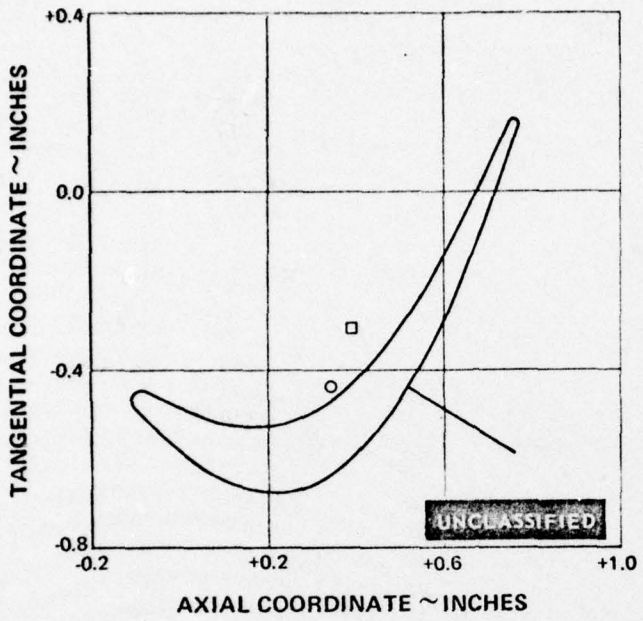

HOT DIMENSIONS

NUMBER OF FOILS	80.00	
DIAMETER	18.9450	IN.
GAGING	0.2763	IN.
PITCH	0.7440	IN.
AXIAL WIDTH	0.8810	IN.
BLADE INLET ANGLE	50.50	DEG
GAS INLET ANGLE	50.50	DEG
BLADE EXIT ANGLE	21.40	DEG
GAS EXIT ANGLE	21.40	DEG
GAGING ANGLE	21.80	DEG
UNCOVERED TURNING	13.72	DEG
PRINCIPAL AXIS	-39.91	DEG
L. E. RADIUS	0.0250	IN.
T. E. RADIUS	0.0100	IN.
METAL AREA	0.1138	$IN.^2$

	X	Y
○ C. G.	0.3454	-0.4429
□ RADIAL REF. GAGE	0.3924	-0.3113
	0.5188	-0.4440

Figure 79 Recambering Design B, Second Vane, Mean Section (CC)

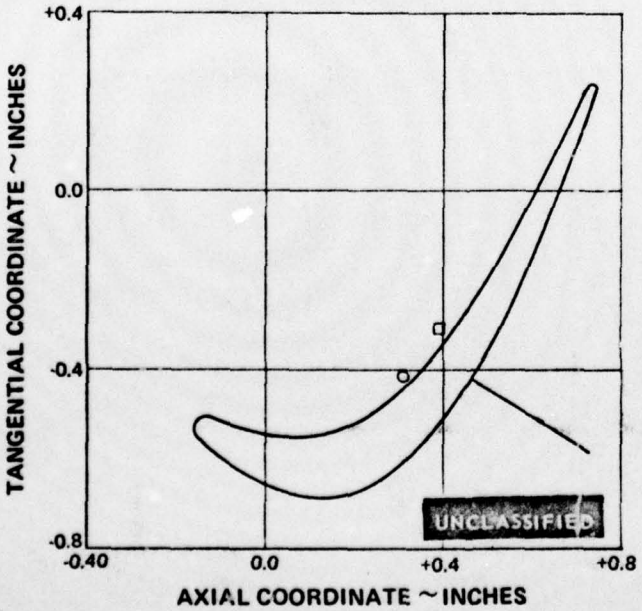

HOT DIMENSIONS

NUMBER OF FOILS	80.00	
DIAMETER	20.9176	IN.
GAGING	0.8077	IN.
PITCH	0.8214	IN.
AXIAL WIDTH	0.9055	IN.
BLADE INLET ANGLE	57.40	DEG
GAS INLET ANGLE	57.40	DEG
BLADE EXIT ANGLE	21.65	DEG
GAS EXIT ANGLE	21.65	DEG
GAGING ANGLE	22.00	DEG
UNCOVERED TURNING	13.71	DEG
PRINCIPAL AXIS	-44.72	DEG
L. E. RADIUS	0.0275	IN.
T. E. RADIUS	0.0100	IN.
METAL AREA	0.1183	$IN.^2$

	X	Y
○ C. G.	0.3085	-0.4201
□ RADIAL REF. GAGE	0.3924	-0.3113
	0.4621	-0.4255

Figure 80 Recambering Design B, Second Vane, 1/4 Tip Section (DD)

AD-A050 537 PRATT AND WHITNEY AIRCRAFT GROUP EAST HARTFORD CONN F/G 21/5
INVESTIGATION OF A HIGHLY LOADED TWO-STAGE FAN-DRIVE TURBINE. V--ETC(U)
JUN 70 H WELNA, D E DAHLBERG, W H HEISER F33615-68-C-1208
UNCLASSIFIED PWA-3967 AFAPL-TR-69-92-VOL-5 NL

2 OF 3
AD
AD50537

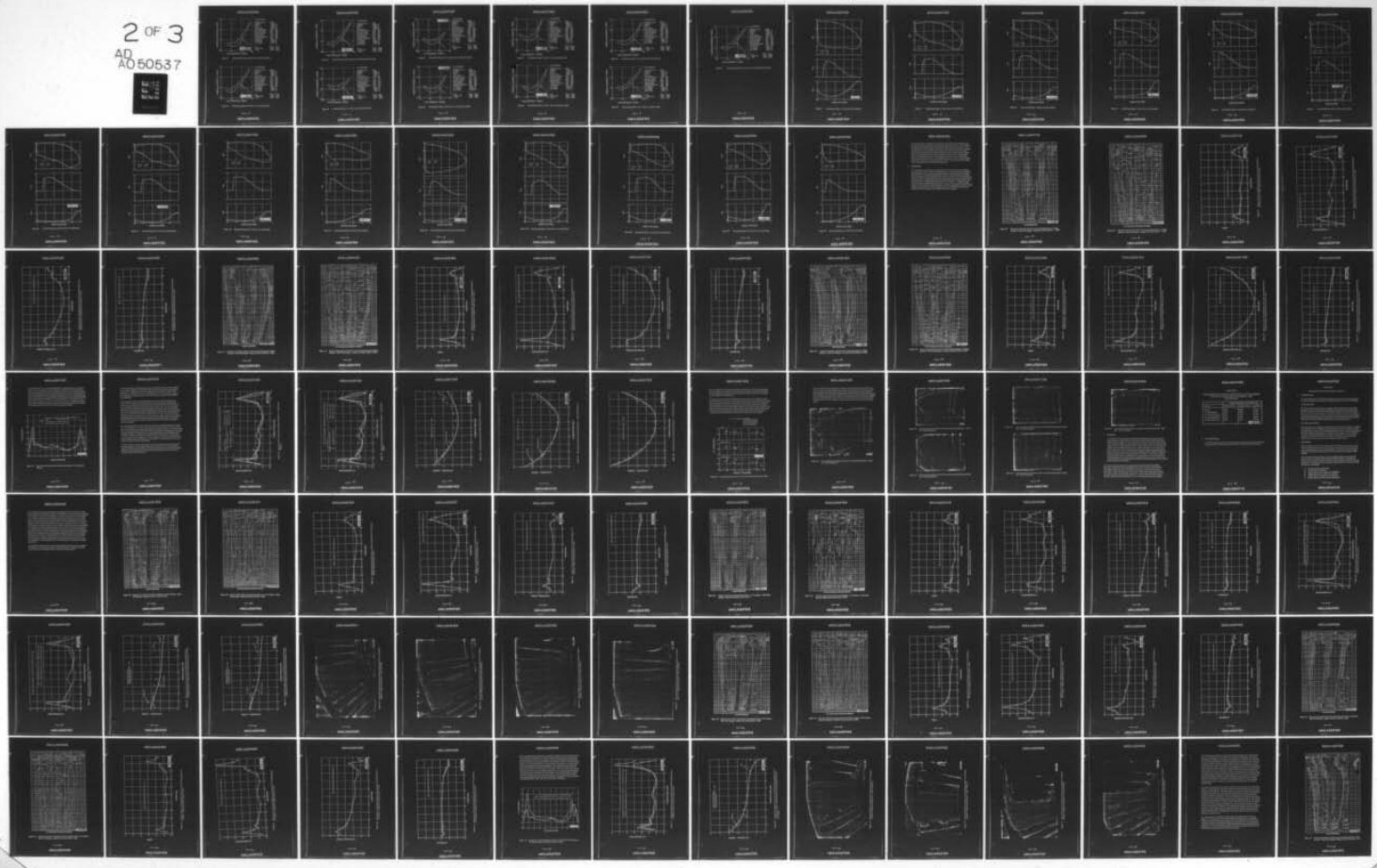

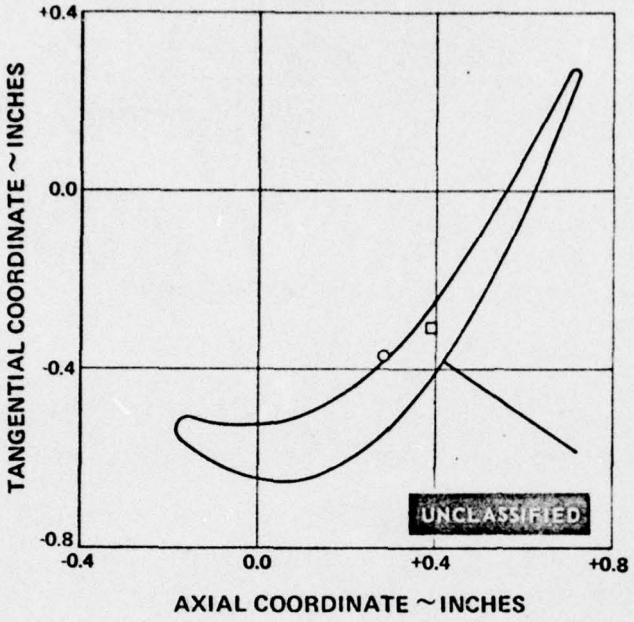

HOT DIMENSIONS

NUMBER OF FOILS	80.00	
DIAMETER	21.7200	IN.
GAGING	0.3521	IN.
PITCH	0.8529	IN.
AXIAL WIDTH	0.9155	IN.
BLADE INLET ANGLE	59.76	DEG
GAS INLET ANGLE	59.90	DEG
BLADE EXIT ANGLE	24.60	DEG
GAS EXIT ANGLE	25.10	DEG
GAGING ANGLE	24.38	DEG
UNCOVERED TURNING	13.46	DEG
PRINCIPAL AXIS	-45.03	DEG
L. E. RADIUS	0.0285	IN.
T. E. RADIUS	0.0100	IN.
METAL AREA	0.1167	$IN.^2$

	X	Y
○ C. G.	0.2854	-0.3740
□ RADIAL REF. GAGE	0.3924	-0.3113
	0.4210	-0.3877

Figure 81 Recambering Design B, Second Vane, Fillet Section (EE)

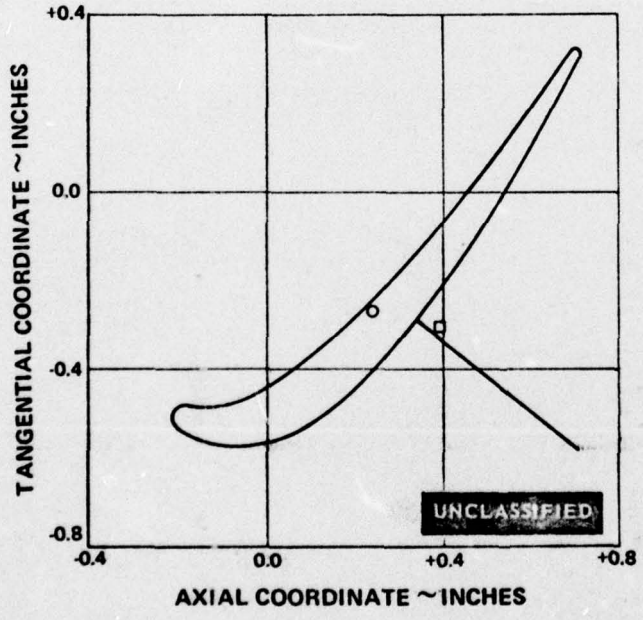

HOT DIMENSIONS

NUMBER OF FOILS	80.00	
DIAMETER	22.8200	IN.
GAGING	0.4598	IN.
PITCH	0.8961	IN.
AXIAL WIDTH	0.9291	IN.
BLADE INLET ANGLE	62.72	DEG
GAS INLET ANGLE	62.75	DEG
BLADE EXIT ANGLE	31.97	DEG
GAS EXIT ANGLE	32.20	DEG
GAGING ANGLE	30.87	DEG
UNCOVERED TURNING	10.93	DEG
PRINCIPAL AXIS	-44.94	DEG
L. E. RADIUS	0.0299	IN.
T. E. RADIUS	0.0100	IN.
METAL AREA	0.1087	$IN.^2$

	X	Y
○ C. G.	0.2401	-0.2759
□ RADIAL REF. GAGE	0.3924	-0.3113
	0.3379	-0.2955

Figure 82 Recambering Design B, Second Vane, Tip Section (HH)

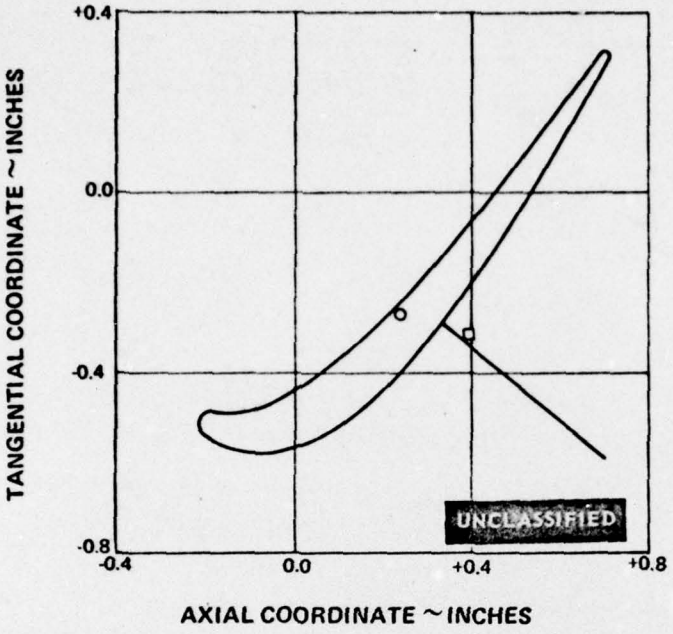

HOT DIMENSIONS

NUMBER OF FOILS	80.00	
DIAMETER	22.8900	IN.
GAGING	0.4687	IN.
PITCH	0.8989	IN.
AXIAL WIDTH	0.9300	IN.
BLADE INLET ANGLE	62.90	DEG
GAS INLET ANGLE	62.90	DEG
BLADE EXIT ANGLE	32.57	DEG
GAS EXIT ANGLE	32.57	DEG
GAGING ANGLE	31.43	DEG
UNCOVERED TURNING	10.58	DEG
PRINCIPAL AXIS	-44.96	DEG
L. E. RADIUS	0.0300	IN.
T. E. RADIUS	0.0100	IN.
METAL AREA	0.1079	$IN.^2$

	X	Y
○ C. G.	0.2365	-0.2683
□ RADIAL REF. GAGE	0.3924	-0.3113
	0.3312	-0.2881

Figure 83 Recambering Design B, Second Vane, Tip Defining Section (GG)

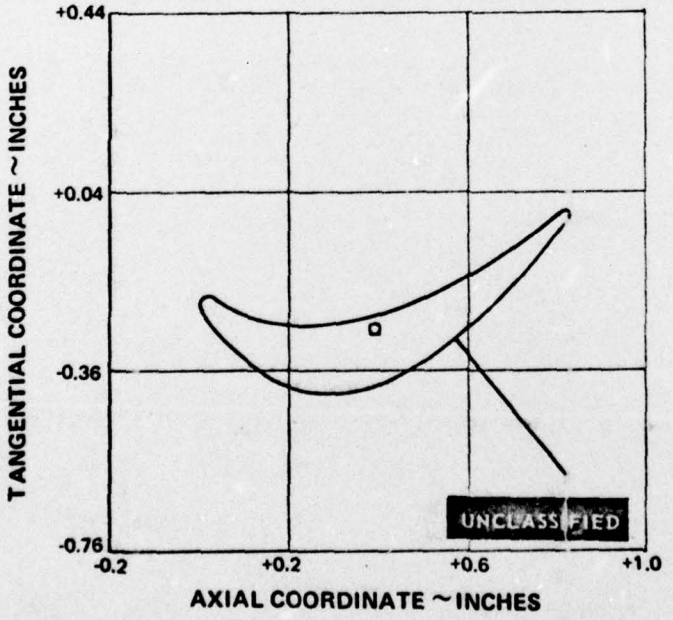

HOT DIMENSIONS

NUMBER OF FOILS	80.00	
DIAMETER	15.0000	IN.
GAGING	0.3860	IN.
PITCH	0.5890	IN.
AXIAL WIDTH	0.8320	IN.
BLADE INLET ANGLE	37.33	DEG
GAS INLET ANGLE	37.33	DEG
BLADE EXIT ANGLE	44.00	DEG
GAS EXIT ANGLE	44.00	DEG
GAGING ANGLE	40.94	DEG
UNCOVERED TURNING	12.06	DEG
PRINCIPAL AXIS	-16.36	DEG
L. E. RADIUS	0.0200	IN.
T. E. RADIUS	0.0100	IN.
METAL AREA	0.0931	$IN.^2$

	X	Y
○ C. G.	0.3919	-0.2691
□ RADIAL REF. GAGE	0.3919	-0.2691
	0.5732	-0.2910

Figure 84 Recambering Design C, Second Vane, Root Section (FF)

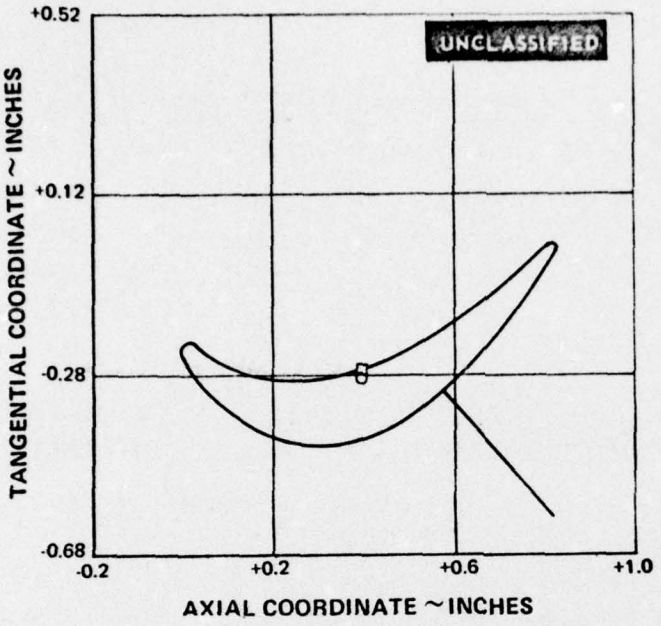

HOT DIMENSIONS		
NUMBER OF FOILS	80.00	
DIAMETER	15.3000	IN.
GAGING	0.3659	IN.
PITCH	0.6008	IN.
AXIAL WIDTH	0.8357	IN.
BLADE INLET ANGLE	37.73	DEG
GAS INLET ANGLE	38.00	DEG
BLADE EXIT ANGLE	40.32	DEG
GAS EXIT ANGLE	39.50	DEG
GAGING ANGLE	37.51	DEG
UNCOVERED TURNING	13.58	DEG
PRINCIPAL AXIS	-17.91	DEG
L. E. RADIUS	0.0204	IN.
T. E. RADIUS	0.0100	IN.
METAL AREA	0.0948	$IN.^2$

	X	Y
○ C. G.	0.3932	-0.2887
□ RADIAL REF.	0.3919	-0.2691
GAGE	0.5704	-0.3154

Figure 85 Recambering Design C, Second Vane, Root Fillet Section (AA)

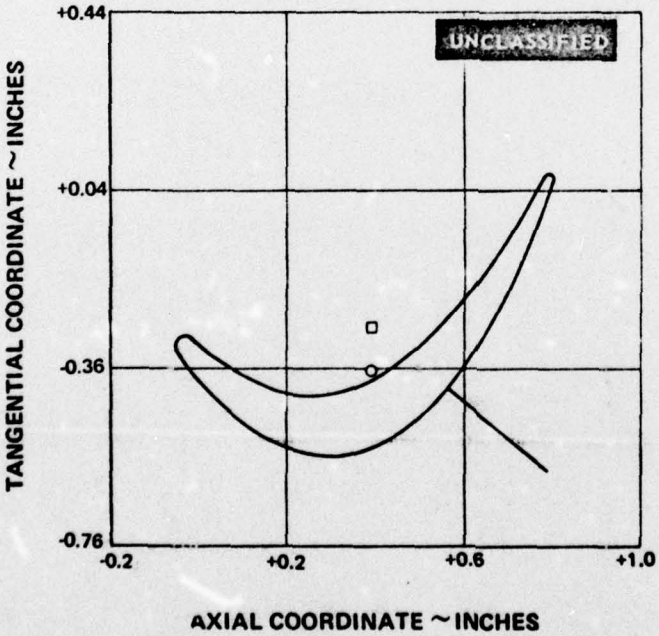

HOT DIMENSIONS		
NUMBER OF FOILS	80.00	
DIAMETER	16.9726	IN.
GAGING	0.2911	IN.
PITCH	0.6665	IN.
AXIAL WIDTH	0.8565	IN.
BLADE INLET ANGLE	42.10	DEG
GAS INLET ANGLE	42.10	DEG
BLADE EXIT ANGLE	25.95	DEG
GAS EXIT ANGLE	25.95	DEG
GAGING ANGLE	25.90	DEG
UNCOVERED TURNING	18.18	DEG
PRINCIPAL AXIS	-27.28	DEG
L. E. RADIUS	0.0225	IN.
T. E. RADIUS	0.0100	IN.
METAL AREA	0.1053	$IN.^2$

	X	Y
○ C. G.	0.3893	-0.3661
□ RADIAL REF.	0.3919	-0.2691
GAGE	0.5594	-0.4057

Figure 86 Recambering Design C, Second Vane, 1/4 Root Section (BB)

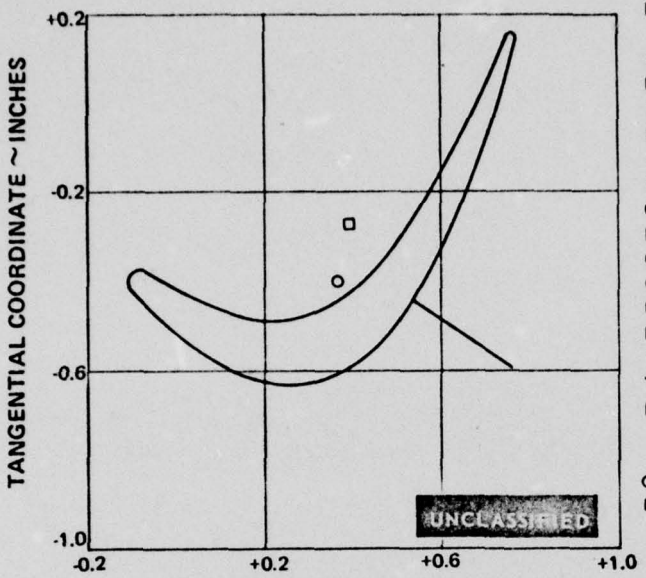

HOT DIMENSIONS

NUMBER OF FOILS	80.00	
DIAMETER	18.9450	IN.
GAGING	0.2620	IN.
PITCH	0.7440	IN.
AXIAL WIDTH	0.8810	IN.
BLADE INLET ANGLE	50.50	DEG
GAS INLET ANGLE	50.50	DEG
BLADE EXIT ANGLE	20.10	DEG
GAS EXIT ANGLE	20.10	DEG
GAGING ANGLE	20.62	DEG
UNCOVERED TURNING	18.18	DEG
PRINCIPAL AXIS	-35.89	DEG
L. E. RADIUS	0.0250	IN.
T. E. RADIUS	0.0100	IN.
METAL AREA	0.1192	IN^2

	X	Y
○ C. G.	0.3649	-0.4037
□ RADIAL REF. GAGE	0.3919	-0.2691
	0.5362	-0.4434

Figure 87 Recambering Design C, Second Vane, Mean Section (CC)

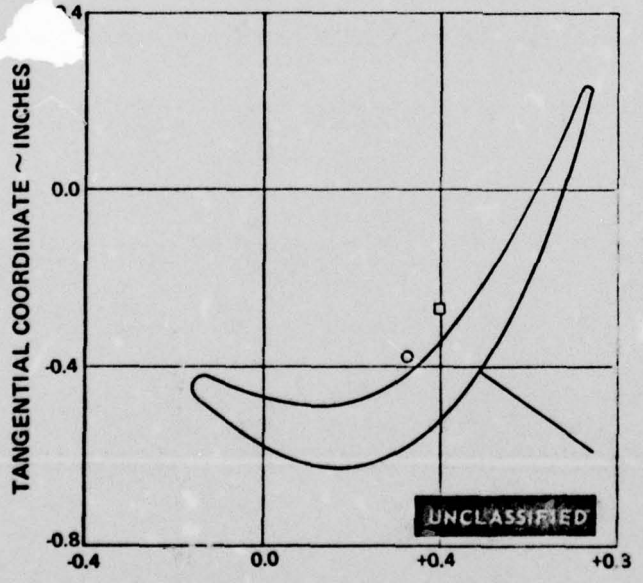

HOT DIMENSIONS

NUMBER OF FOILS	80.00	
DIAMETER	20.9176	IN.
GAGING	0.2969	IN.
PITCH	0.8214	IN.
AXIAL WIDTH	0.9055	IN.
BLADE INLET ANGLE	57.40	DEG
GAS INLET ANGLE	57.40	DEG
BLADE EXIT ANGLE	20.60	DEG
GAS EXIT ANGLE	20.60	DEG
GAGING ANGLE	21.19	DEG
UNCOVERED TURNING	17.80	DEG
PRINCIPAL AXIS	-40.47	DEG
L. E. RADIUS	0.0275	IN.
T. E. RADIUS	0.0100	IN.
METAL AREA	0.1236	IN^2

	X	Y
○ C. G.	0.3240	-0.3762
□ RADIAL REF. GAGE	0.3919	-0.2691
	0.4789	-0.4194

Figure 86 Recambering Design C, Second Vane, 1/4 Tip Section (DD)

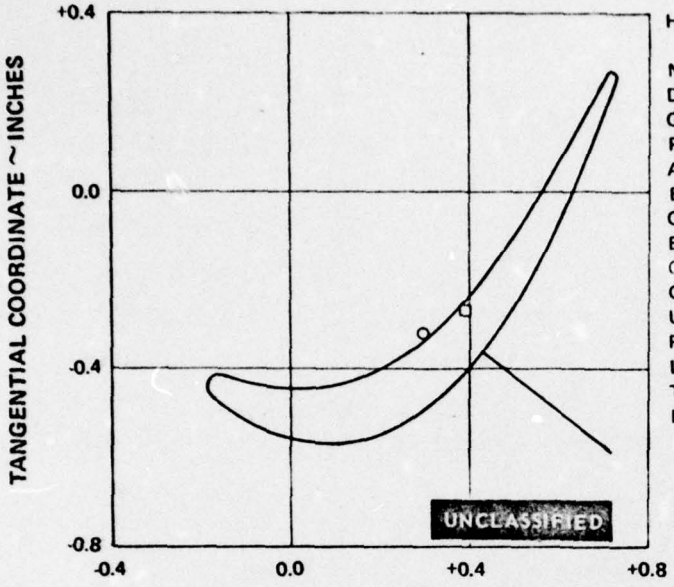

HOT DIMENSIONS

NUMBER OF FOILS	80.00	
DIAMETER	21.7200	IN.
GAGING	0.3579	IN.
PITCH	0.8529	IN.
AXIAL WIDTH	0.9155	IN.
BLADE INLET ANGLE	59.76	DEG
GAS INLET ANGLE	59.90	DEG
BLADE EXIT ANGLE	25.14	DEG
GAS EXIT ANGLE	24.65	DEG
GAGING ANGLE	24.81	DEG
UNCOVERED TURNING	17.11	DEG
PRINCIPAL AXIS	-40.62	DEG
L. E. RADIUS	0.0285	IN.
T. E. RADIUS	0.0100	IN.
METAL AREA	0.1167	$IN.^2$

	X	Y
○ C. G.	0.2956	-0.3218
□ RADIAL REF. GAGE	0.3919	-0.2691
	0.4308	-0.3645

Figure 89 Recambering Design C, Second Vane, Fillet Section (EE)

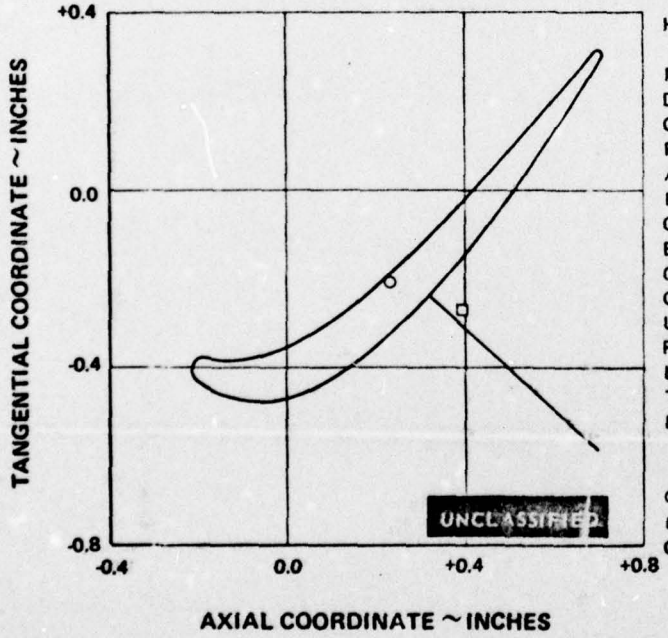

HOT DIMENSIONS

NUMBER OF FOILS	80.00	
DIAMETER	22.8200	IN.
GAGING	0.5111	IN.
PITCH	0.8961	IN.
AXIAL WIDTH	0.9291	IN.
BLADE INLET ANGLE	62.72	DEG
GAS INLET ANGLE	62.75	DEG
BLADE EXIT ANGLE	36.63	DEG
GAS EXIT ANGLE	36.55	DEG
GAGING ANGLE	34.77	DEG
UNCOVERED TURNING	10.09	DEG
PRINCIPAL AXIS	-40.99	DEG
L. E. RADIUS	0.0299	IN.
T. E. RADIUS	0.0100	IN.
METAL AREA	0.0965	$IN.^2$

	X	Y
○ C. G.	0.2328	-0.2084
□ RADIAL REF.	0.3919	-0.2691
GAGE	0.3212	-0.2364

Figure 90 Recambering Design C, Second Vane, Tip Section (HH)

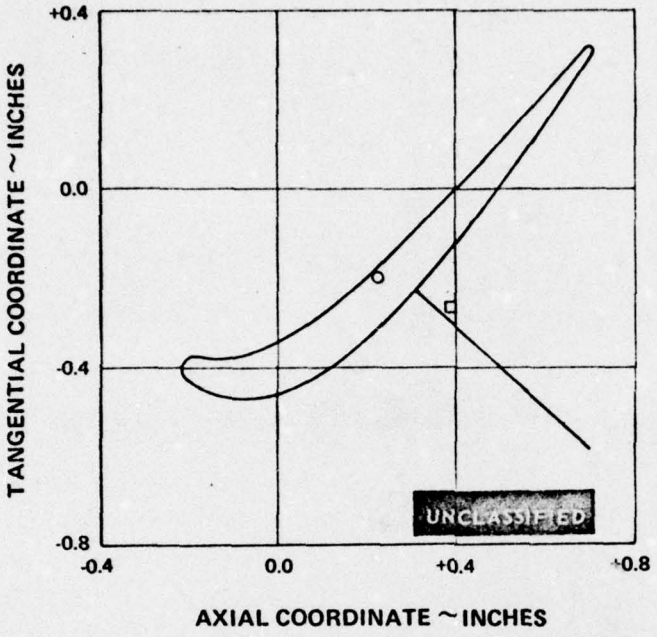

HOT DIMENSIONS

NUMBER OF FOILS	80.00	
DIAMETER	22.8900	IN.
GAGING	0.5234	IN.
PITCH	0.8989	IN.
AXIAL WIDTH	0.9300	IN.
BLADE INLET ANGLE	62.90	DEG
GAS INLET ANGLE	62.90	DEG
BLADE EXIT ANGLE	37.57	DEG
GAS EXIT ANGLE	37.57	DEG
GAGING ANGLE	35.61	DEG
UNCOVERED TURNING	9.15	DEG
PRINCIPAL AXIS	-41.10	DEG
L. E. RADIUS	0.0300	IN.
T. E. RADIUS	0.0100	IN.
METAL AREA	0.0947	$IN.^2$

	X	Y
O C. G.	0.2272	-0.2003
□ RADIAL REF. GAGE	0.3919	-0.2691
	0.3107	-0.2283

Figure 91 Recambering Design C, Second Vane, Tip Defining Section (GG)

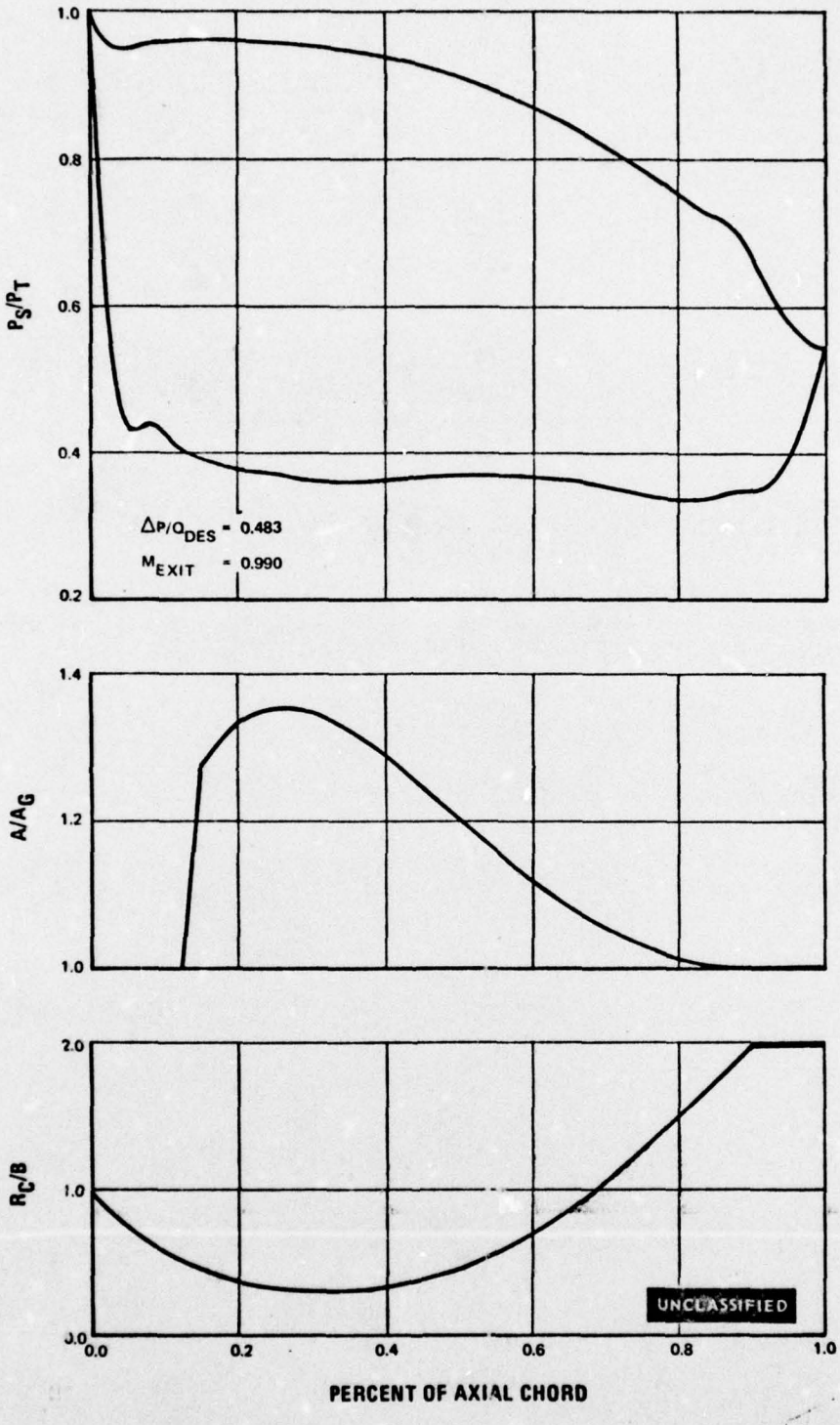

Figure 92 Recambering Design A Second Vane, Root Section

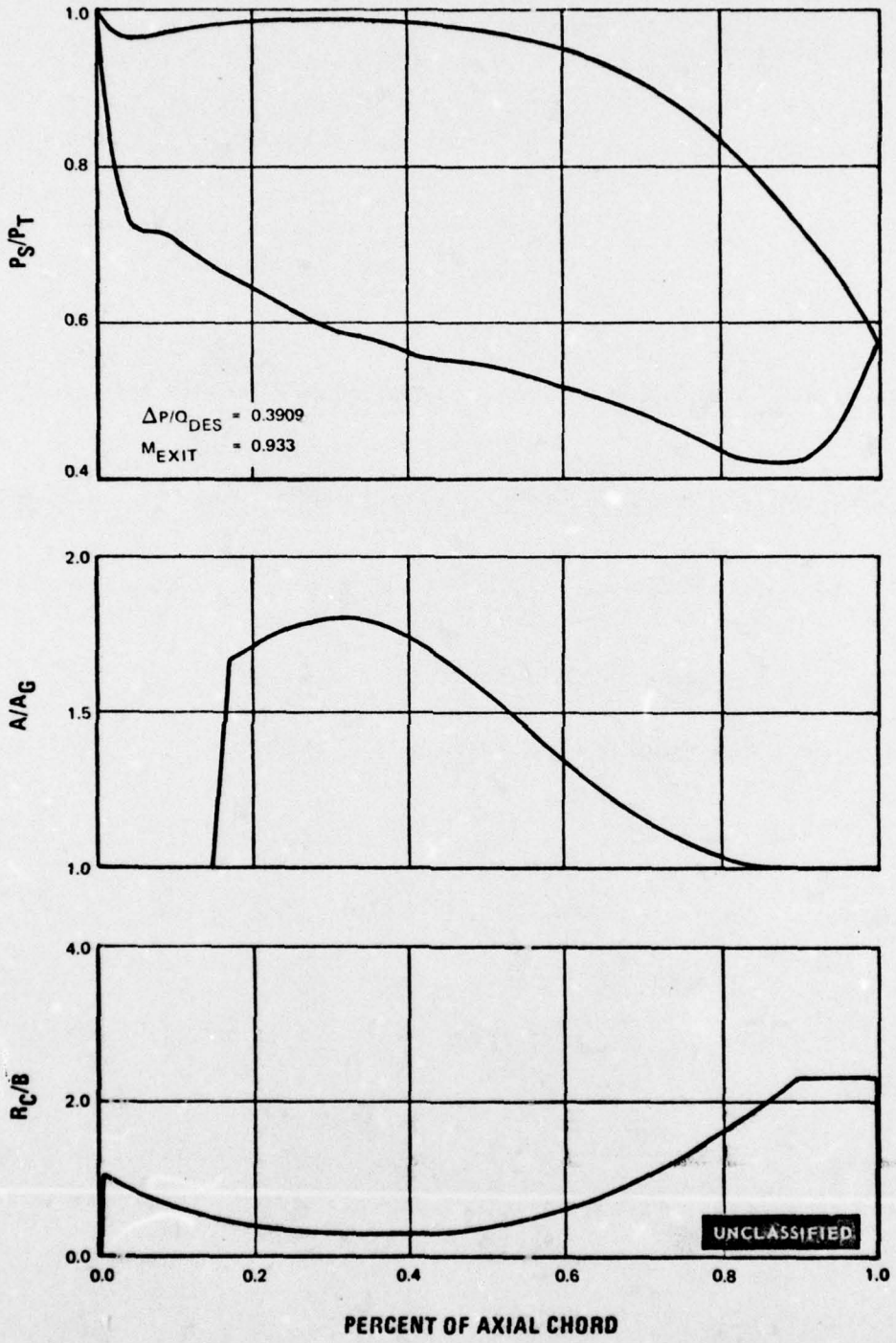

Figure 93 Recambering Design A, Second Vane, 1/4 Root Section

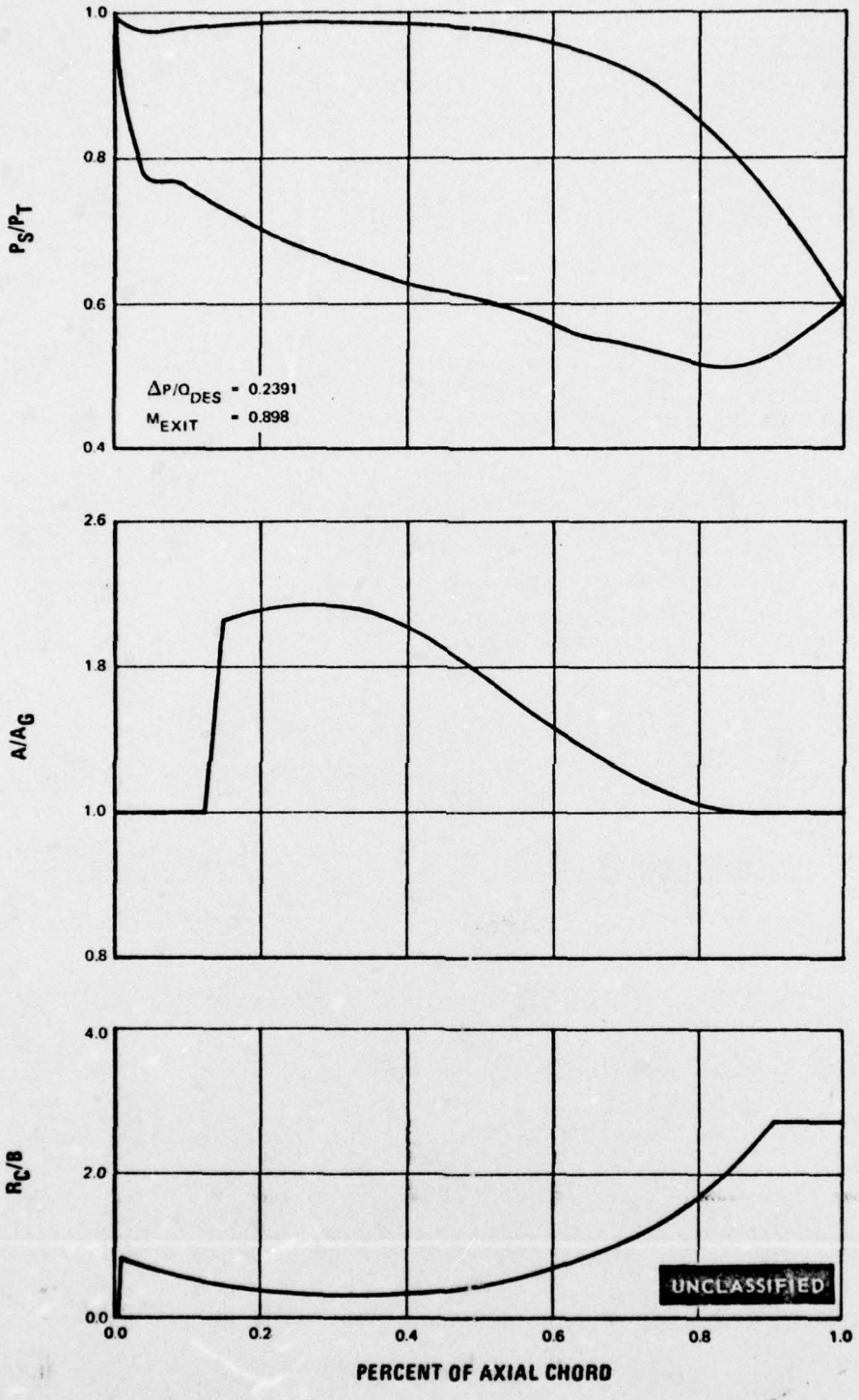

Figure 94 Recambering Design A., Second Vane, Mean Section

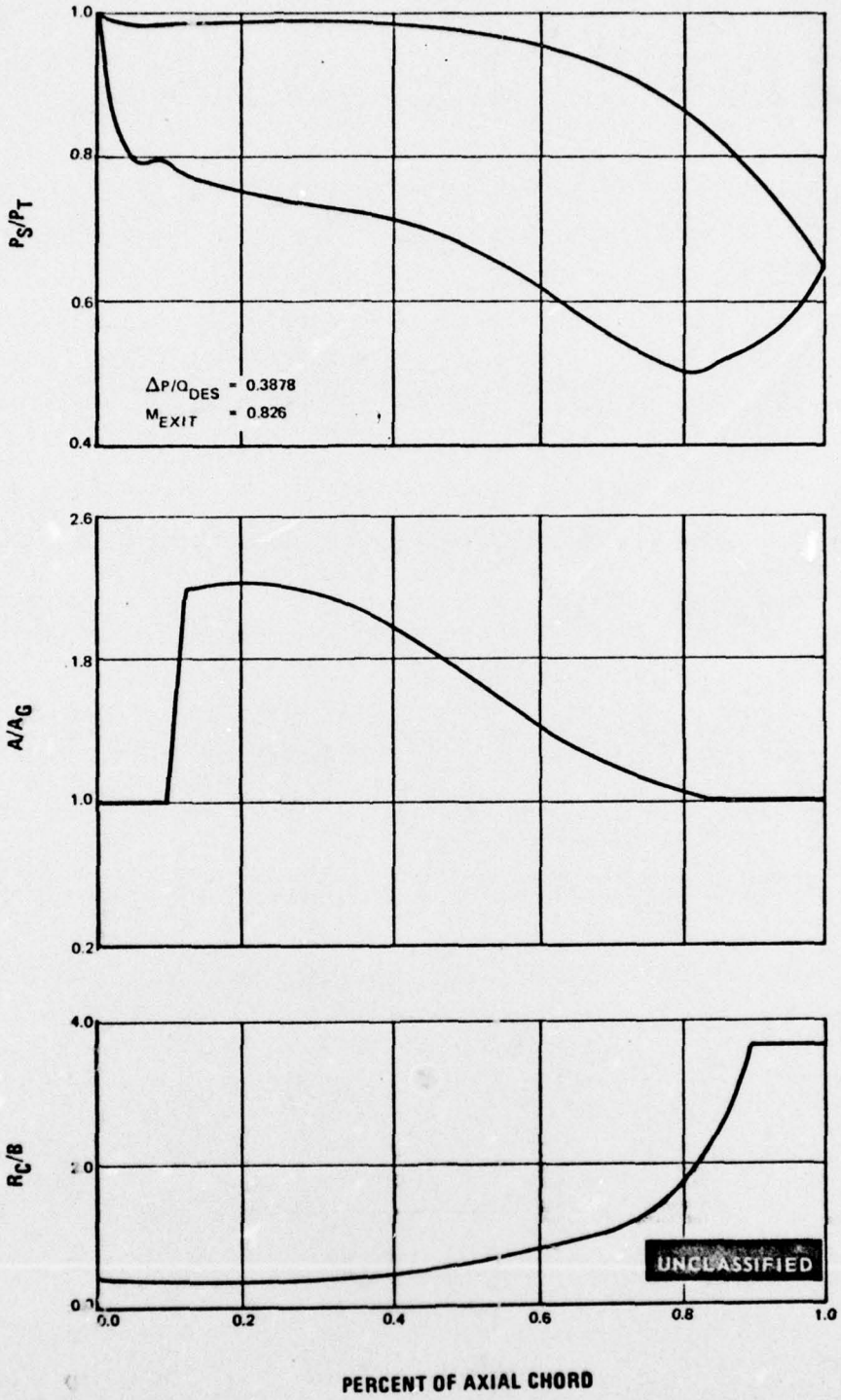

Figure 95 Recambering Design A, Second Vane, 1/4 Tip Section

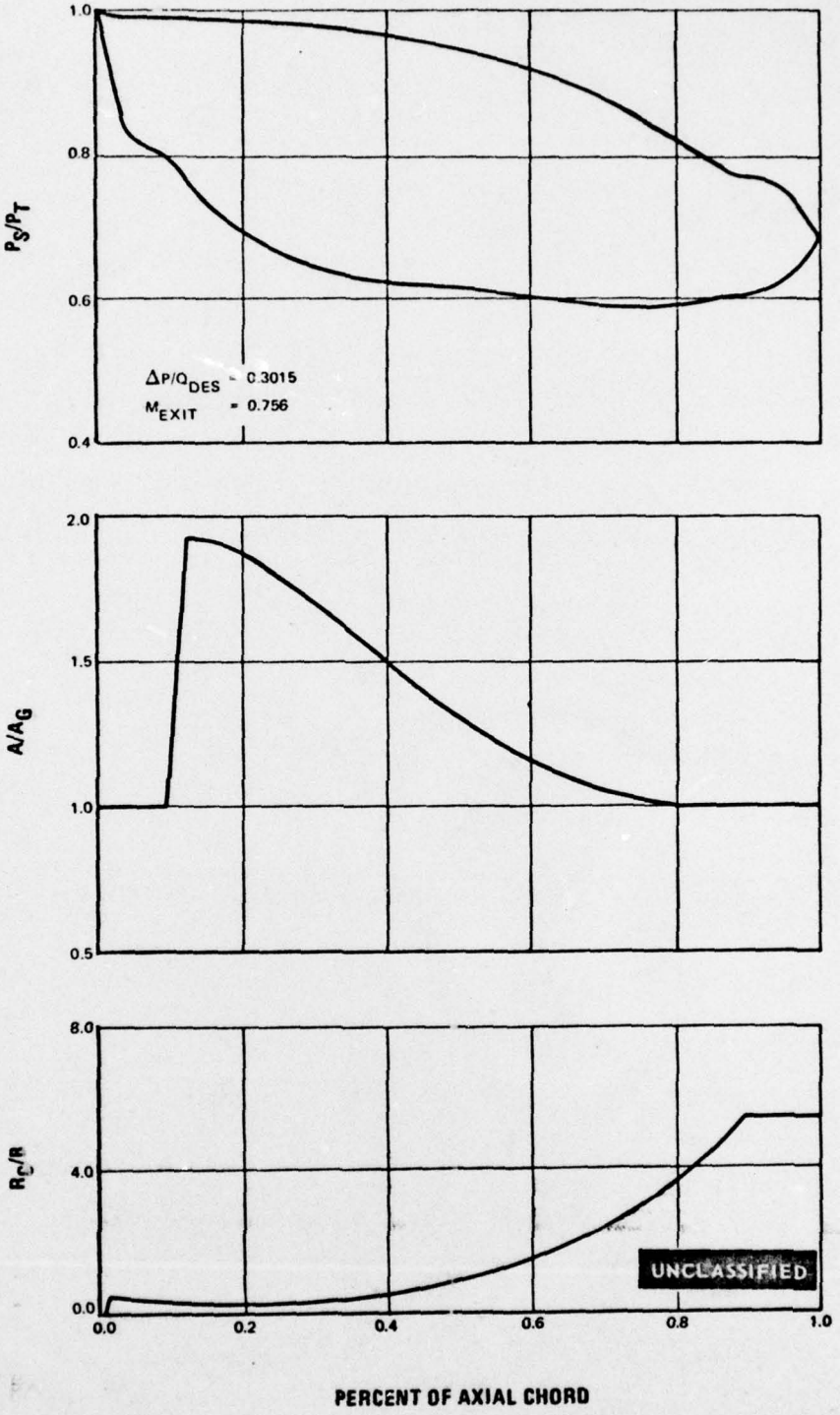

Figure 96 Recambering Design A, Second Vane, Tip Section

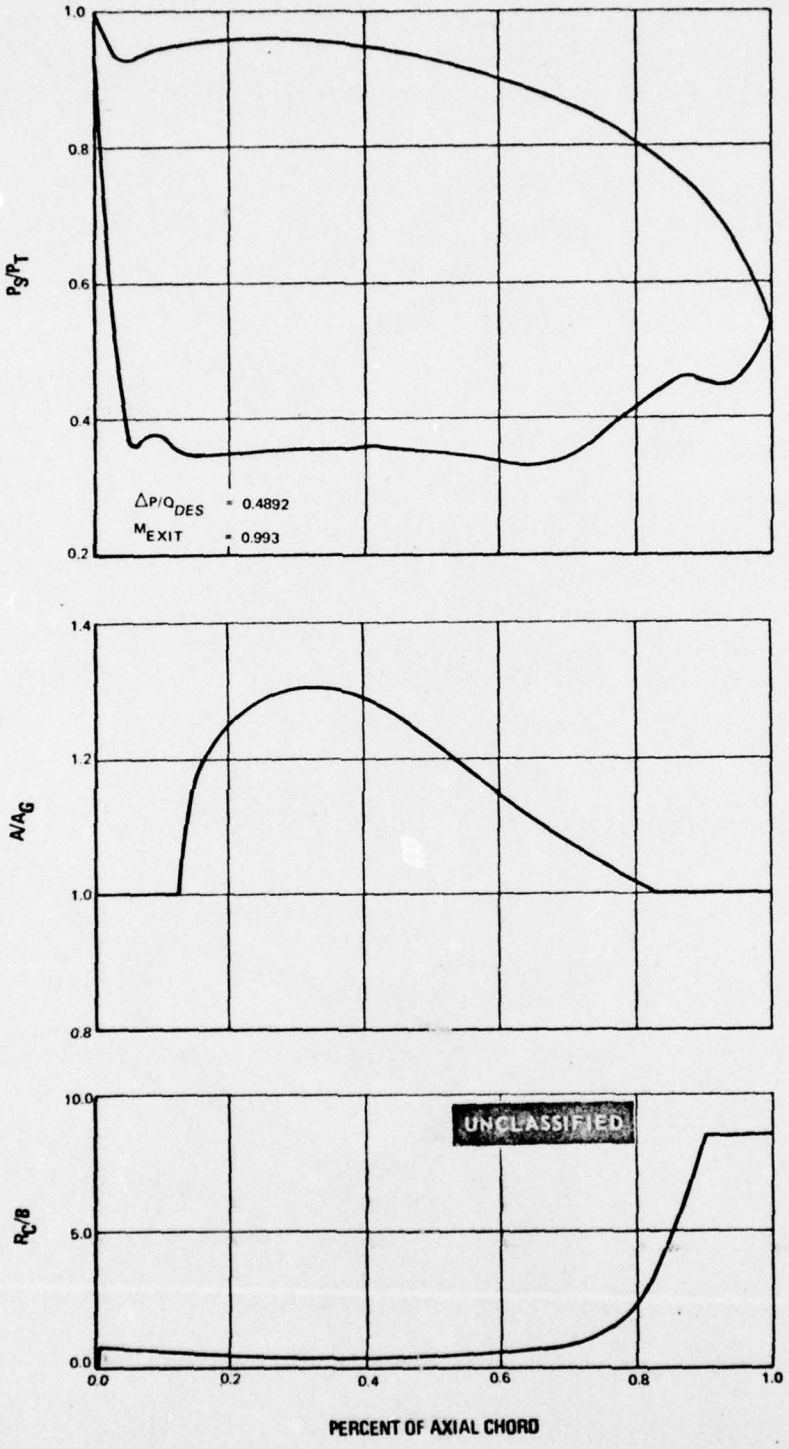

Figure 97 Recambering Design B, Second Vane, Root Section

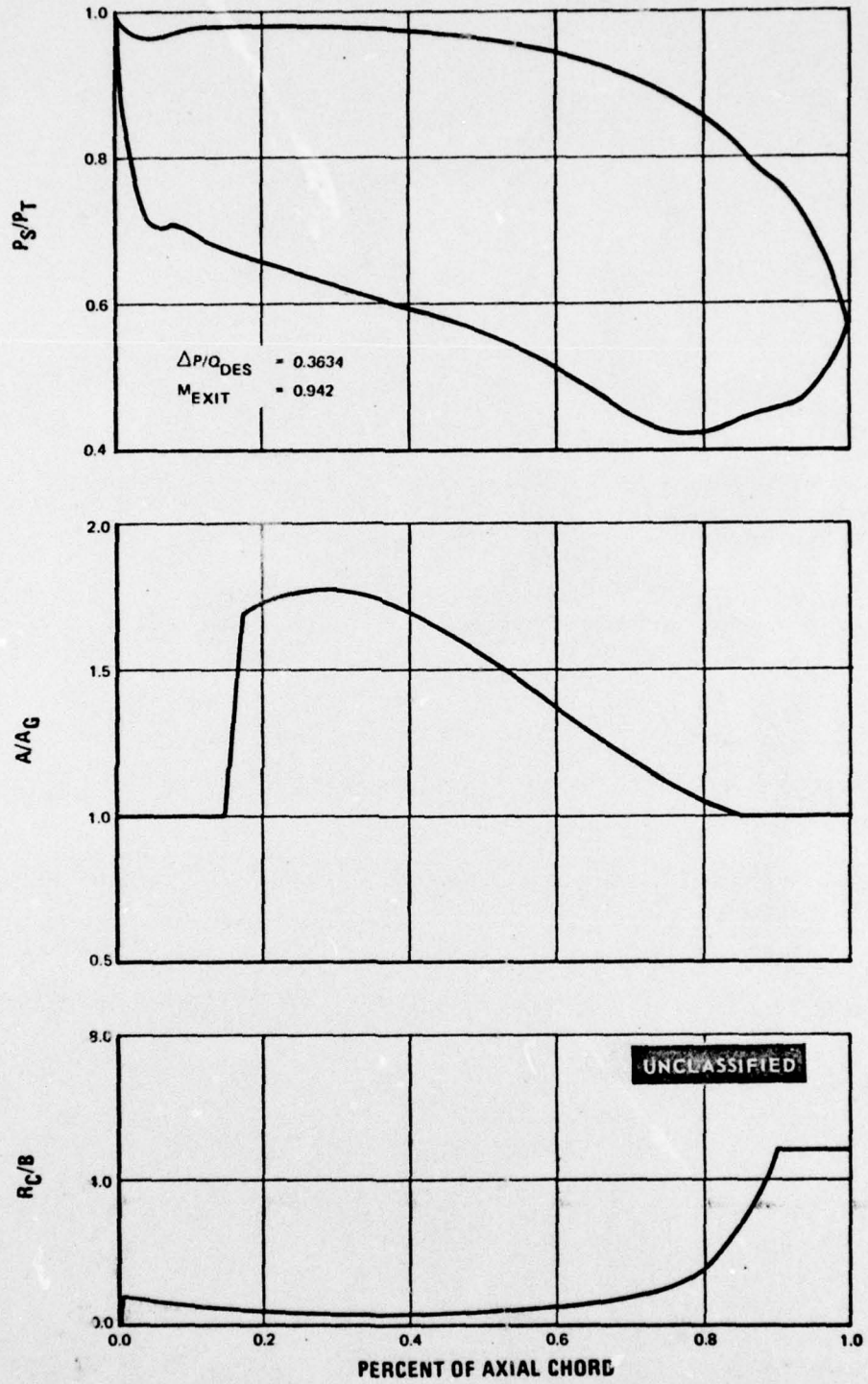

Figure 98 Recambering Design B, Second Vane, 1/4 Root Section

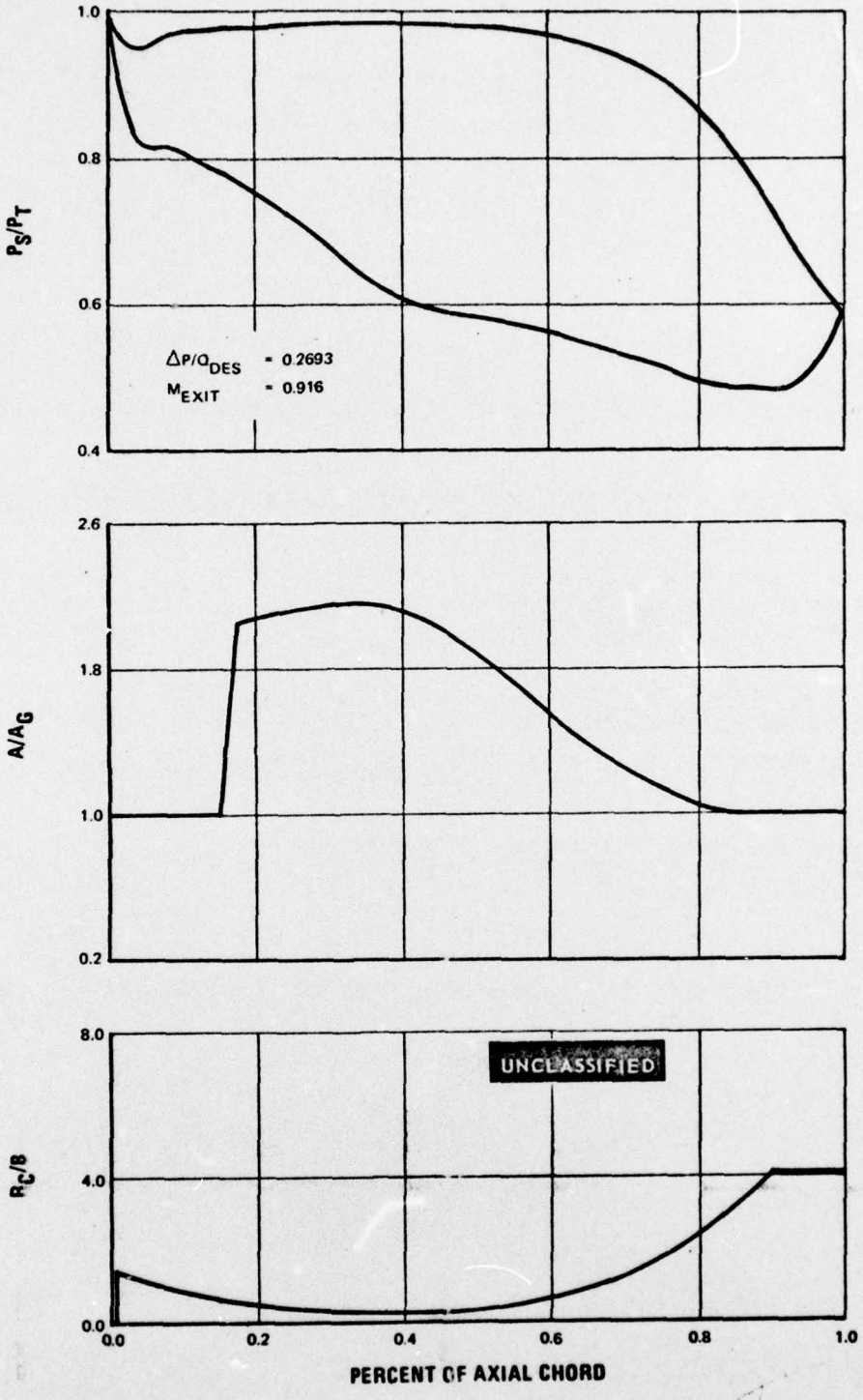

Figure 99 Recambering Design B, Second Vane, Mean Section

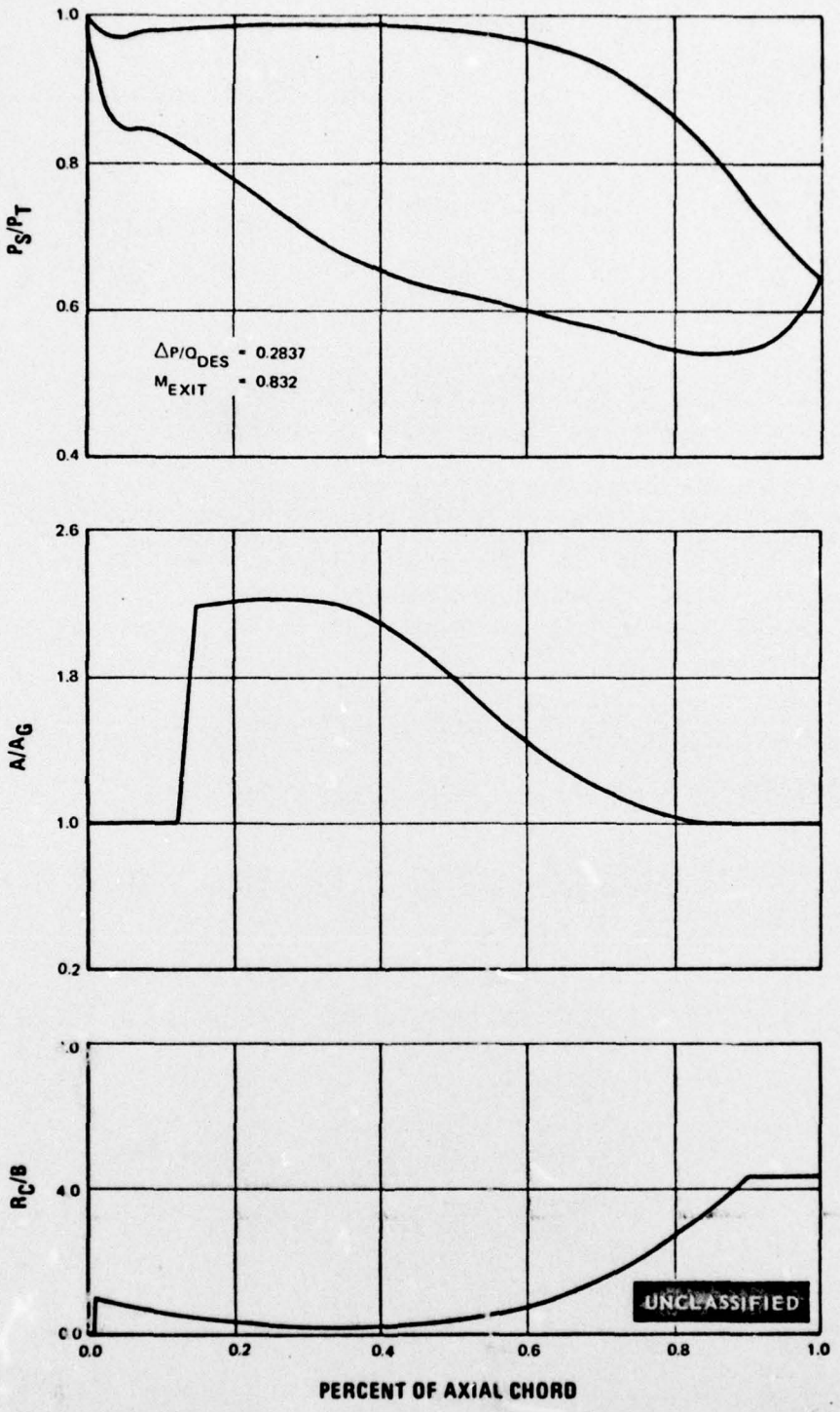

Figure 100 Recambering Design B, Second Vane, 1/4 Tip Section

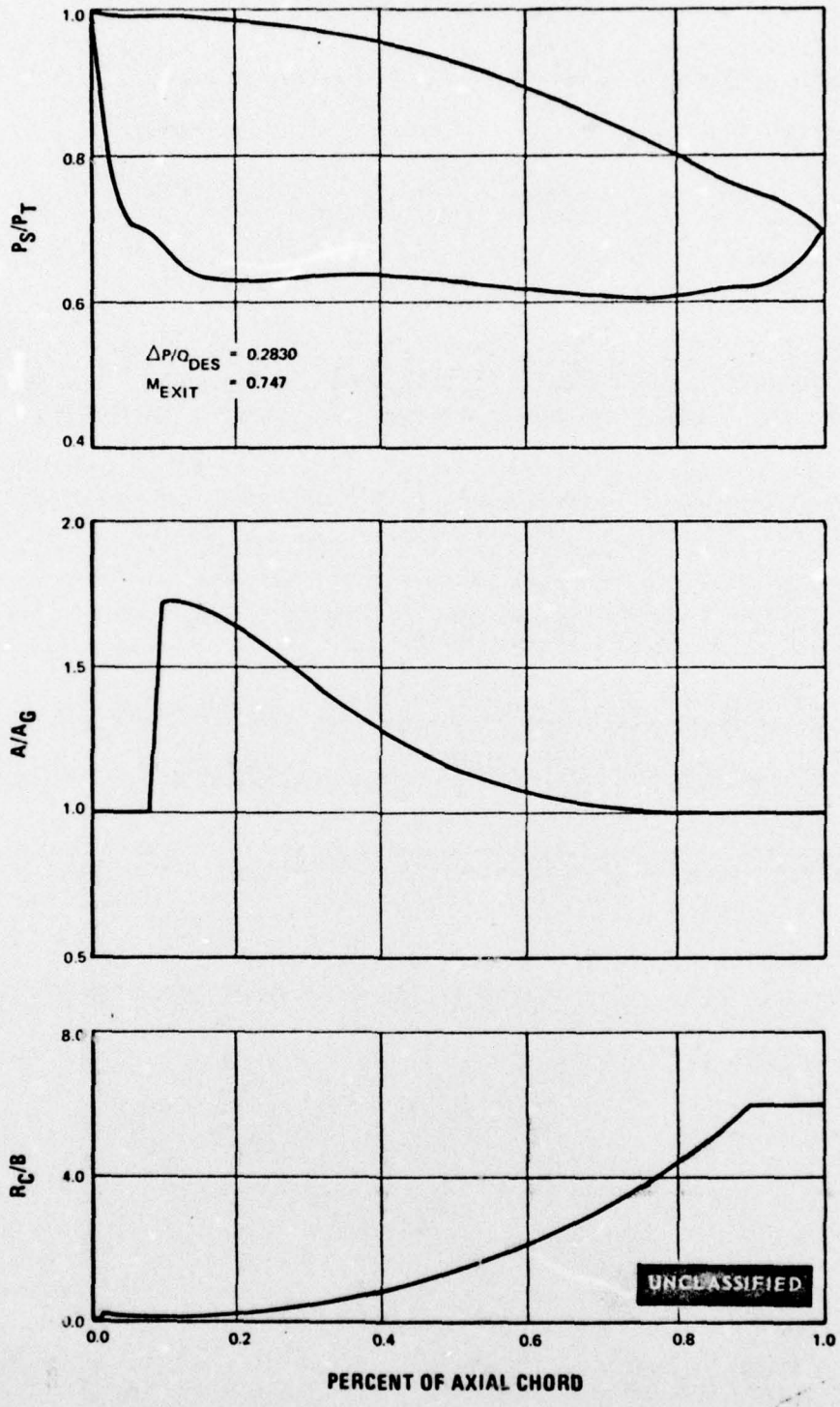

Figure 101 Recambering Design B, Second Vane, Tip Section

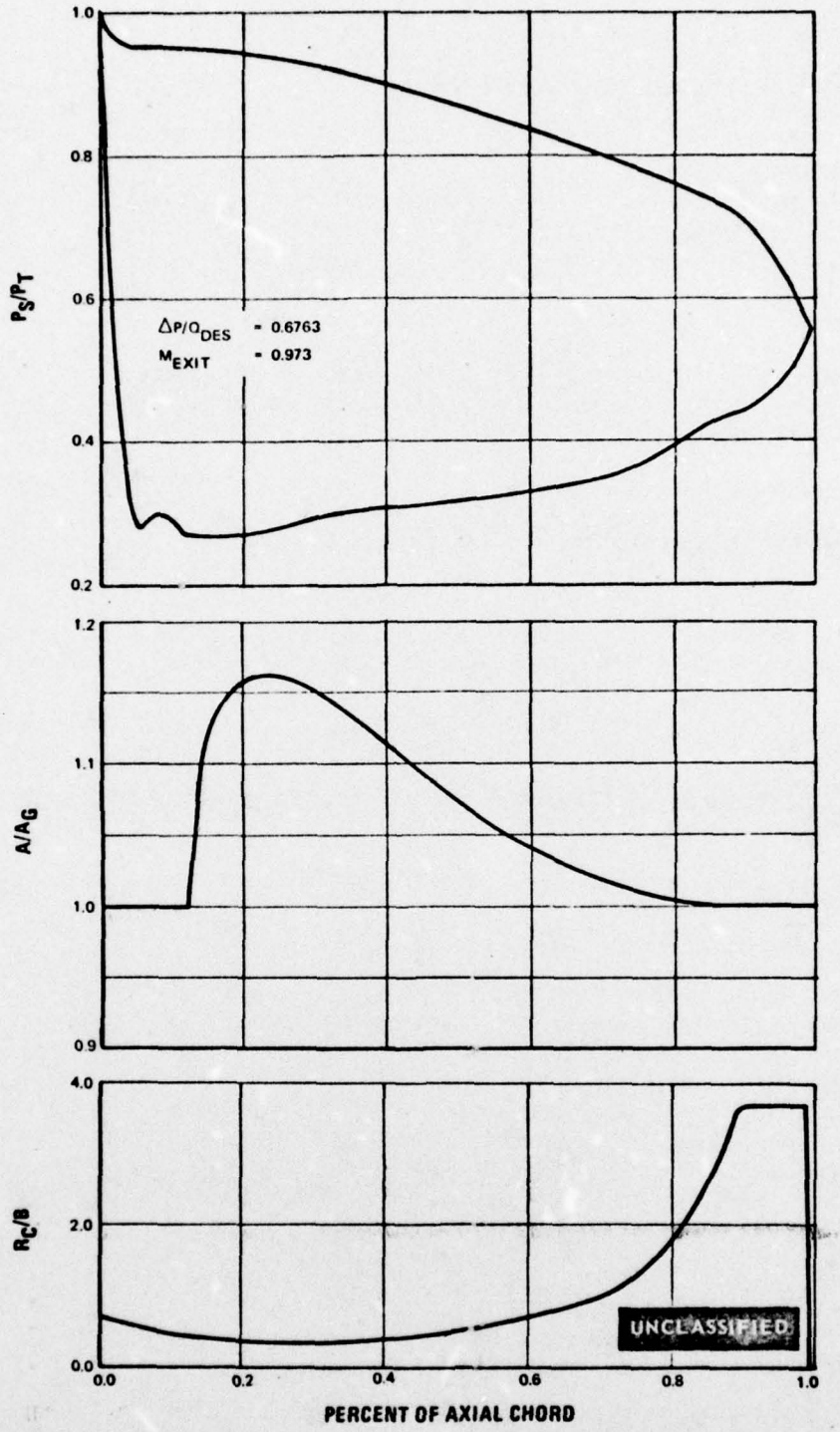

Figure 102 Recambering Design C, Second Vane, Root Section

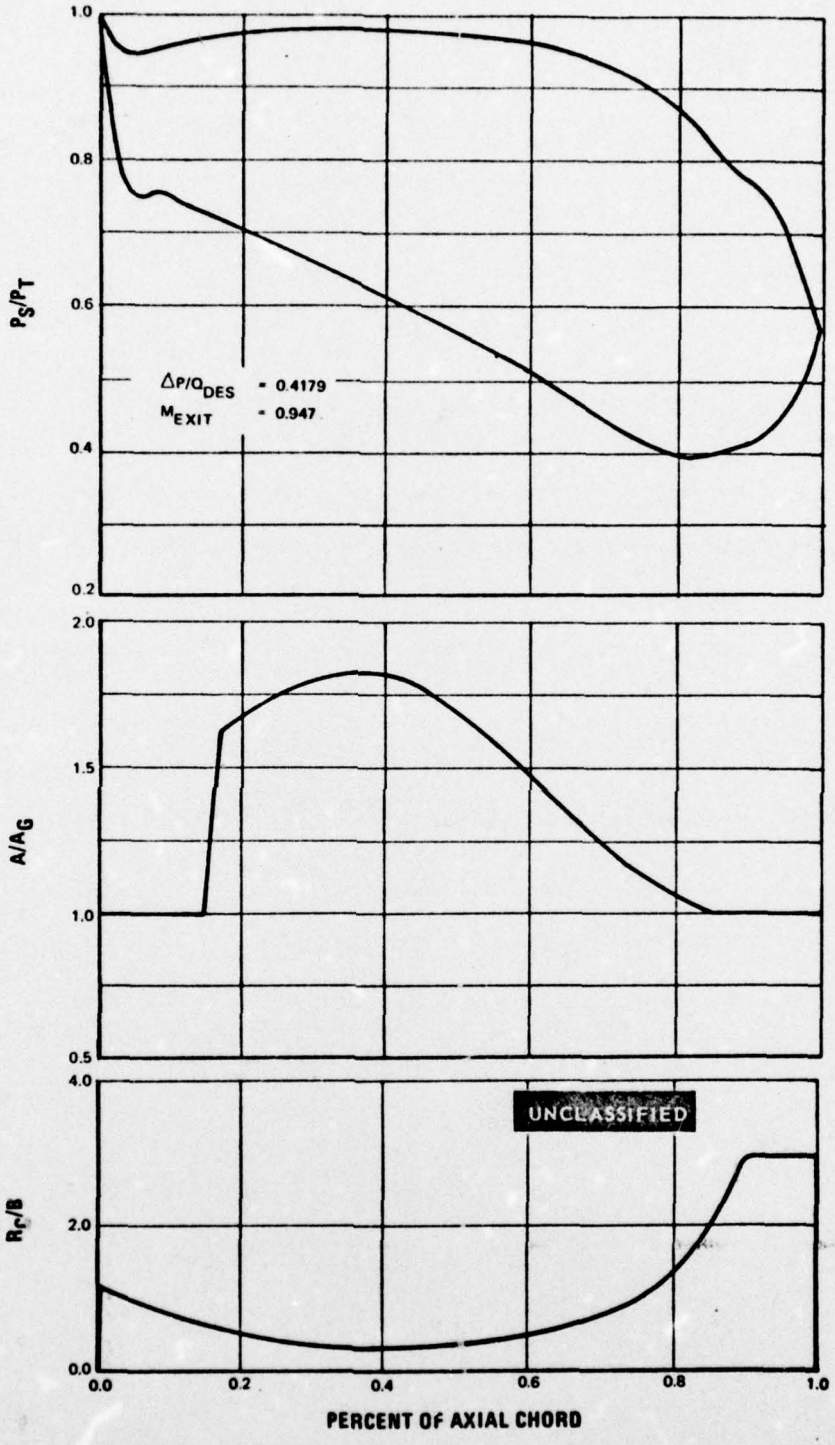

Figure 103 Recambering Design C, Second Vane, 1/4 Root Section

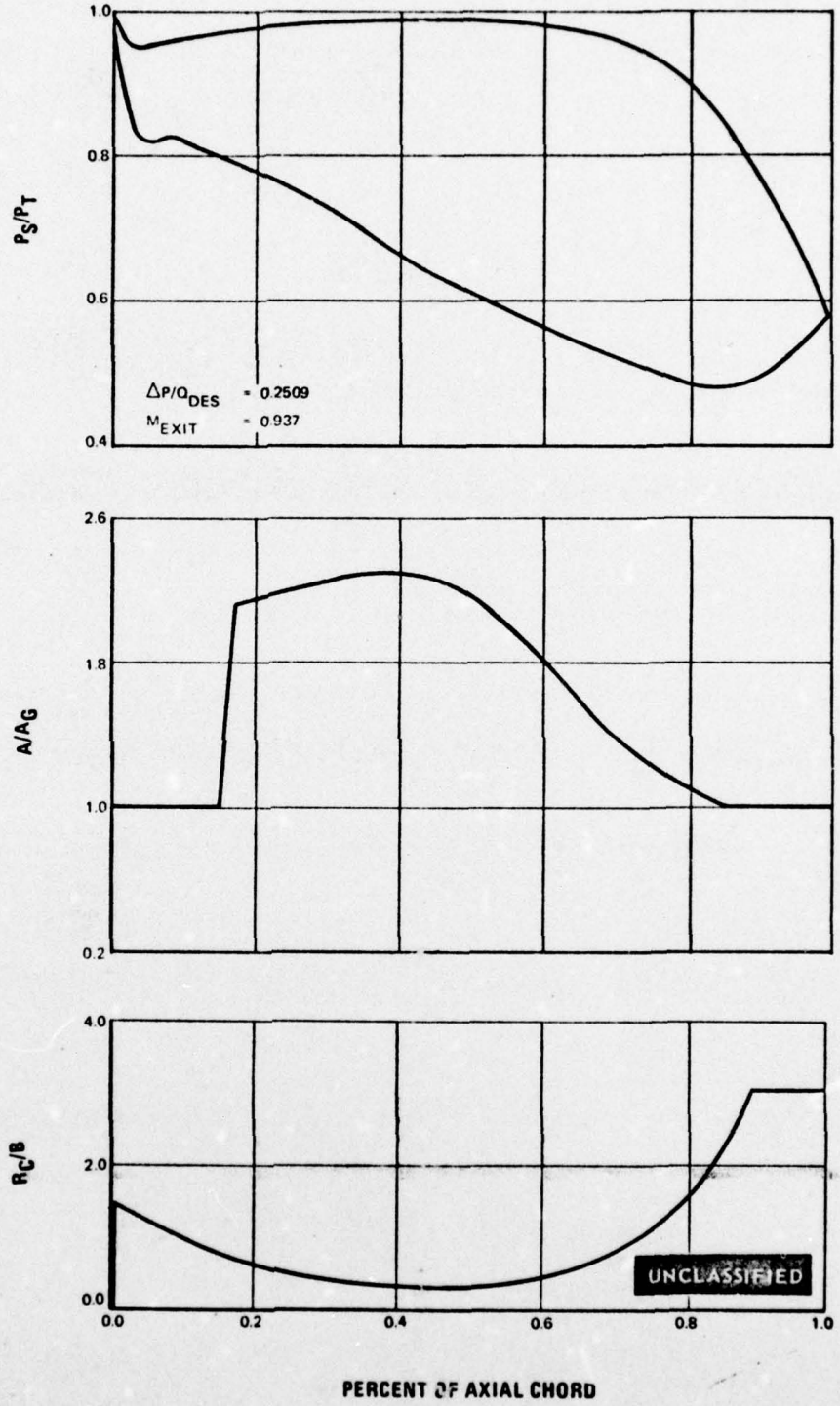

Figure 104 Recambering Design C, Second Vane, Mean Section

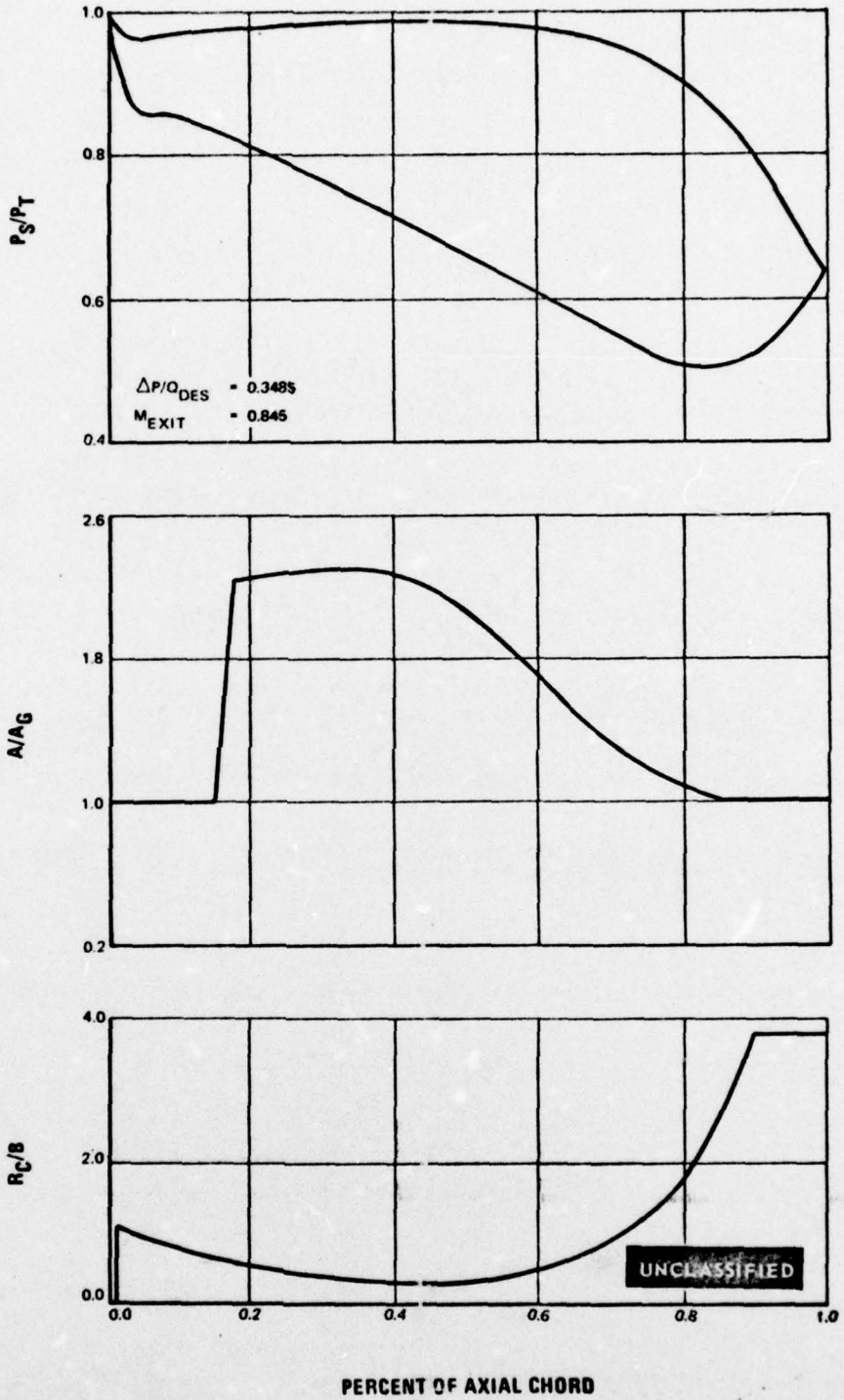

Figure 105 Recambering Design C, Second Vane, 1/4 Tip Section

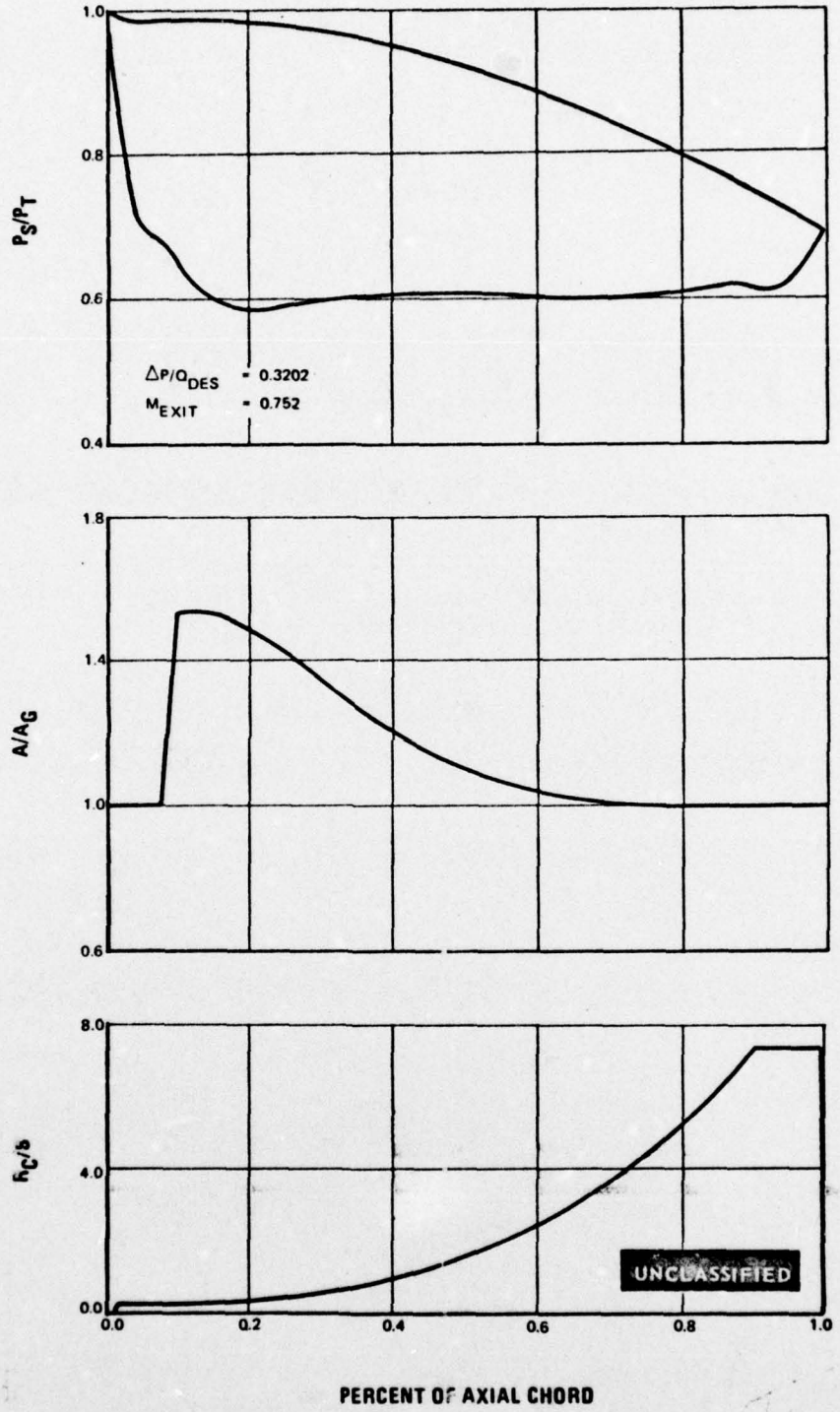

Figure 106 Recambering Design C, Second Vane, Tip Section

(U) Except for the test airfoils, the cascade rig used in this Task was identical to the one used to evaluate the first recambered second vane airfoil (Task II c). This was the normal solidity, annular segment, cascade rig described in detail in Reference 2. The inlet guide vanes used in testing the three local recambering designs were the redesigned inlet guide vanes described in Reference 4, Section IV, since the inlet angles of the three recambered airfoils were identical to both the baseline and the first recambered designs. In keeping with the Task II c evaluations, inlet boundary layer bleed slots were also used during these tests. The boundary layer slots were cut into the inlet guide vane pack inside diameter and outside diameter walls, and were 0.094 and 0.047 inches wide, respectively. The inlet screen of Task IIc was also in the cascade in order to generate a more realistic turbulence intensity level.

4. DISCUSSION

(U) The performance data at the exit Mach number nearest the design value (0.869) are presented for each of the three recambering designs. For each geometrical variation, the pressure loss contours, the exit gas angle contours, spanwise pressure loss distributions, spanwise loss coefficient distributions, spanwise exit gas angle distributions and spanwise exit Mach number distributions are shown. These plots are found in Figure 107 through 112 for recambering design A at an exit midspan Mach number of 0.846. Data were also taken at exit midspan Mach numbers of 0.787 and 0.972. Similar plots are found for recambering design B in Figures 113 through 118 at an exit midspan Mach number of 0.856, and for recambering design C at an exit midspan Mach number of 0.862 in Figures 119 through 124. Data were also taken at exit midspan Mach numbers of 0.799 and 0.995 for design B, and at 0.800 and 1.008 for design C.

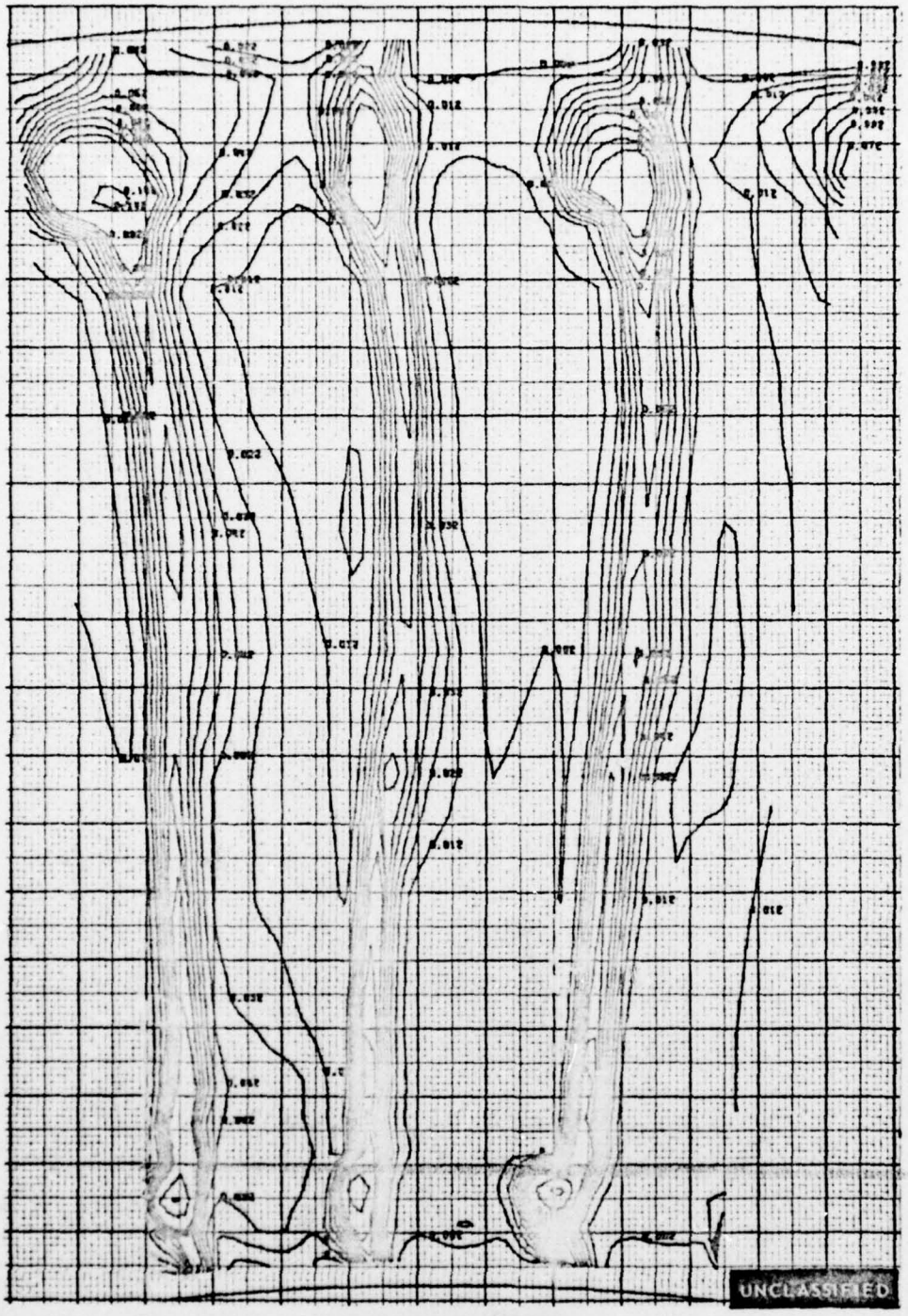

Δ PO/PO CONTOURS

Figure 107 Pressure Loss Contours, Second Vane Recambering Design A at Design Incidence. Three Flow Passages. Midspan Exit Mach Number = 0.846

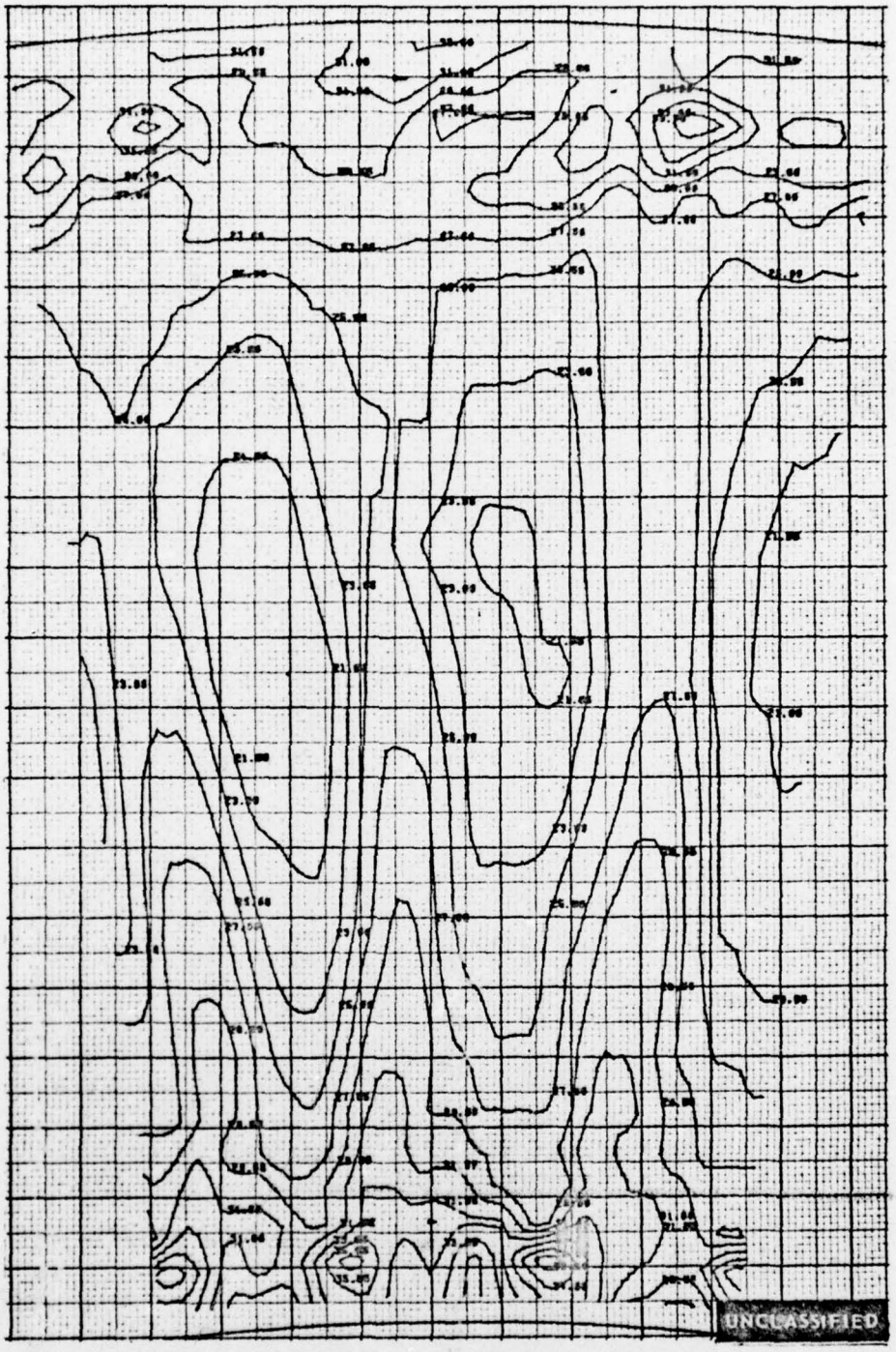

EXIT GAS ANGLE CONTOURS, DEGREES

Figure 108 Exit Gas Angle Contours, Second Vane Recambering Design A at Design Incidence. Three Flow Passages. Midspan Exit Mach Number = 0.846

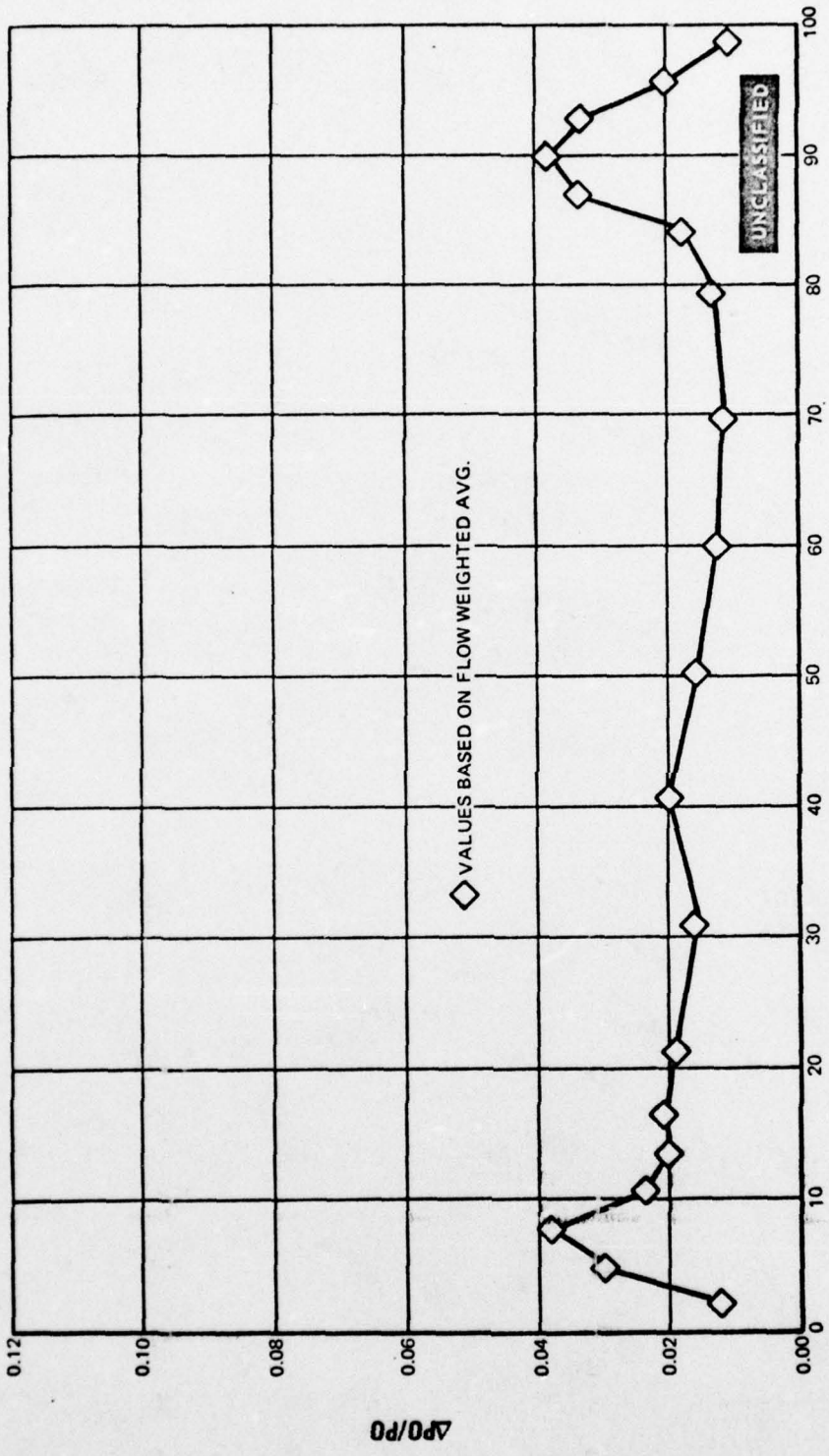

Figure 109 Spanwise Pressure Loss Distribution, Second Vane Recambering Design A at Design Incidence. Midspan Exit Mach Number = 0.846

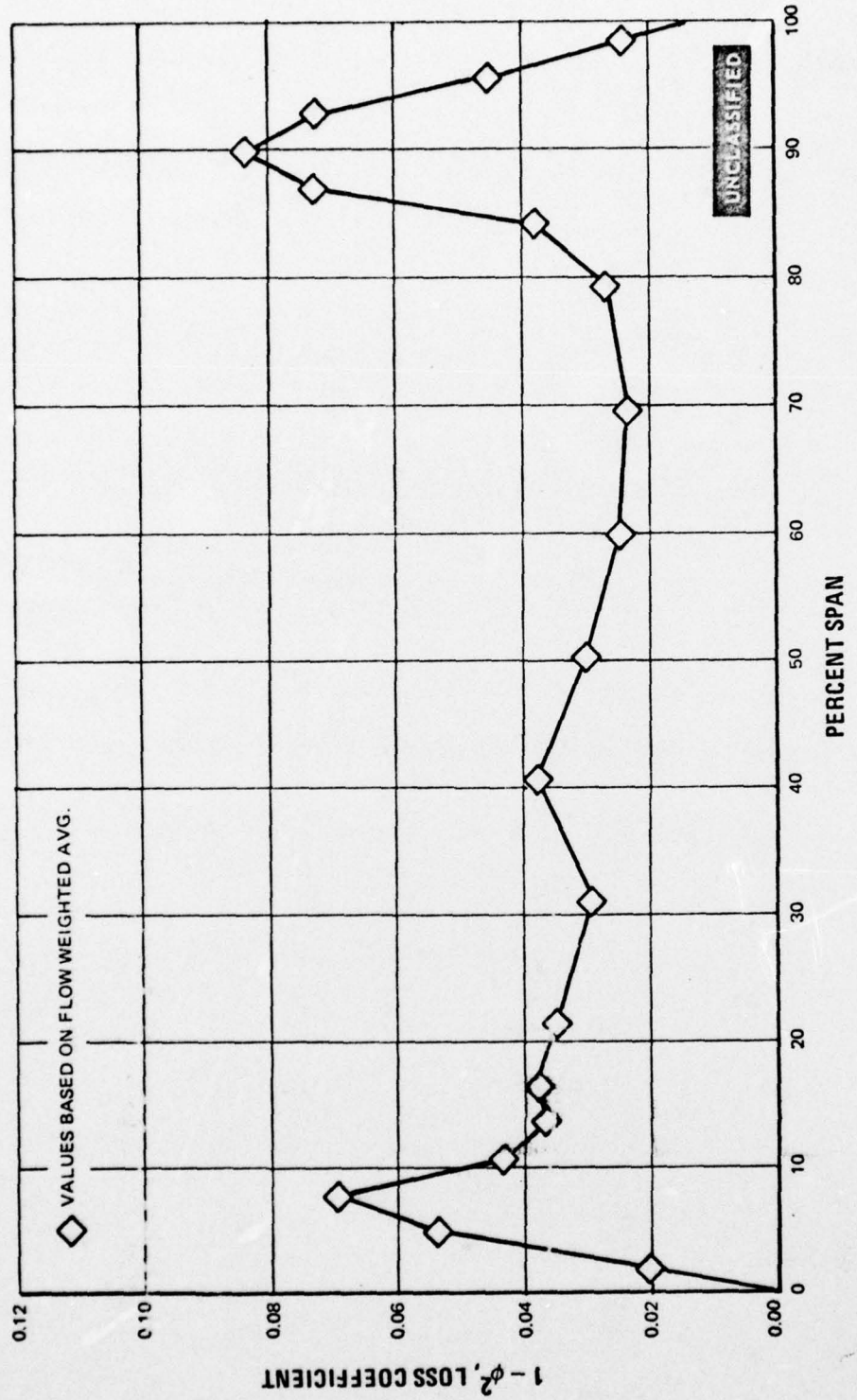

Figure 110 Spanwise Loss Coefficient Distribution, Second Vane Recambering Design A at Design Incidence. Midspan Exit Mach Number = 0.846

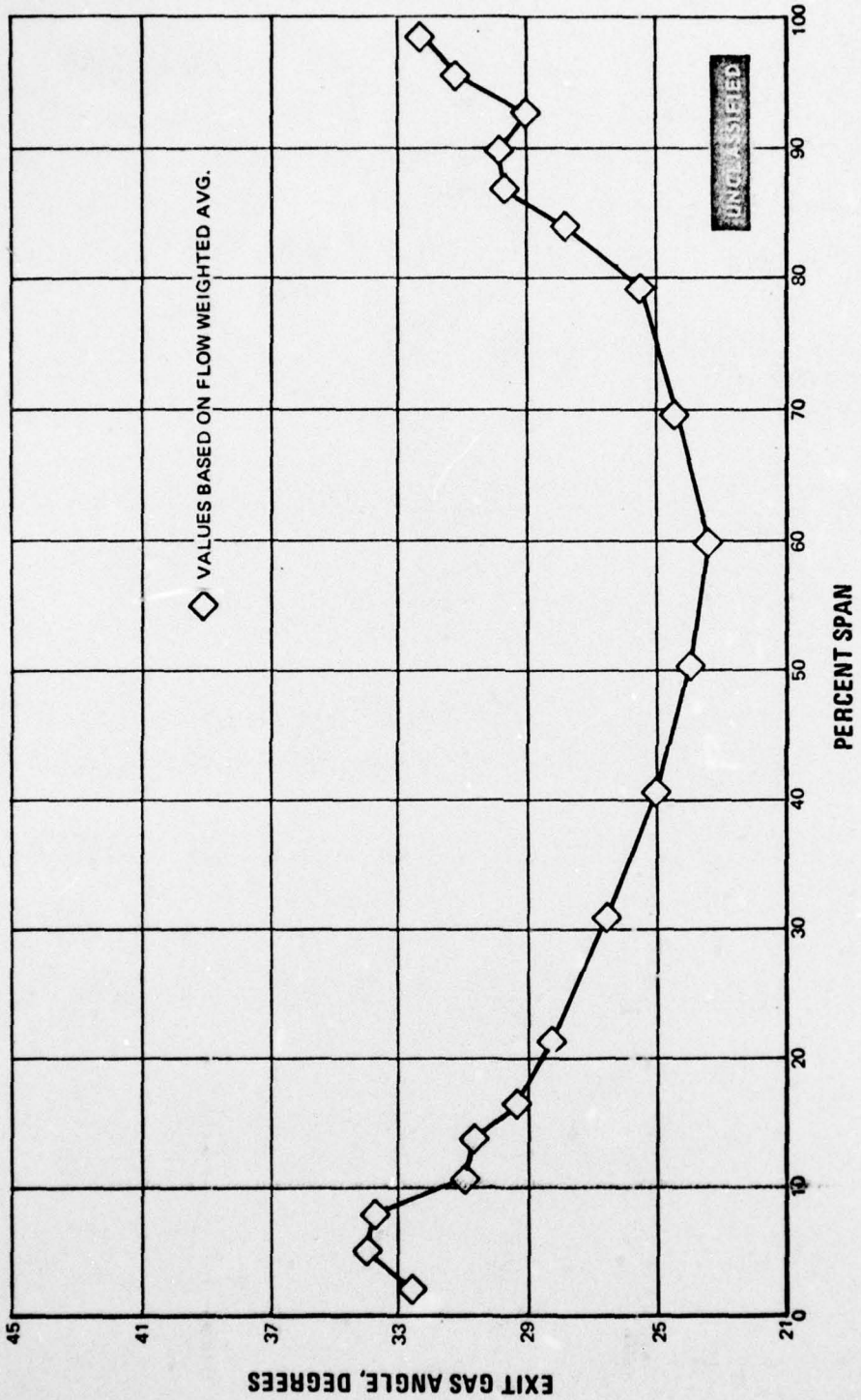

Figure 111 Spanwise Exit Gas Angle Distribution, Second Vane Recambering Design A at Design Incidence. Midspan Exit Mach Number = 0.846

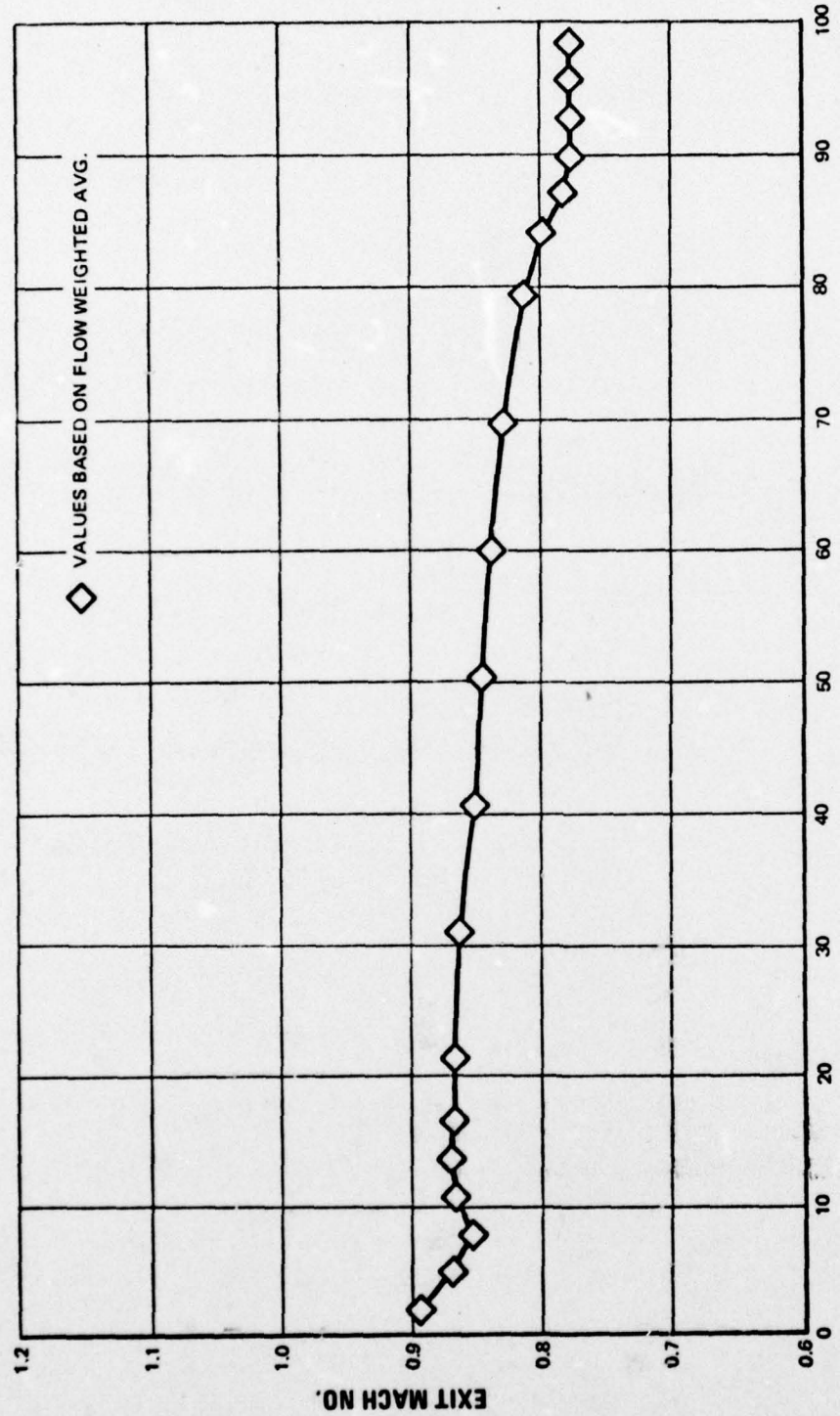

Figure 112 Spanwise Exit Mach Number Distribution, Second Vane Recambering Design A at Design Incidence. Midspan Exit Mach Number = 0.846

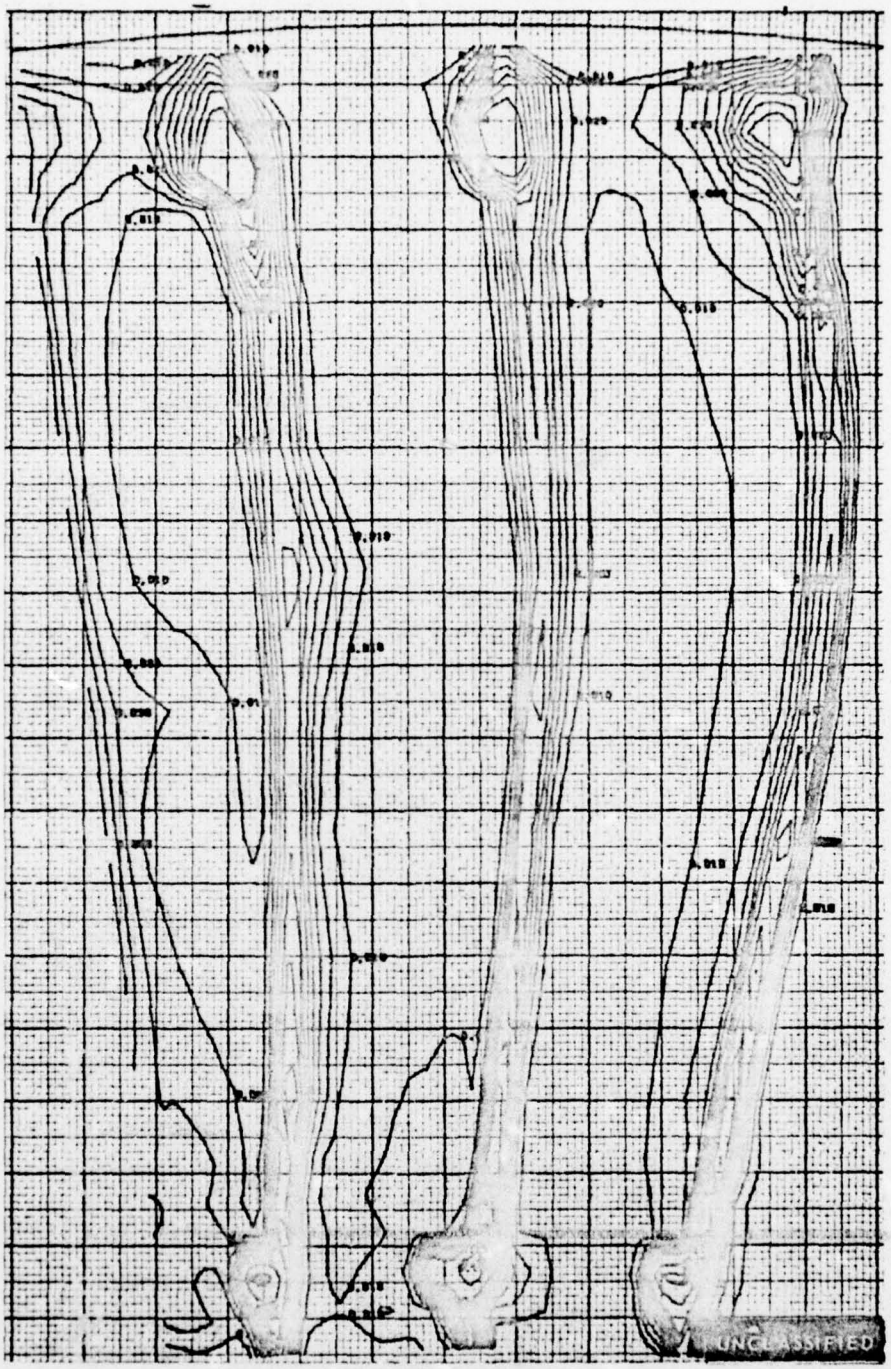

ΔPO/PO CONTOURS

Figure 113 Pressure Loss Contours, Second Vane Recambering Design B at Design Incidence. Three Flow Passages. Midspan Exit Mach Number = 0.856

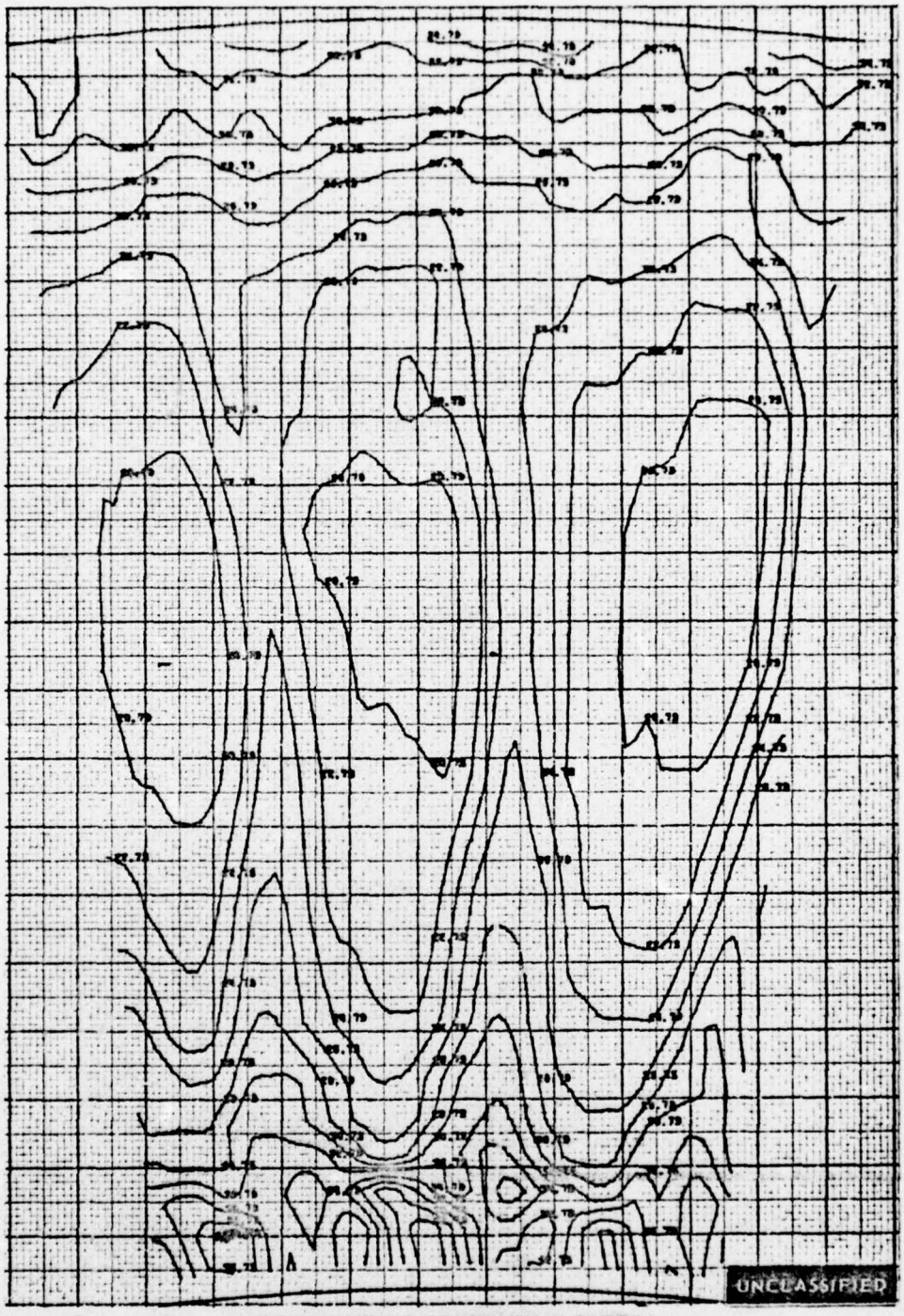

EXIT GAS ANGLE CONTOURS, DEGREES

Figure 114 Exit Gas Angle Contours, Second Vane Recambering Design B at Design Incidence. Three Flow Passages. Midspan Exit Mach Number = 0.856

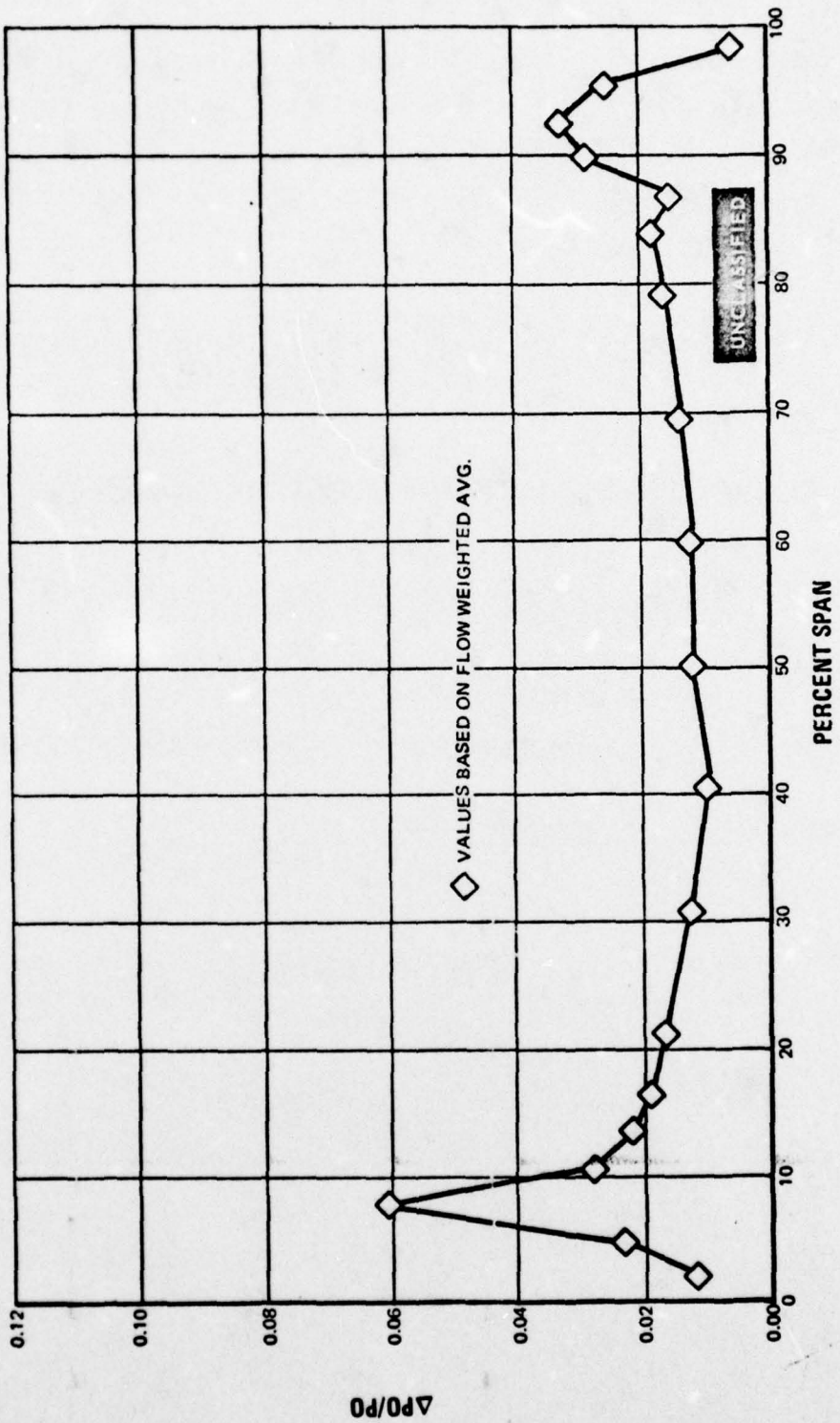

Figure 115 Spanwise Pressure Loss Distribution, Second Vane Recambering Design B at Design Incidence. Midspan Exit Mach Number = 0.856

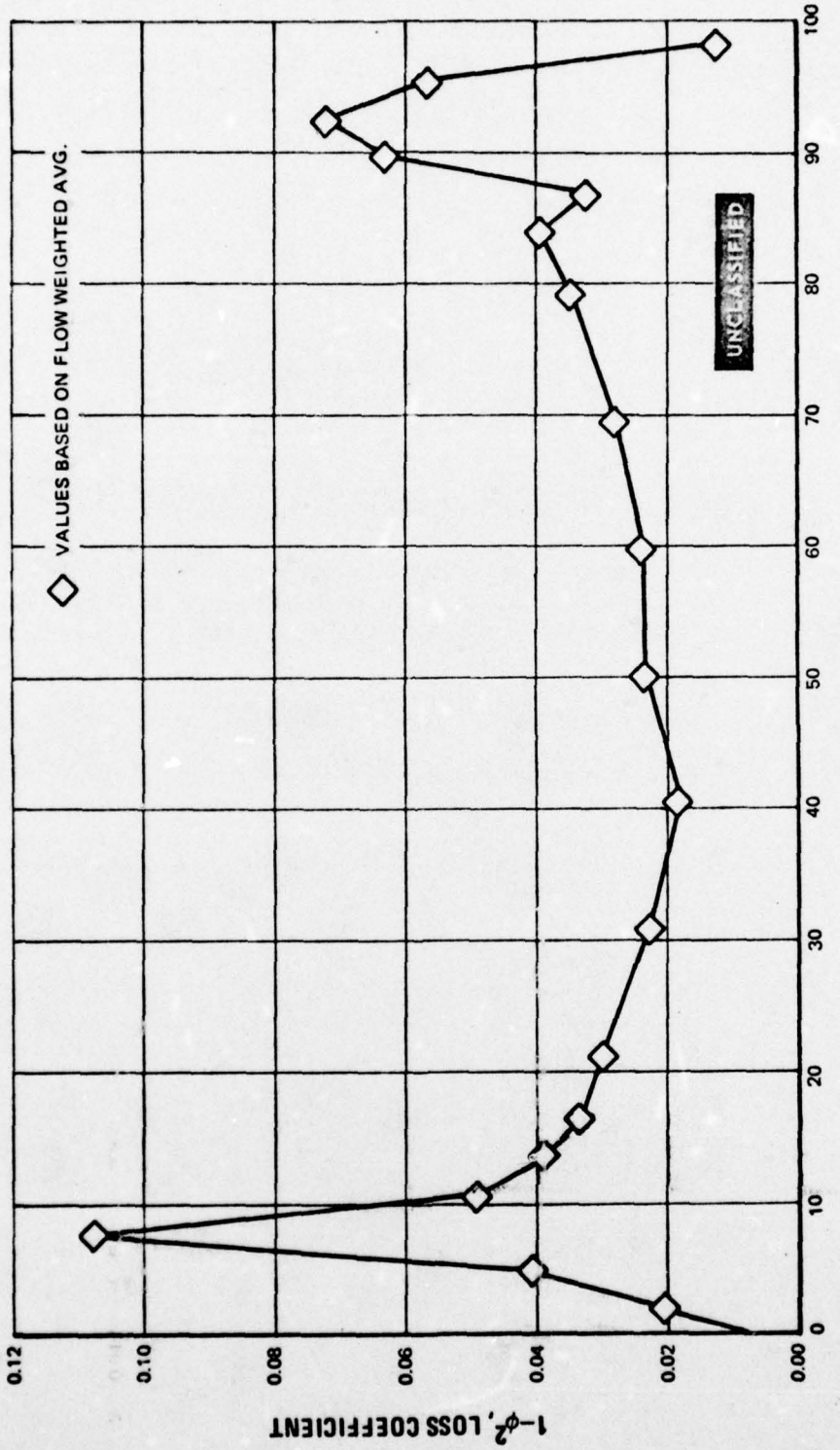

Figure 116 Spanwise Loss Coefficient Distribution, Second Vane Recambering Design B at Design Incidence. Midspan Exit Mach Number = 0.856

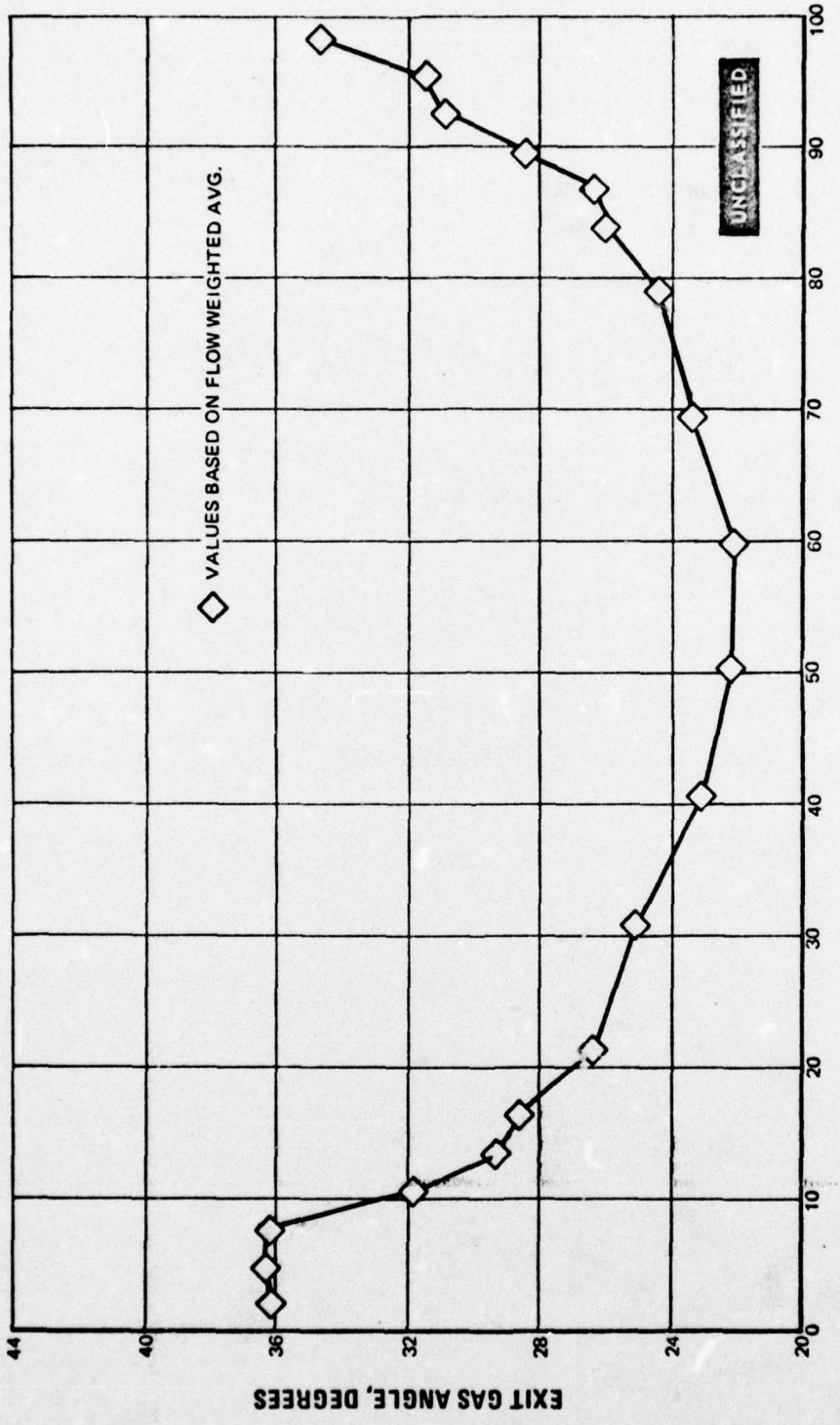

Figure 117 Spanwise Exit Gas Angle Distribution, Second Vane Recambering Design B at Design Incidence. Midspan Exit Mach Number = 0.856

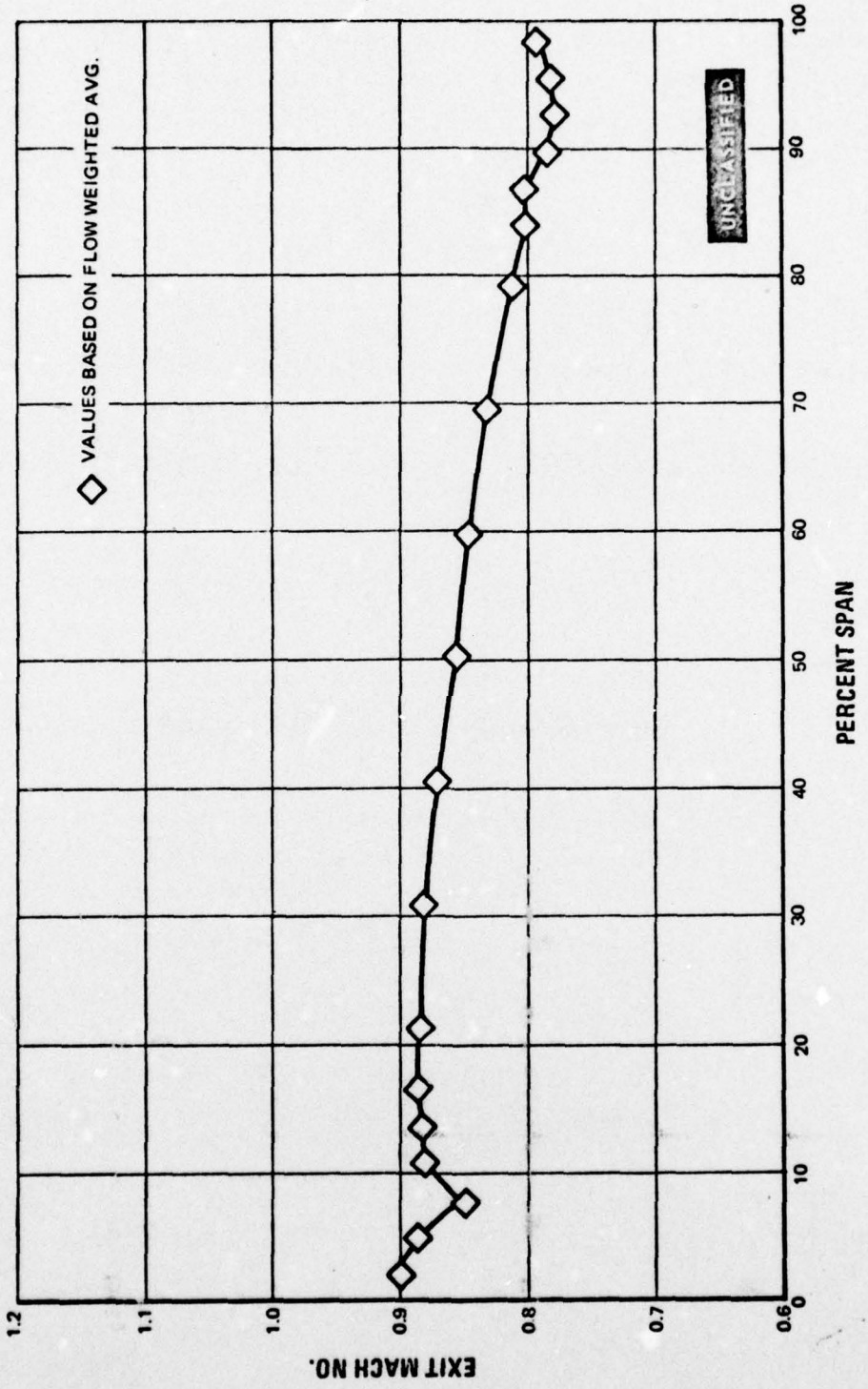

Figure 118 Spanwise Exit Mach Number Distribution, Second Vane Recambering Design B at Design Incidence. Midspan Exit Mach Number = 0.856

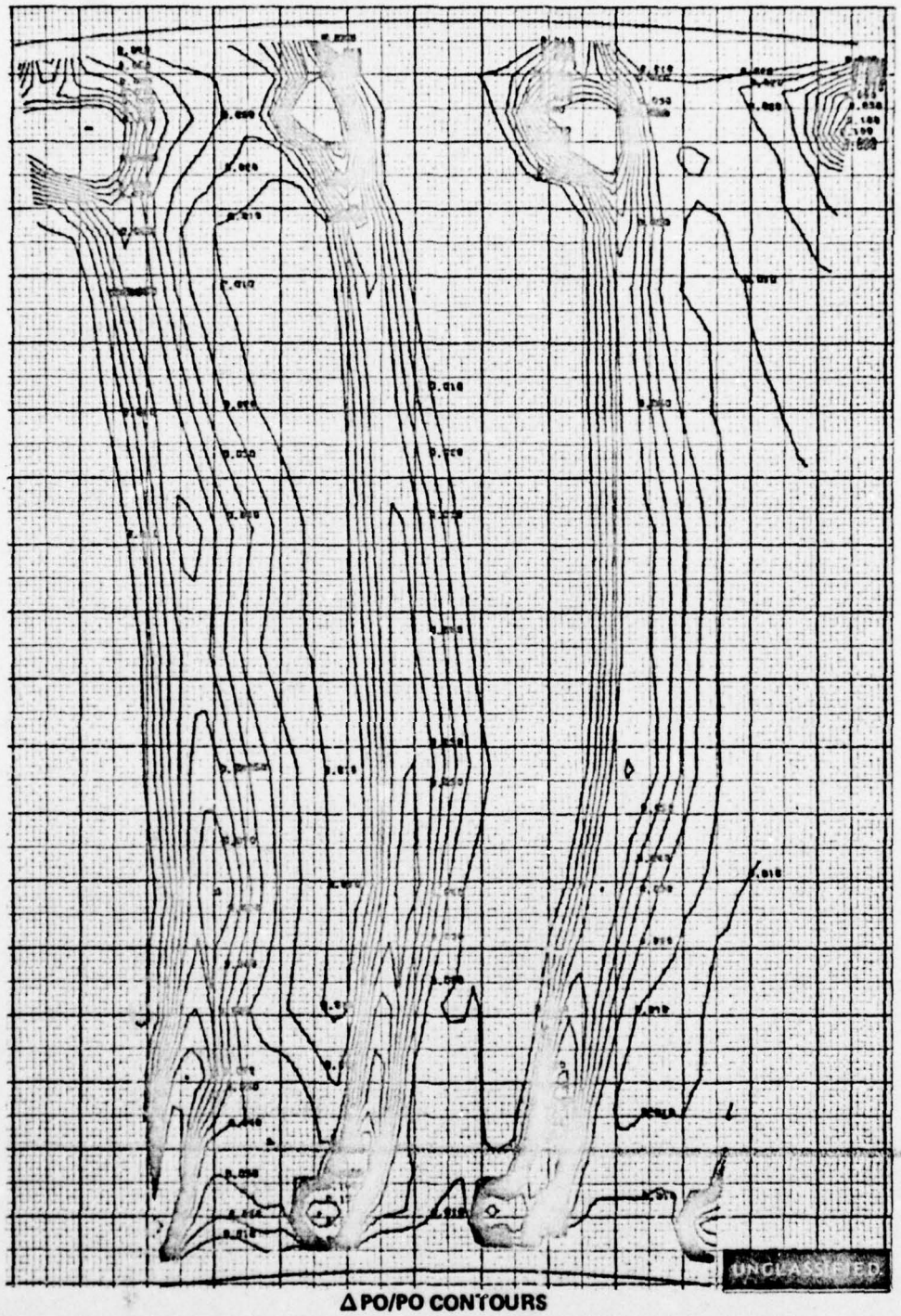

Figure 119 Pressure Loss Contours, Second Vane Recambering Design C at Design Incidence. Three Flow Passages. Midspan Exit Mach Number = 0.862

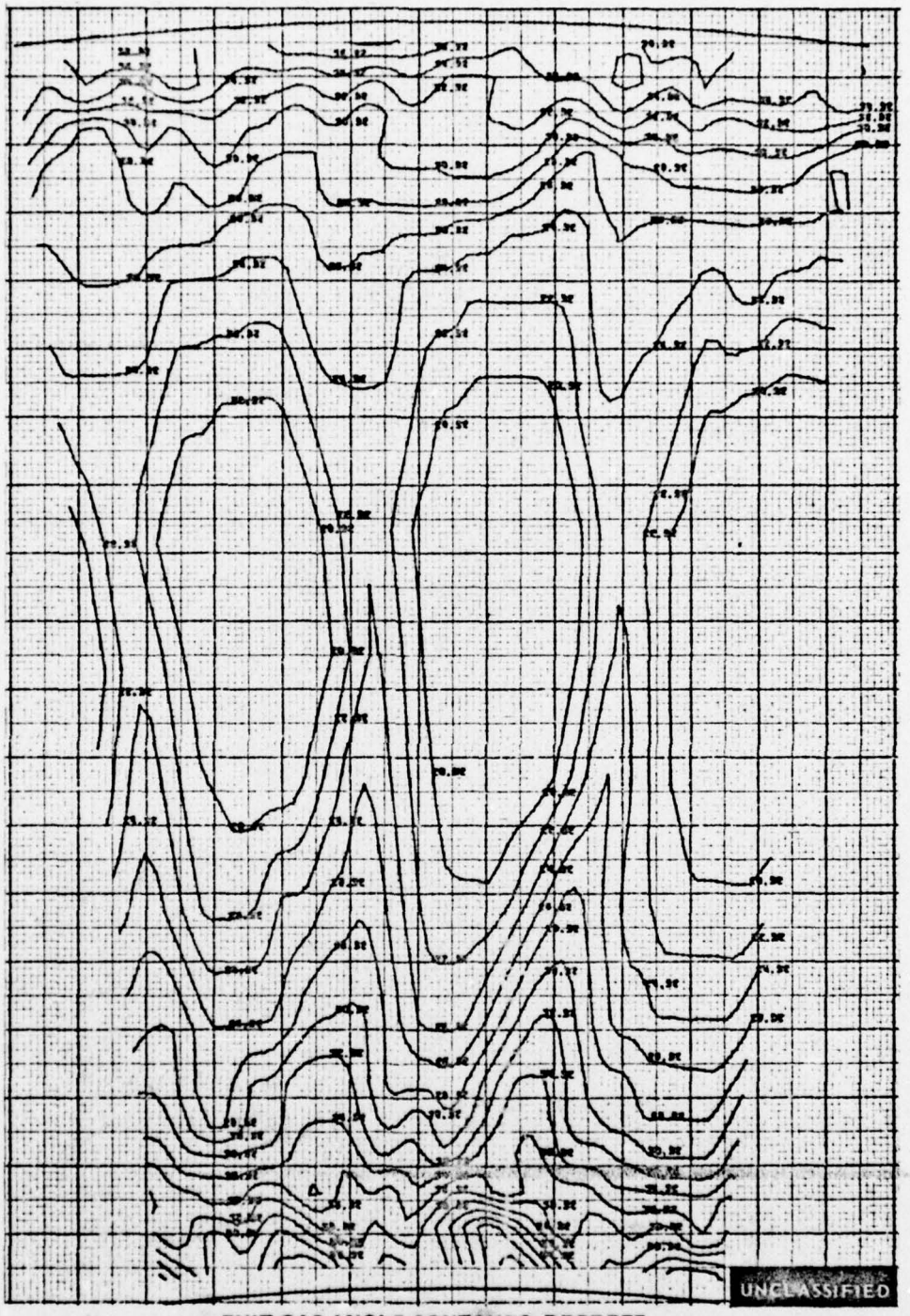

EXIT GAS ANGLE CONTOURS, DEGREES

Figure 120 Exit Gas Angle Contours, Second Vane Recambering Design C at Design Incidence. Three Flow Passages. Midspan Exit Mach Number = 0.862

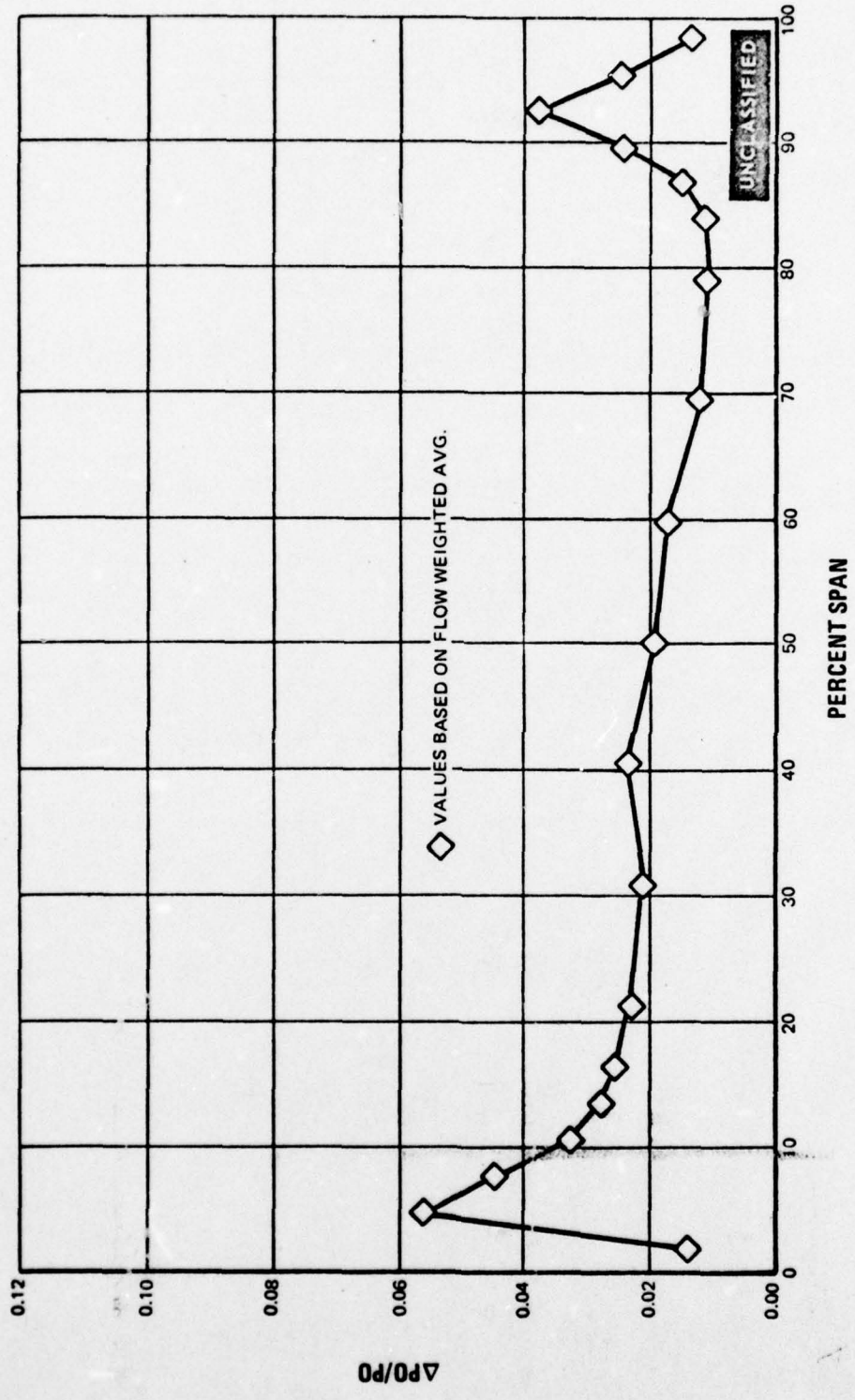

Figure 121 Spanwise Pressure Loss Distribution, Second Vane Recambering Design C at Design Incidence. Midspan Exit Mach Number = 0.862

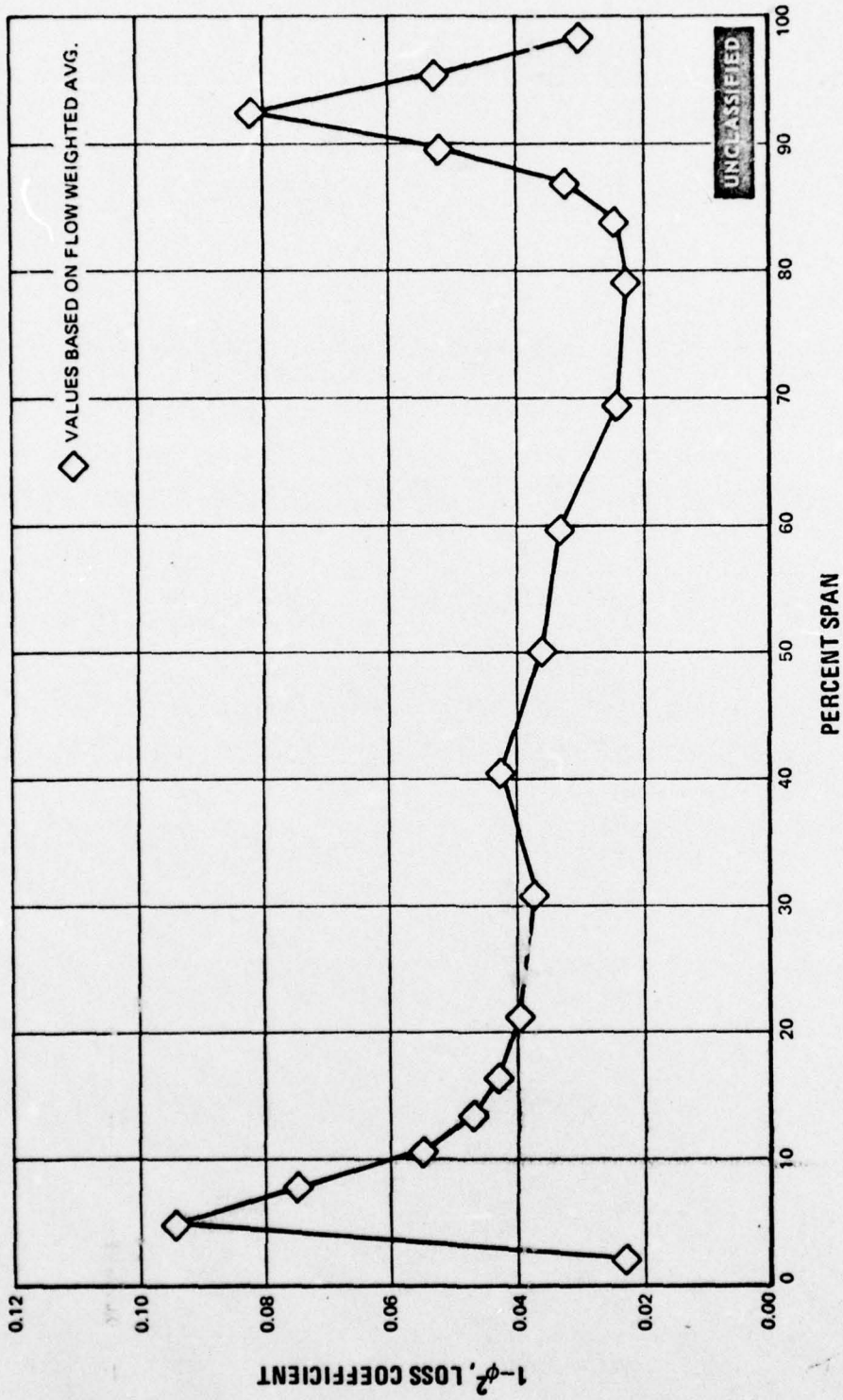

Figure 122 Spanwise Loss Coefficient Distribution, Second Vane Recambering Design C at Design Incidence. Midspan Exit Mach Number = 0.862

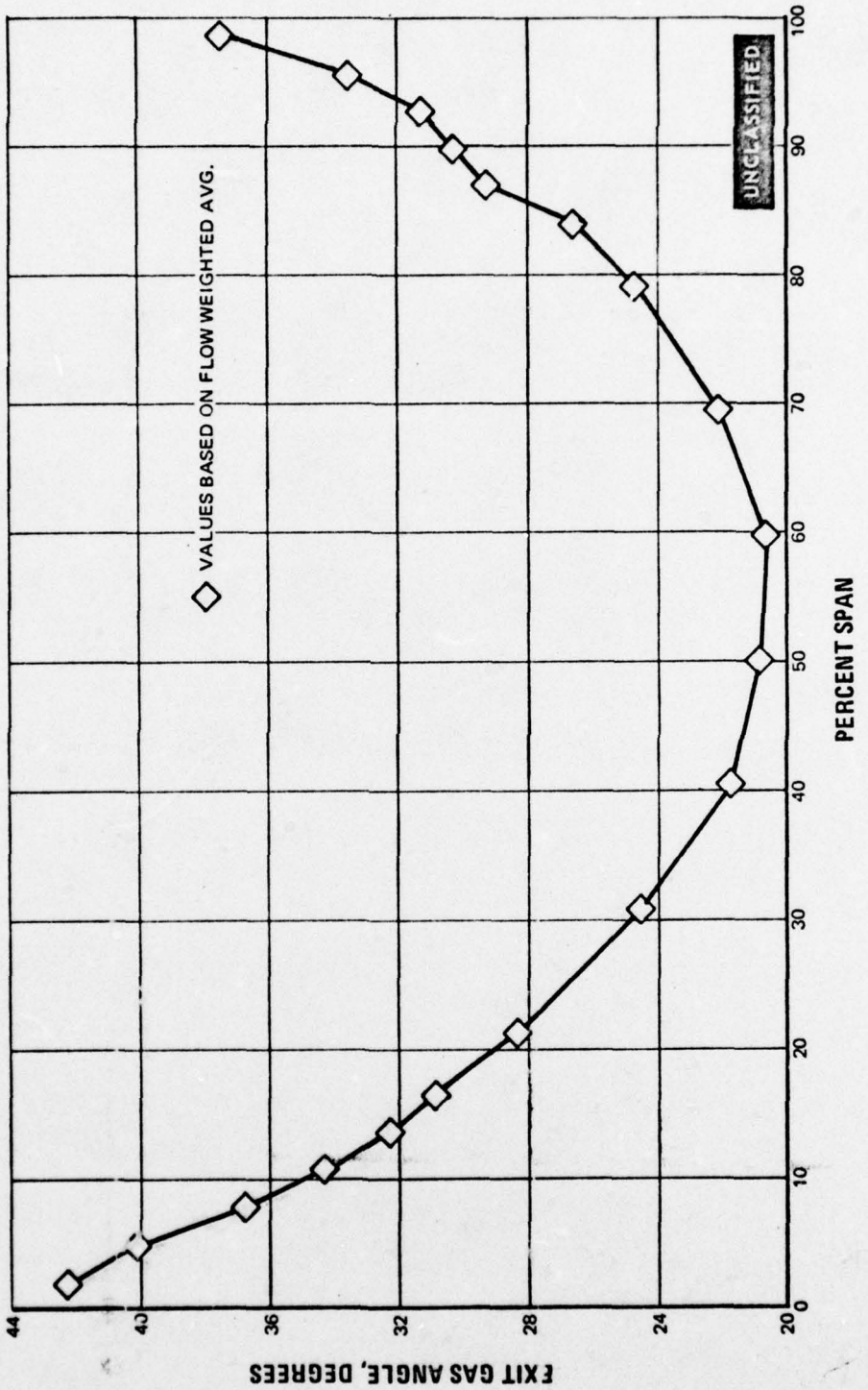

Figure 123 Spanwise Exit Gas Angle Distribution, Second Vane Recambering Design C at Design Incidence. Midspan Exit Mach Number = 0.862

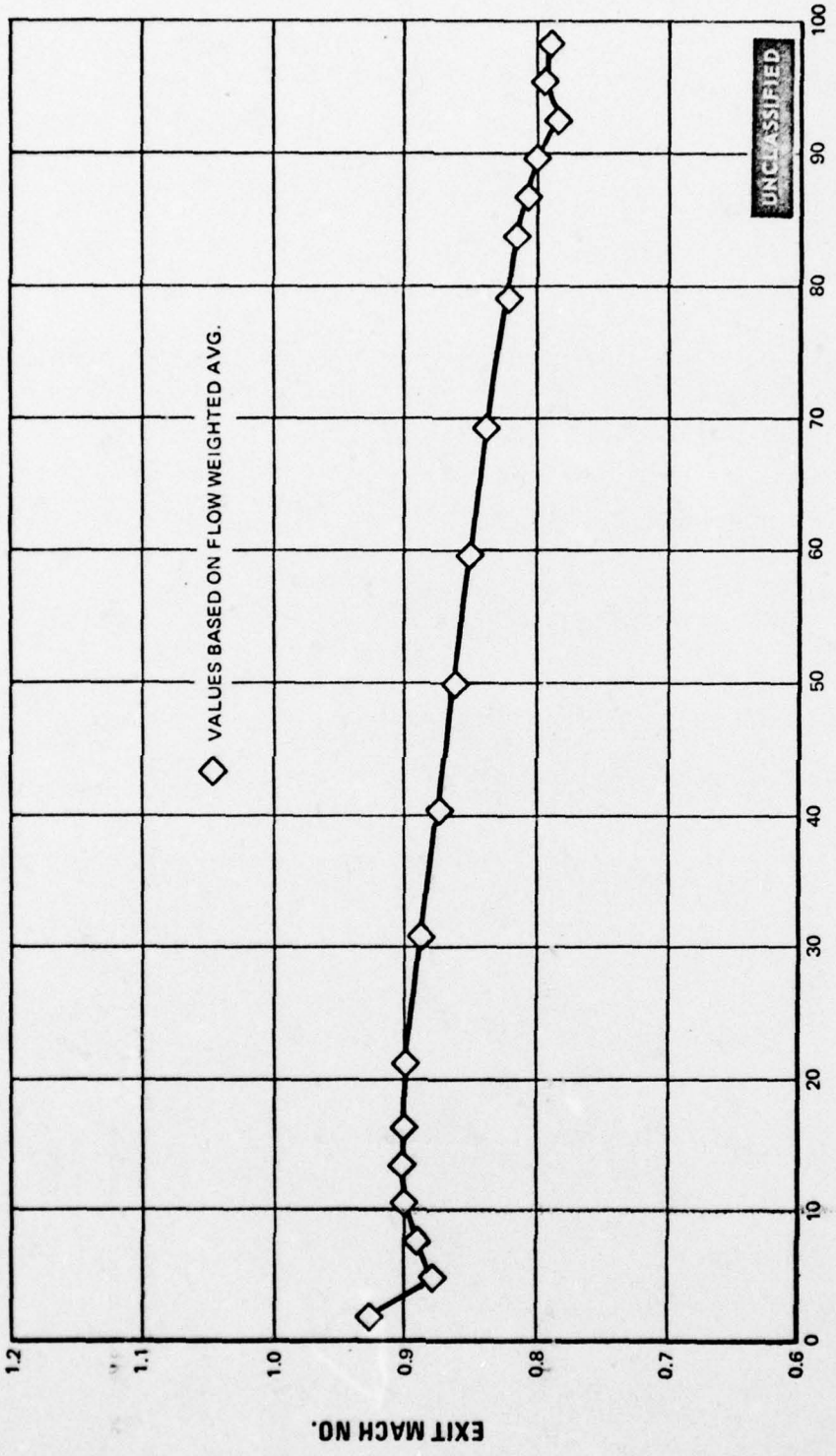

Figure 124 Spanwise Exit Mach Number Distribution, Second Vane Recambering Design C at Design Incidence. Midspan Exit Mach Number = 0.862

(U) The spanwise loss coefficient distribution for recambering design A is shown in Figure 125. For comparison, the loss coefficient distributions are included for the second vane baseline airfoil and for the baseline airfoil after the first recambering was applied. The peak loss near the inside diameter of design A agreed well with that for the first recambered test, but the integrated midspan-to-root loss coefficient increased from 0.029 to 0.036. The midspan-to-tip integrated loss decreased from 0.038 for the first recambering to 0.035 for design A, reflecting the effect of opening the tip exit angle by approximately 10 degrees. The overall integrated loss coefficient indicated a slight increase (0.036) as compared to that for the first recambering (0.033). Losses at the midspan were close to the loss levels for the baseline airfoil

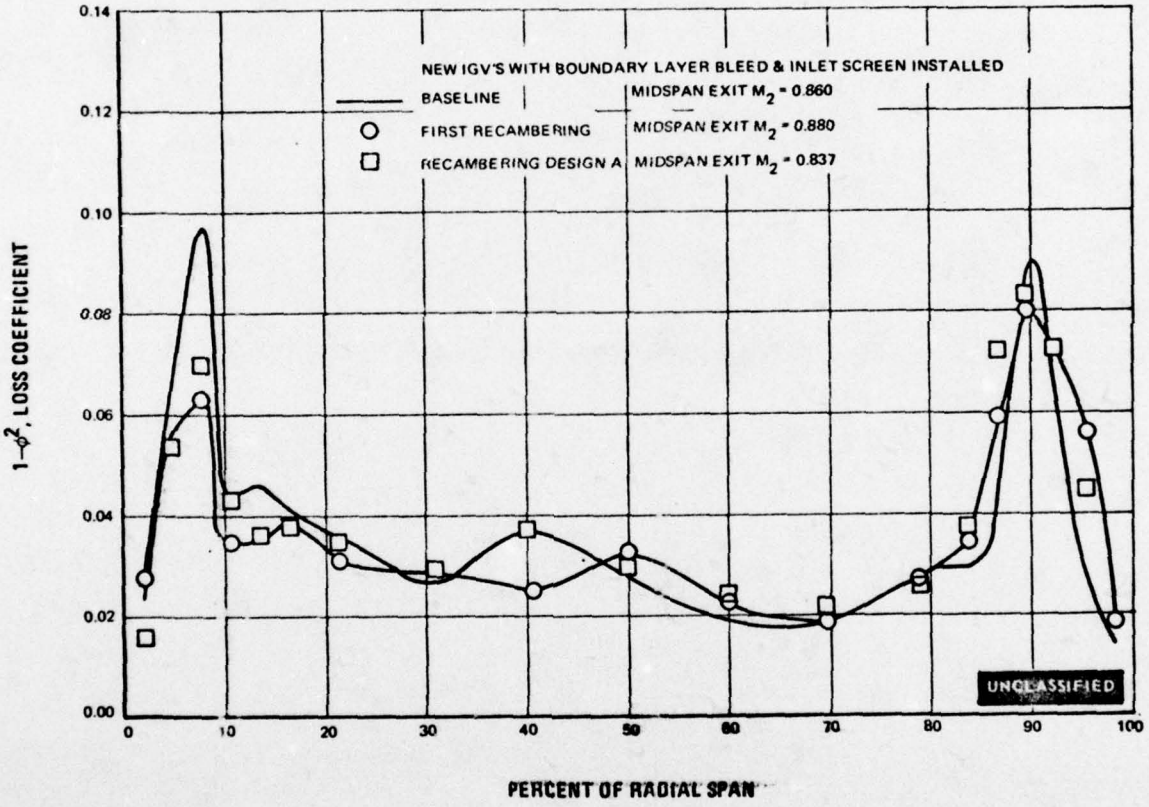

Figure 125 Spanwise Flow Weighted Loss Coefficient Distribution – Recambering Design A

(U) As noted above, the differences between the measured loss values of these airfoils are very small. Therefore, the loss values that are quoted are integrated flow-weighted values, since it is difficult to evaluate the differences by observing the spanwise loss distributions. The quoted values are the midspan design exit Mach number, arrived at by extrapolation of plotted test data. These values will be compiled in Table XXXII in the Summary.

(U) The spanwise loss coefficient distribution for recambering design B is shown in Figure 126 for comparision with the baseline and first recambering. Although the root exit angle was increased by approximately 8.5 degrees from the baseline airfoil design, the peak loss at the root was identical to the baseline value. The integrated midspan-to-root loss coefficients were also essentially the same, since the loss coefficient for the baseline foil was 0.035, while for design B it was 0.031. This compares to 0.036 for design A and 0.029 for the first recambered airfoil. The design B exit tip angle was increased by about 10 degrees above that for the baseline value. Again, the peak and integrated losses for design B were almost identical to the baseline airfoil. The integrated midspan-to-tip loss coefficient for the baseline airfoil was 0.035, while for design B it was 0.033. This compares to 0.035 and 0.038 for design A and the first recambered airfoil, respectively.

(U) A similar comparison of loss coefficients is made for recambering design C in Figure 127. For this design, the root exit angle was increased approximately 13.5 degrees and the tip exit angle was increased by approximately 15 degrees over the baseline airfoil angles. The root losses for design C were almost identical to design B, and slightly greater than the baseline airfoil value. The tip losses were lower (0.034) than both the baseline (0.035) and design A (0.035) and higher than design B (0.033), with the peak shifting closer to the wall. Design C had the highest overall loss coefficient (0.038) when compared to the baseline (0.035), design A (0.0350) and design B (0.032). The midspan loss for design C was greater than the baseline airfoil design.

(U) The measured exit gas angles agreed well with the airfoil design angles for three recambering changes. These are presented in Figures 128, 129 and 130. Although the inlet flow angles were not completely defined by mapping the test channel (only a single radial traverse was made), the exit angle measurements indicate that the airfoils were turning the flow to the desired value.

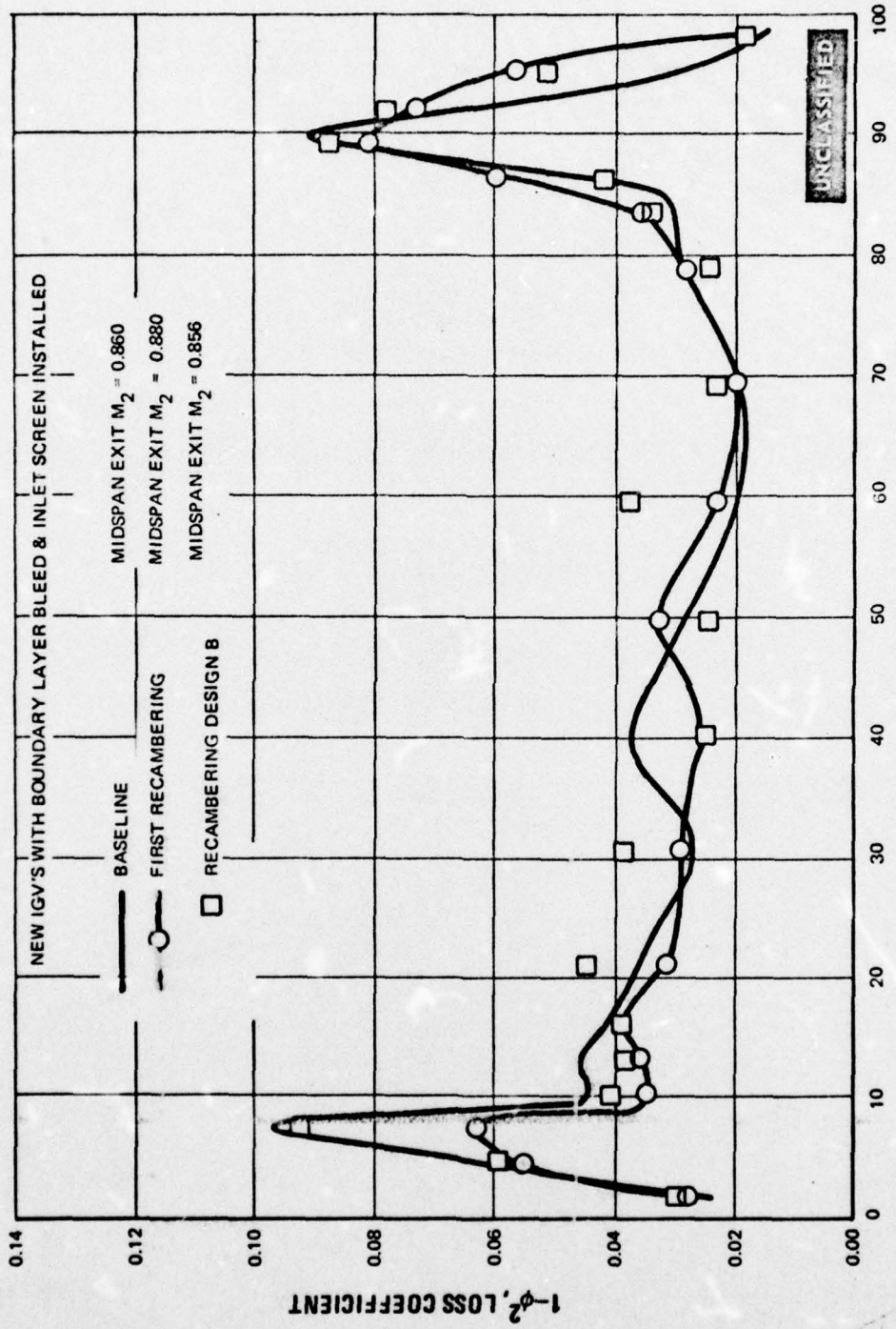

Figure 126 Spanwise Flow Weighted Loss Coefficient Distribution – Recambering Design B

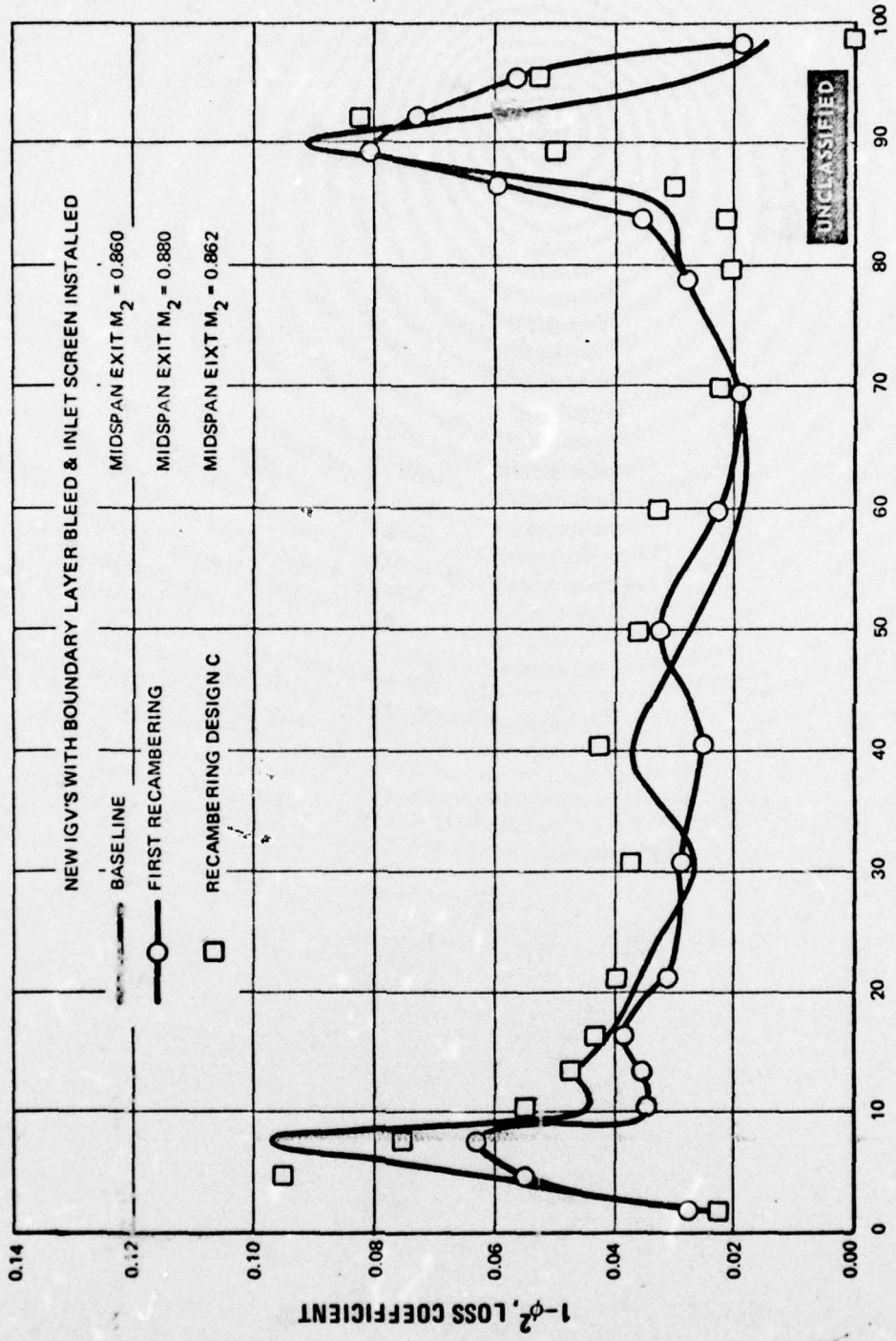

Figure 127 Spanwise Flow Weighted Loss Coefficient Distribution -- Recambering Design C

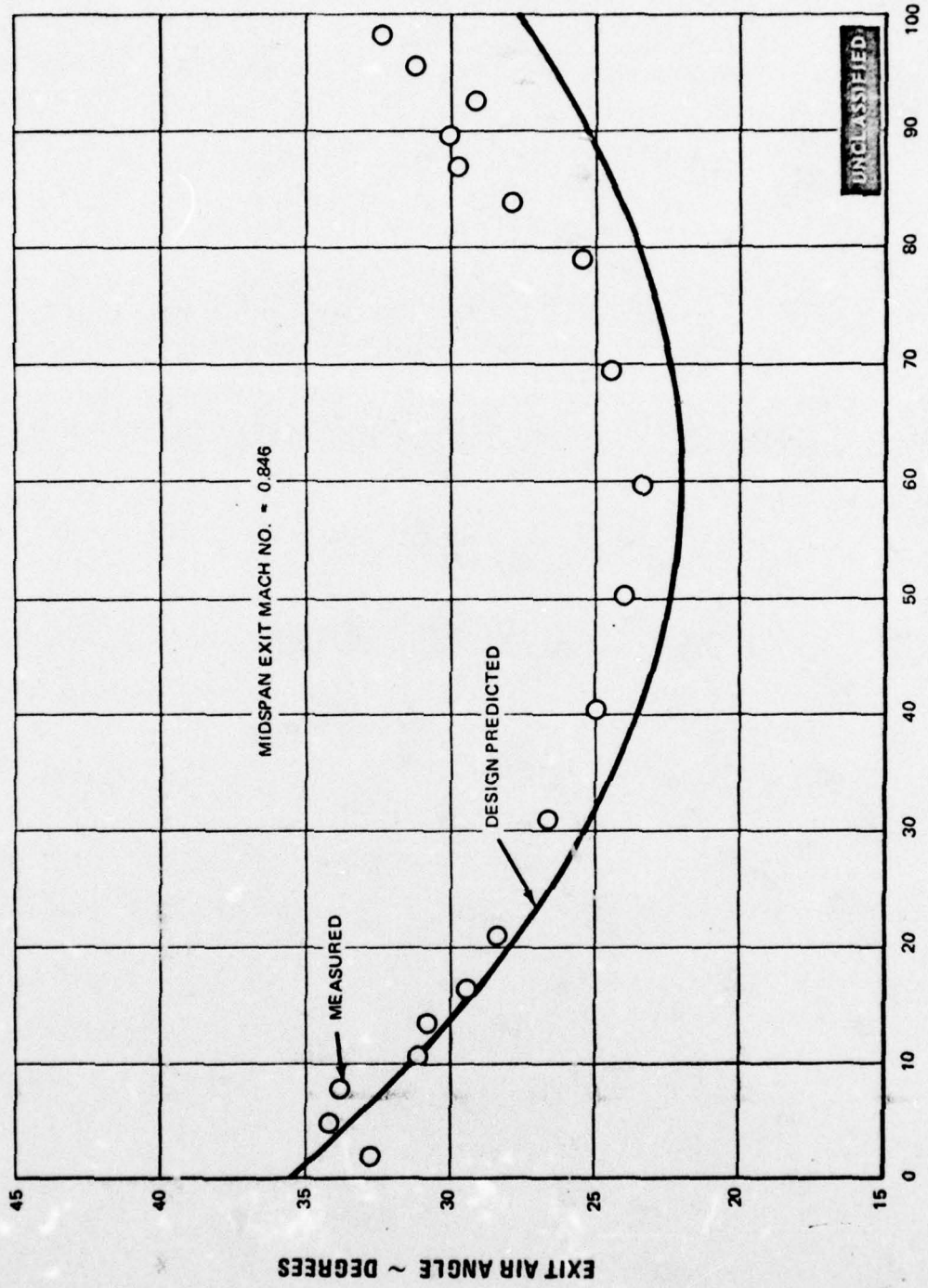

Figure 128 Measured Spanwise Exit Gas Angle Distribution – Recambering Design A

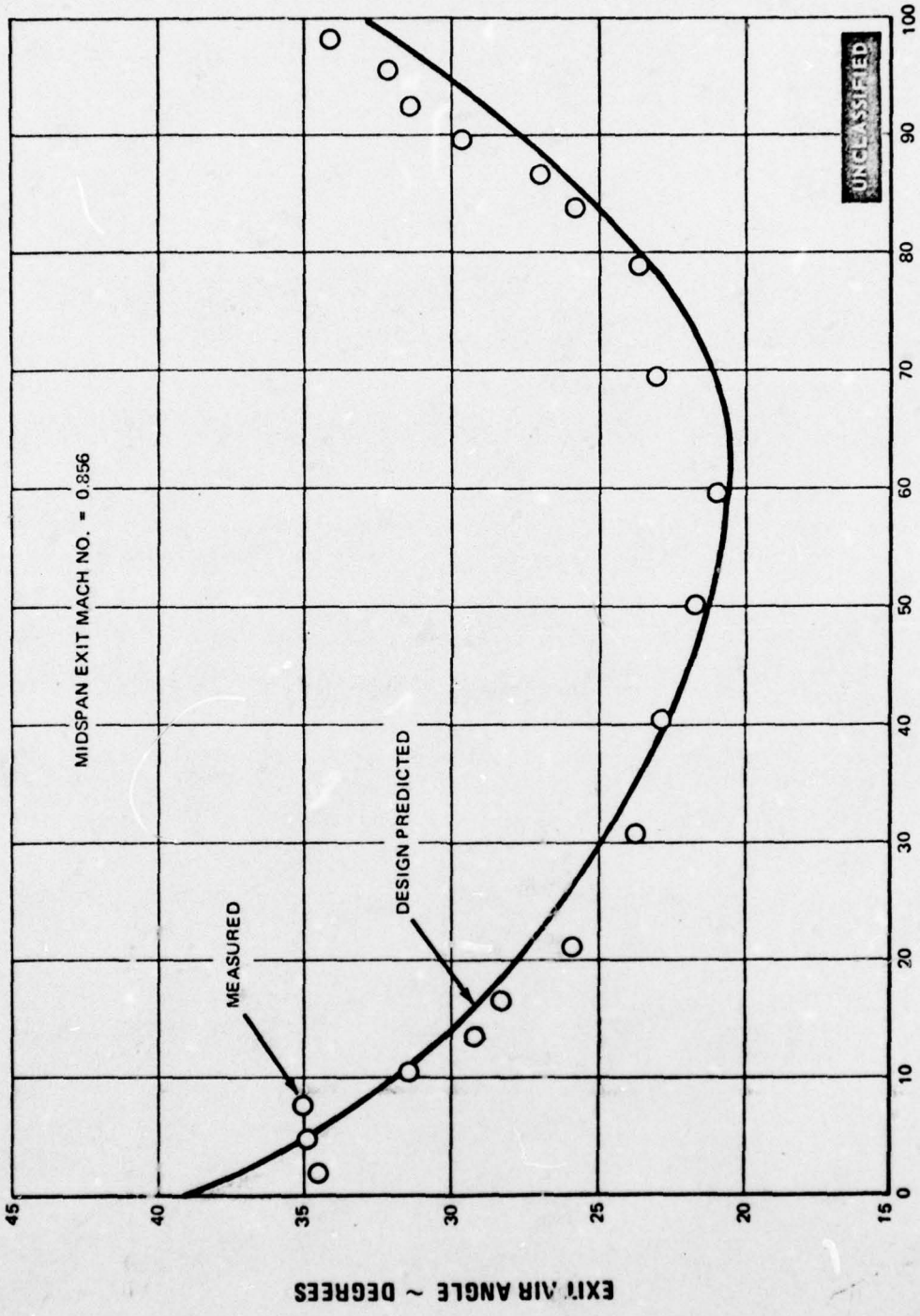

Figure 129 Measured Spanwise Exit Gas Angle Distribution – Recambering Design B

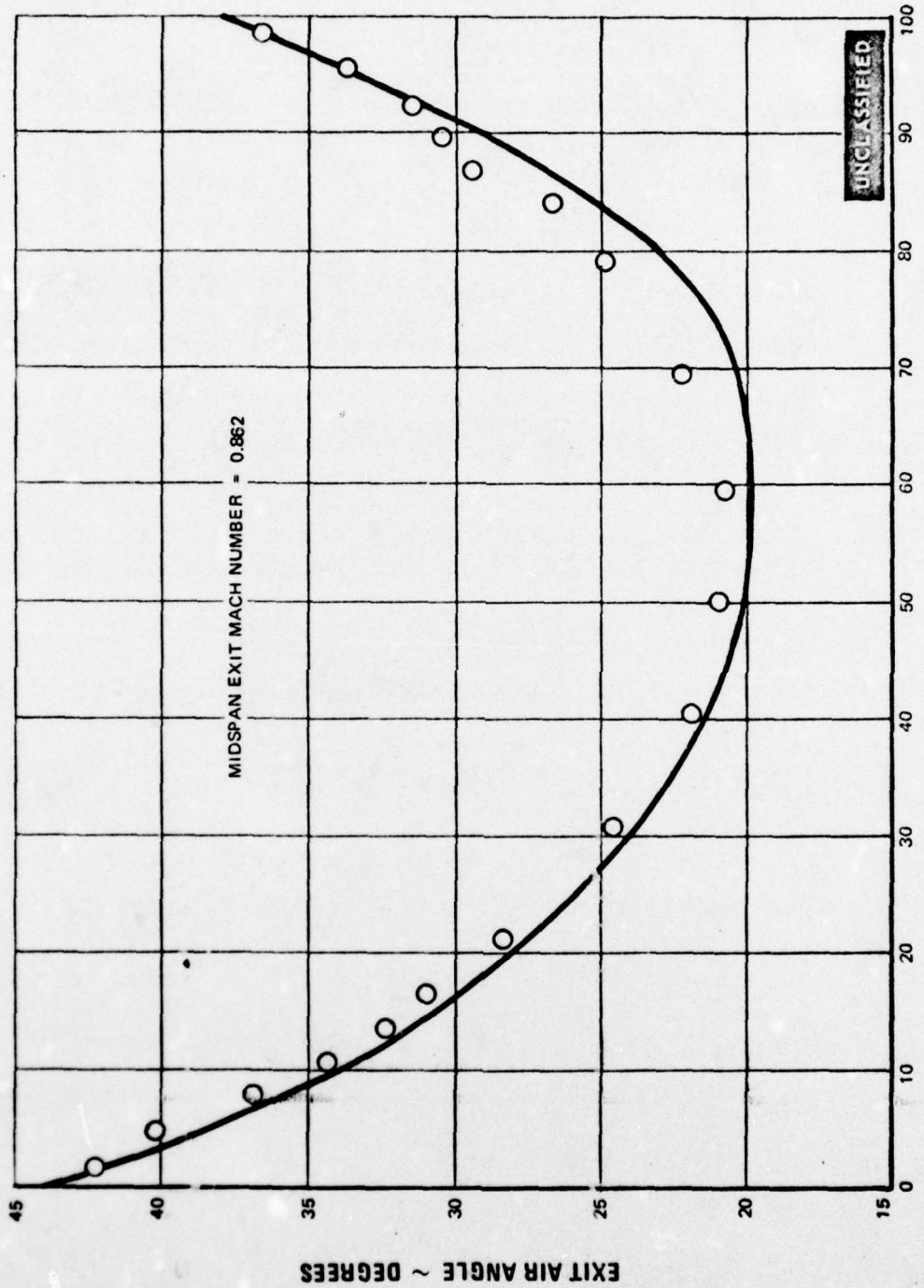

Figure 130 Measured Spanwise Exit Gas Angle Distribution – Recambering Design C

Design A exhibited a few degrees of underturning at the tip. The same order of magnitude of underturning was observed for the baseline test in the same region (Reference 4). This underturning disappears for designs B and C, indicating that better control of flow was obtained in the tip section.

(U) There was very small effect of Mach number variation on loss coefficient for the recambered airfoils. This is seen in Figure 131. None of the airfoils exhibited a transonic drag rise over the Mach number range tested. The Reynolds number was not held constant during these tests, and any variation of loss may be partly attributed to the fact that Reynolds number increased with Mach number in the annular segment cascade. The plane cascade tests of the baseline airfoil sections (Section III), where Reynolds number could be controlled idependently of Mach number, indicated that there was only a small effect of Reynolds number on loss within the range of that investigation.

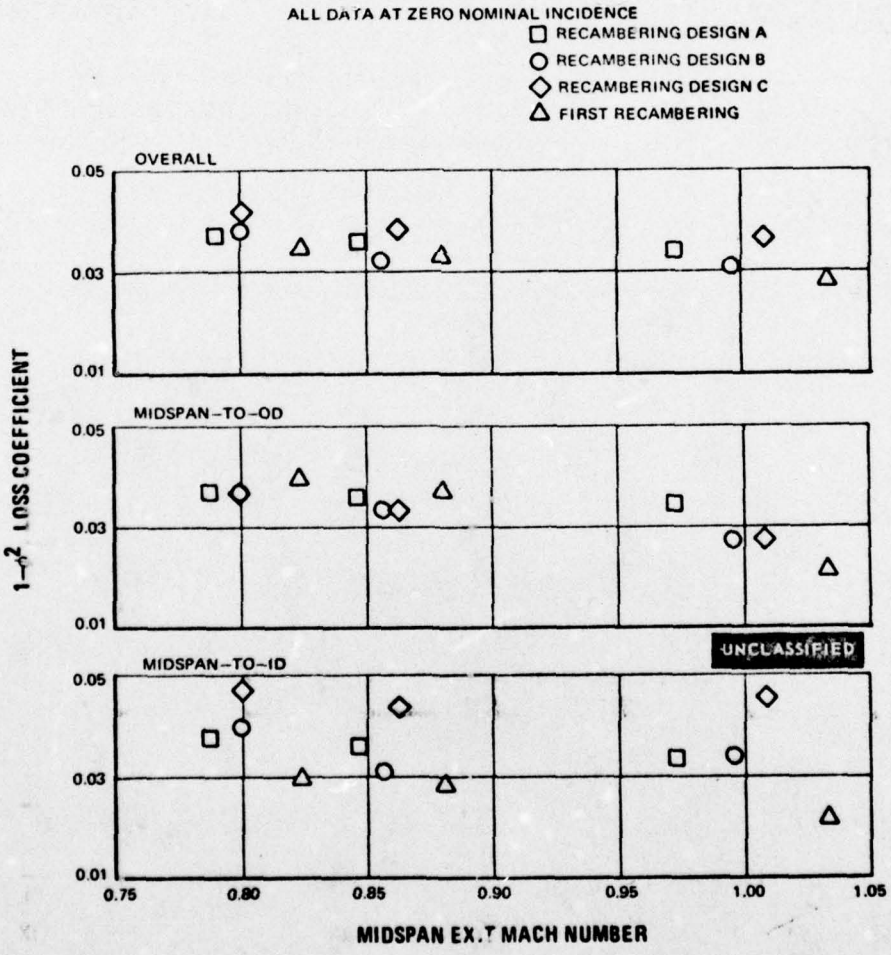

Figure 131 Effect of Mach Number on Loss for the Various Recambering Designs

(U) As was done in the previous tasks, a mixture of oil and graphite was painted on the airfoils in order to provide additional information about the behavior of the flow in these recambered airfoil cascades. Photographs of the resulting patterns were taken and are shown in Figures 132 and 133 for recambering design A, in Figures 134 and 135 for design B, and in Figures 136 and 137 for design C. These patterns indicate that the flow remained attached on the airfoils and end-walls. Cross-flow patterns can be seen from these photographs at the walls, but no separation on these walls in the vicinity of the airfoils was detected.

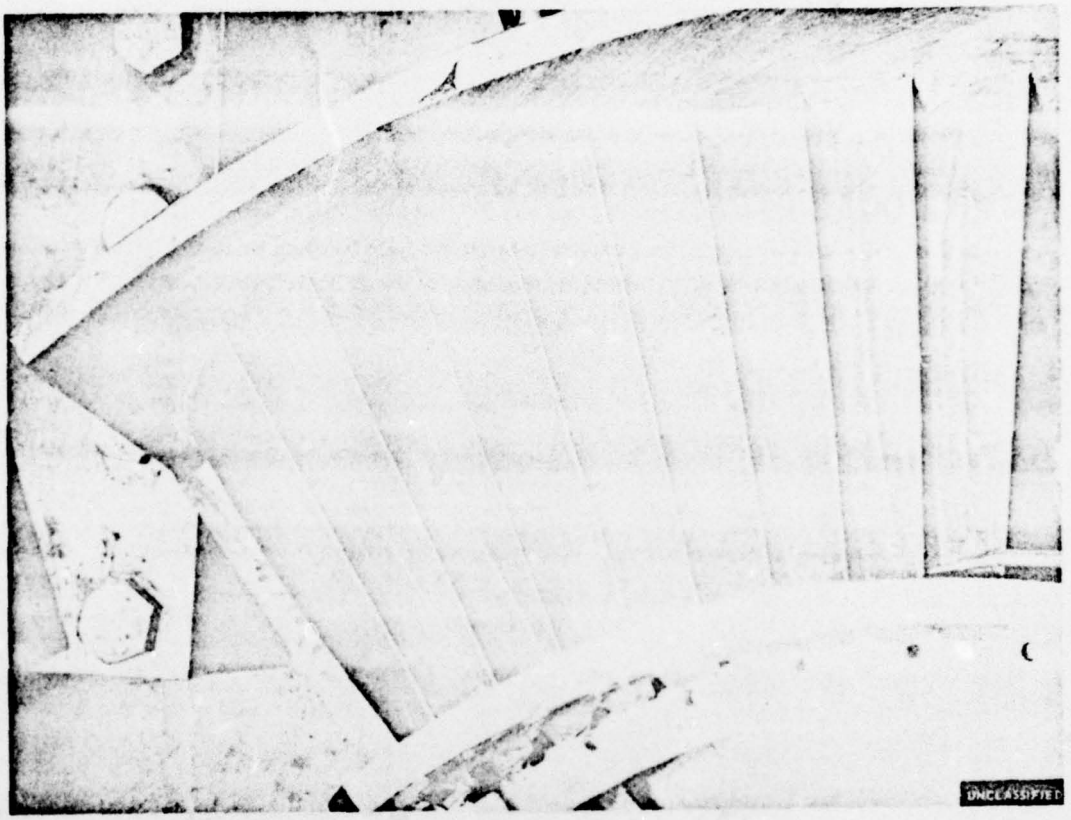

Figure 132 Oil and Graphite Flow Patterns, Second Vane Recambering Design A, Mach No. = 0.846 (FE95157)

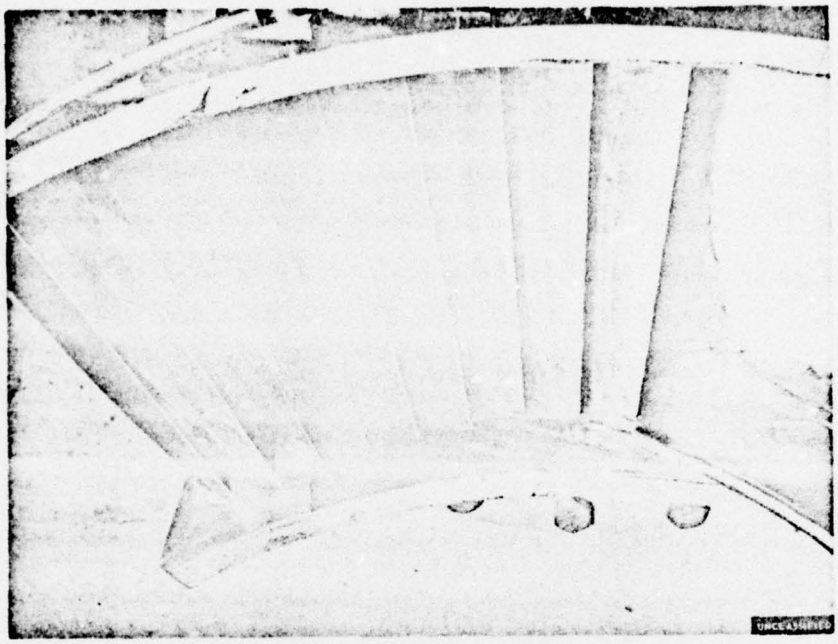

Figure 133 Oil and Graphite Flow Patterns, Second Vane Recambering Design A, Mach No. = 0.846 (FE95158)

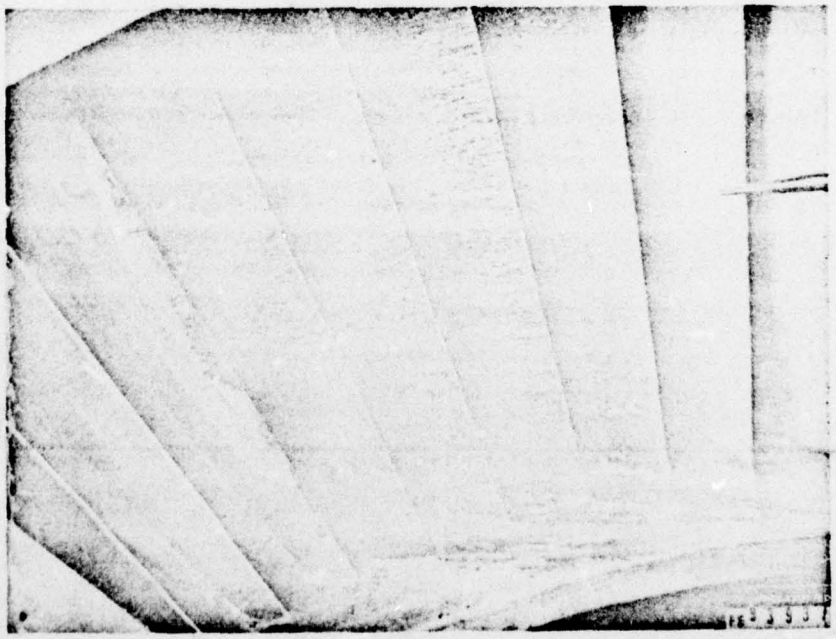

Figure 134 Oil and Graphite Flow Patterns, Second Vane Recambering Design B, Mach No. = 0.856 (FE93931)

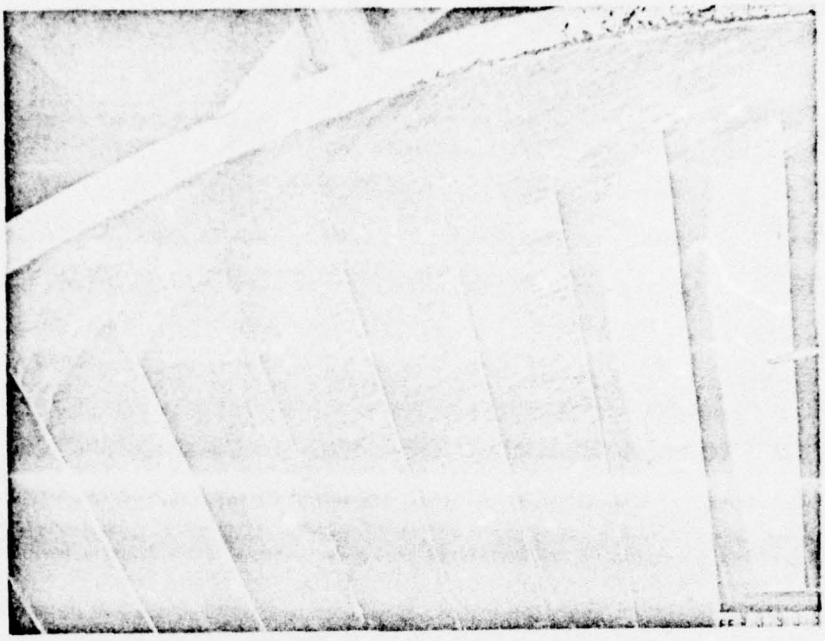

Figure 135 Oil and Graphite Flow Patterns, Second Vane Recambering Design B, Mach No. = 0.856 (FE 93939)

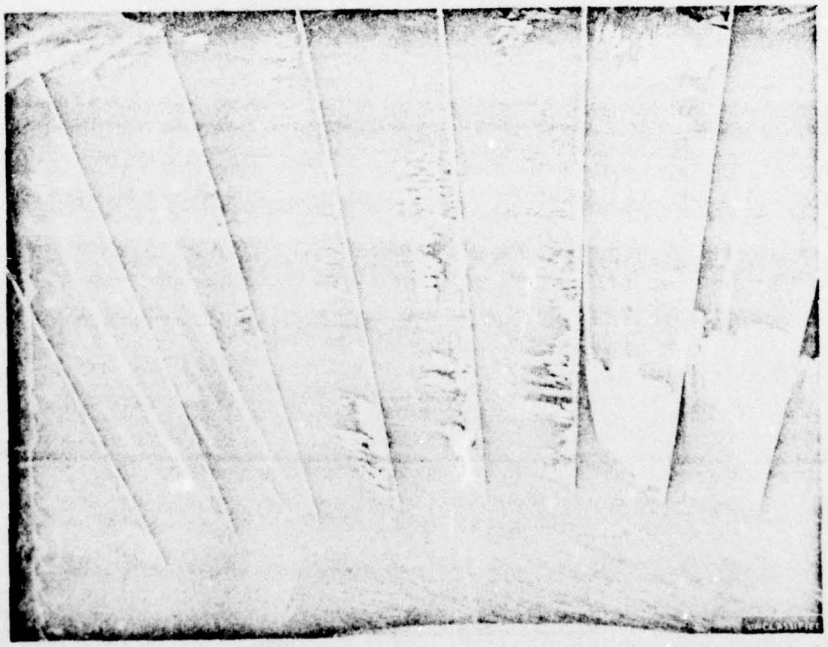

Figure 136 Oil and Graphite Flow Patterns, Second Vane Recambering Design C, Mach No. = 0.862 (FE95165)

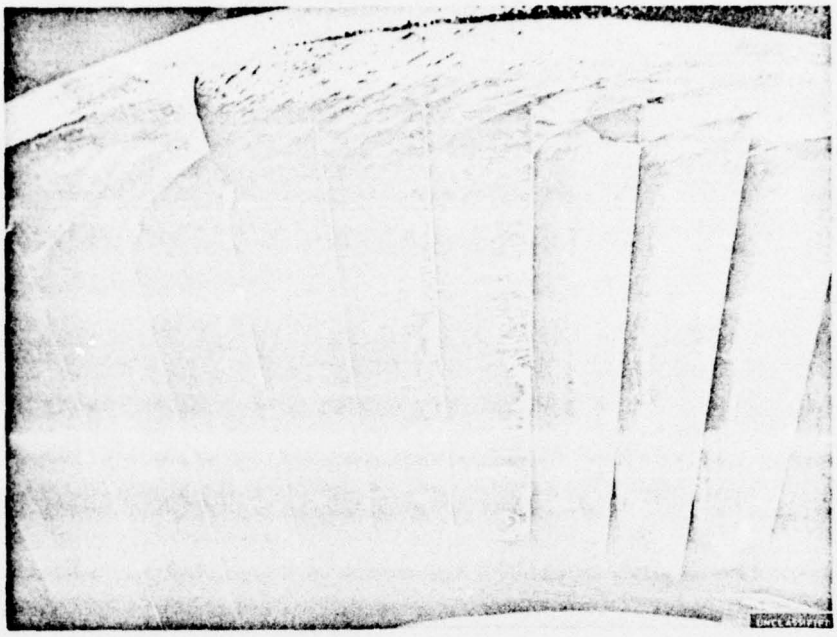

Figure 137 Oil and Graphite Flow Patterns, Second Vane Recambering Design C, Mach No. = 0.862 (FE95166)

5. SUMMARY

(U) Results of the second vane recambering test evaluation at zero incidence and at nominal design exit Mach number are tabulated in Table XXXII. During these tests, three levels (approximately 5, 10 and 15 degrees) of local uncambering at the end-walls were investigated. With such large changes in local airfoil geometry, the end-wall losses could not be substantially reduced. The 10 degree uncambered cascade (Design B) had a slightly lower overall loss than the 5 and 15 degree uncambered cascades (Designs A and C, respectively). The root end loss was the lowest for recambering design B with small differences in tip end loss for the three recambered designs. Midspan profile losses increased as expected with an increasing amount of midspan overcambering applied in each of the three cascades to maintain constant overall work. The exit flow angles for recambering designs A, B and C behaved in a predictable manner, indicating that such uncambering can be a potentially useful technique for improving entrance flow conditions for the following row of airfoils.

(U) This Task IIIa information will be applied in the demonstrator turbine design (Phase IV). Data shows that the overall loss coefficient for the same overall work was only slightly affected by a large redistribution of turning. Furthermore, the data indicates that a slight reduction of end-wall loss results from a small amount of the type of recambering that was investigated. As a result, the final design studies (Phase IV) will attempt to gain some advantage from the direct and indirect benefits of such recambering. The indirect benefits include better flow control and better spanwise distribution.

TABLE XXXII

COMPARISON OF LOSS COEFFICIENTS FOR SECOND VANE RECAMBERING
CORRECTED TO DESIGN POINT MACH NUMBER = 0.869
ZERO INCIDENCE

	MEASURED LOSS COEFFICIENT, $1-\phi^2$		
Airfoil	Midspan-To-Root	Midspan-To-Tip	Overall
Baseline	0.035	0.035	0.035
First Recambering	0.029	0.038	0.033
Recambering Design A	0.036	0.035	0.036
Recambering Design B	0.031	0.033	0.032
Recambering Design C	0.044	0.034	0.038

UNCLASSIFIED

6. TEST PROCEDURE

(U) The test procedure employed during this task was identical to that of the Task II b baseline evaluation. This procedure was described in complete detail in Reference 3.

SECTION VI

OFF-DESIGN EVALUATION (TASK IIIb AND IIIc)

1. RFP OBJECTIVE

(U) Determine the effect of off-design operation on the aerodynamic performance of the selected airfoil geometries having the optimum boundary control method applied.

2. TASK OBJECTIVE

(U) The purpose of these tasks was to evaluate off-design performance of the airfoil geometries which showed optimum end-wall losses during the Task IIIa investigation. These cascades were tested at three Mach numbers, including the design point, and at positive and negative incidence angles. The incidence angle was varied by changing the inlet guide vane geometry. Exit flow survey data were obtained and local and integrated losses and flow angle deviation were evaluated. This data will provide the basis for the airfoil loss system which will be integrated with the turbine design system.

3. CASCADE PACK DESIGN

(U) New turning vane assemblies were fabricated for the off-design evaluations. Initially, it was decided to test at ±10 degree incidence. However, in order to build the ±10 degree incidence inlet guide vane, a new inlet bellmouth would have to have been fabricated. The largest negative incidence guide vane which could have been fabricated within the second vane bellmouth limitations was -6 degrees. This, therefore, was the negative incidence at which the tests were run. There was no problem in attaining the +10 degrees incidence inlet guide vanes for the bellmouth design on hand.

4. DISCUSSION

(U) Four airfoils were tested at incidence angles of +10 degrees and -6 degrees. These airfoils included the second vane baseline airfoil, the second vane with first recambering, recambering design A, and recambering design C. The results of these off-design tests will be discussed in the same order, and later tabulated in the Summary (Table XXXIII).

(U) The baseline airfoil performance data at an incidence angle of +10 degrees are presented for an exit midspan Mach number of 0.835 in Figures 138 through 143. Care was taken to choose a passage that was free of inlet guide vane wakes for spanwise evaluations. As in Reference 4, the following is included whenever "performance data" is referred to in this Report:

- total pressure loss contour plots
- exit gas angle contour plots
- average spanwise total pressure loss distribution
- average spanwise loss coefficient distribution
- average spanwise exit flow angle distribution
- average spanwise exit Mach number distribution

(U) The performance data are presented for an incidence angle of -6 degrees at a mid-span exit Mach number of 0.865 in Figures 144 through 149. Baseline airfoil comparisons of the spanwise loss coefficient distribution at +10 degrees incidence with zero incidence and -6 degrees incidence with zero incidence are shown in Figures 150 and 151, respectively. The root end-wall losses were greater at the positive incidence, and less at the negative incidence than the zero incidence values. The tip end-wall losses at the positive incidence were almost identical at the zero incidence, and again less than zero incidence for the negative incidence condition. On an overall integrated basis, the positive incidence loss coefficient was greater, and the negative incidence loss coefficient was less than the zero incidence value. The measured exit gas angles for positive and negative incidence are shown in Figures 152 and 153, respectively. These results indicate that the measured angles were, in general, in close agreement with the predicted values as was the case for previous tests (Task III a). Oil and graphite flow visualization tests were made on the test airfoils at both incidence angles and these are shown in Figures 154 through 157. These photographs indicate attached flow over the airfoil and end-walls and, as in the zero incidence case, some radial inflow at the end-walls due to the usual suction surface corner vortex.

(U) Performance data for the second vane first recambered airfoil are shown in Figures 158 through 163 at the positive incidence angle of +10 degrees. Similar data for the negative incidence of -6 degrees are shown in Figures 164 through 169.

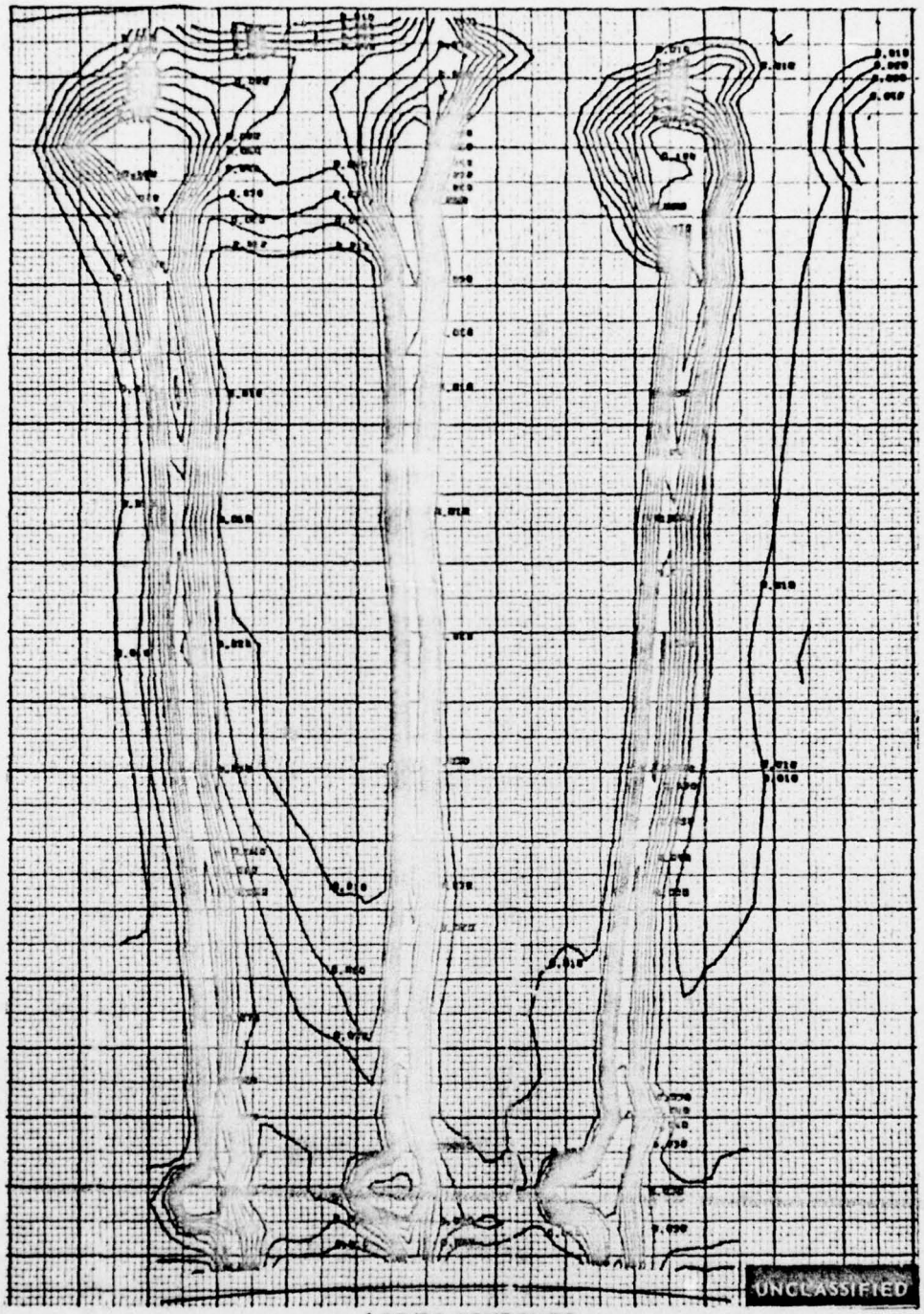

Figure 138 Pressure Loss Contours, Second Vane Baseline at +10° Incidence. Three Flow Passages. Midspan Exit Mach Number - 0.835

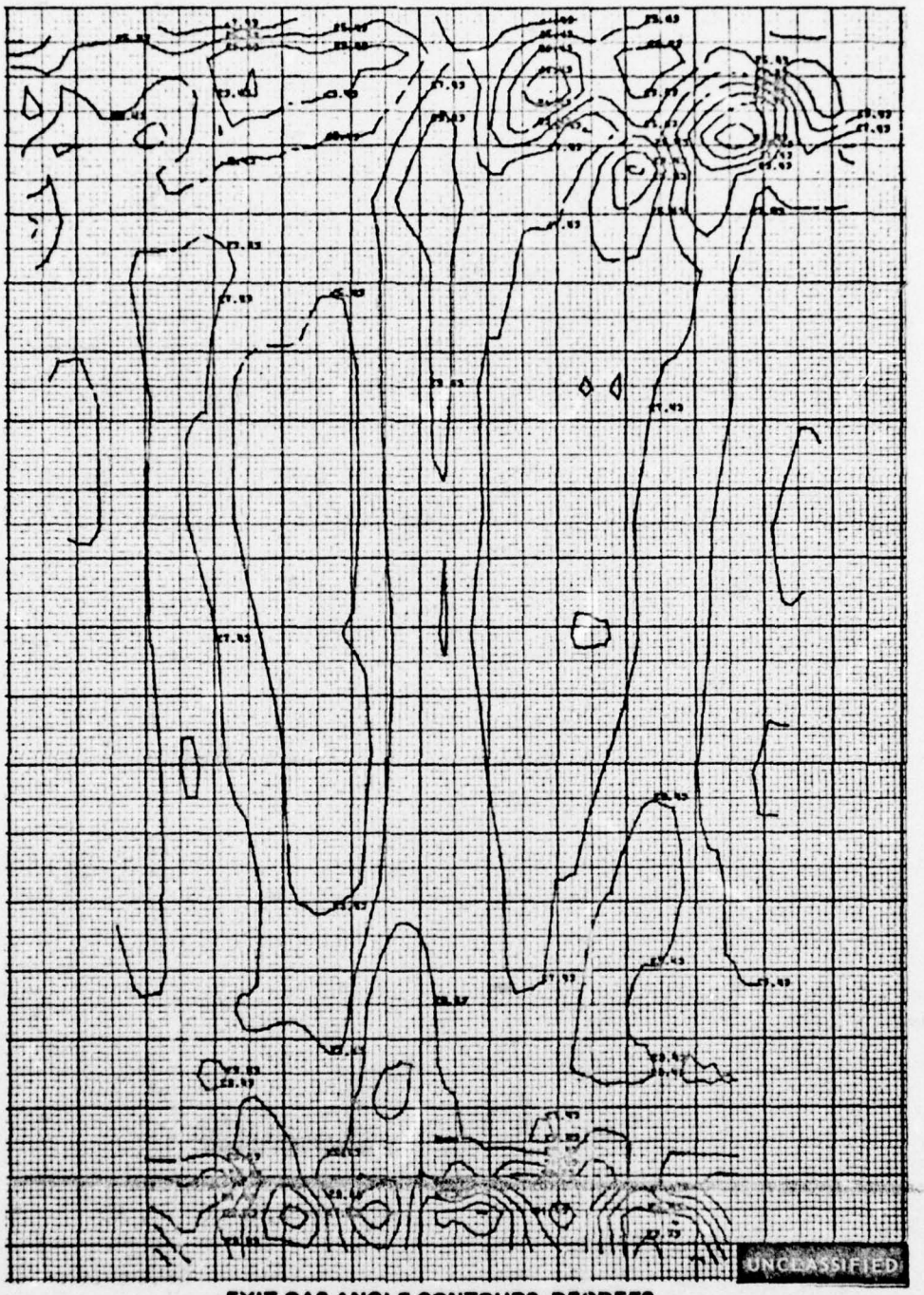

Figure 139 Exit Gas Angle Contours, Second Vane Baseline at +10° Incidence. Three Flow Passages. Midspan Exit Mach Number = 0.835

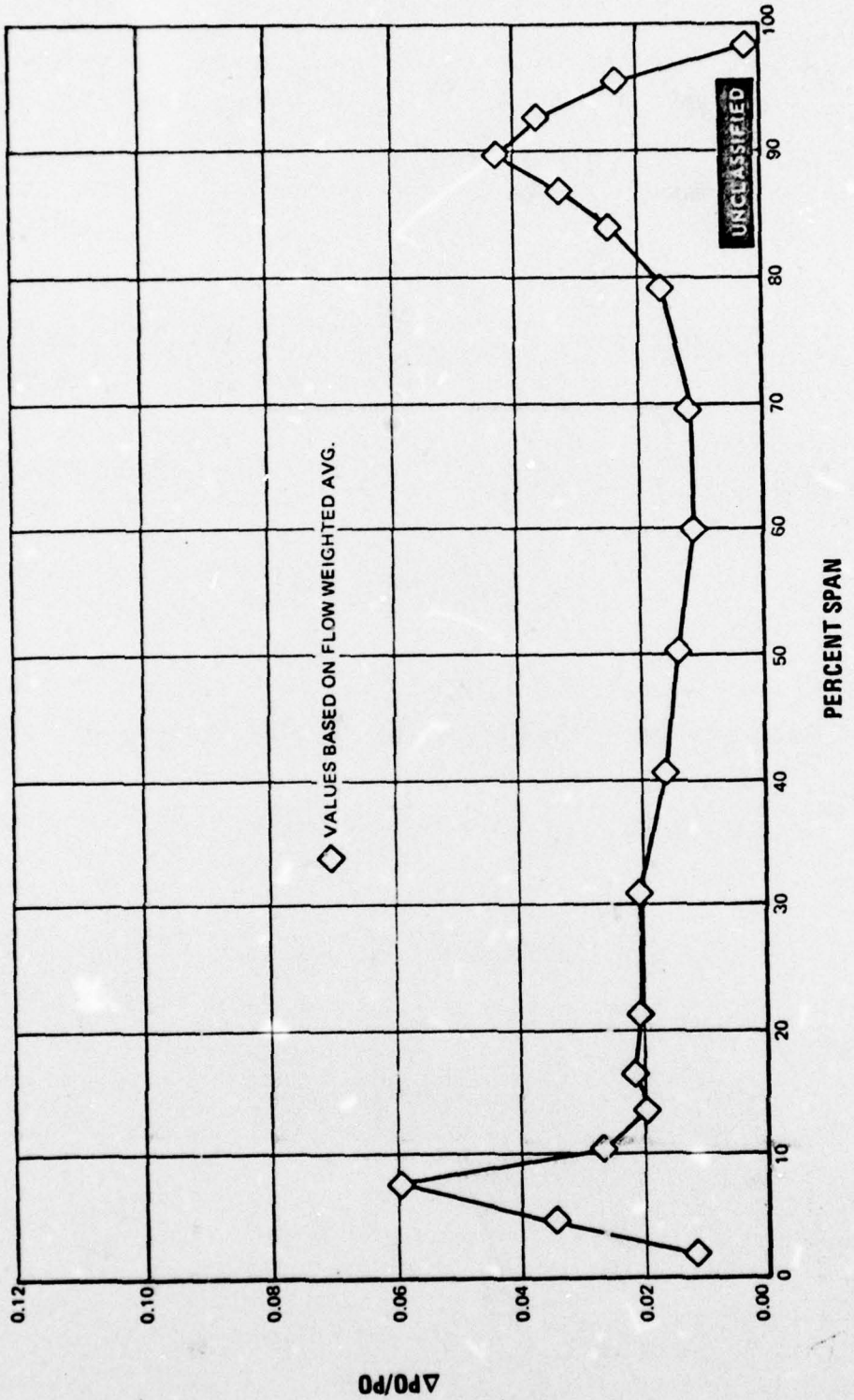

Figure 140 Spanwise Pressure Loss Distribution, Second Vane Baseline at +10° Incidence. Midspan Exit Mach Number = 0.835

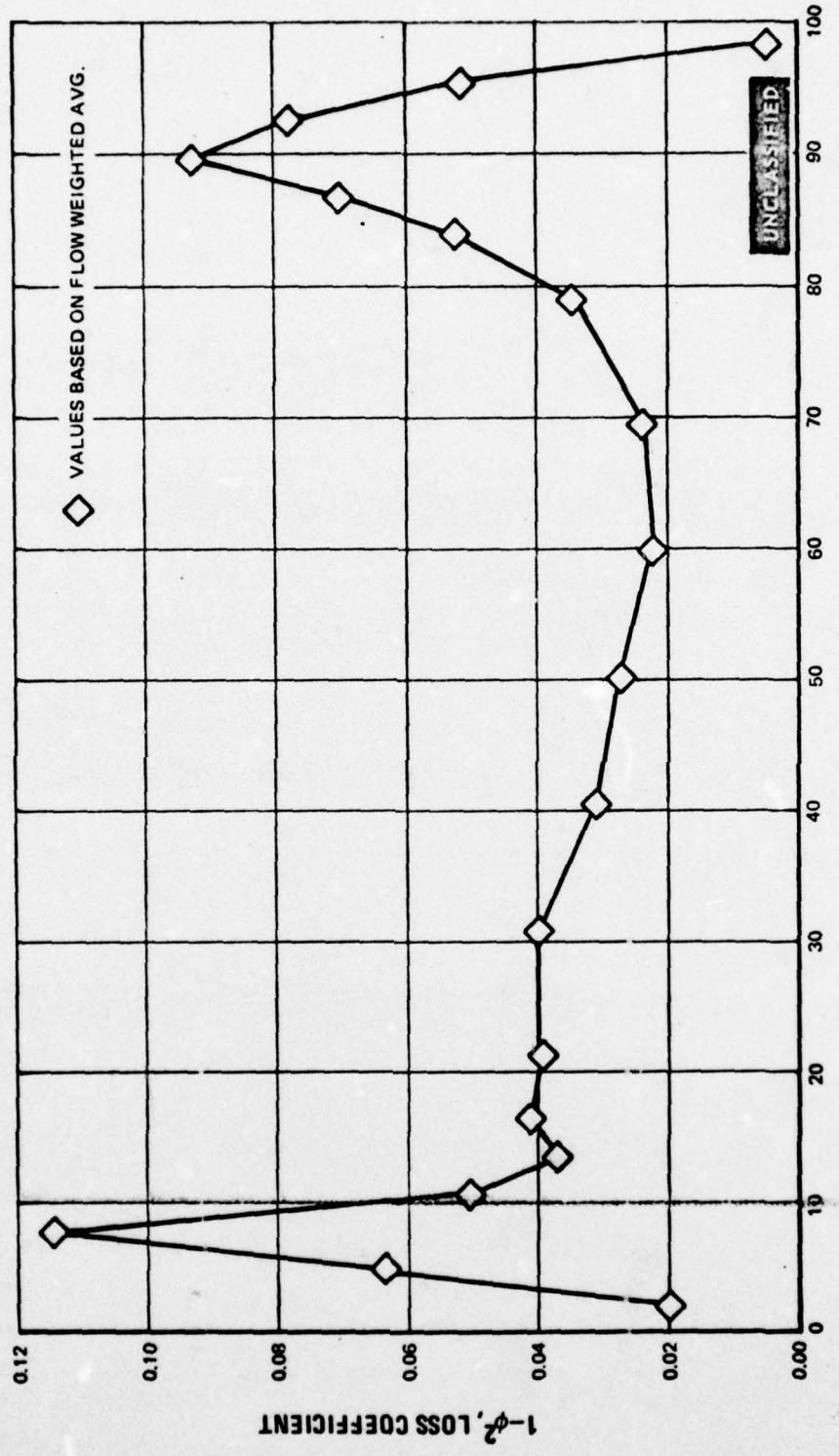

Figure 141 Spanwise Loss Coefficient Distribution, Second Vane Baseline at +10° Incidence. Midspan Exit Mach Number = 0.835

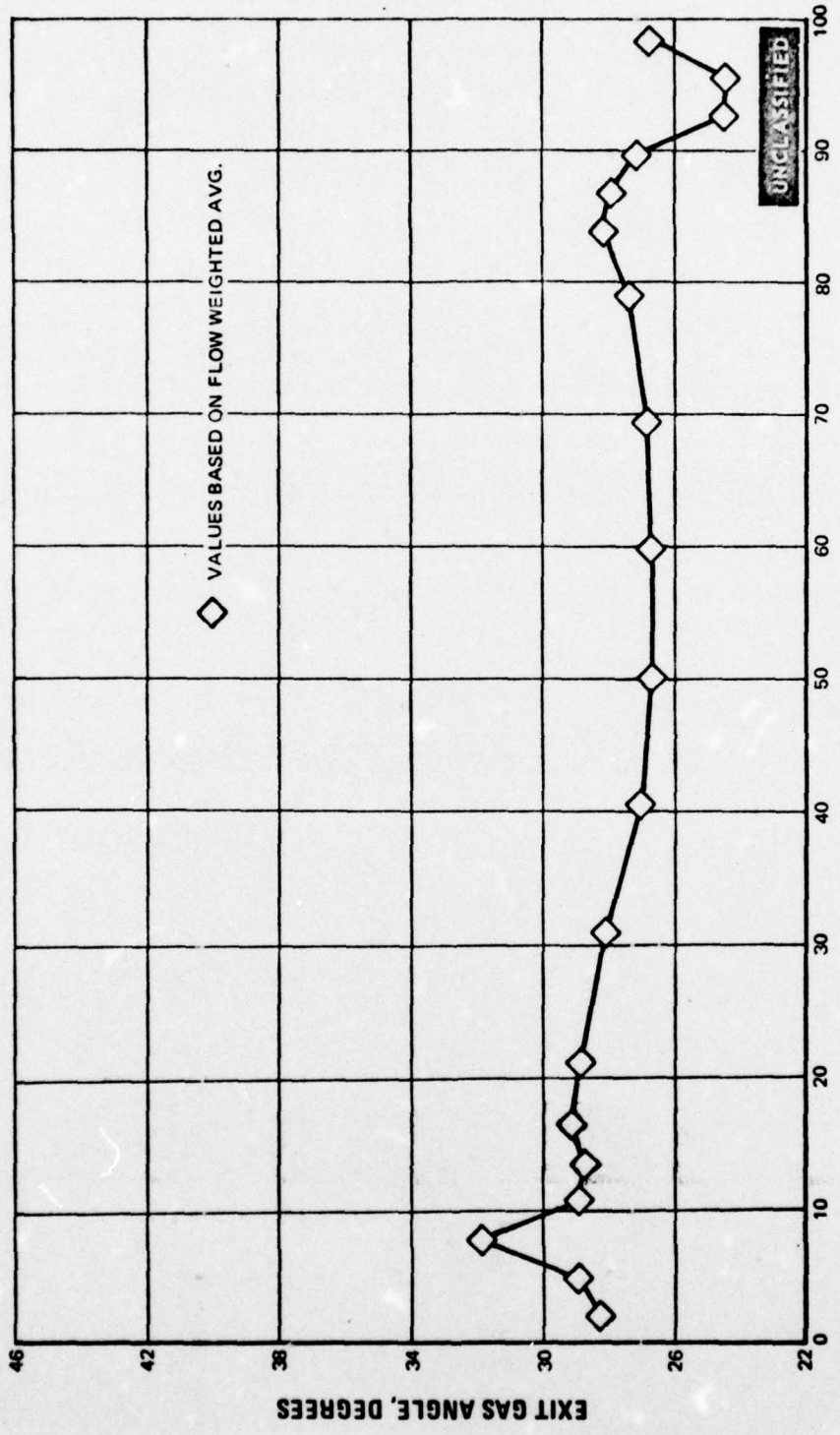

Figure 142 Spanwise Exit Gas Angle Distribution, Second Vane Baseline at +10° Incidence. Midspan Exit Mach Number = 0.835

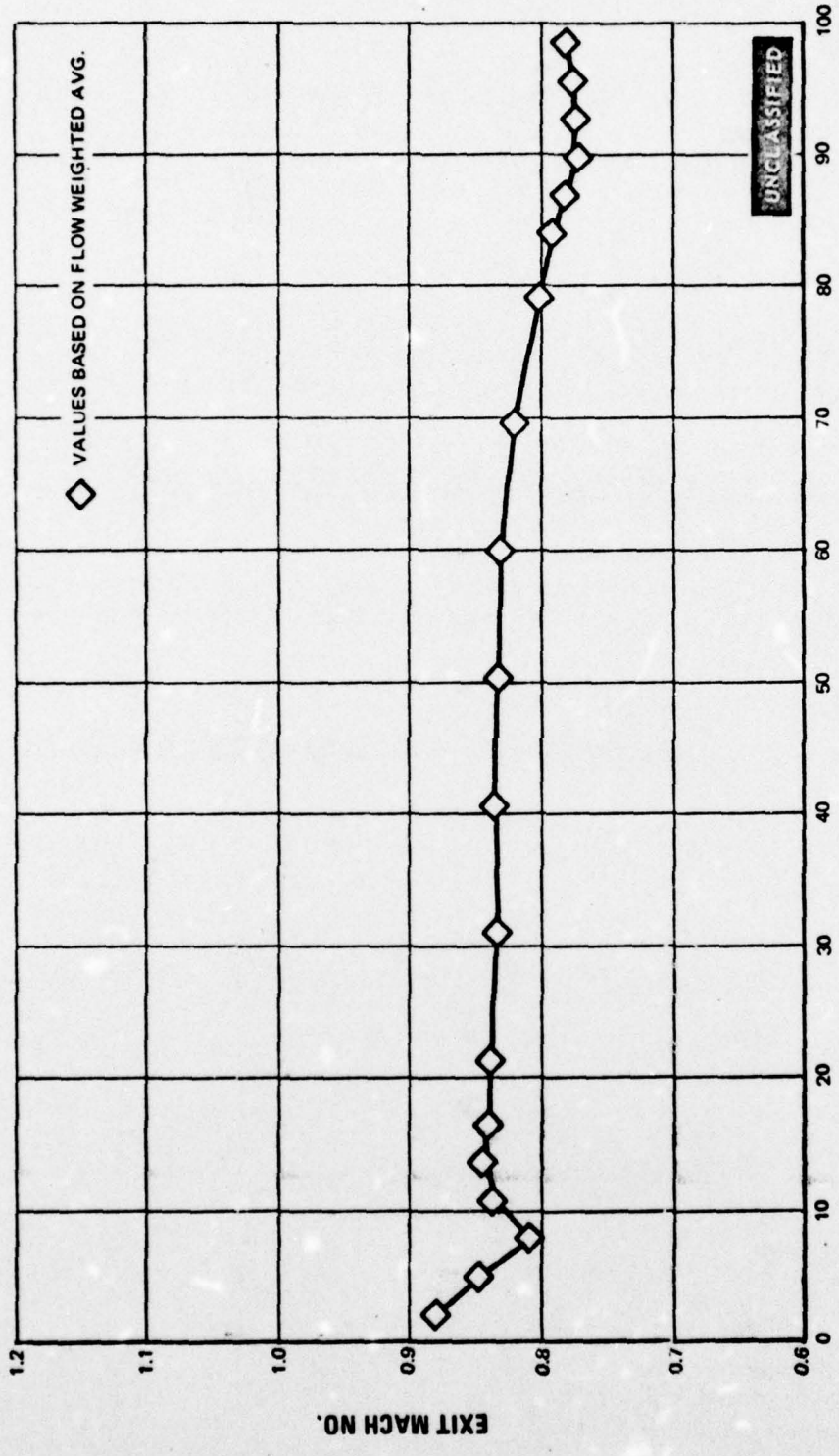

Figure 143 Spanwise Exit Mach Number Distribution, Second Vane Baseline at +10° Incidence. Midspan Exit Mach Number = 0.835

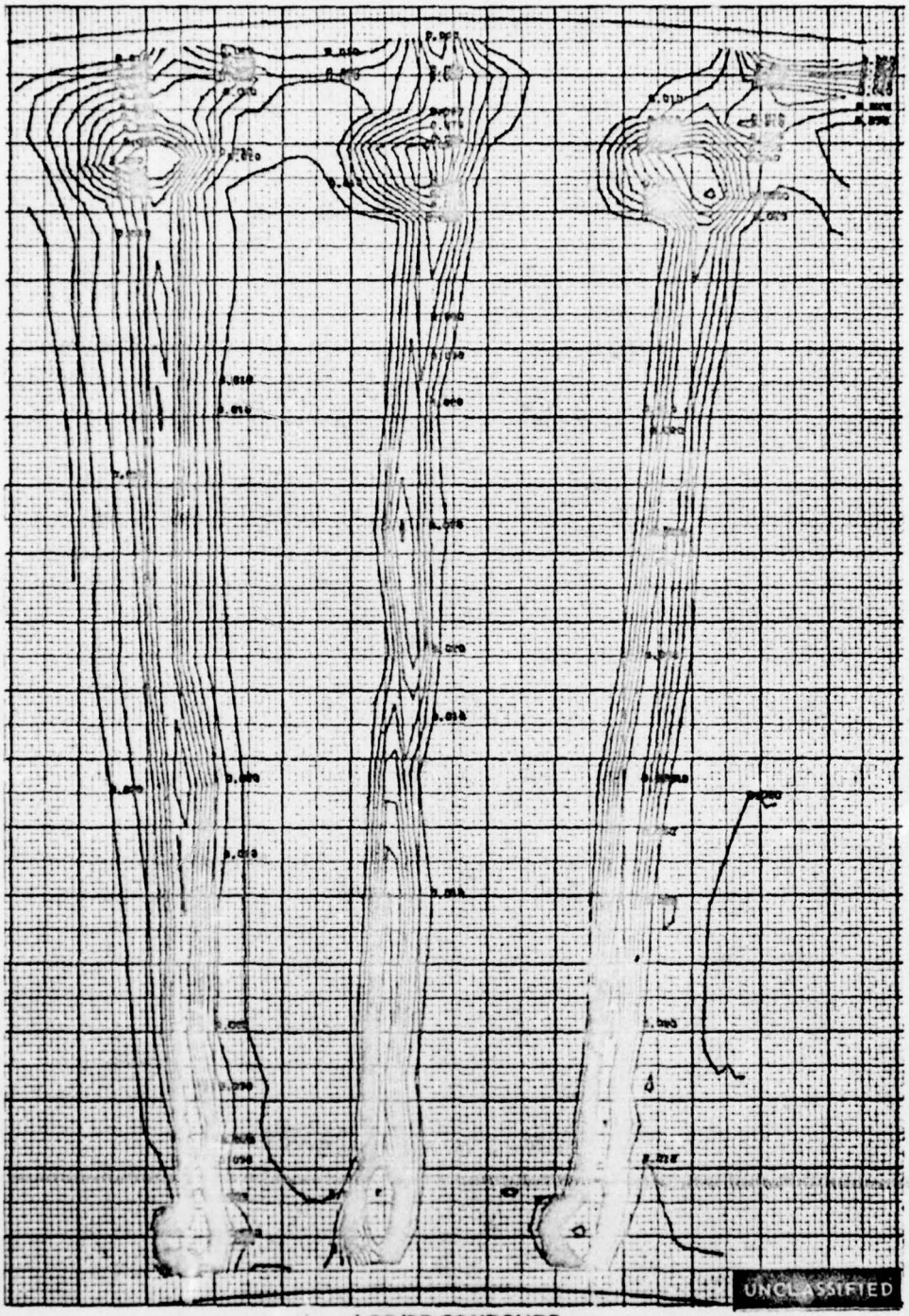

ΔPO/PO CONTOURS

Figure 144 Pressure Loss Contours, Second Vane Baseline at -6° Incidence. Three Flow Passages. Midspan Exit Mach Number = 0.865

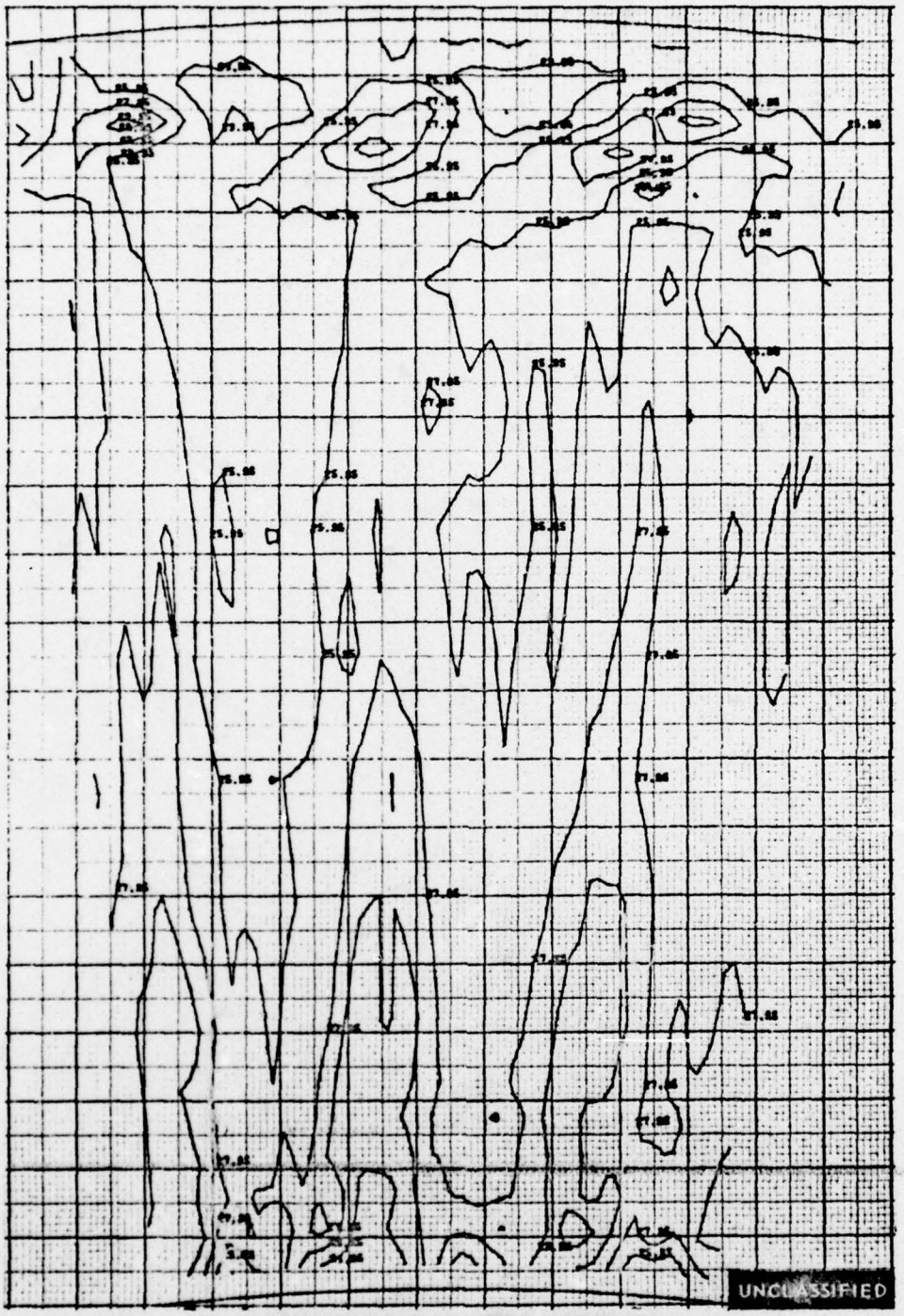

EXIT GAS ANGLE CONTOURS, DEGREES

Figure 145 Exit Gas Angle Contours, Second Vane Baseline at -6° Incidence. Three Flow Passages. Midspan Exit Mach Number = 0.865

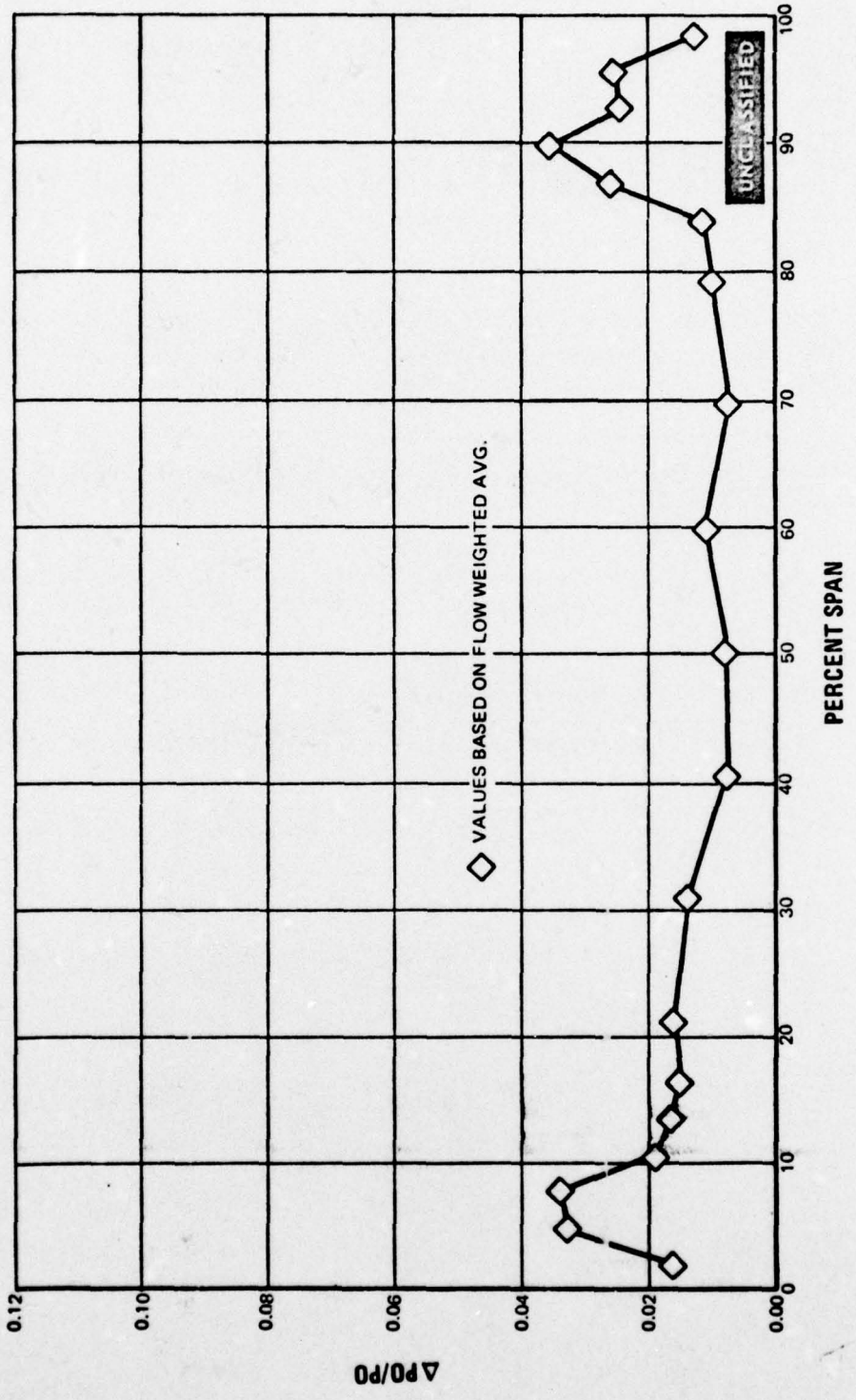

Figure 146 Spanwise Pressure Loss Distribution, Second Vane Baseline at -6° Incidence. Midspan Exit Mach Number = 0.865

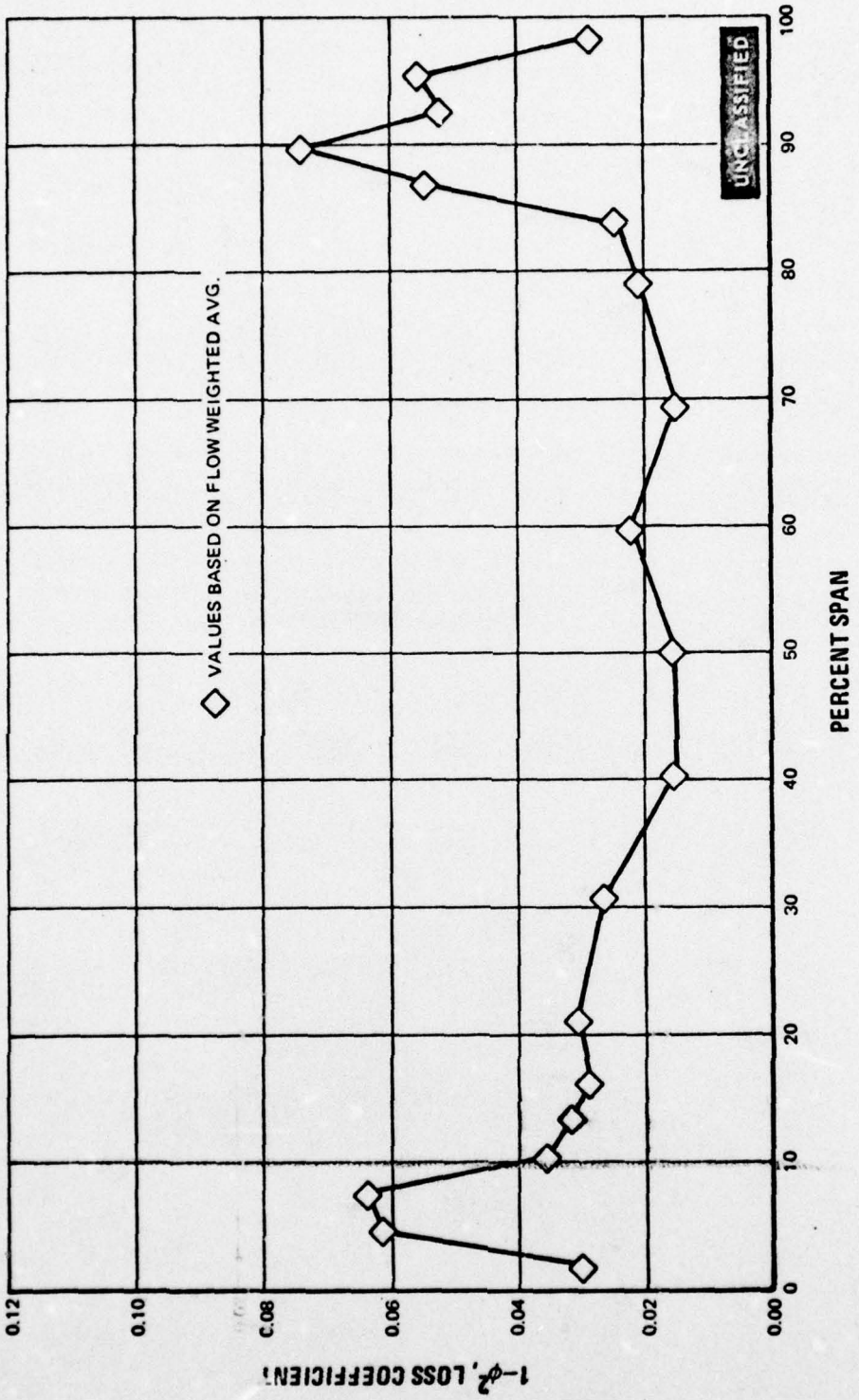

Figure 147 Spanwise Loss Coefficient Distribution, Second Vane Baseline at -6° Incidence. Midspan Exit Mach Number = 0.865

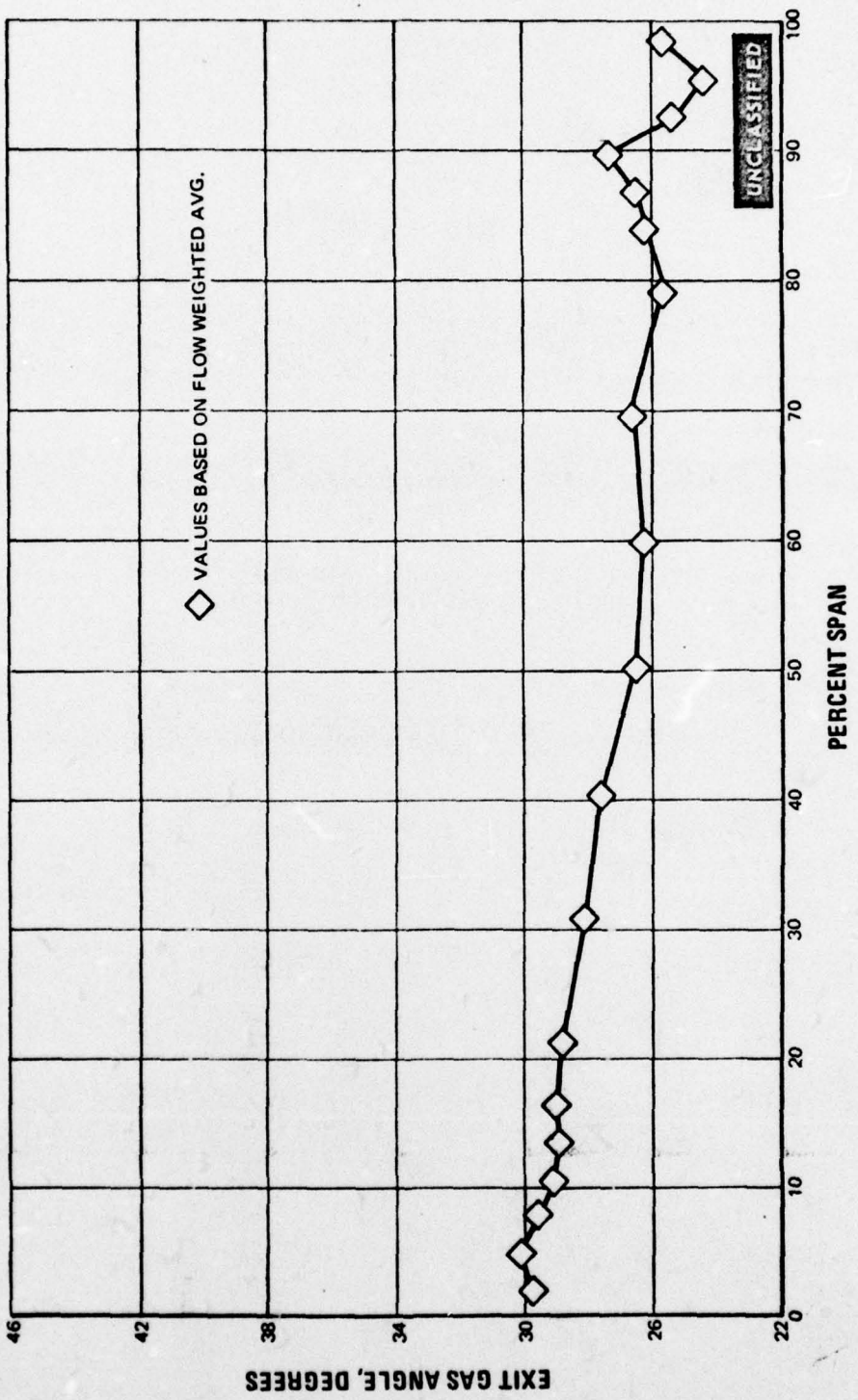

Figure 148 Spanwise Exit Gas Angle Distribution, Second Vane Baseline at -6° Incidence. Midspan Exit Mach Number = 0.865

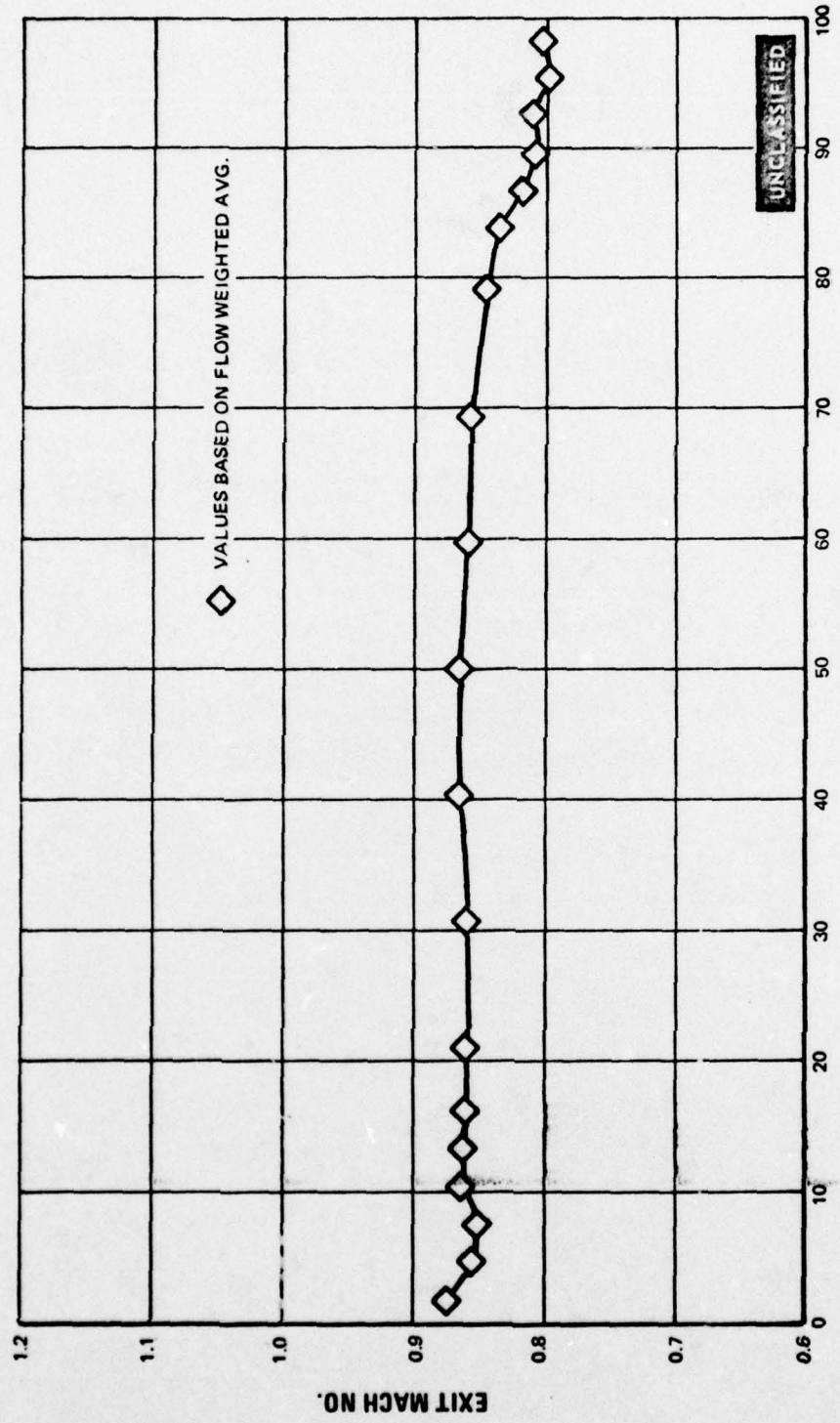

Figure 149 Spanwise Exit Mach Number Distribution, Second Vane Baseline at -6° Incidence. Midspan Exit Mach Number = 0.865

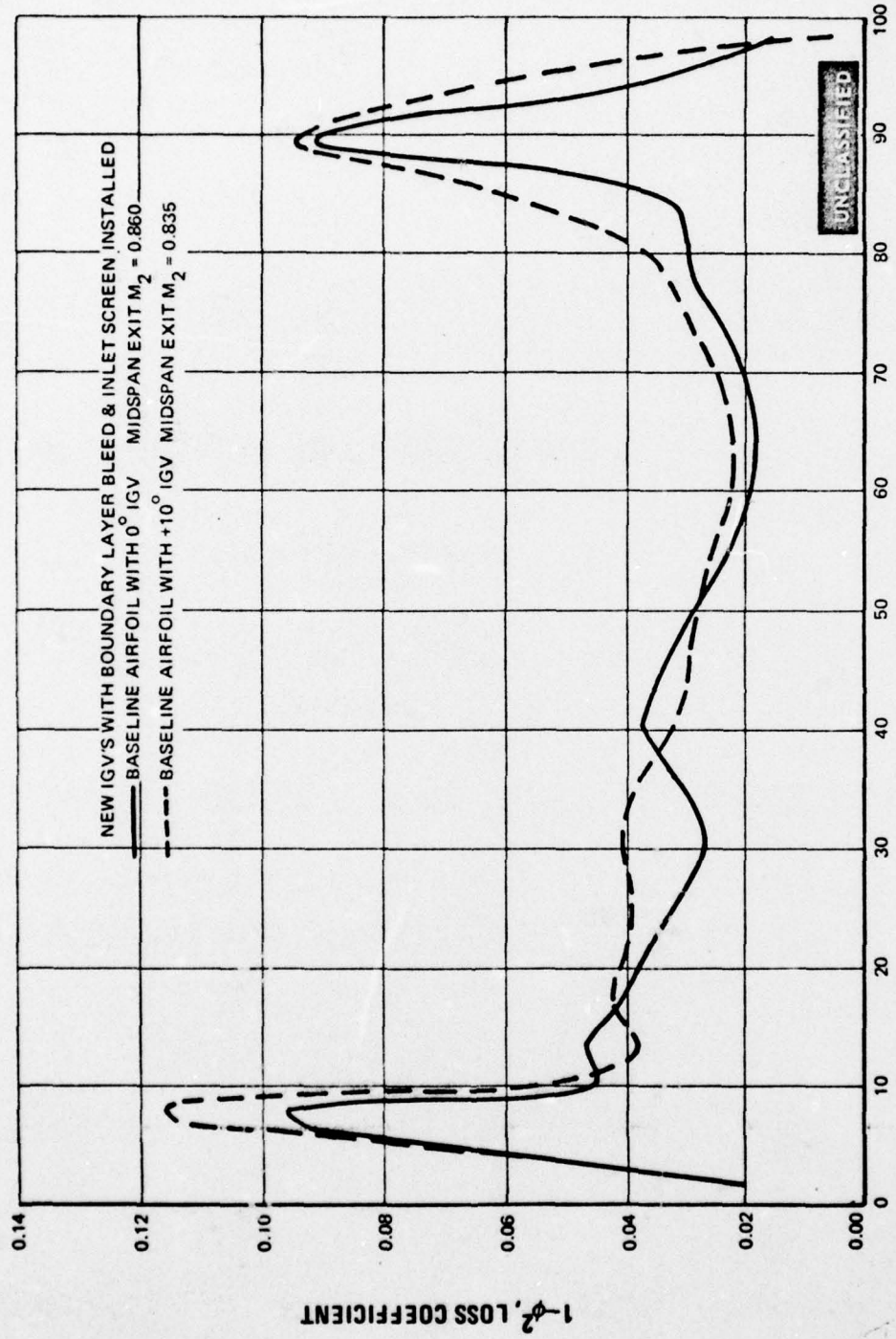

Figure 150 Comparison of Baseline Airfoil Loss Coefficient Distribution at +10° Incidence With Zero Incidence Values

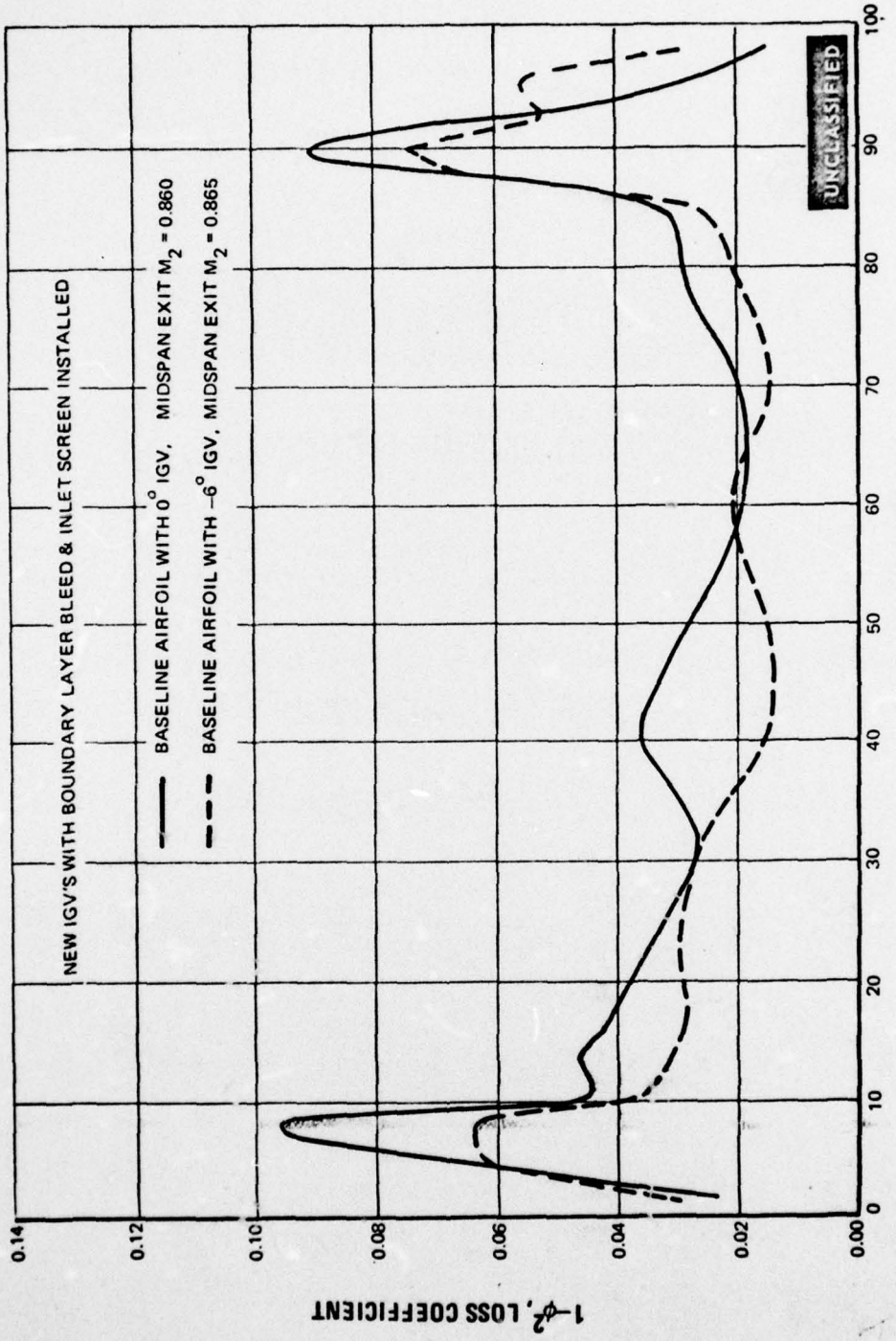

Figure 151 Comparison of Baseline Airfoil Loss Coefficient Distribution at -6 Degree Incidence With Zero Incidence Values

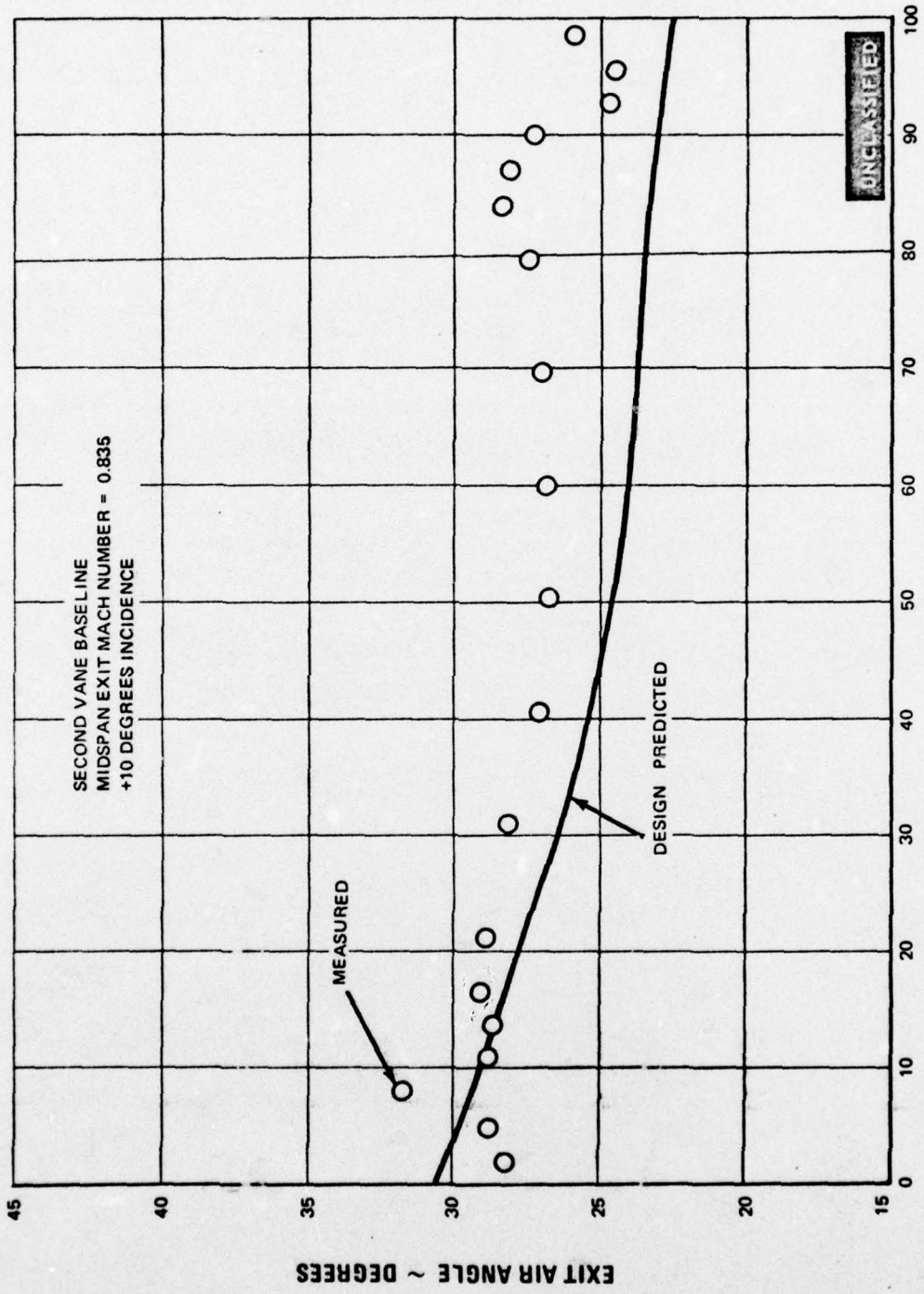

Figure 152 Comparison of Measured Exit Gas Angle With Predicted Design Values at +10 Degrees Incidence. Baseline Airfoil at Midspan Exit Mach No. = 0.835

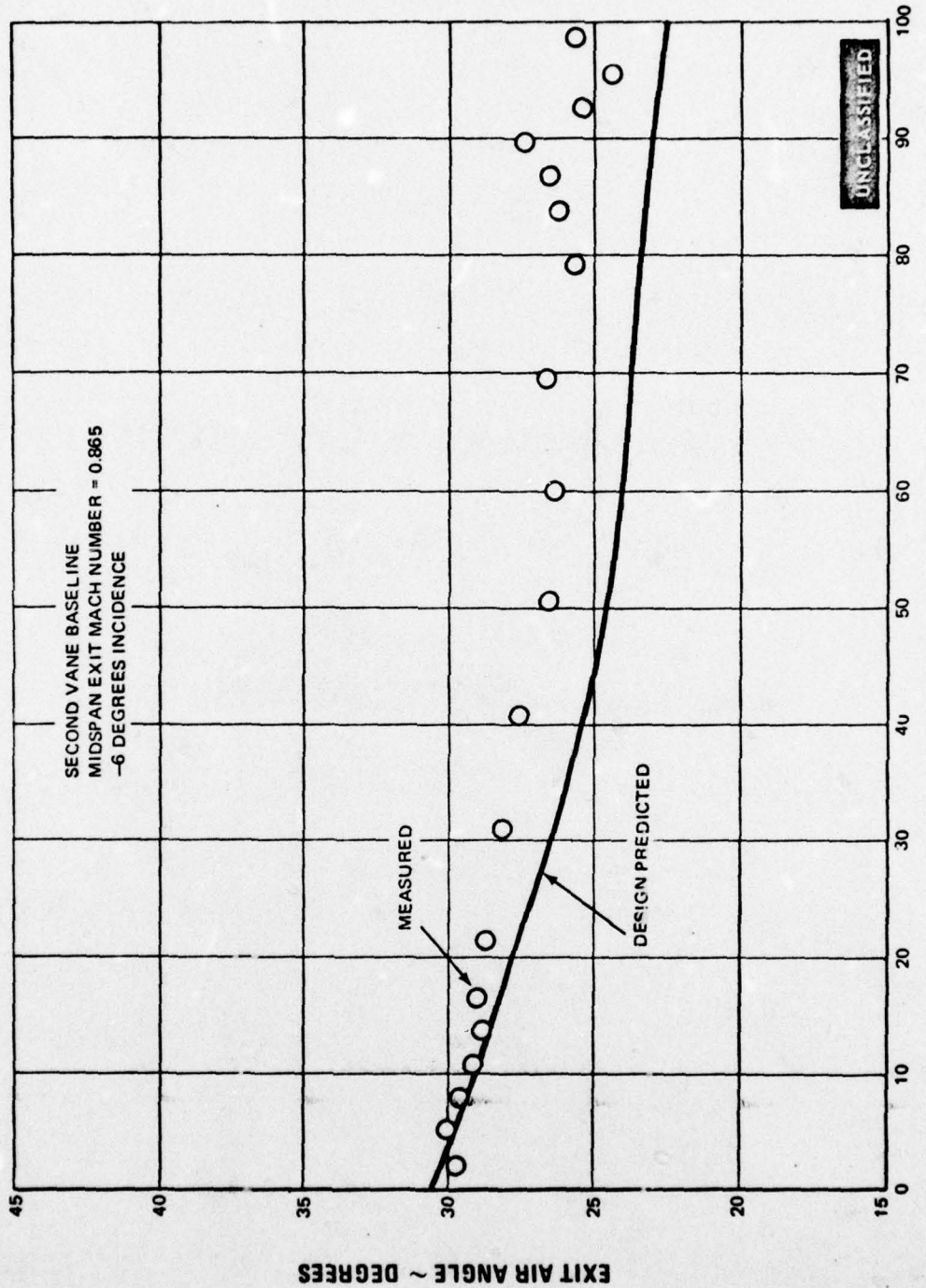

Figure 153 Comparison of Measured Exit Gas Angle With Predicted Design Values at -6 Degrees Incidence. Baseline Airfoil at Midspan Exit Mach No. = 0.865

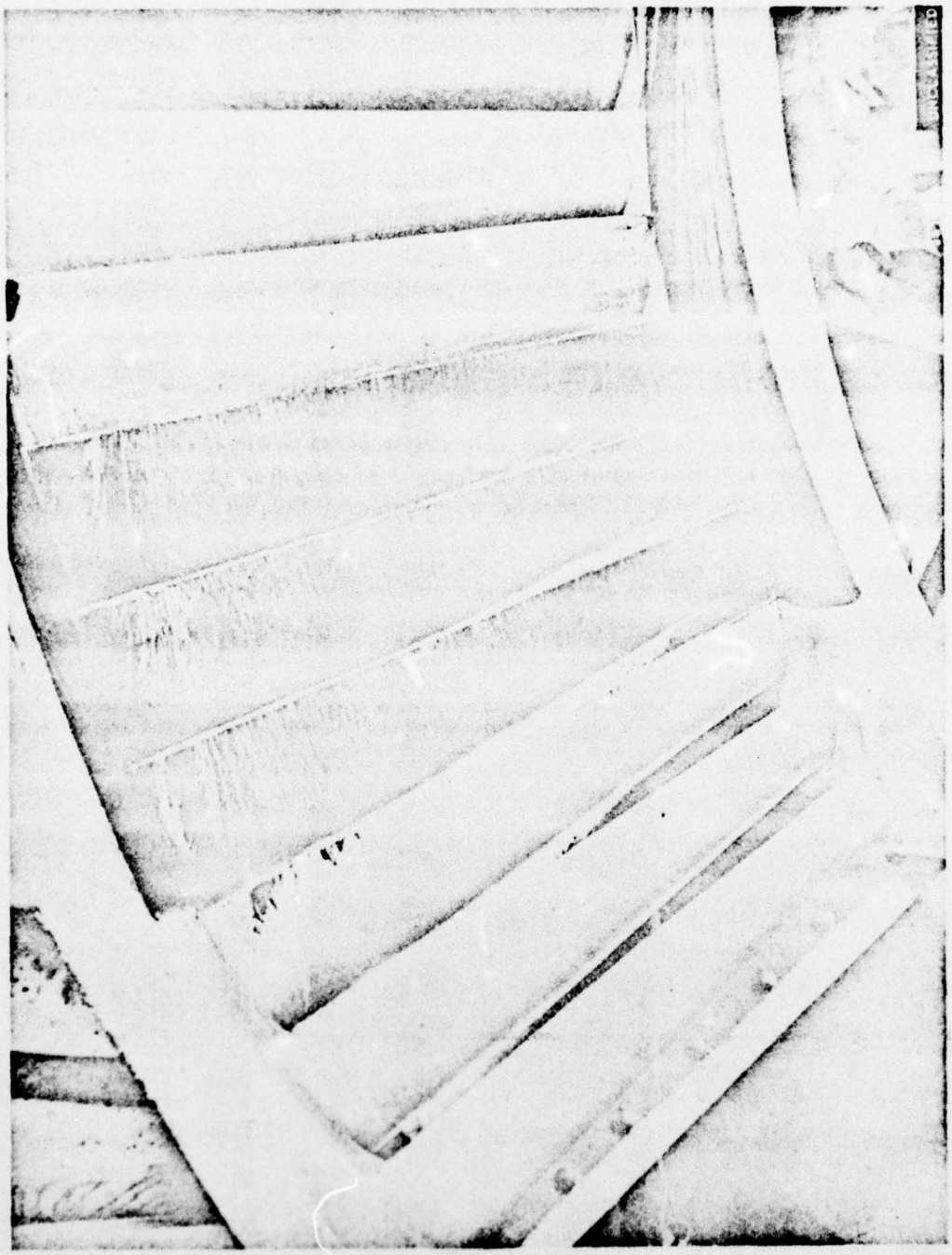

Figure 154 Oil and Graphite Flow Patterns, Second Vane Baseline Airfoil at +10 Degrees Incidence. Midspan Exit Mach No. = 0.835 (FE95349)

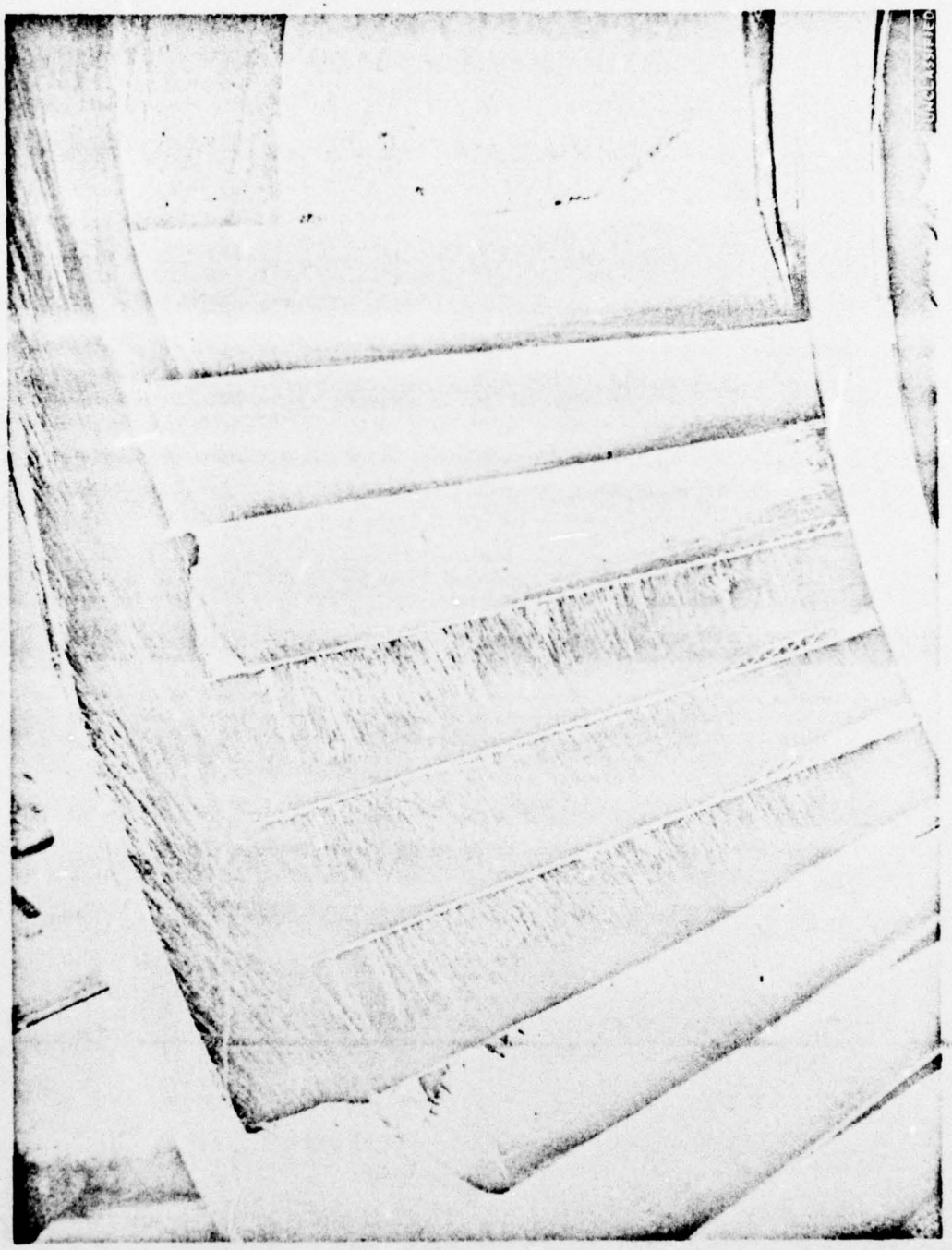

Figure 155 Oil and Graphite Flow Patterns, Second Vane Baseline Airfoil at +10 Degrees Incidence. Midspan Exit Mach No. = 0.835 (FE95350)

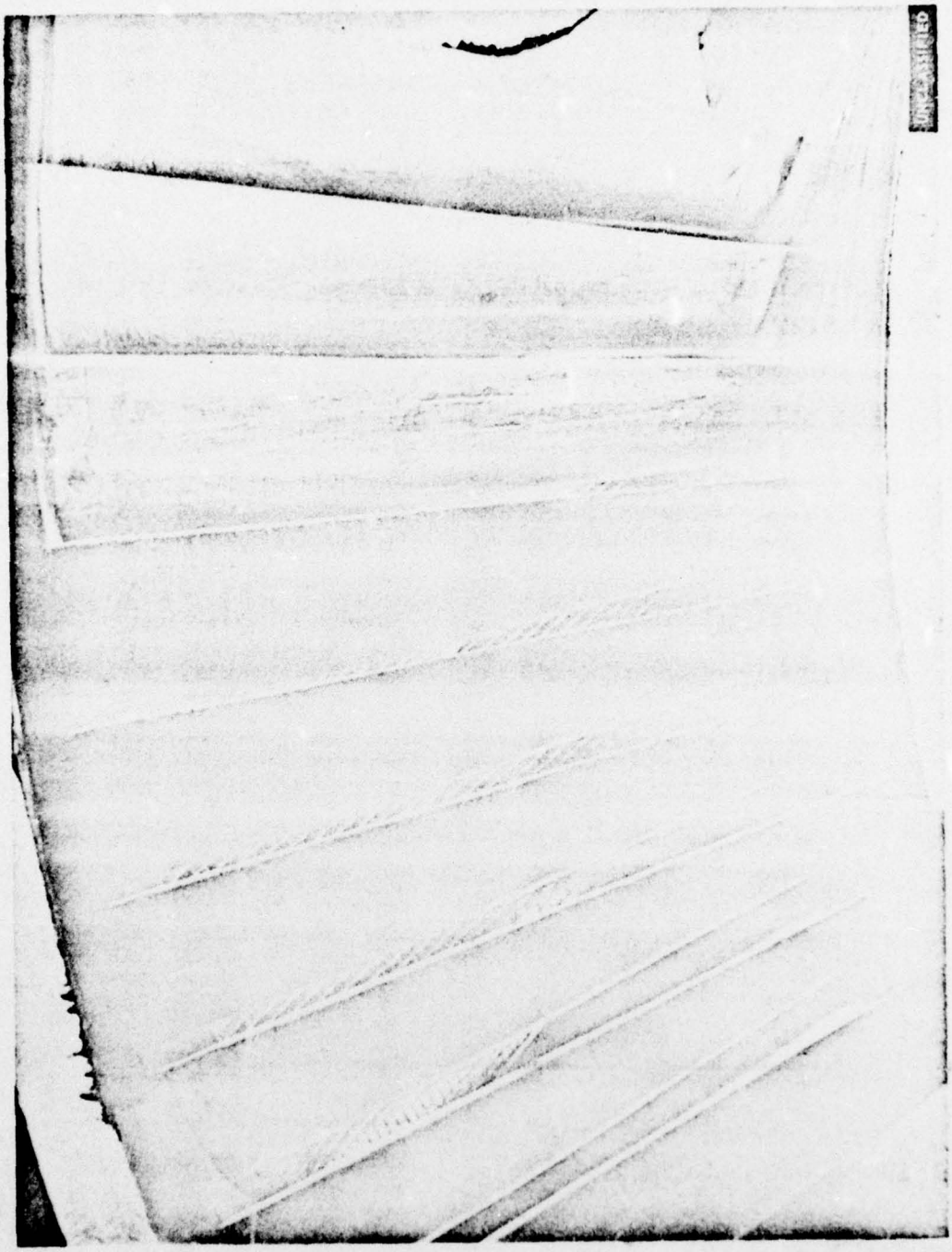

Figure 156 Oil and Graphite Flow Patterns, Second Vane Baseline Airfoil at -6 Degrees Incidence. Midspan Exit Mach No. = 0.865 (FE95432)

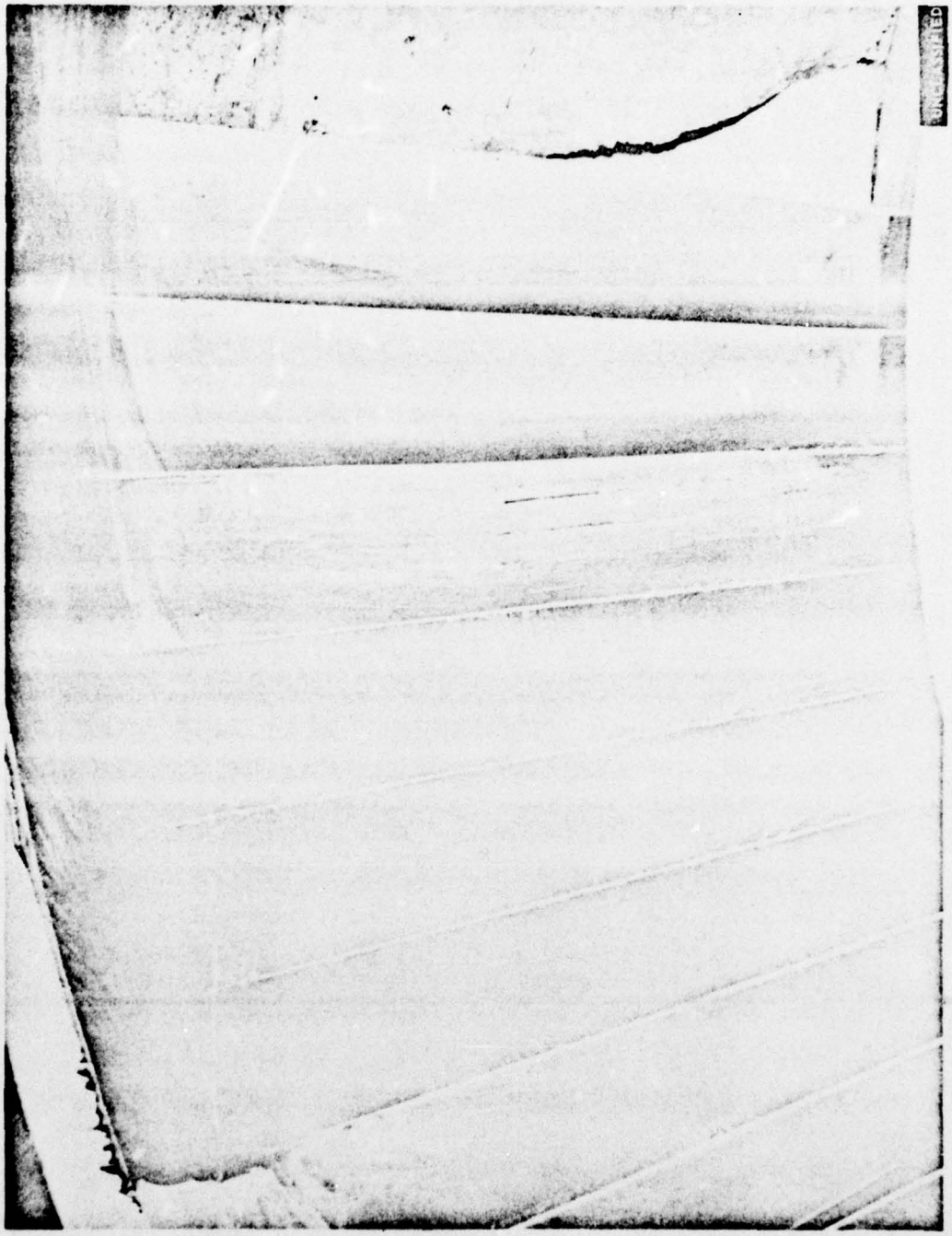

Figure 157 Oil and Graphite Flow Patterns, Second Vane Baseline Airfoil at -6 Degrees Incidence, Midspan Exit Mach No. = 0.865 (FE95433)

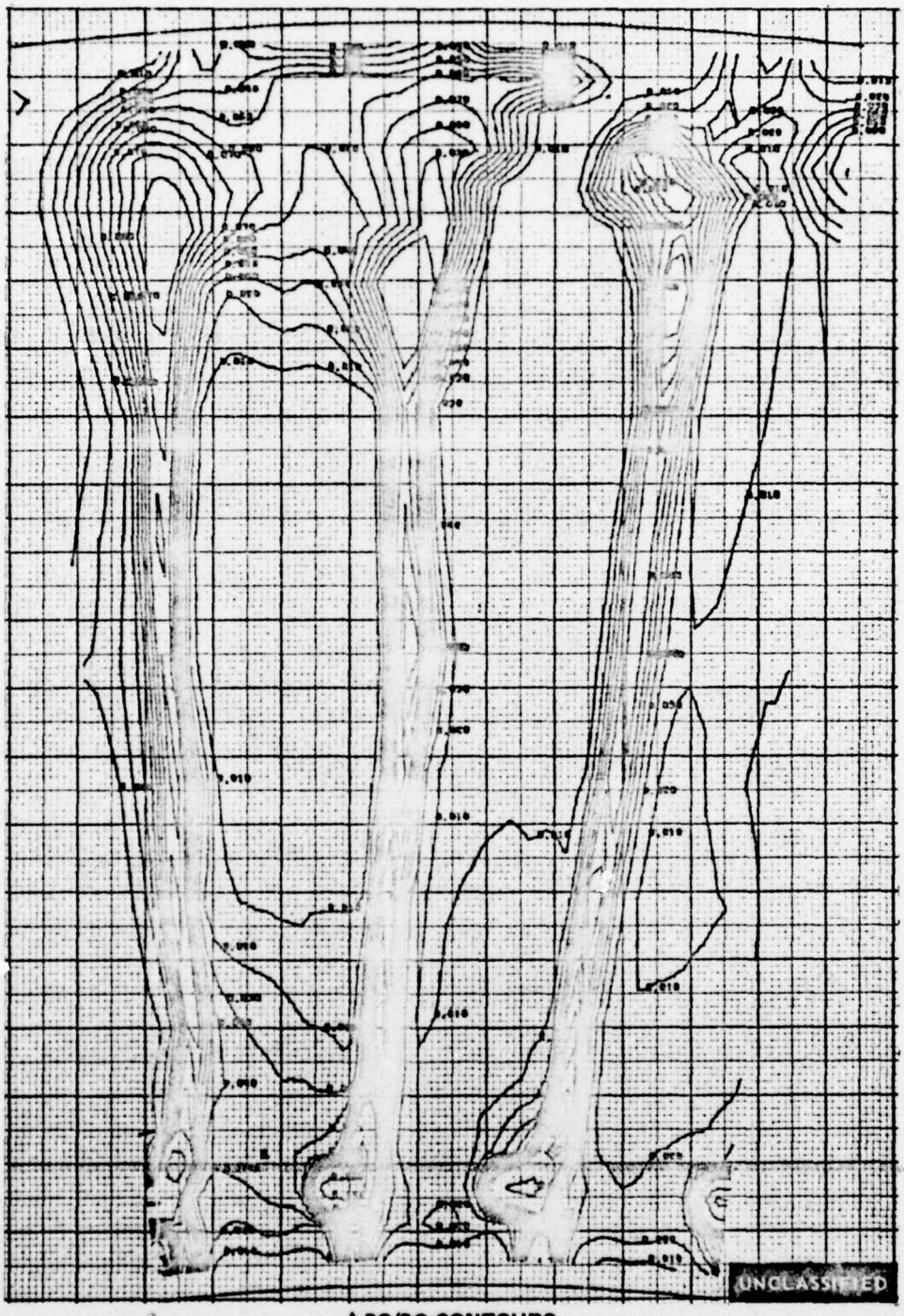

ΔPO/PO CONTOURS

Figure 158 Pressure Loss Contours, Second Vane First Recambering at +10° Incidence. Three Flow Passages. Midspan Exit Mach Number = 0.840

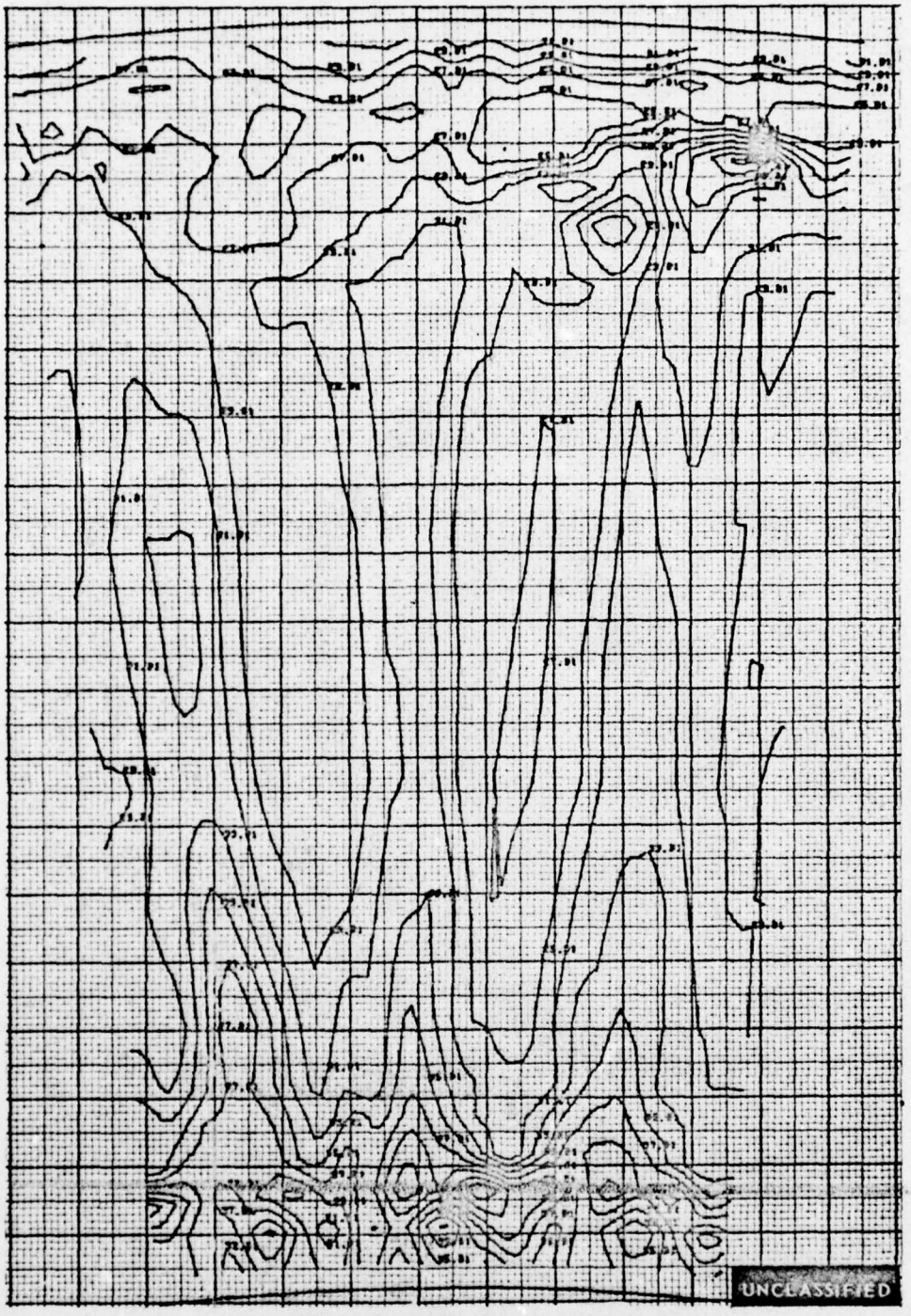

EXIT GAS ANGLE CONTOURS, DEGREES

Figure 159 Exit Gas Angle Contours, Second Vane First Recambering at +10° Incidence. Three Flow Passages. Midspan Exit Mach Number = 0.840

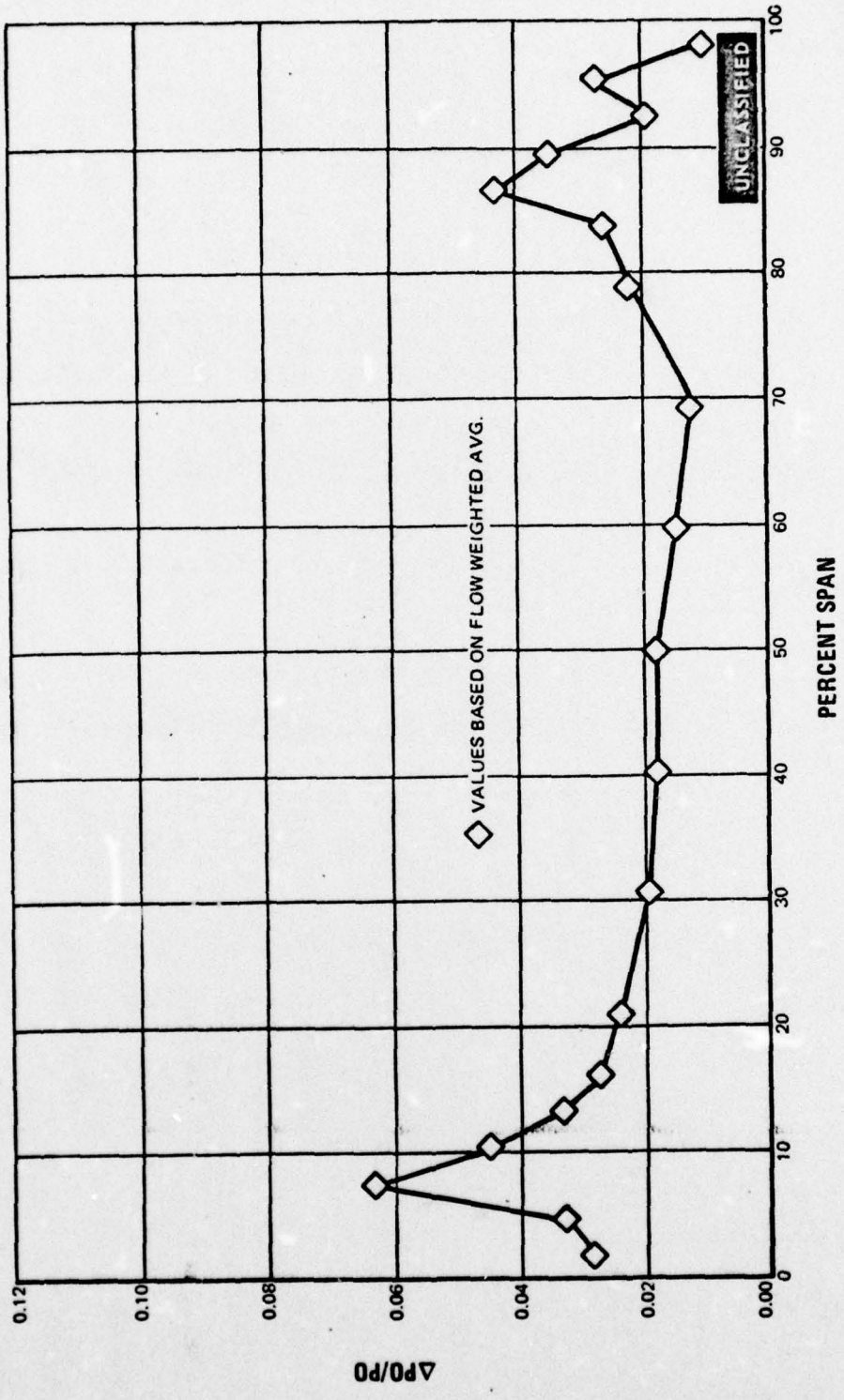

Figure 160 Spanwise Pressure Loss Distribution, Second Vane First Recambering at +10° Incidence. Midspan Exit Mach Number = 0.840

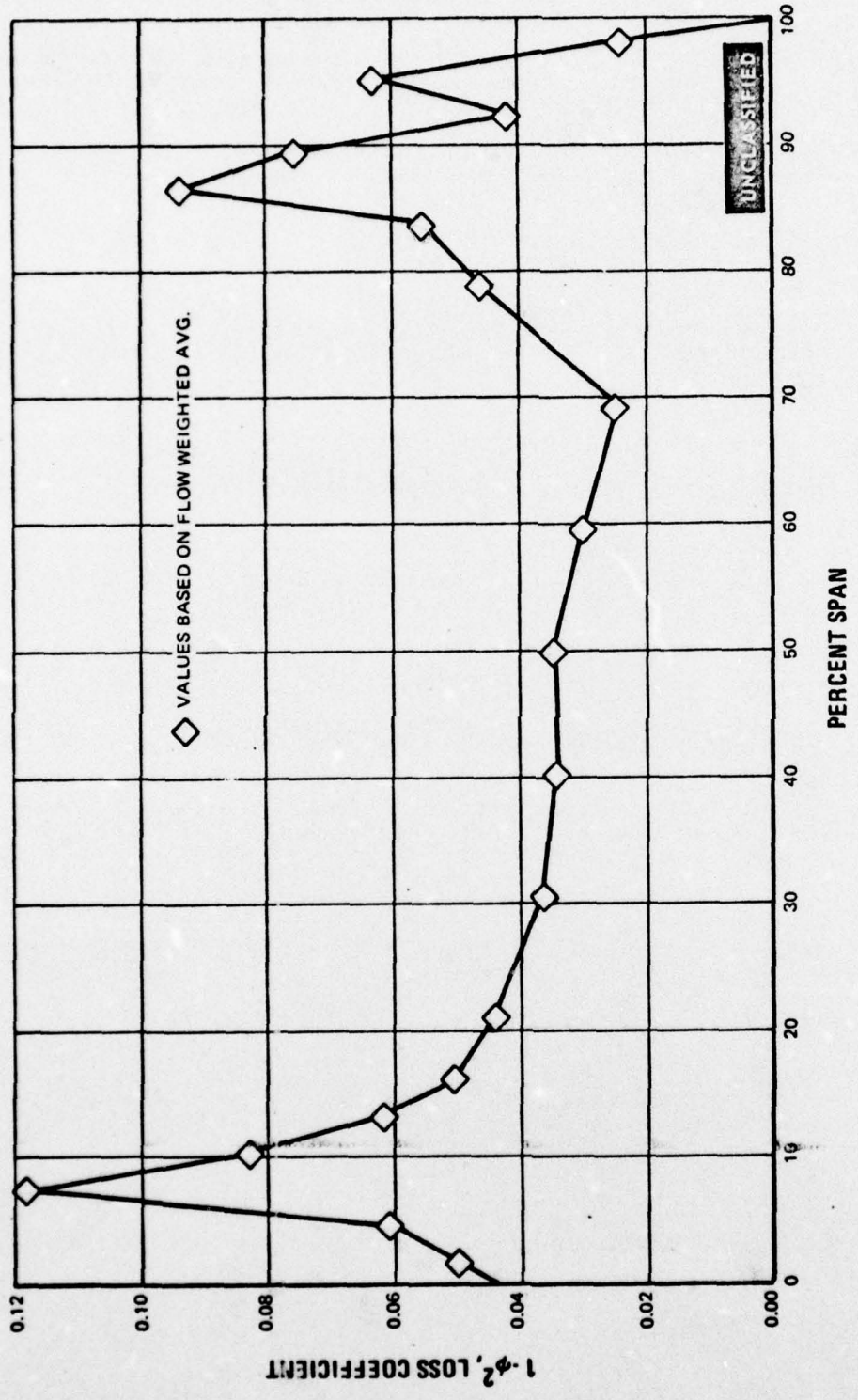

Figure 161 Spanwise Loss Coefficient Distribution, Second Vane First Recambering at +10° Incidence. Midspan Exit Mach Number = 0.840

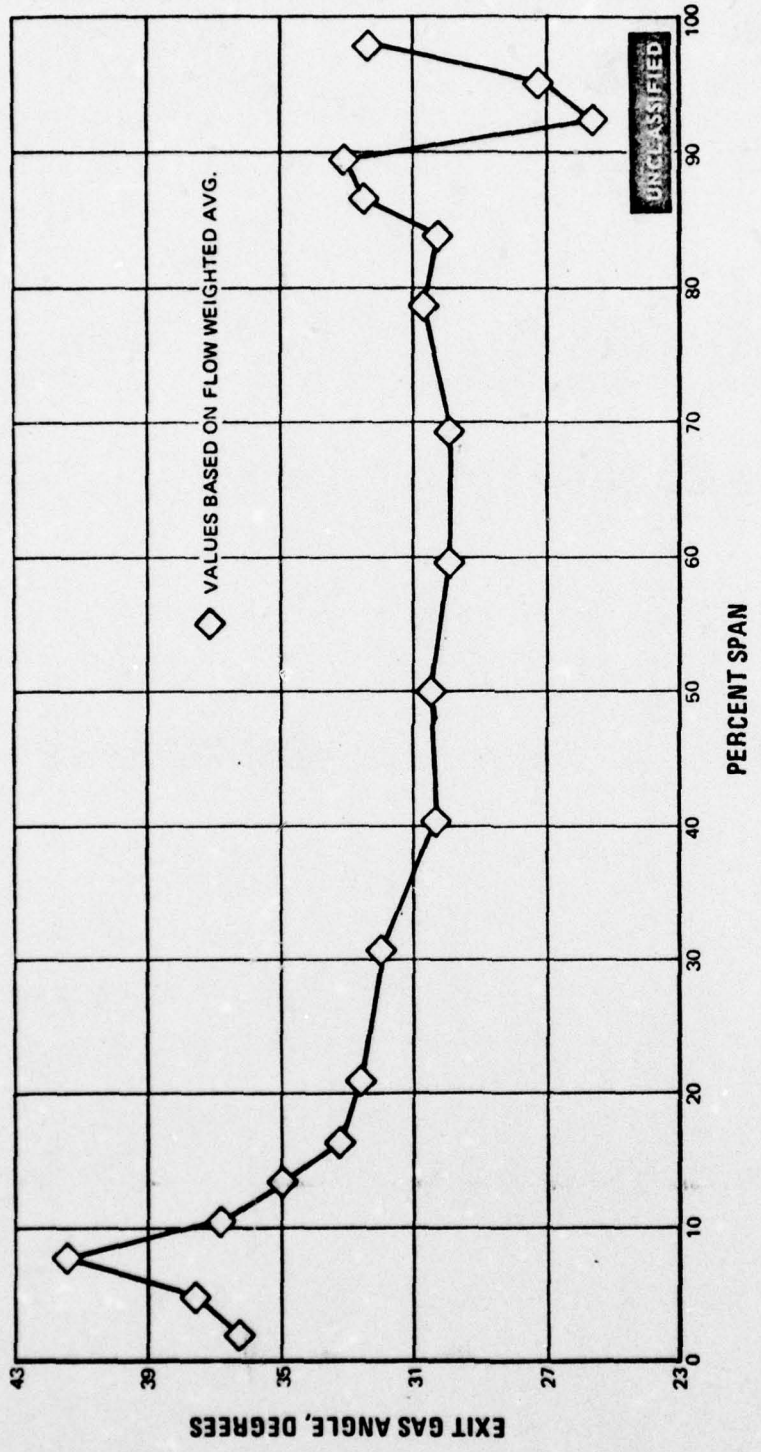

Figure 162 Spanwise Exit Gas Angle Distribution, Second Vane First Recambering at +10° Incidence. Midspan Exit Mach Number = 0.840

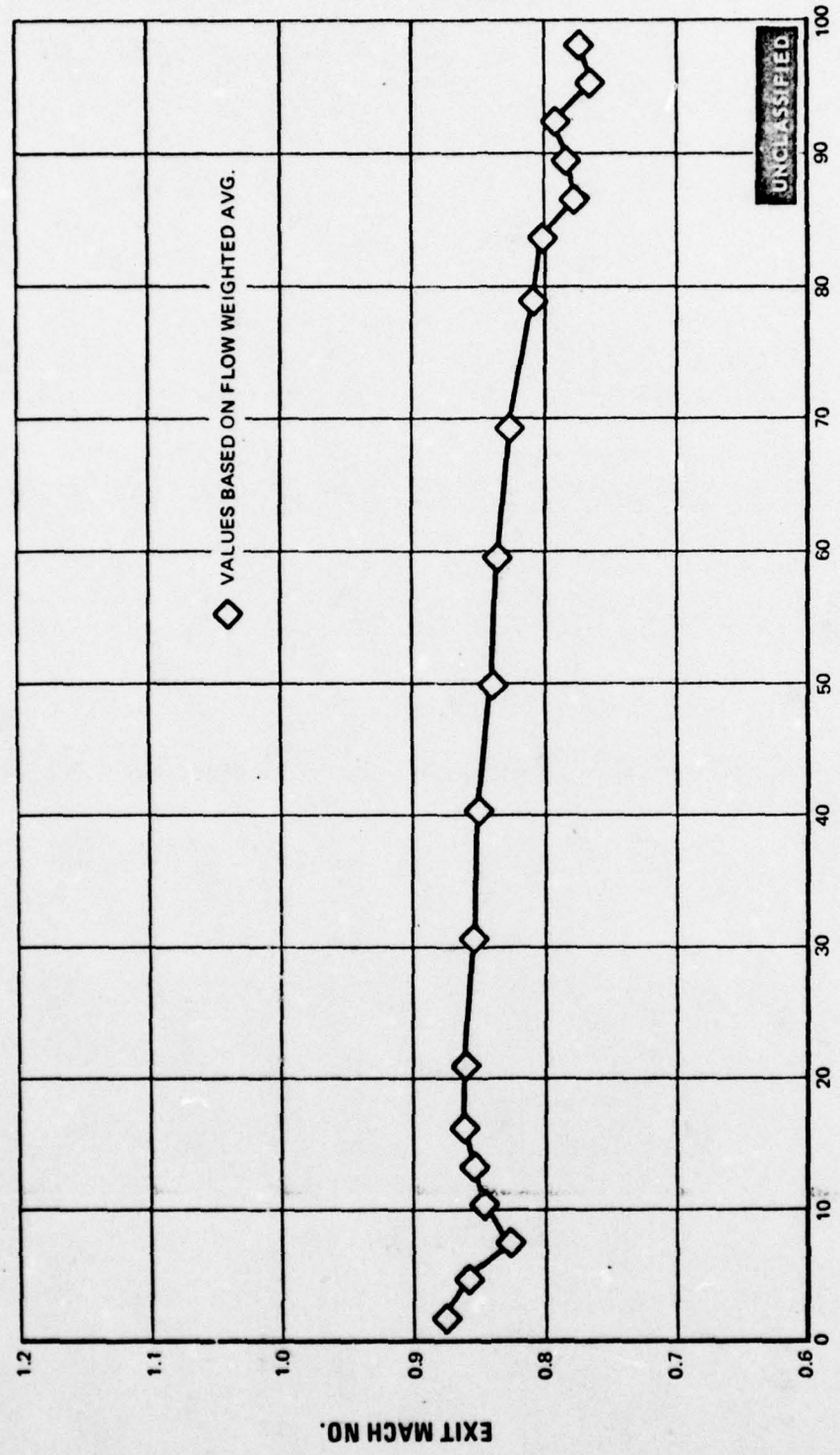

Figure 163 Spanwise Exit Mach Number Distribution, Second Vane First Recambering at +10° Incidence. Midspan Exit Mach Number = 0.840

Δ PO/PO CONTOURS

Figure 164 Pressure Loss Contours, Second Vane First Recambering at -6° Incidence. Three Flow Passages. Midspan Exit Mach Number = 0.883

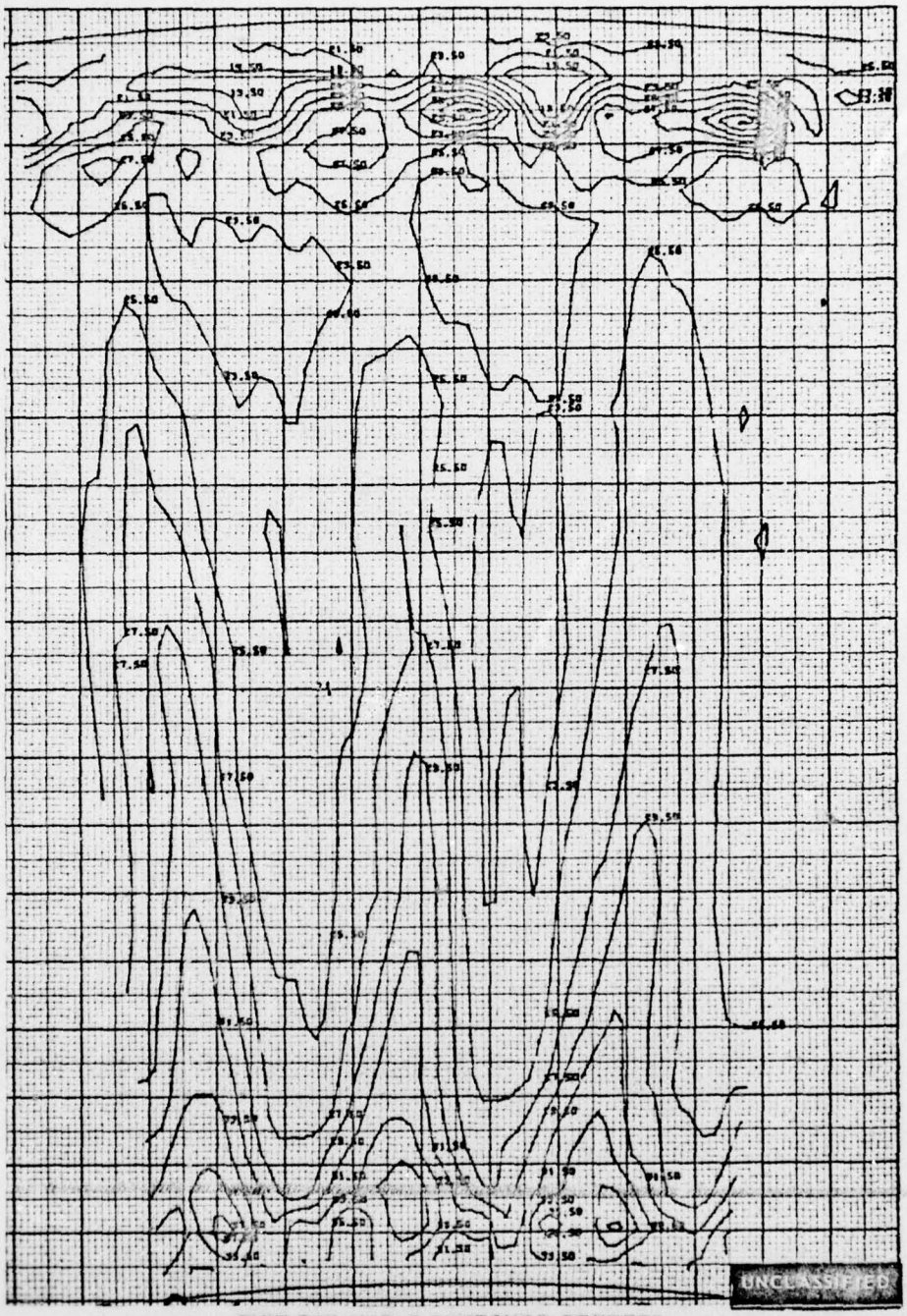

Figure 165 Exit Gas Angle Contours, Second Vane First Recambering at -6° Incidence. Three Flow Passages. Midspan Exit Mach Number = 0.883

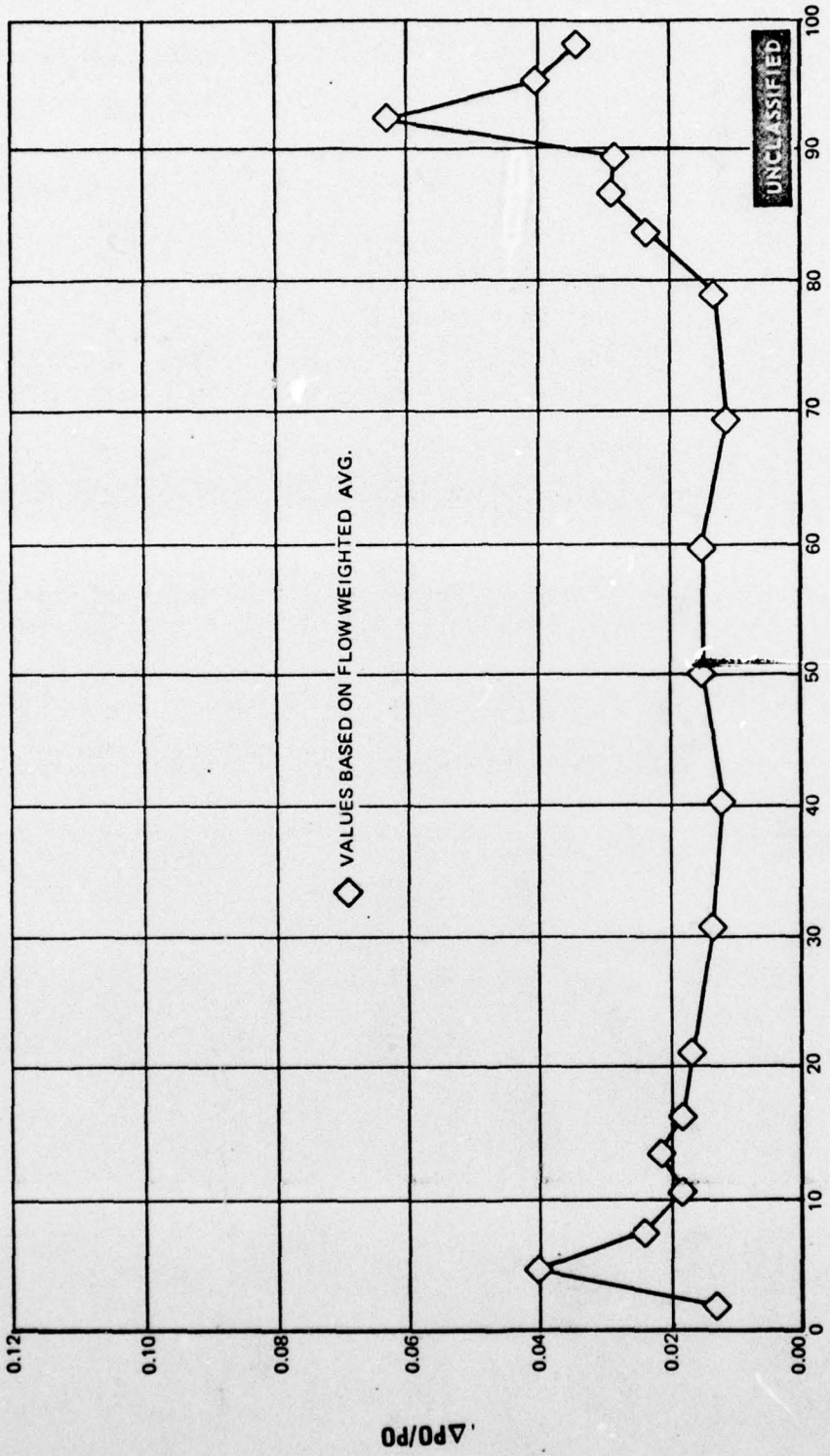

Figure 166 Spanwise Pressure Loss Distribution, Second Vane First Recambering at -6° Incidence. Midspan Exit Mach Number = 0.883

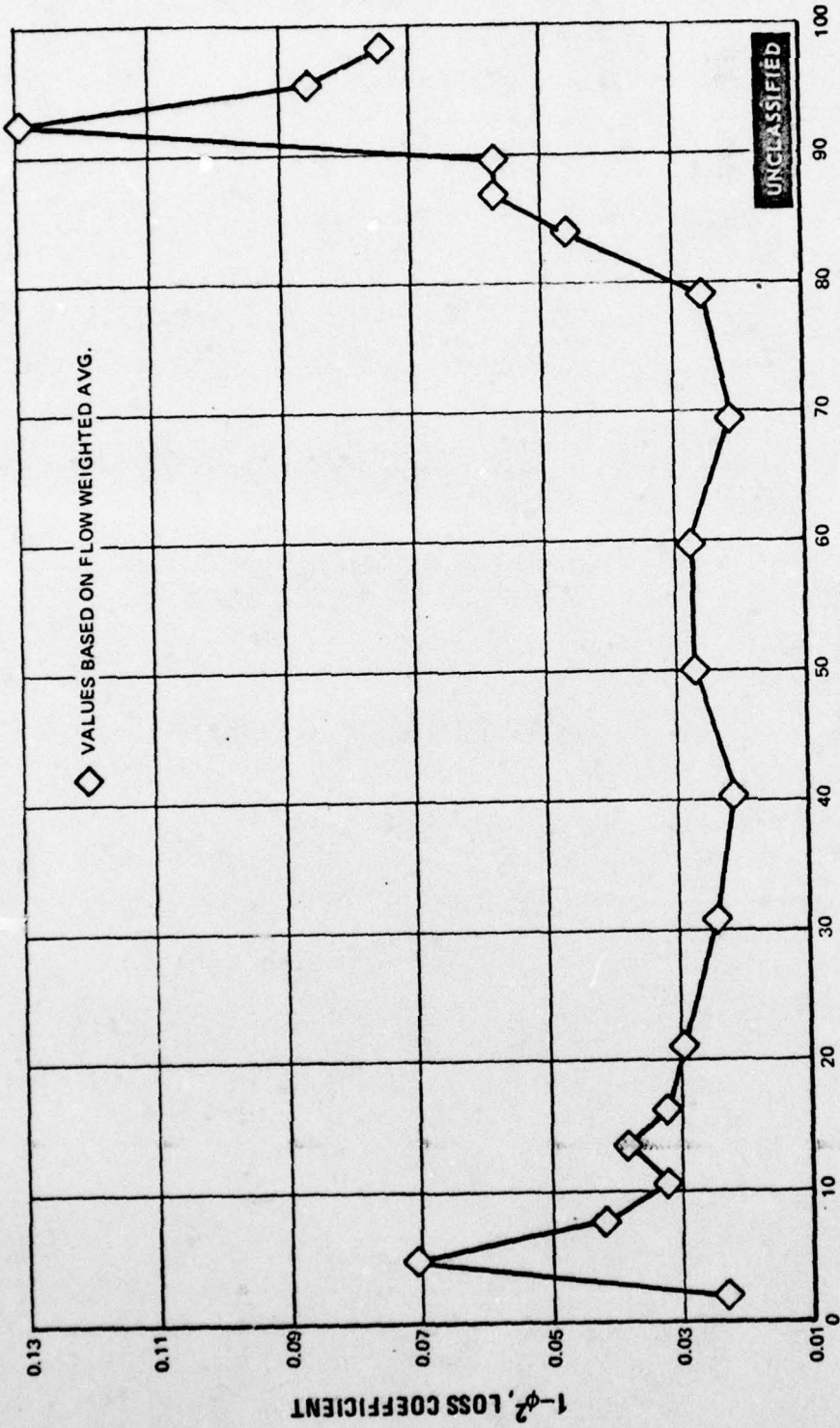

Figure 167 Spanwise Loss Coefficient Distribution, Second Vane First Recambering at -6° Incidence. Midspan Exit Mach Number = 0.883

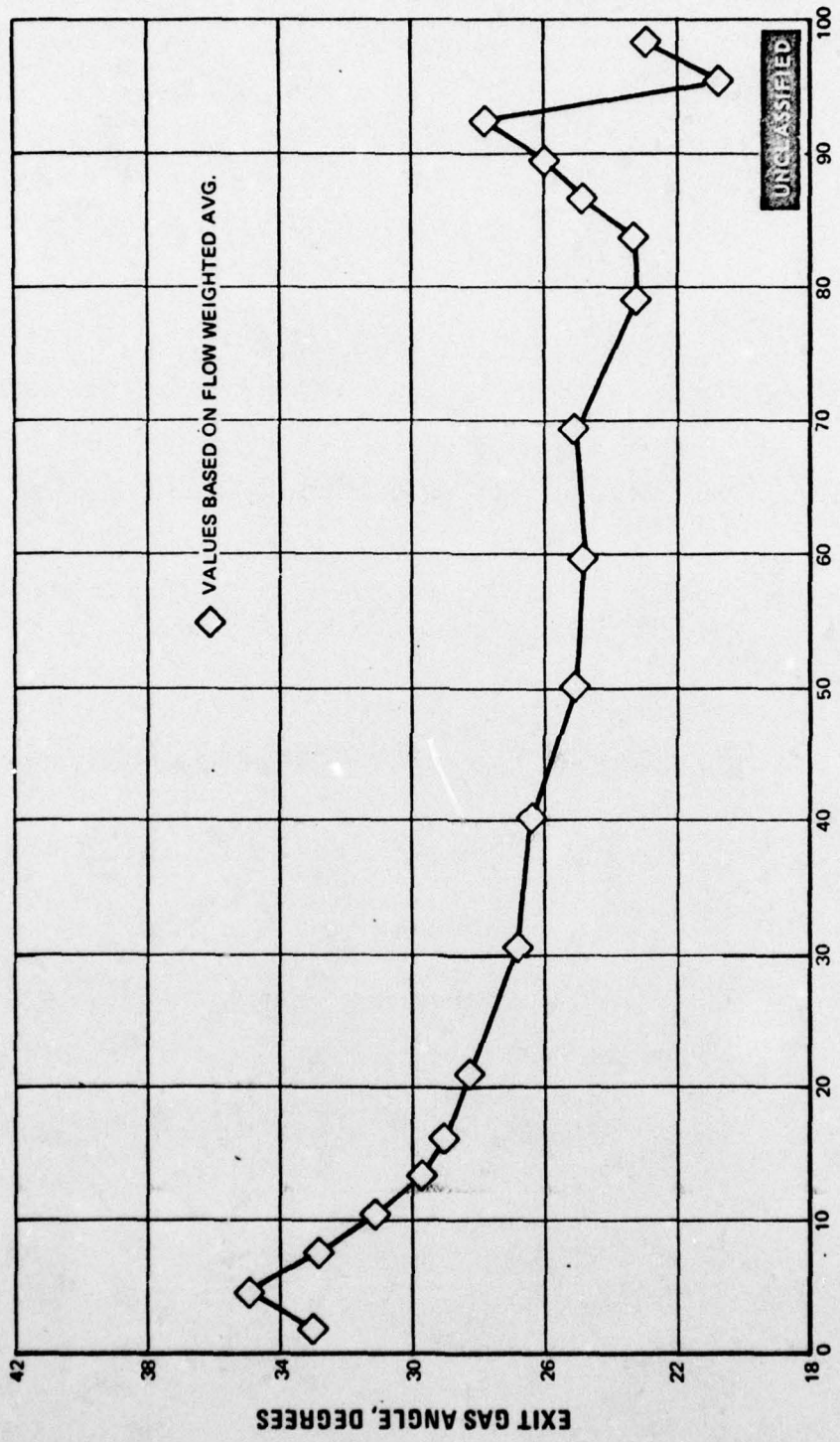

Figure 168 Spanwise Exit Gas Angle Distribution, Second Vane First Recambering at -6° Incidence. Midspan Exit Mach Number = 0.883

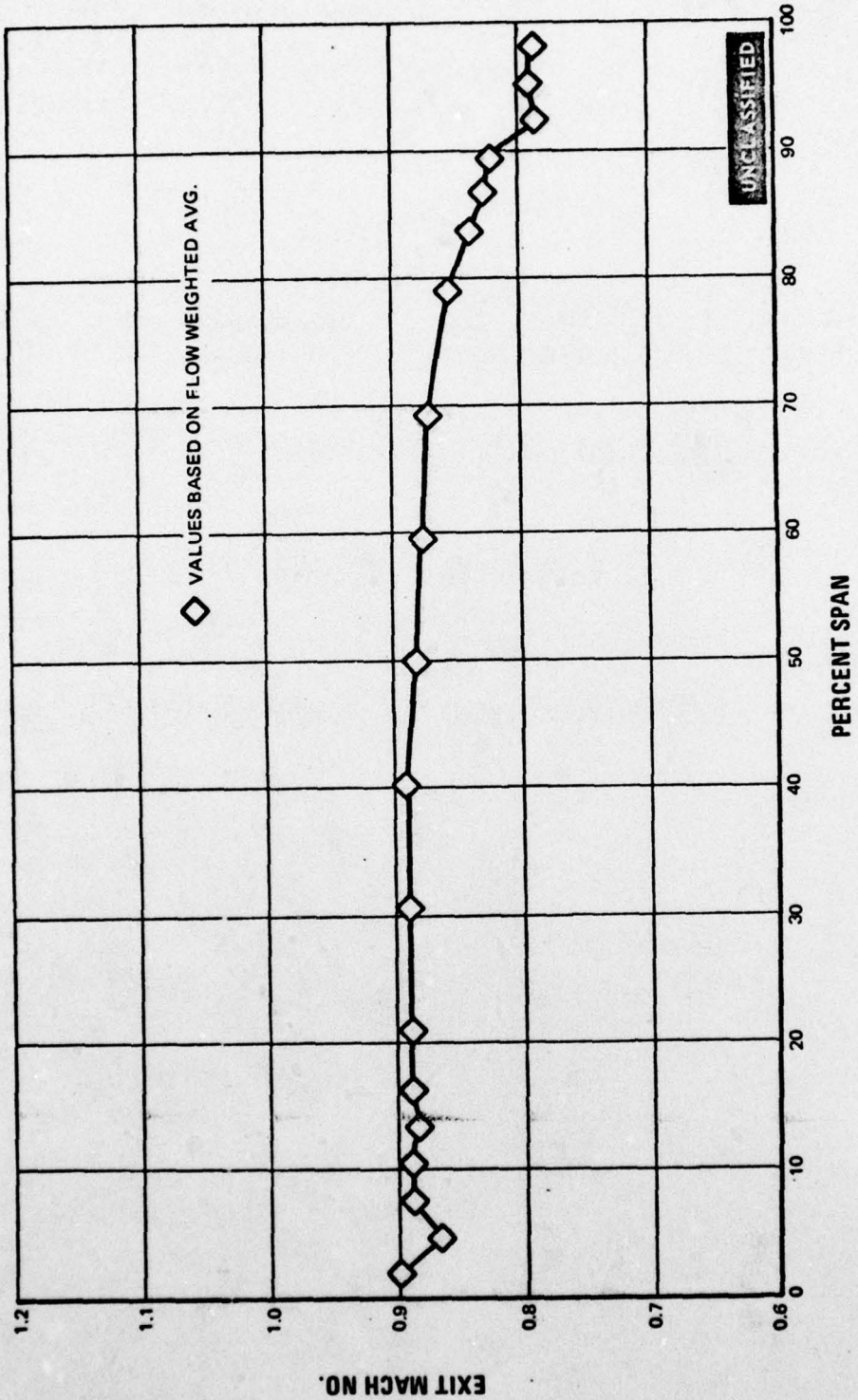

Figure 169 Spanwise Exit Mach Number Distribution, Second Vane First Recambering at -6° Incidence. Midspan Exit Mach Number = 0.883

(U) Comparisons of the spanwise loss coefficient distribution at +10 degrees incidence with zero degrees incidence, and -6 degrees incidence with zero degrees incidence are shown in Figures 170 and 171, respectively. The root end-wall losses were larger for the positive incidence and almost identical for the negative incidence values when compared to the zero incidence results. The tip end-wall losses showed very little variation for the three incidences that were investigated. On an overall basis, the positive incidence loss coefficient was substantially larger, and the negative incidence value was slightly greater than for the zero incidence condition. The measured exit gas angles are shown only for the -6 degree condition (Figure 172), since probe problems during the +10 degree test produced erroneous angle readings. The measured angles, as was the case for the baseline tests, were in good agreement with the design predicted values. Oil and graphite flow patterns are shown in Figures 173 through 176 for both positive and negative incidence tests. The flow was, as usual, well-behaved.

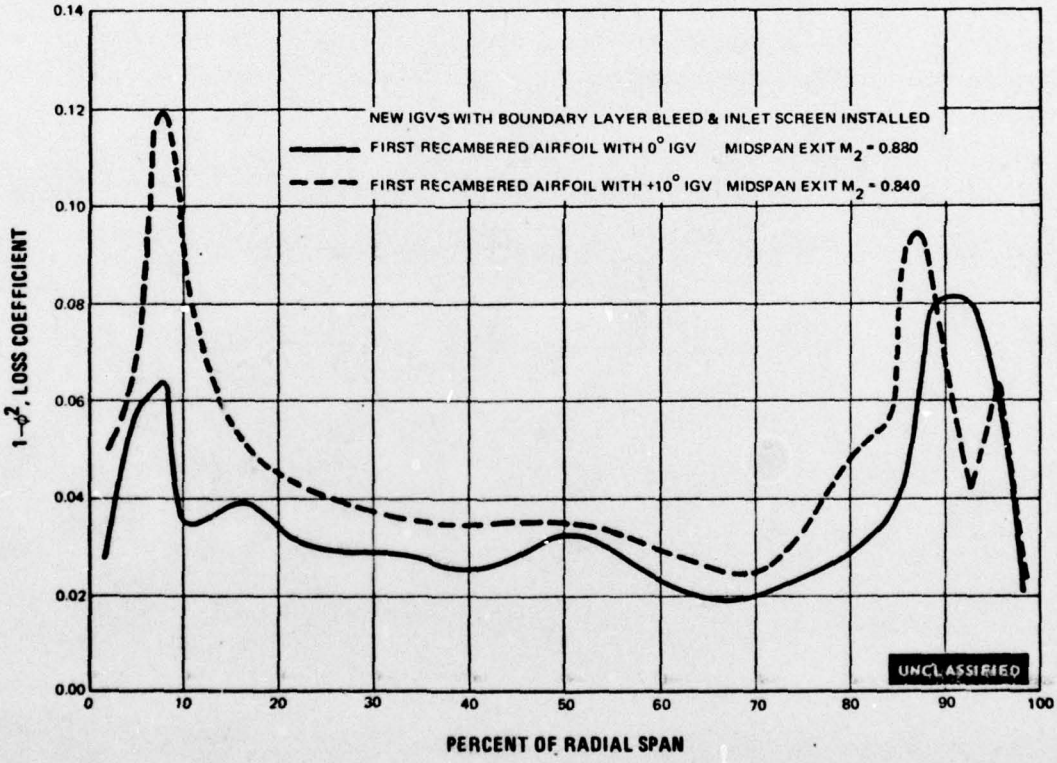

Figure 170 Comparison of First Recambered Airfoil Loss Coefficient Distribution at +10 Degrees Incidence With Zero Incidence Values

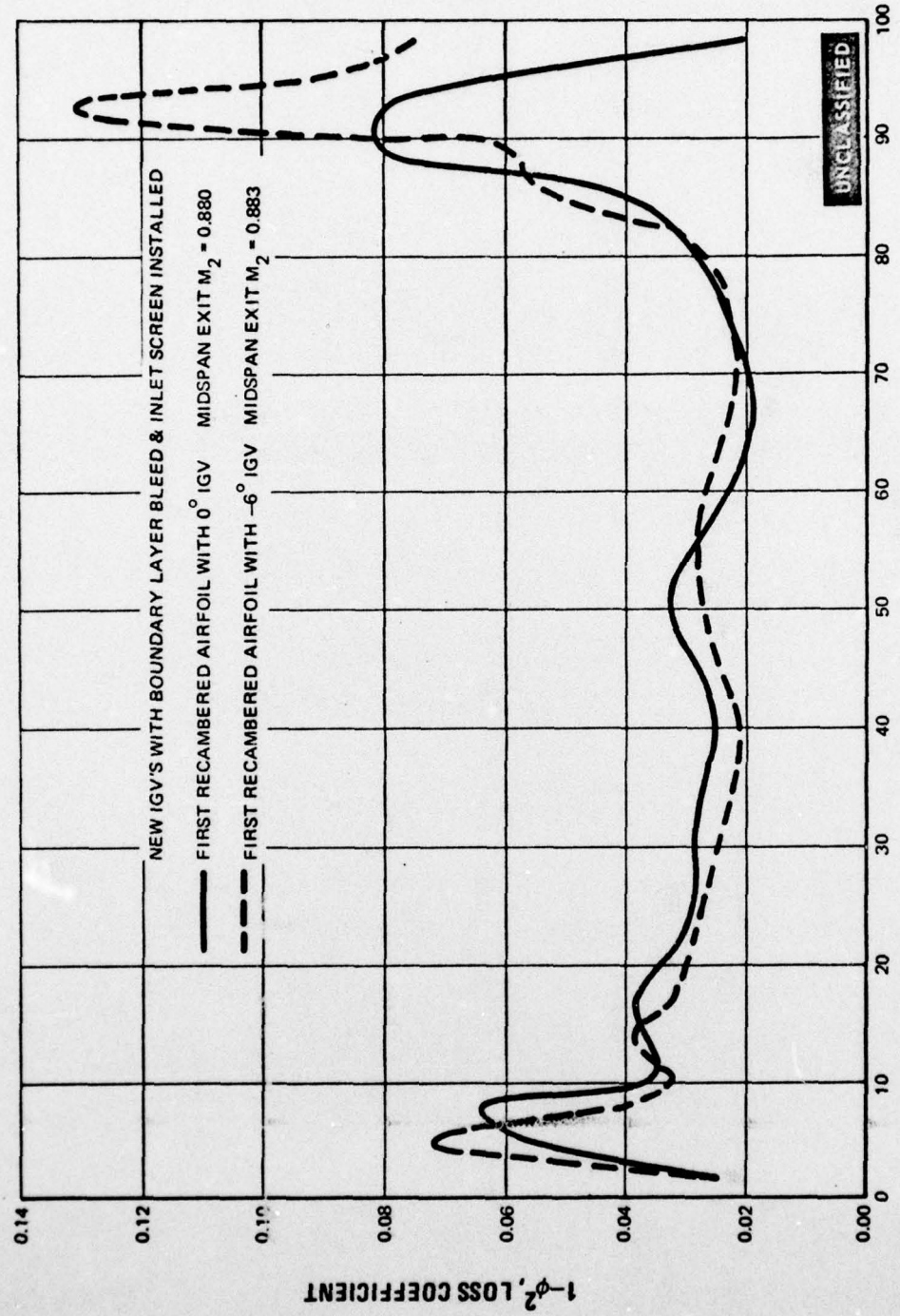

Figure 171 Comparison of First Recambered Airfoil Loss Coefficient Distribution at -6 Degrees Incidence With Zero Incidence Values

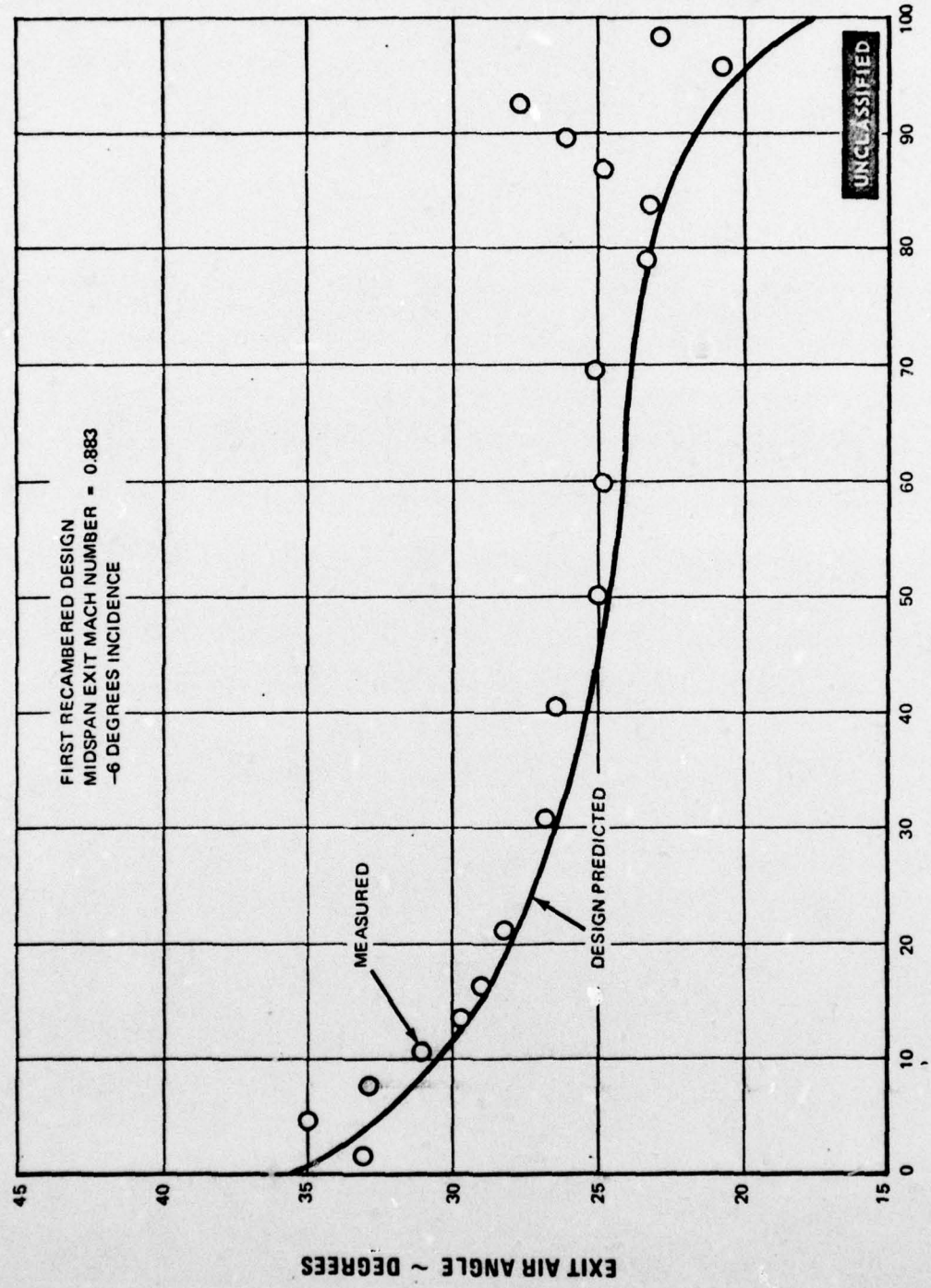

Figure 172 Comparison of Measured Exit Gas Angle With Predicted Design Values at -6 Degrees Incidence. First Recambered Airfoil at Midspan Exit Mach No. = 0.883

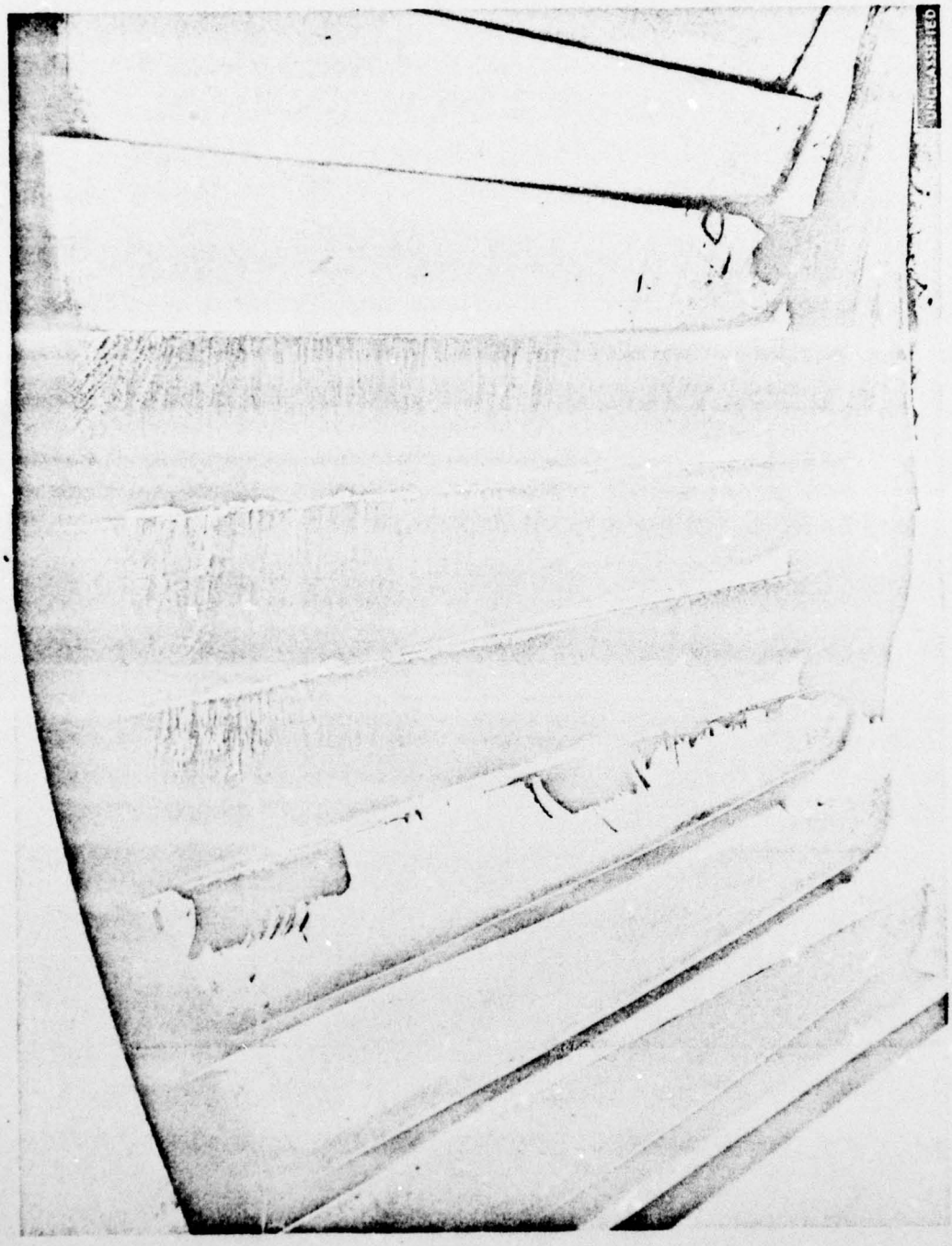

Figure 173 Oil and Graphite Flow Patterns, First Recambered Airfoil at +10 Degrees Incidence. Midspan Exit Mach No. = 0.840 (FE95376)

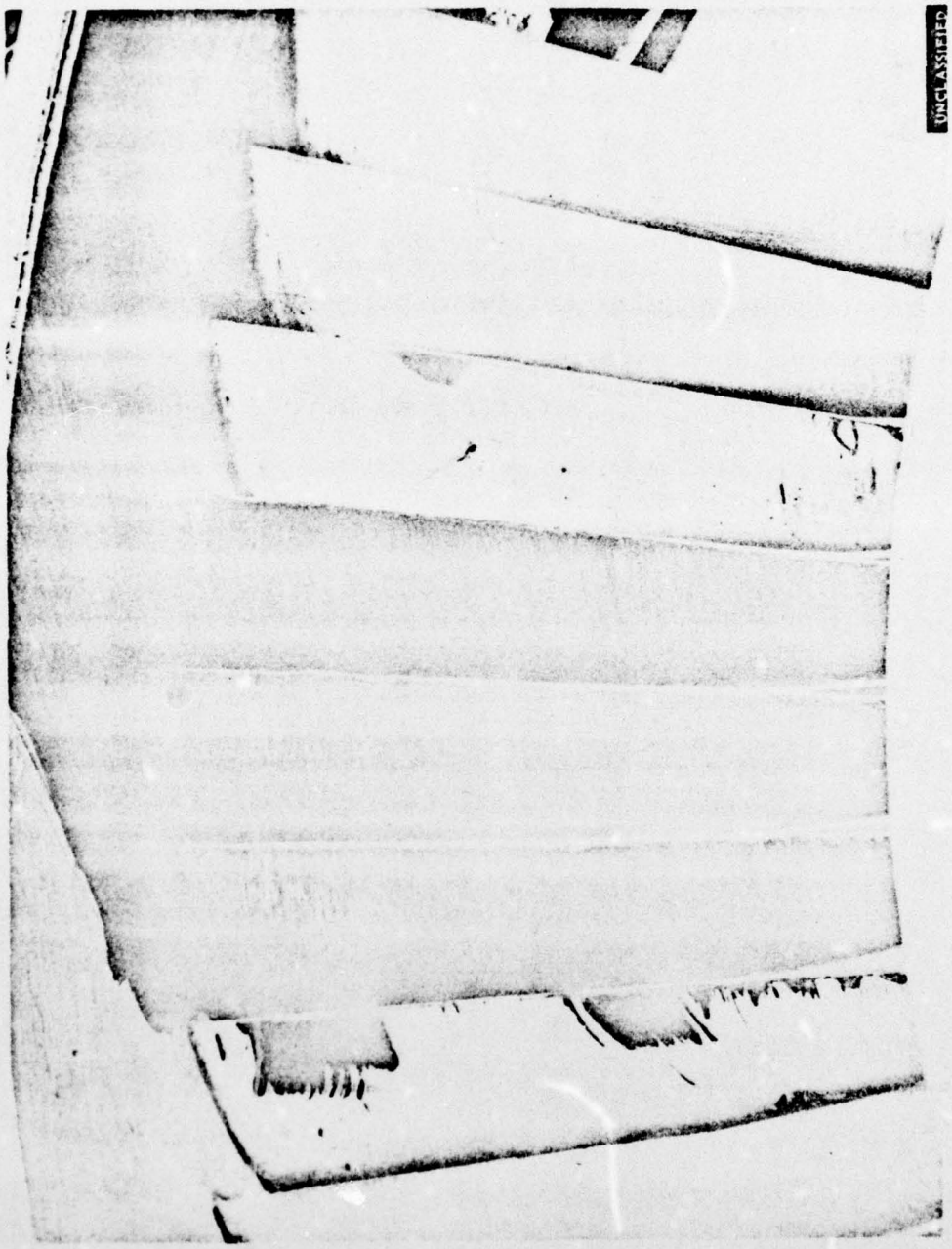

Figure 174 Oil and Graphite Flow Patterns, First Recambered Airfoil at +10 Degrees Incidence. Midspan Exit Mach No. = 0.840 (FE95377)

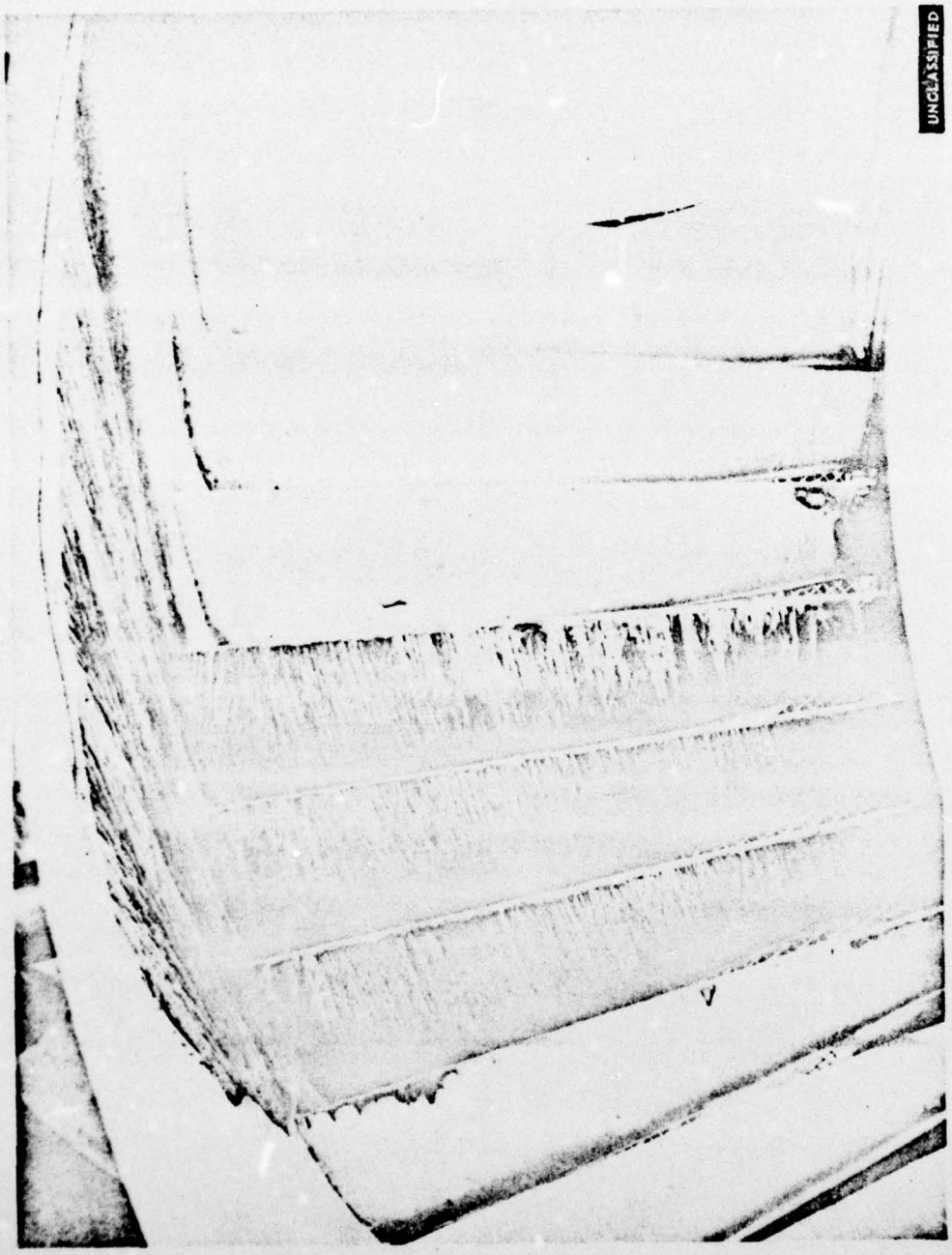

Figure 175 Oil and Graphite Flow Patterns, First Recambered Airfoil at -6 Degrees Incidence. Midspan Exit Mach No. = 0.883 (FE95504)

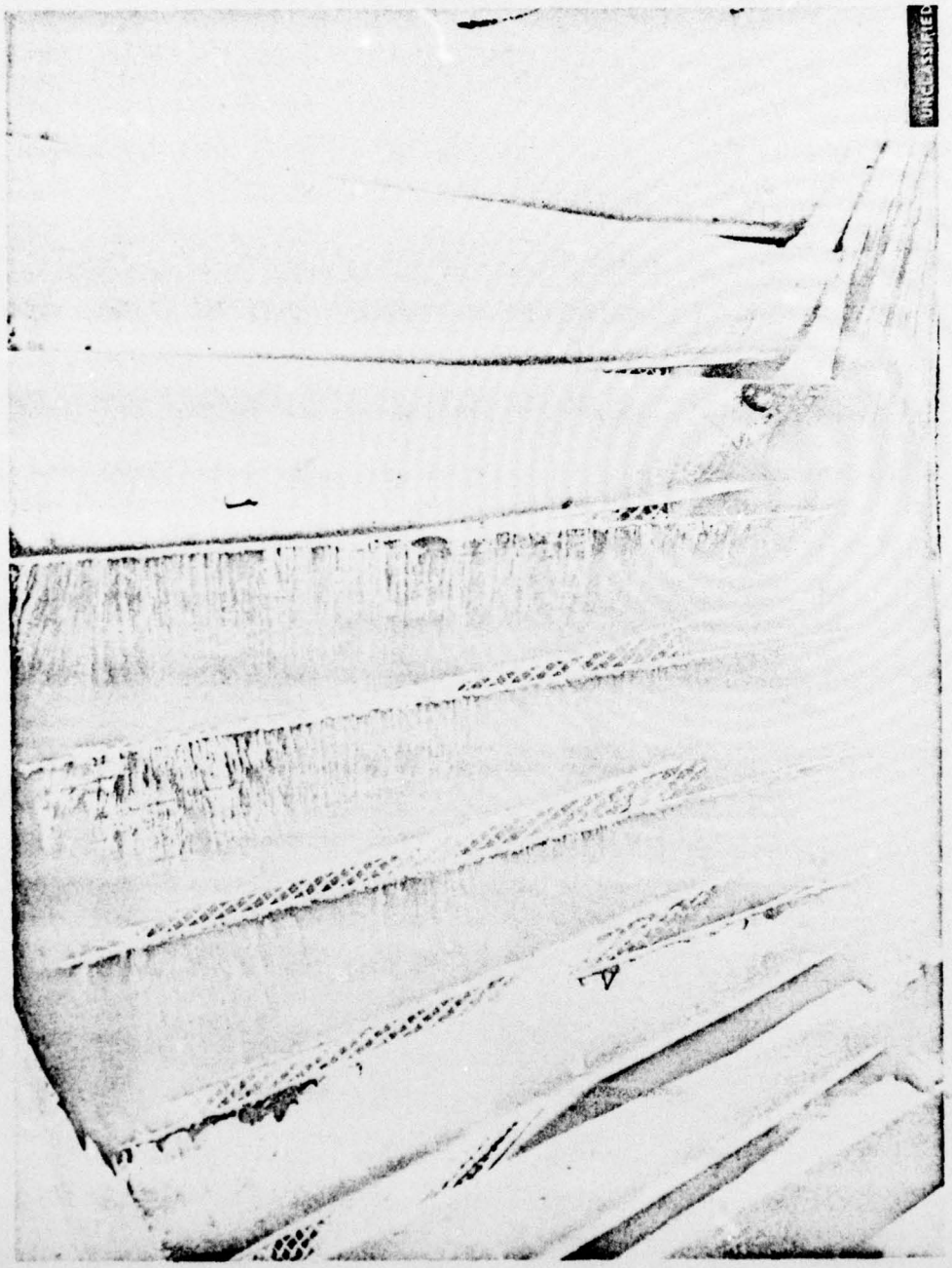

Figure 176 Oil and Graphite Flow Patterns, First Recambered Airfoil at -6 Degrees Incidence. Midspan Exit Mach No. = 0.883 (FE95503)

(U) Performance data for the second vane recambering design A airfoil are shown in Figures 177 through 182 at the positive incidence angle of 10 degrees. Similar data for a negative incidence of 6 degrees are shown in Figures 183 through 188. Spanwise loss coefficient distributions at +10 degrees incidence and -6 degrees incidence are compared to zero degrees incidence values in Figures 189 and 190, respectively. The root end-wall losses were larger for positive incidence and showed little difference for the negative incidence, when compared to the zero incidence results. The tip end-wall losses were much larger at the positive incidence and slightly lower at the negative incidence, when compared to the zero incidence condition. Overall, the positive incidence loss was greater and the negative incidence less when compared to the zero incidence curve. The measured exit gas angles are shown in Figures 191 and 192 for the +10 degrees and -6 degrees evaluations, respectively. Slight underturning is indicated at the tip in both cases with good agreement with design predicted values over the rest of the airfoils. This was also true at the zero incidence test condition (Section V). Oil and graphite flow patterns are shown in Figures 193 through 196 for both positive and negative incidence tests.

(U) The last airfoil subjected to off-design evaluation was the second vane recambering design C. The performance data for this airfoil at +10 degrees incidence are presented in Figures 197 through 202. The same type of data for the -6 degree incidence is shown in Figures 203 through 208. Comparisons of the spanwise loss coefficient distributions at positive incidence and negative incidence are made with zero incidence values in Figures 209 and 210, respectively. The root end-wall losses were slightly lower at the +10 degrees and -6 degrees incidence than at the zero incidence condition. The positive incidence tip end-wall loss was greater than, and the negative incidence tip end-wall loss was about the same as the zero incidence value. The overall loss coefficient was slightly higher at the positive incidence, and slightly lower at the negative incidence, in comparison to zero incidence conditions. The measured exit gas angles are shown in Figures 211 and 212. Good agreement was obtained with design values for both positive and negative incidence angles. Oil and graphite flow patterns for these tests are shown in Figures 213 through 216. Well behaved flow with some end-wall radial shift, is again verified from these patterns.

(U) The variation of loss coefficient with midspan exit Mach number is shown in Figures 217, 218 and 219 for the second vane first recambered airfoil, recambering design A and recambering design C, respectively. The contribution of each end to the overall loss is shown, in order to indicate the effect of incidence on each end-wall uncambering. For these same airfoils, the effect of incidence on loss coefficient is shown in Figure 220. It is noted that these airfoils were not overly sensitive to incidence, and that the loss level generally goes up with incidence angle.

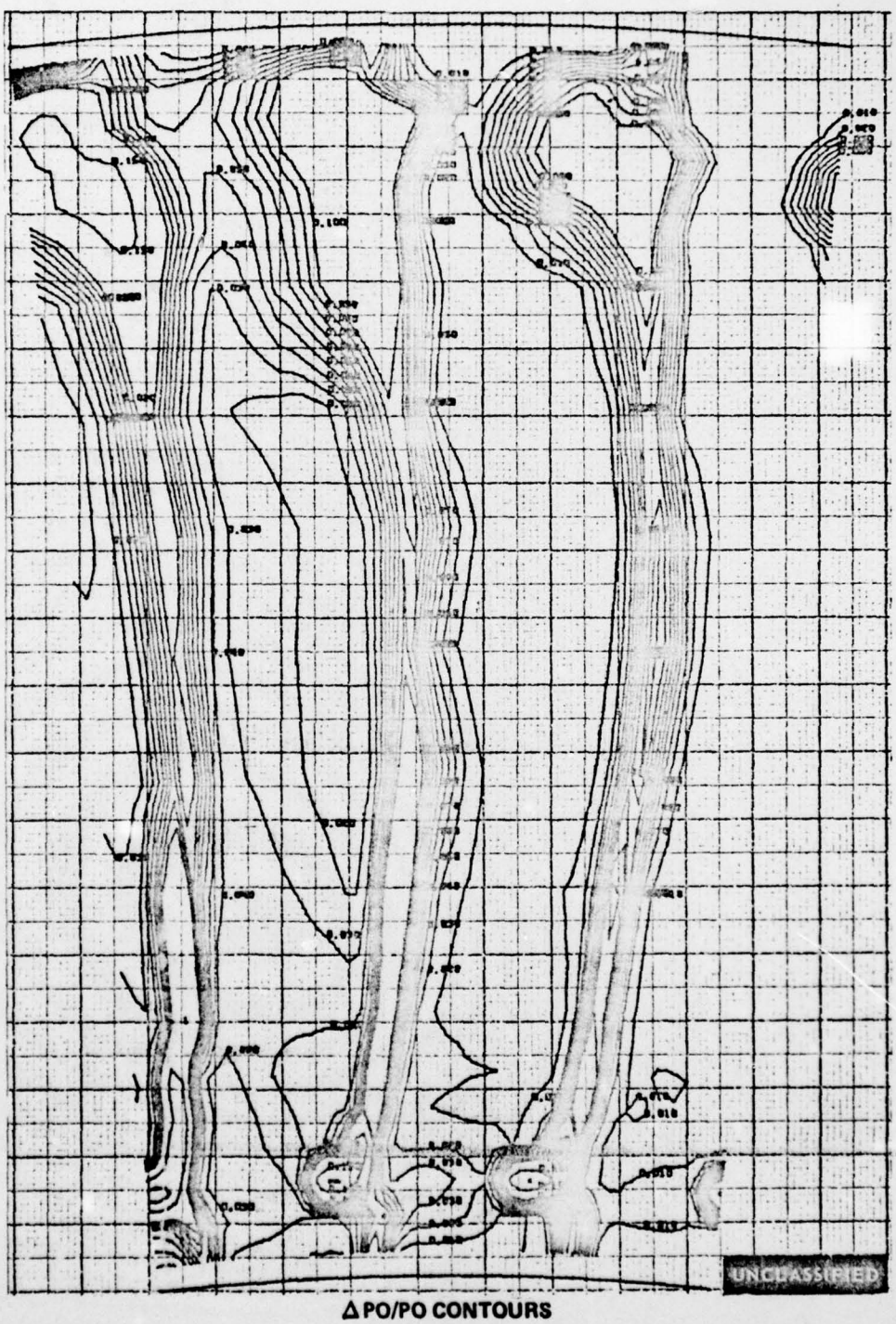

Figure 177 Pressure Loss Contours, Second Vane Recambering Design A at +10° Incidence. Three Flow Passages. Midspan Exit Mach Number = 0.837

AD-A050 537 PRATT AND WHITNEY AIRCRAFT GROUP EAST HARTFORD CONN F/G 21/5
INVESTIGATION OF A HIGHLY LOADED TWO-STAGE FAN-DRIVE TURBINE. V--ETC(U)
JUN 70 H WELNA, D E DAHLBERG, W H HEISER F33615-68-C-1208
UNCLASSIFIED PWA-3967 AFAPL-TR-69-92-VOL-5 NL

3 OF 3
AD
AD 50537

END
DATE FILMED
4 -78
DDC

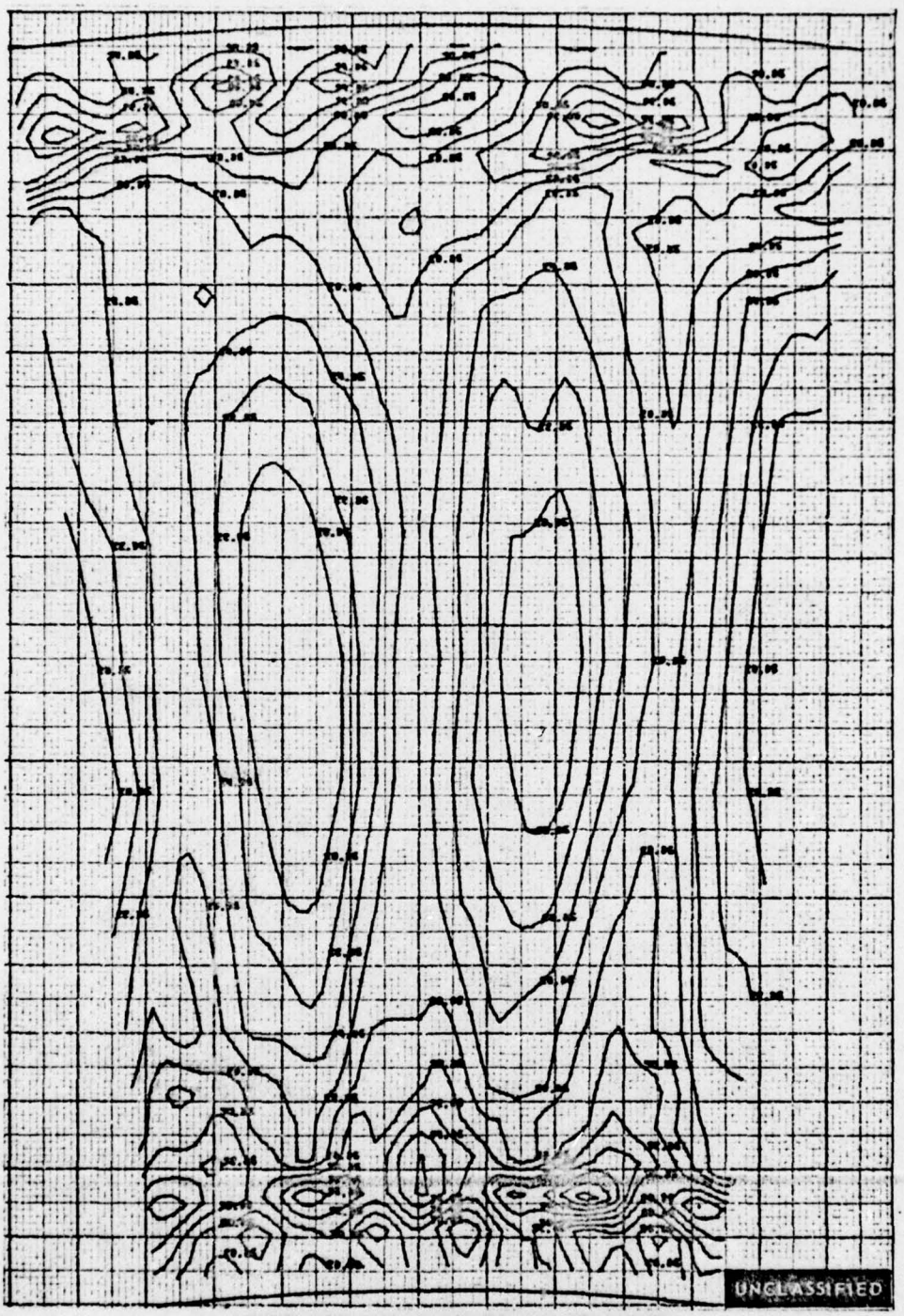

EXIT GAS ANGLE CONTOURS, DEGREES

Figure 178 Exit Gas Angle Contours, Second Vane Recambering Design A at +10° Incidence. Three Flow Passages. Midspan Exit Mach Number = 0.837

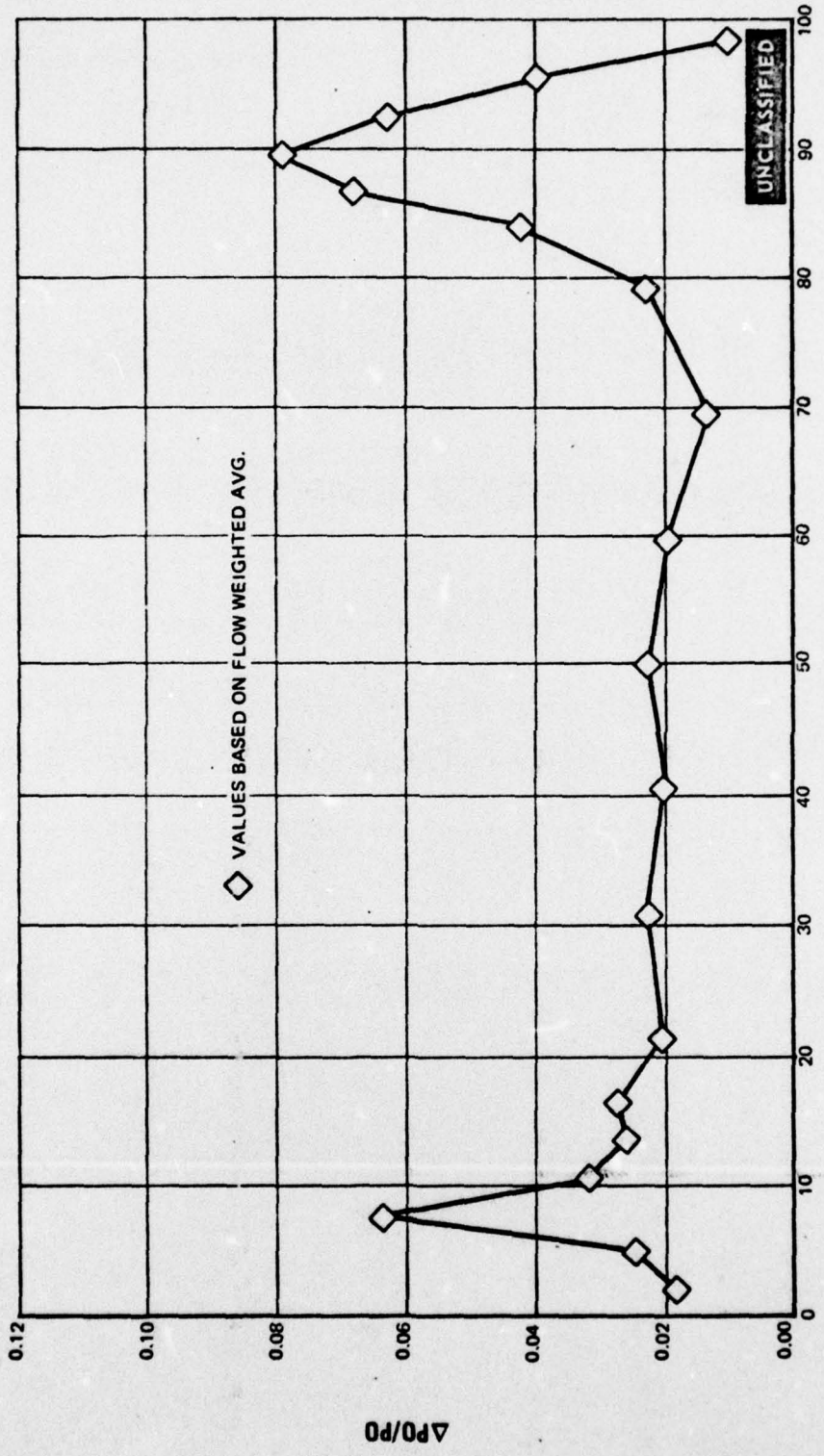

Figure 179 Spanwise Pressure Loss Distribution, Second Vane Recambering Design A at +10° Incidence. Midspan Exit Mach Number = 0.837

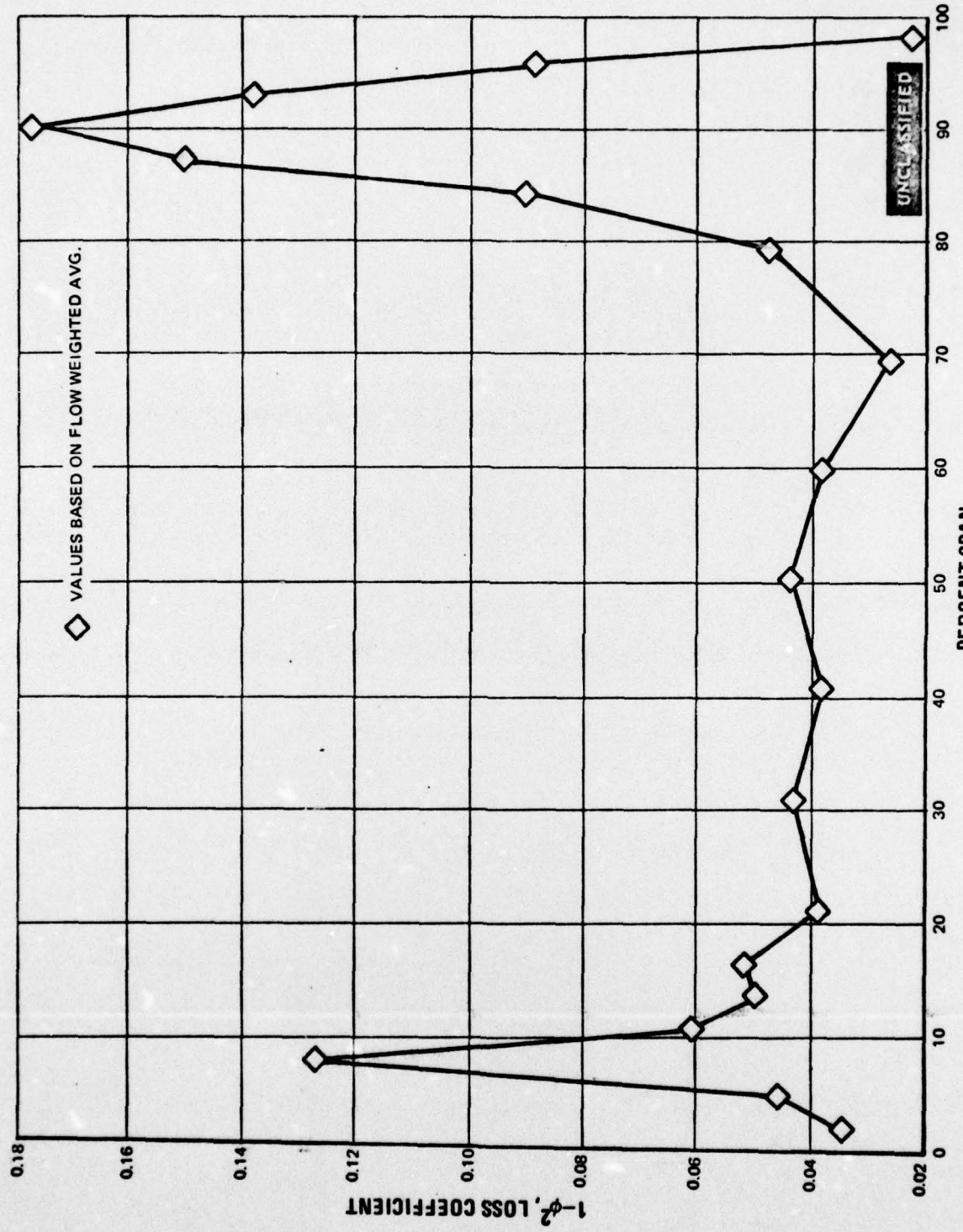

Figure 180 Spanwise Loss Coefficient Distribution, Second Vane Recambering Design A at [illegible] Incidence. Midspan Exit Mach Number = 0.837

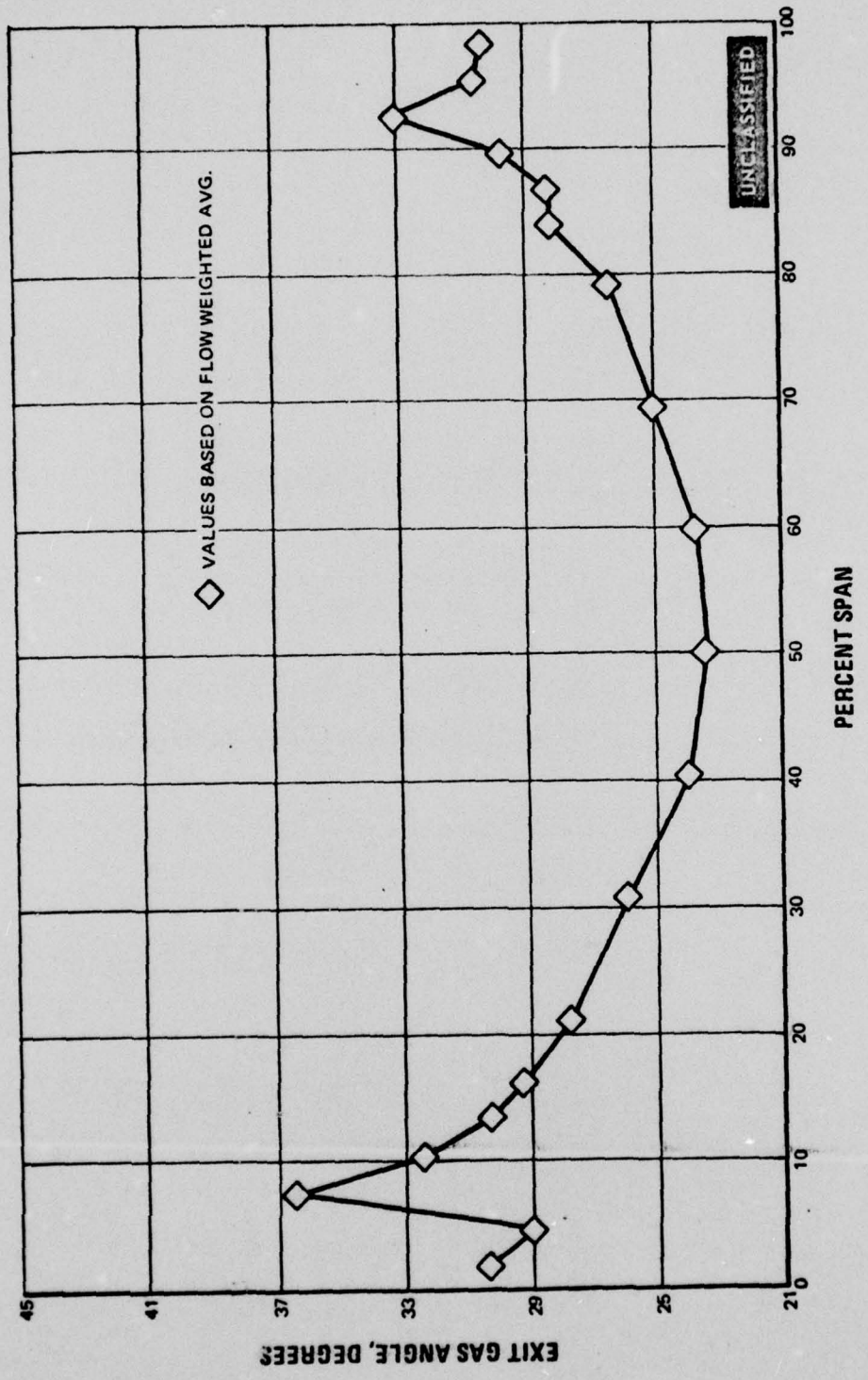

Figure 181 Spanwise Exit Gas Angle Distribution, Second Vane Recambering Design A at +10° Incidence. Midspan Exit Mach Number = 0.837

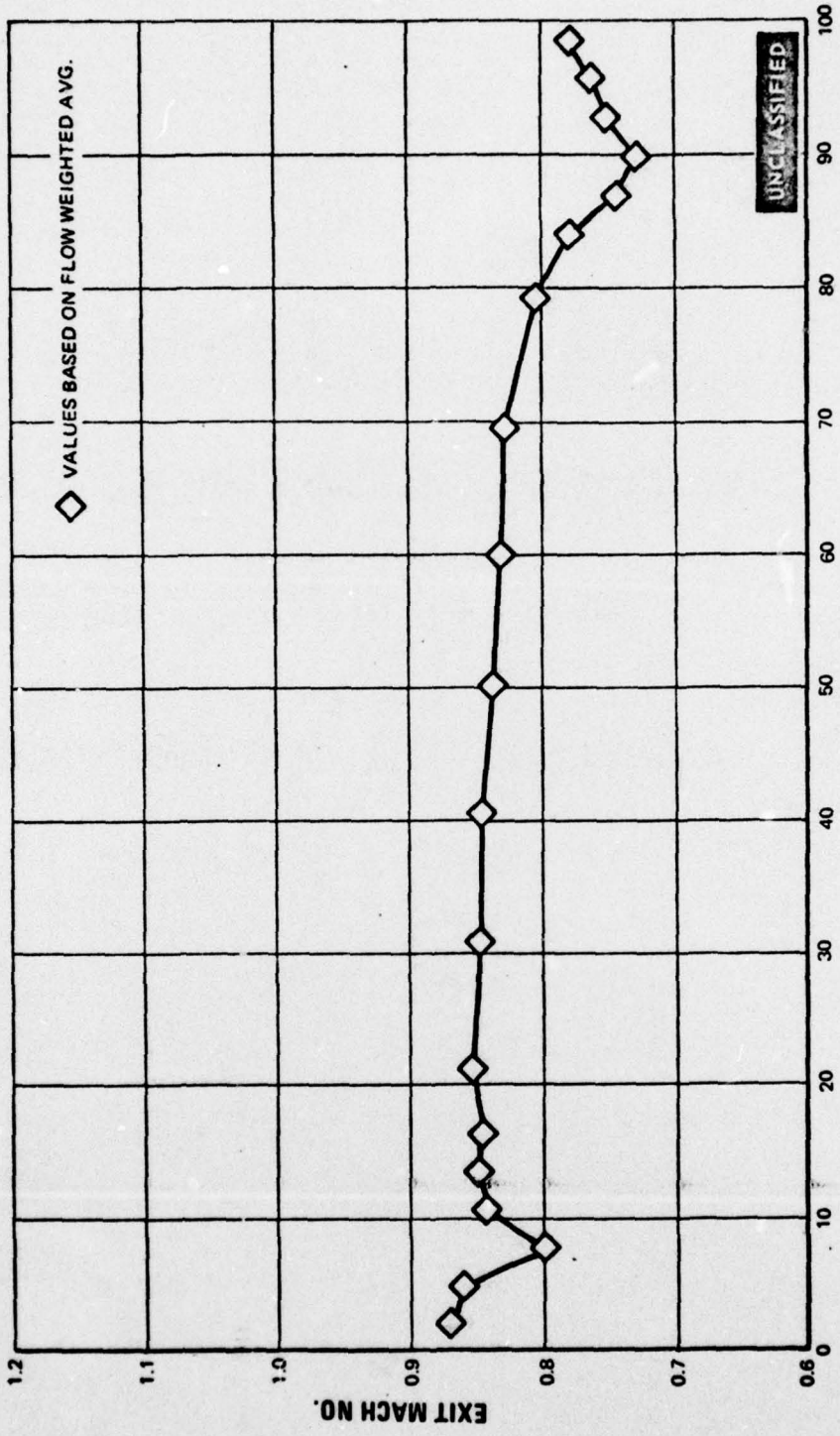

Figure 182 Spanwise Exit Mach Number Distribution, Second Vane Recambering Design A at +10° Incidence. Midspan Exit Mach Number = 0.837

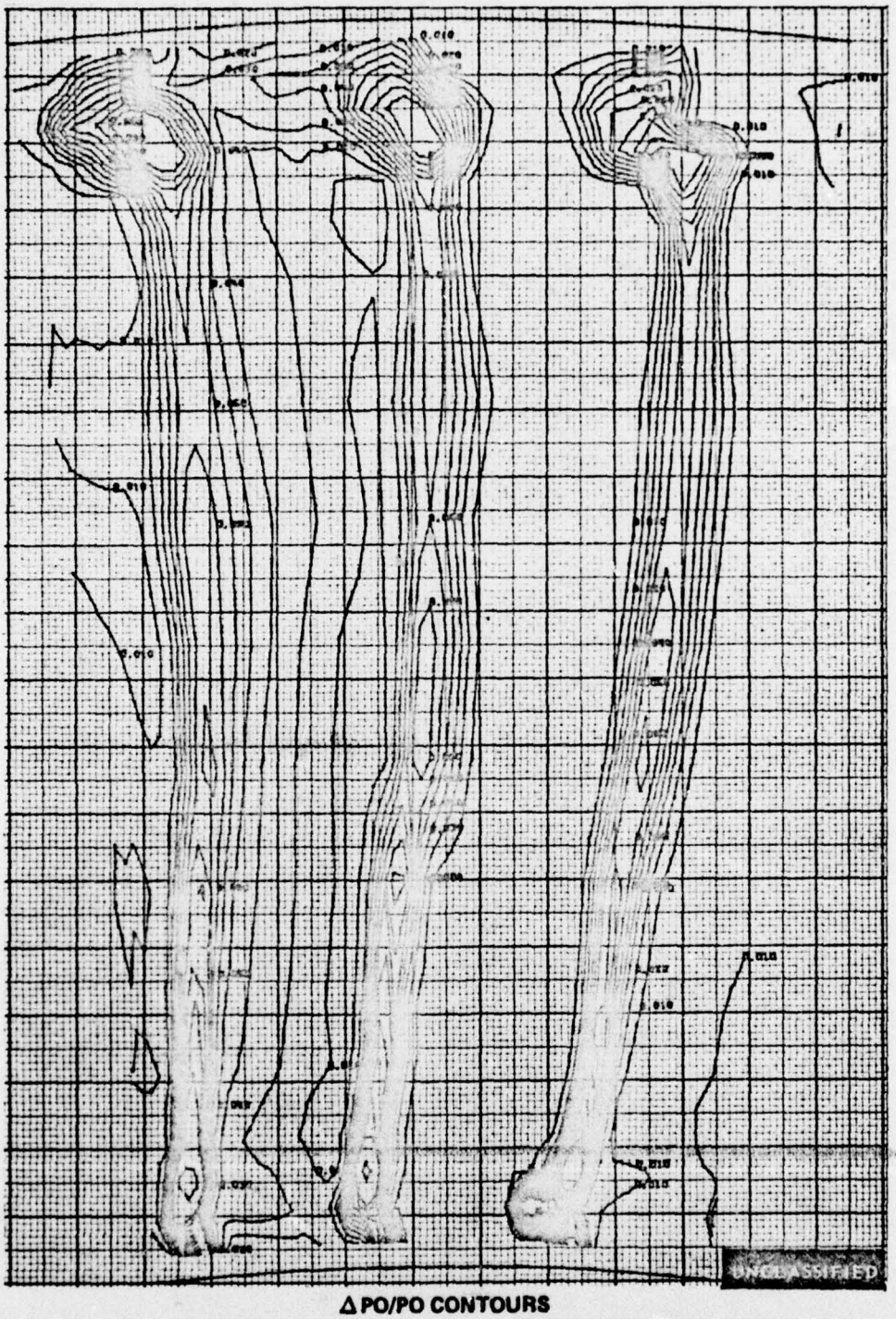

Δ PO/PO CONTOURS

Figure 183 Pressure Loss Contours, Second Vane Recambering Design A at -6° Incidence. Three Flow Passages. Midspan Exit Mach Number = 0.869

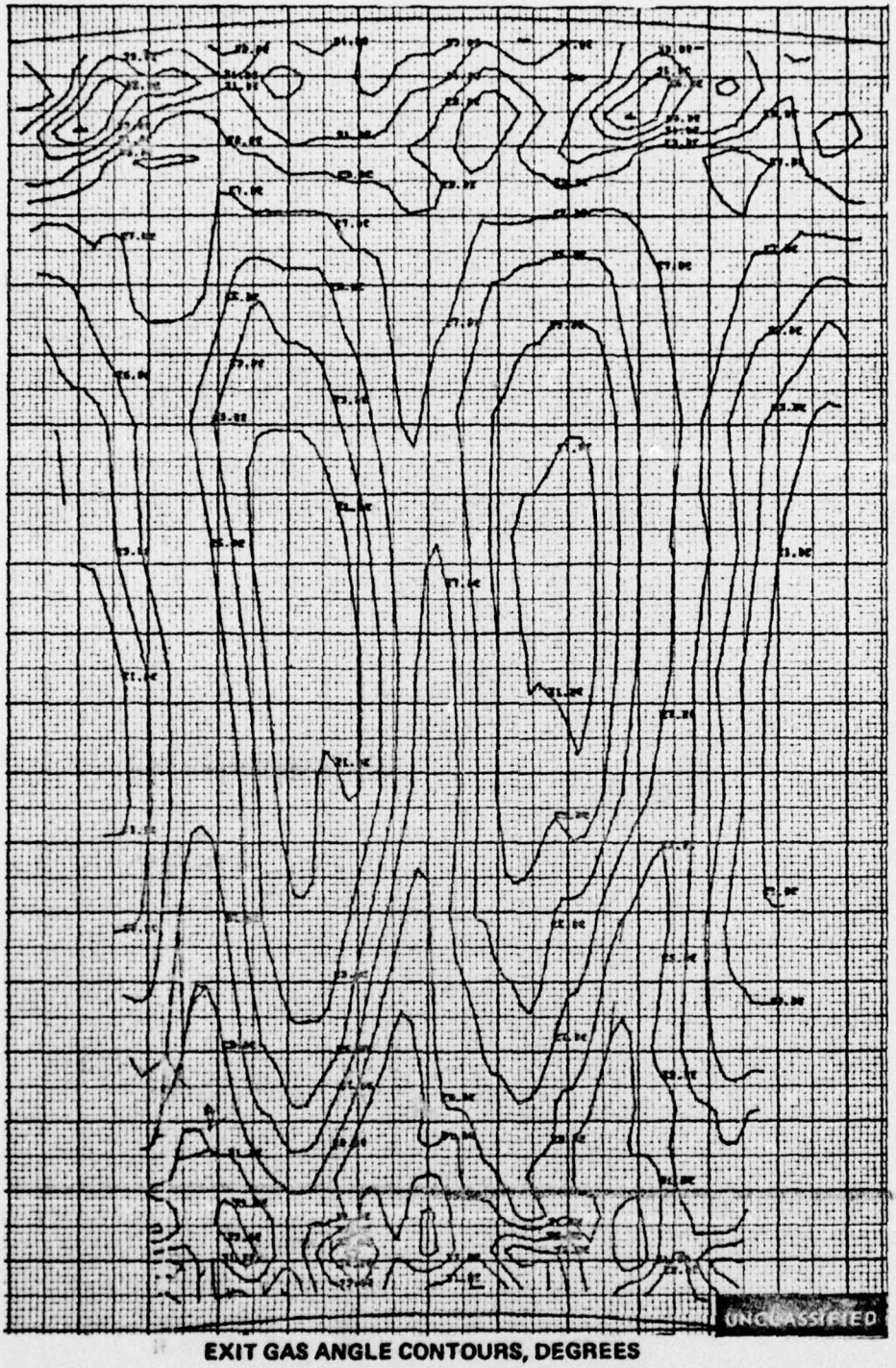

EXIT GAS ANGLE CONTOURS, DEGREES

Figure 184 Exit Gas Angle Contours, Second Vane Recambering Design A at -6° Incidence. Three Flow Passages. Midspan Exit Mach Number = 0.869

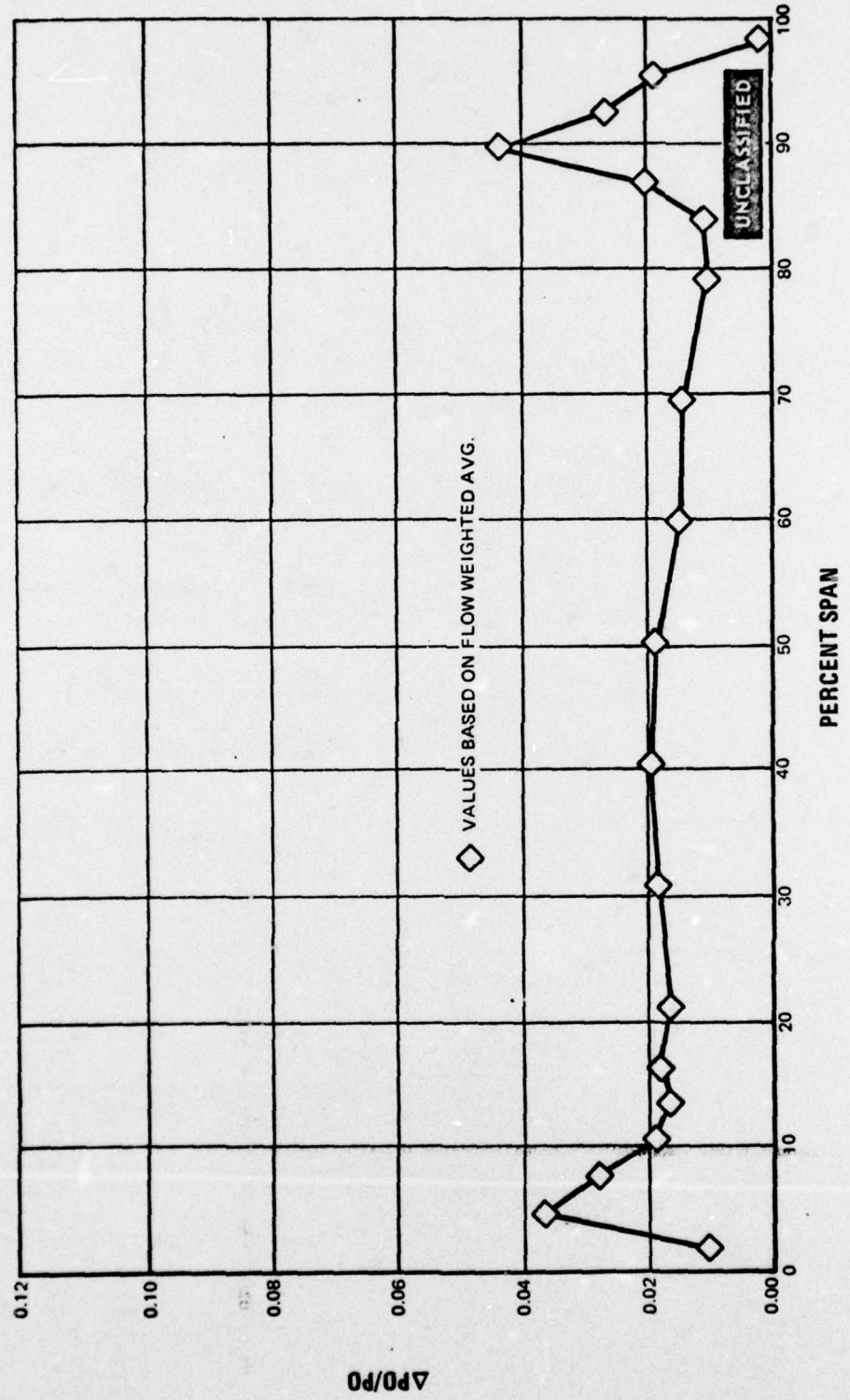

Figure 185 Spanwise Pressure Loss Distribution, Second Vane Recambering Design A at -6° Incidence. Midspan Exit Mach Number = 0.869

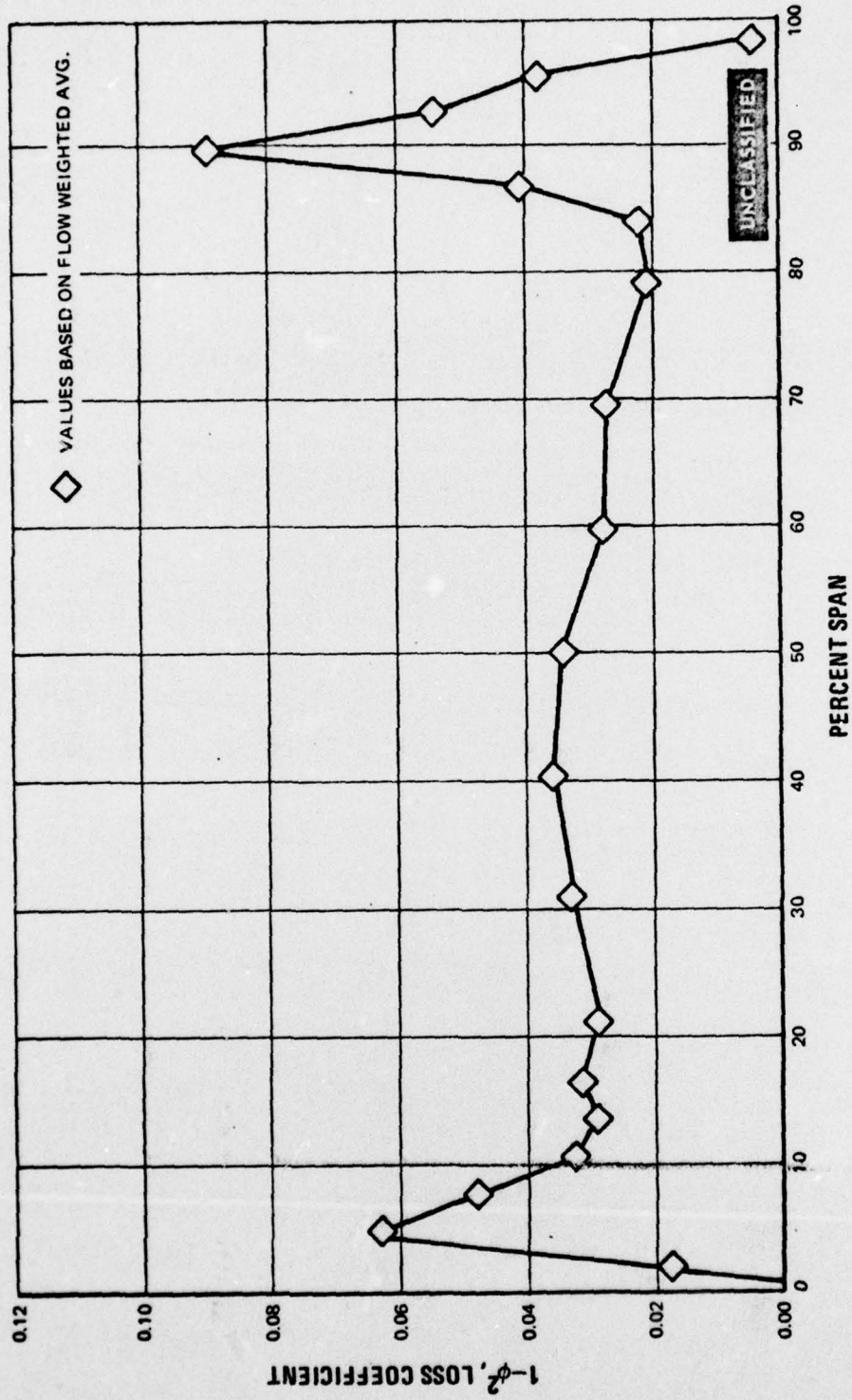

Figure 186 Spanwise Loss Coefficient Distribution, Second Vane Recambering Design A at -6° Incidence. Midspan Exit Mach Number = 0.869

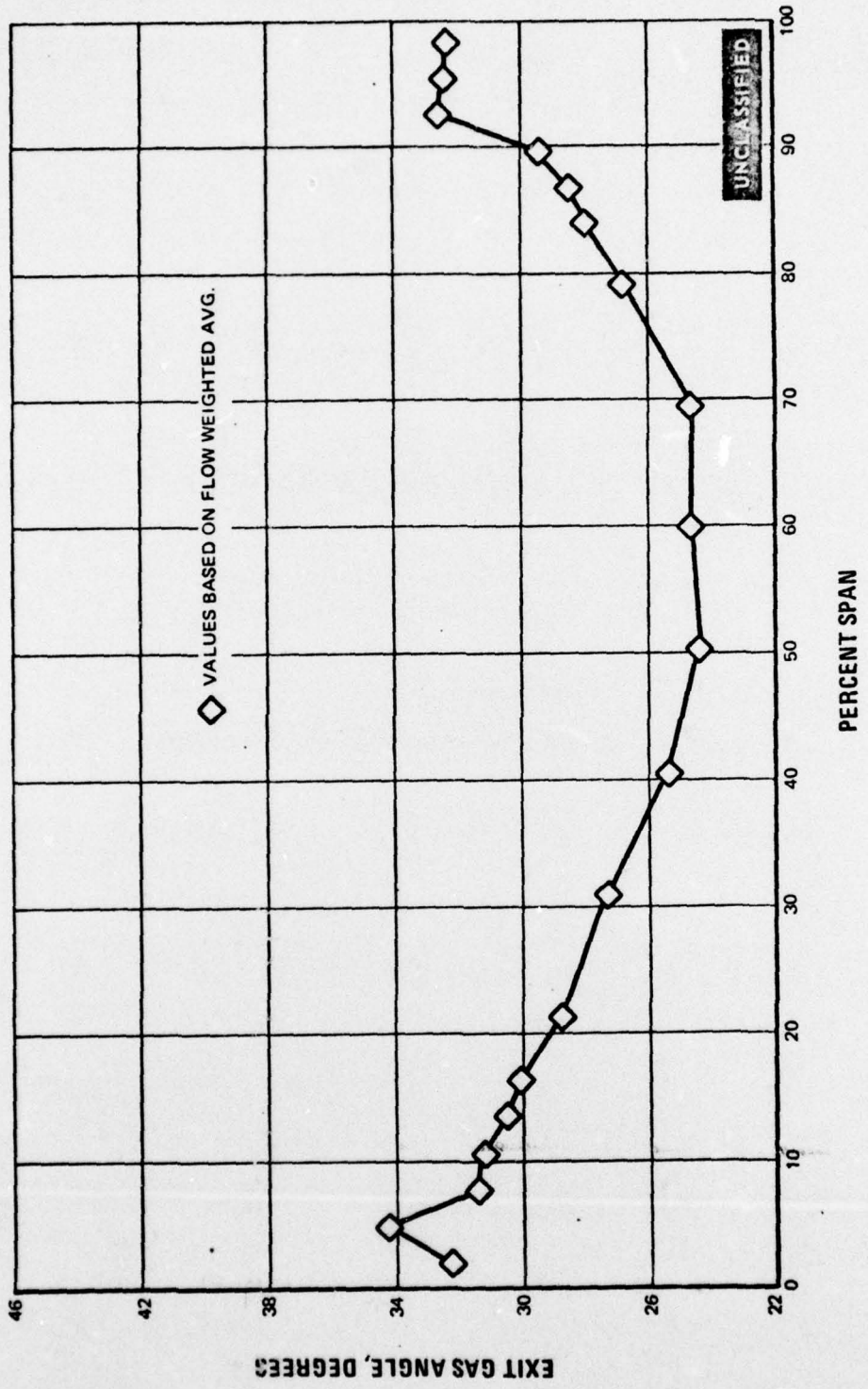

Figure 187 Spanwise Exit Gas Angle Distribution, Second Vane Recambering Design A at -6° Incidence. Midspan Exit Mach Number = 0.869

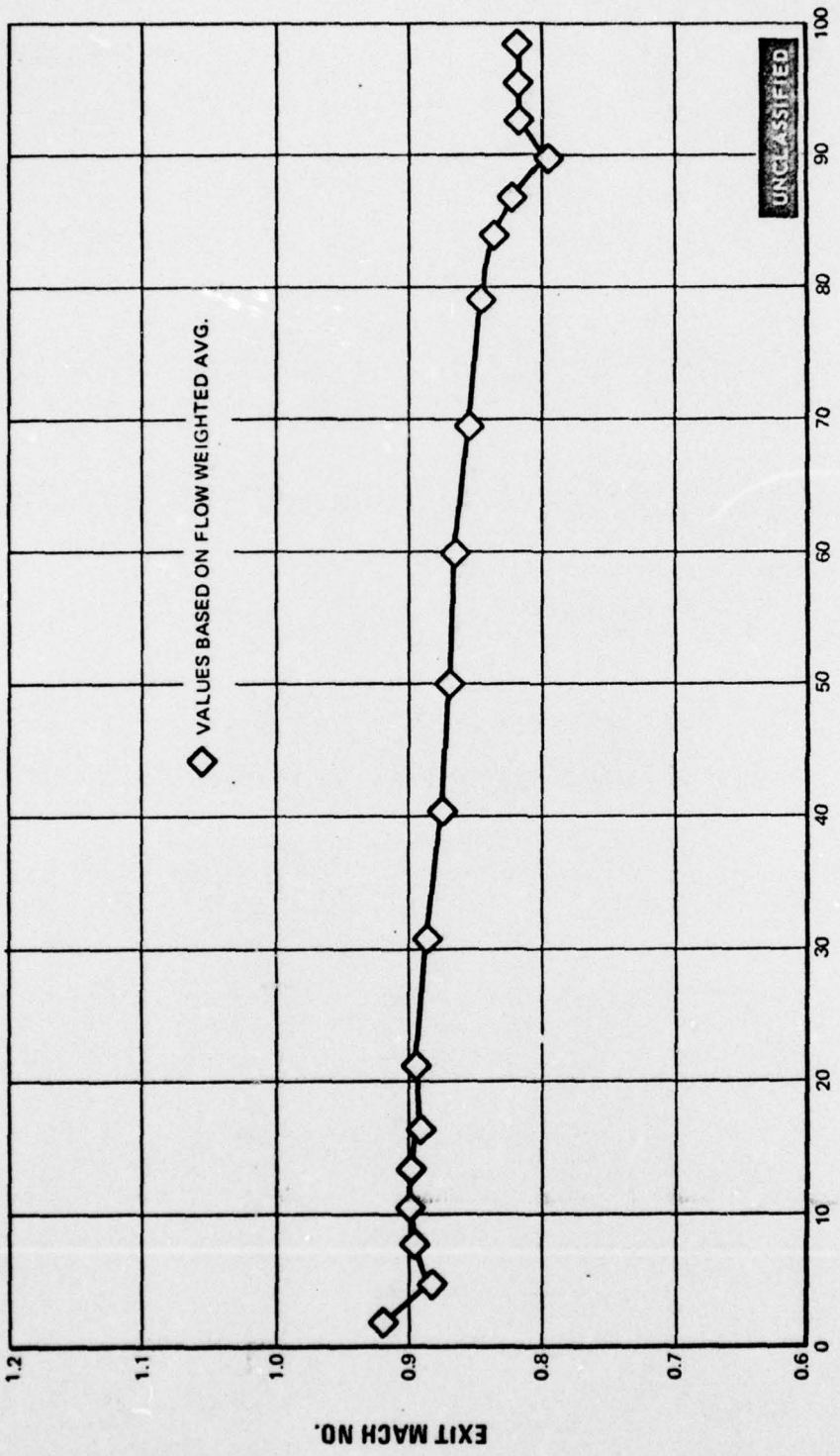

Figure 188 Spanwise Exit Mach Number Distribution, Second Vane Recambering Design A at -6° Incidence. Midspan Exit Mach Number = 0.869

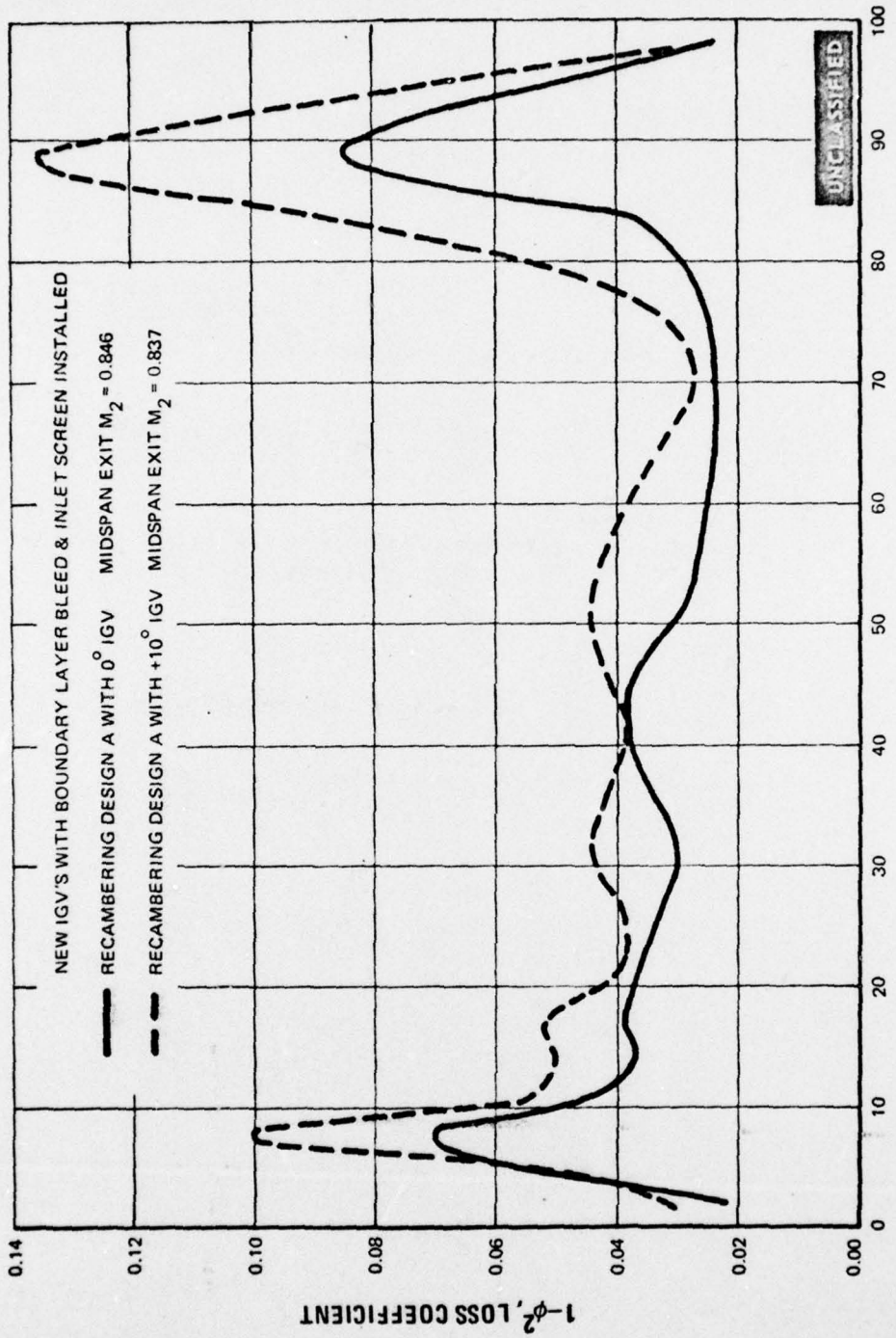

Figure 189 Comparison of Recambering Design A Airfoil Loss Coefficient Distribution at +10 Degrees Incidence With Zero Incidence Values

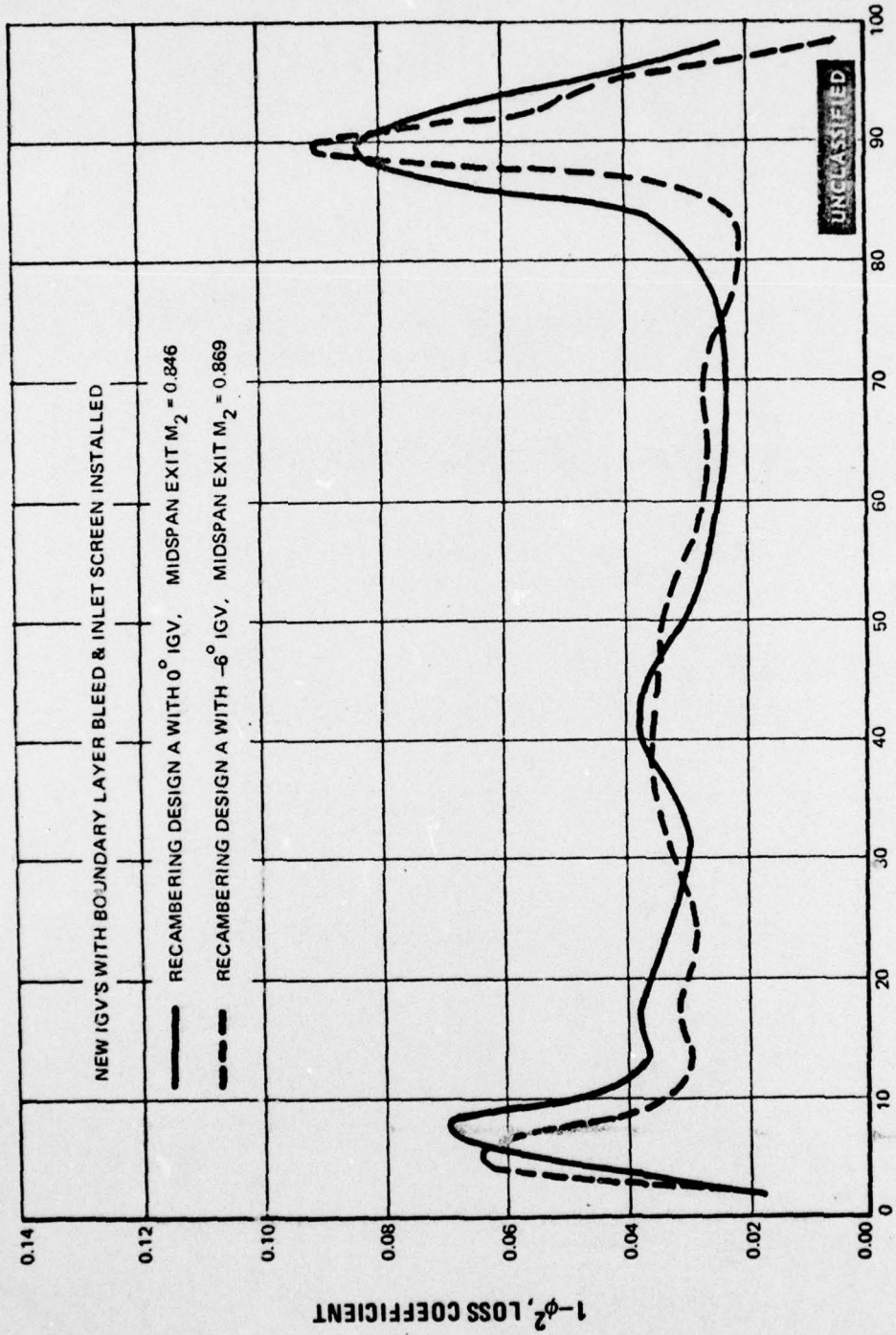

Figure 190 Comparison of Recambering Design A Airfoil Loss Coefficient Distribution at -6 Degrees Incidence With Zero Incidence Values

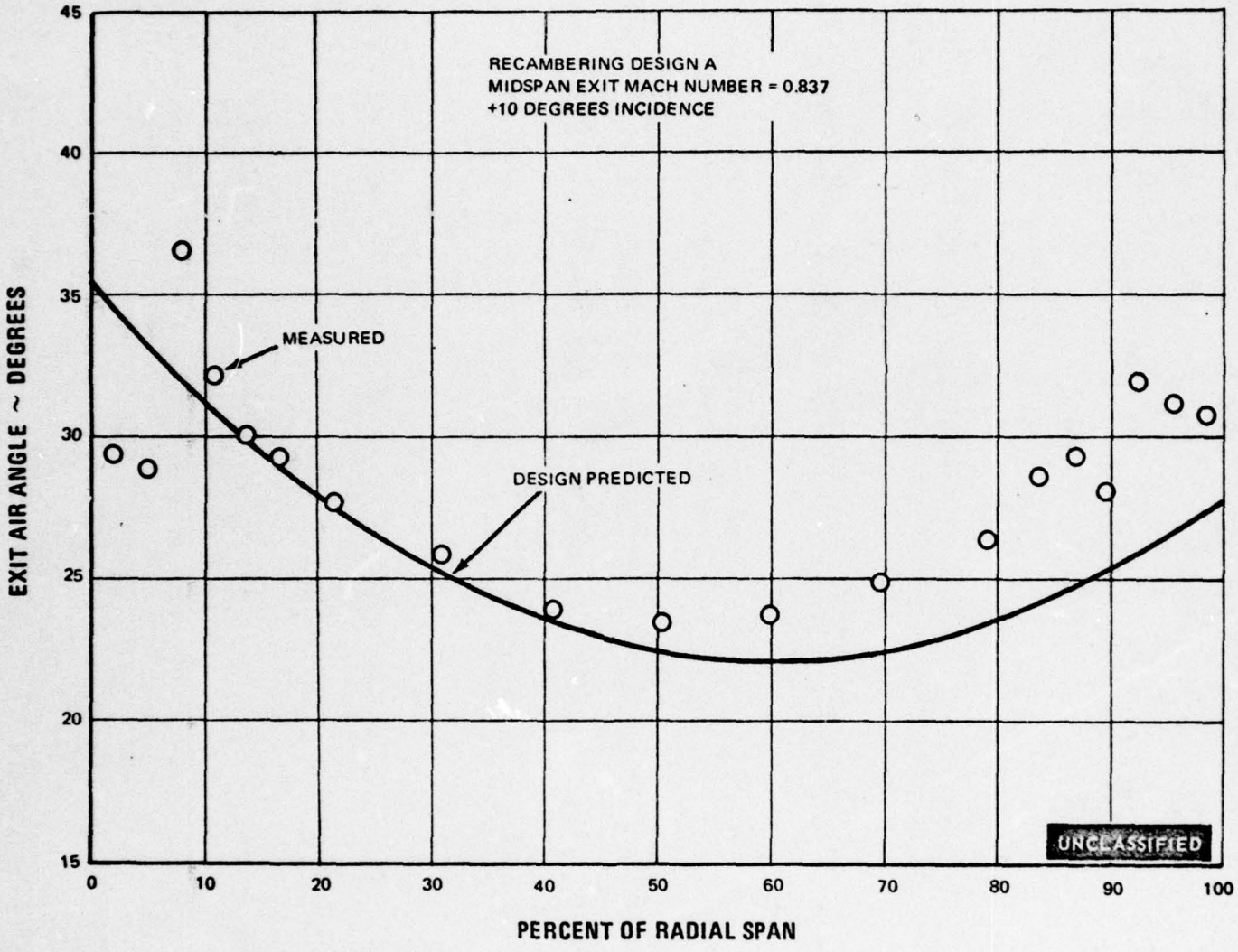

Figure 191 Comparison of Measured Exit Gas Angle With Predicted Design Values at +10 Degrees Incidence. Design A Airfoil at Midspan Exit Mach No. = 0.837

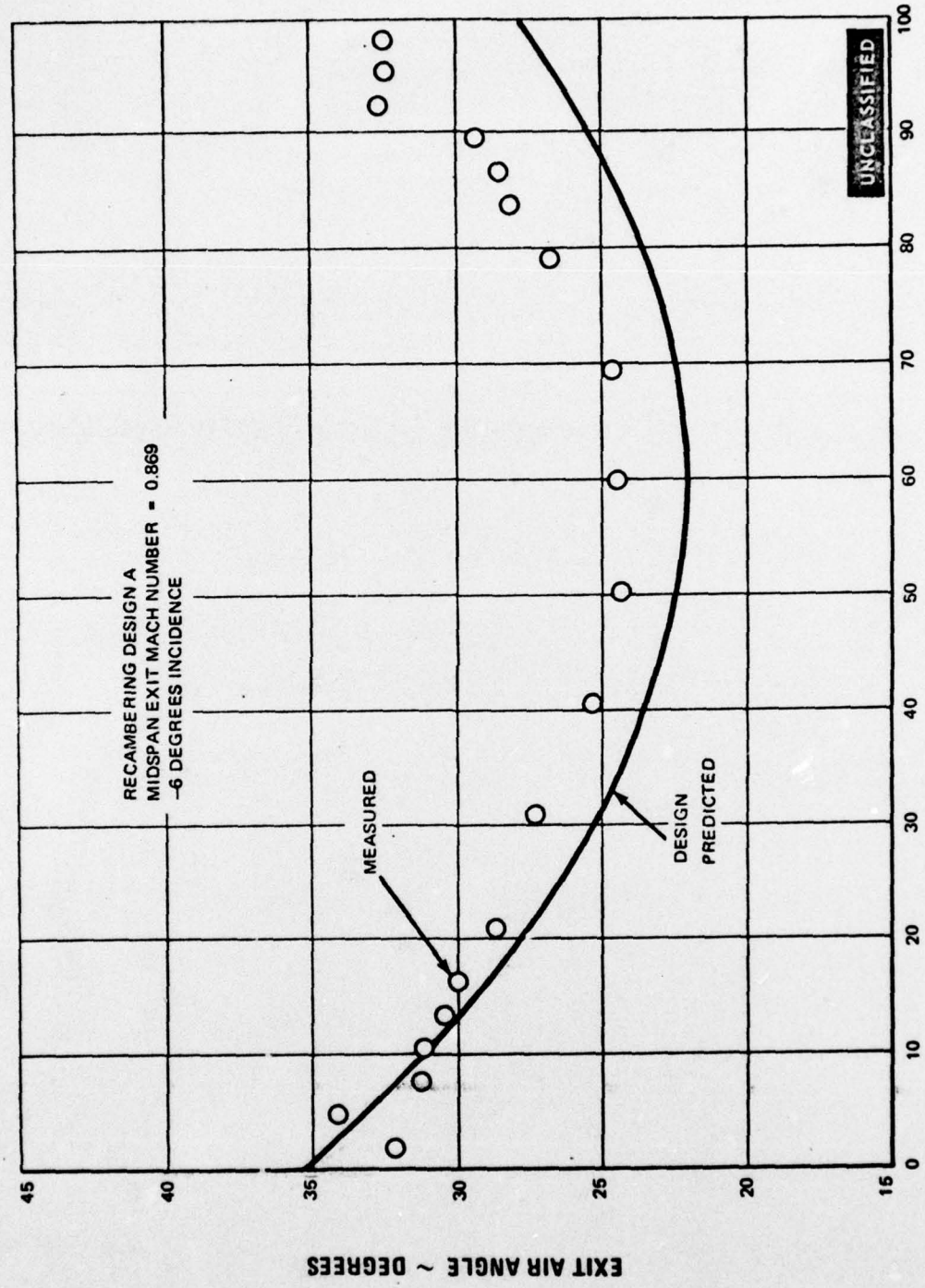

Figure 192 Comparison of Measured Exit Gas Angle With Predicted Design Values at -6 Degrees Incidence. Design A Airfoil at Midspan Exit Mach No. = 0.869

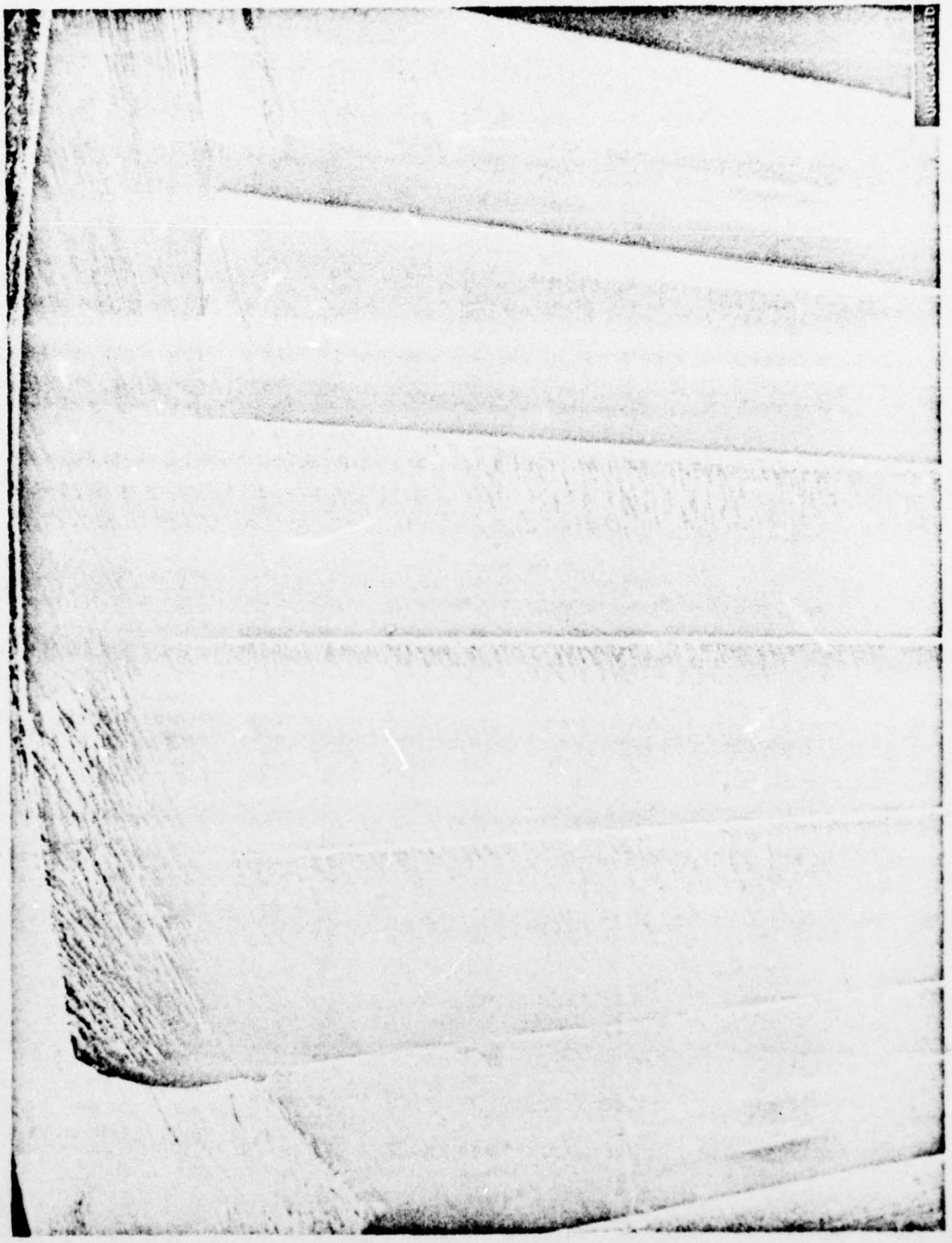

Figure 193 Oil and Graphite Flow Patterns, Second Vane Recambering Design A Airfoil at +10 Degrees Incidence. Midspan Exit Mach No. = 0.837 (FE95732)

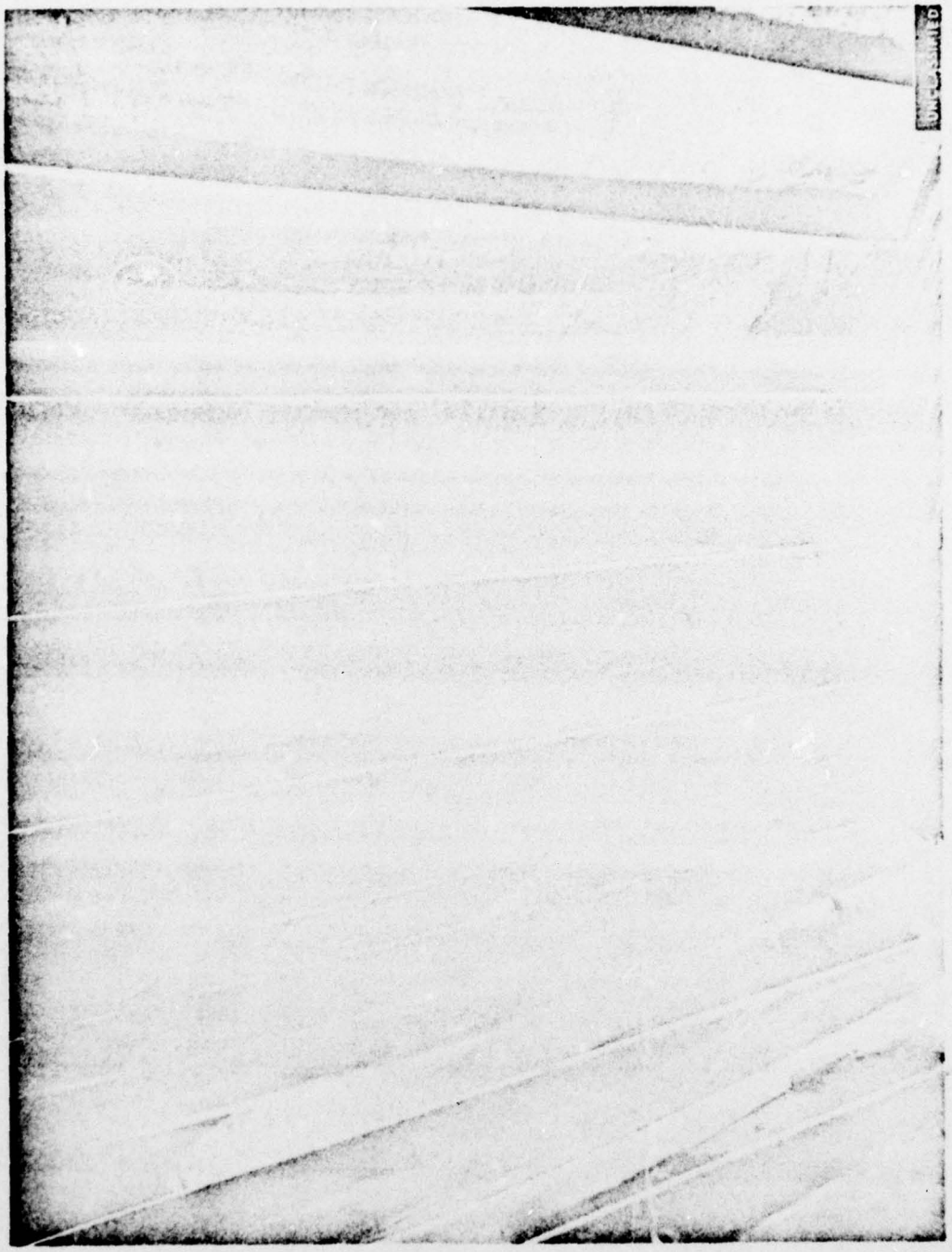

Figure 194 Oil and Graphite Flow Patterns, Second Vane Recambering Design A Airfoil at +10 Degrees Incidence. Midspan Exit Mach No. = 0.837 (FE95733)

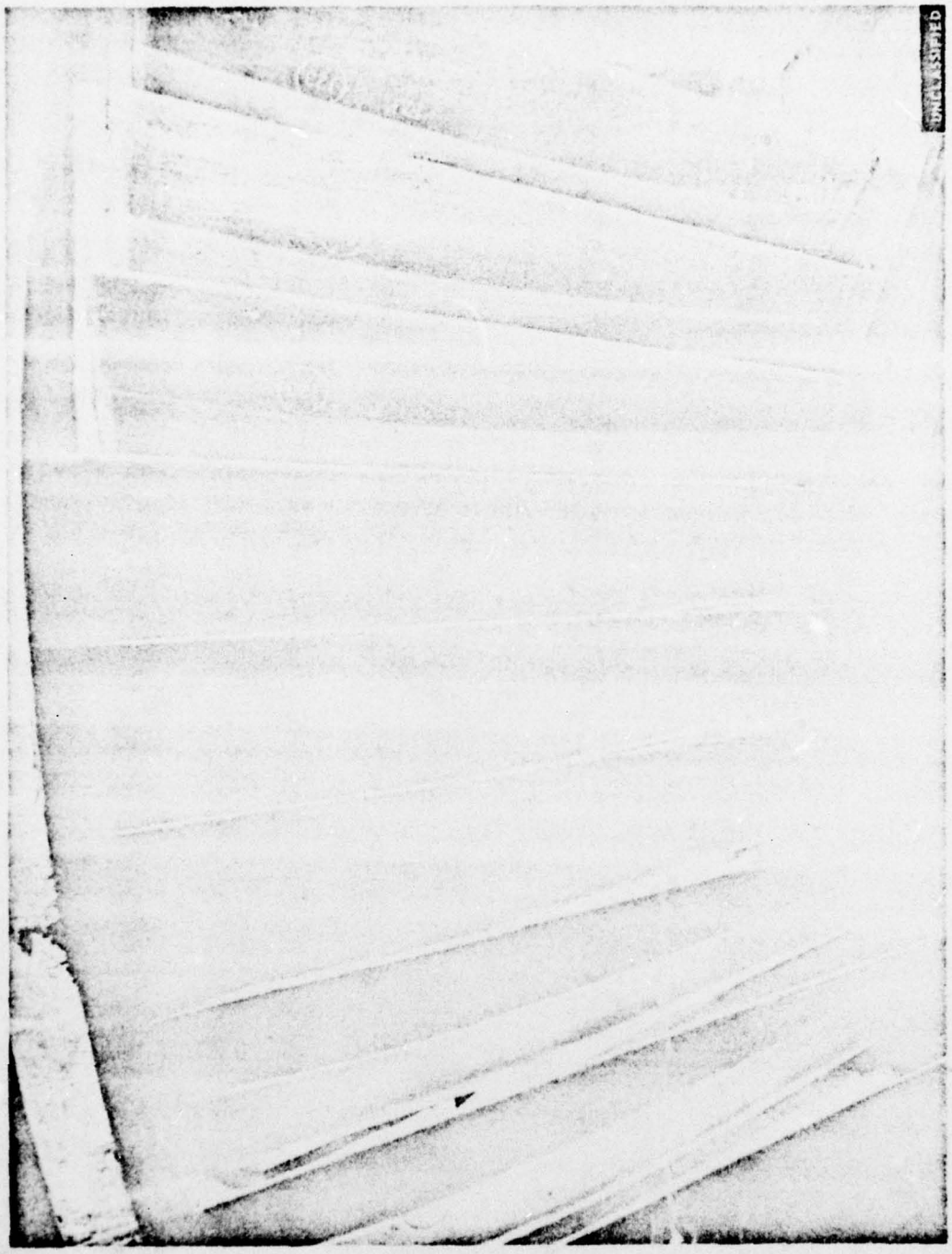

Figure 195 Oil and Graphite Flow Patterns, Second Vane Recambering Design A Airfoil at -6 Degrees Incidence. Midspan Exit Mach No. = 0.869 (FE95863)

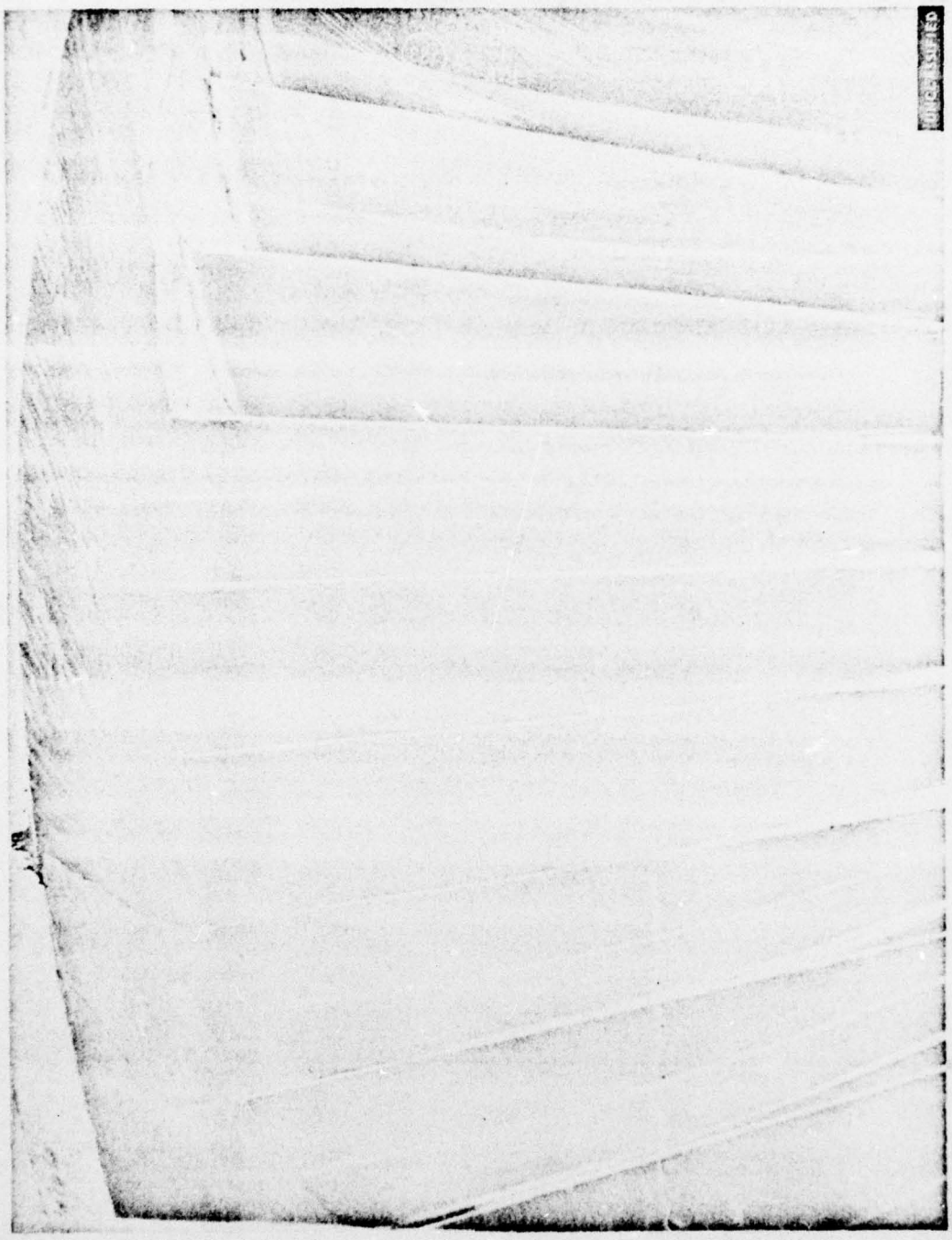

Figure 196 Oil and Graphite Flow Patterns, Second Vane Recambering Design A Airfoil at -6 Degrees Incidence. Midspan Exit Mach No. = 0.869 (FE95864)

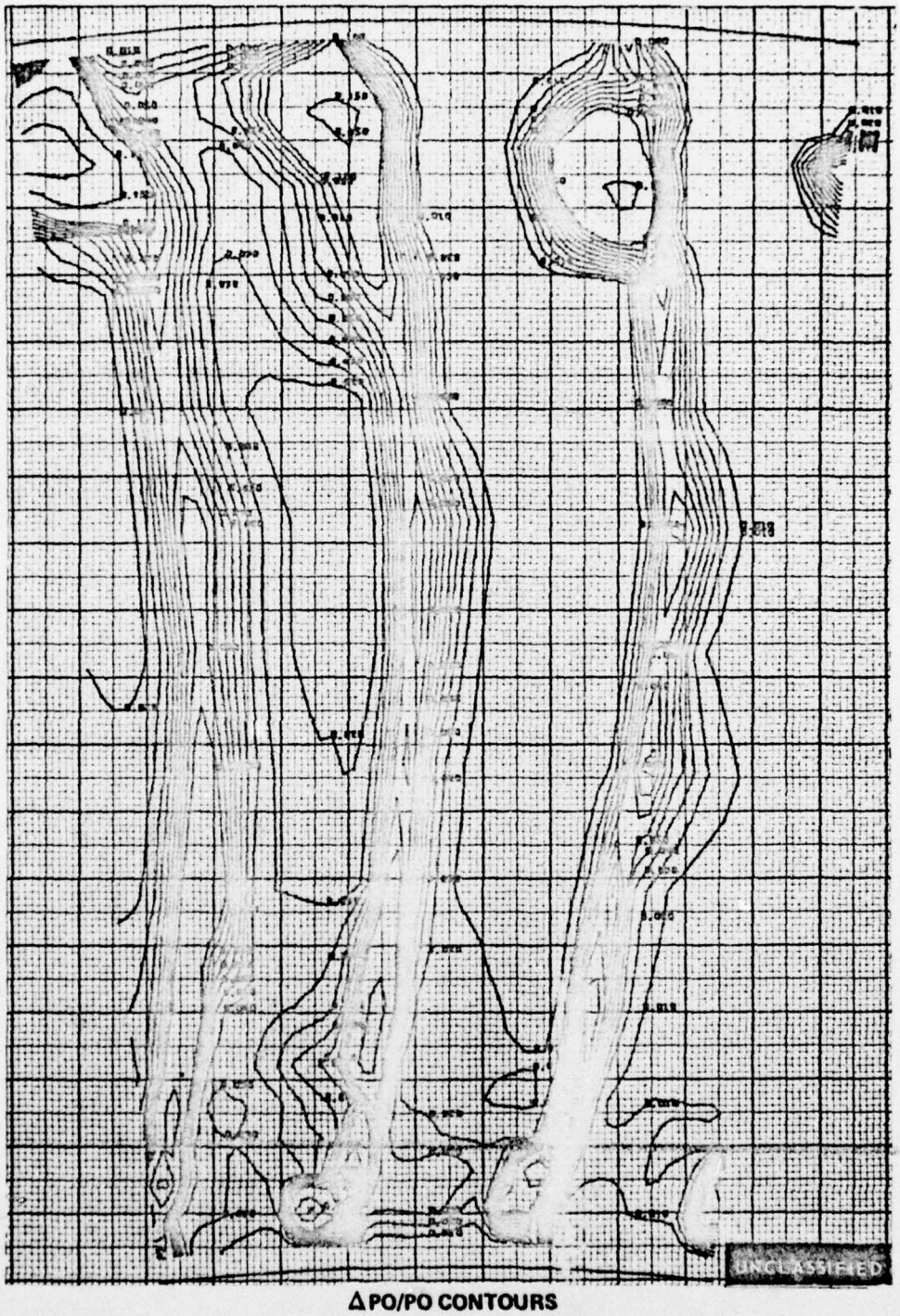

ΔPO/PO CONTOURS

Figure 197 Pressure Loss Contours, Second Vane Recambering Design C at +10° Incidence. Three Flow Passages. Midspan Exit Mach Number = 0.858

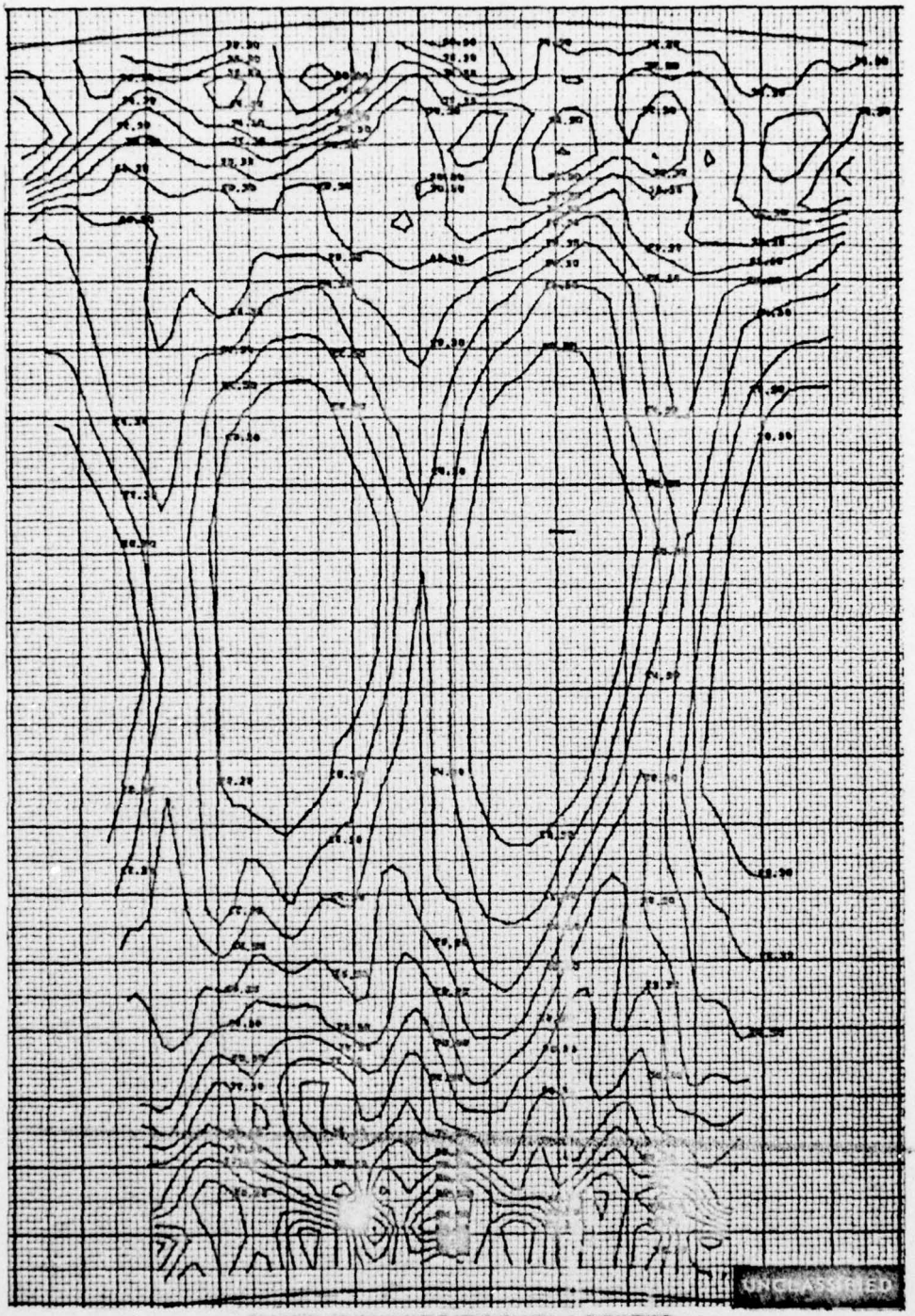

EXIT GAS ANGLE CONTOURS, DEGREES

Figure 198 Exit Gas Angle Contours, Second Vane Recambering Design C at +10° Incidence. Three Flow Passages. Midspan Exit Mach Number = 0.858

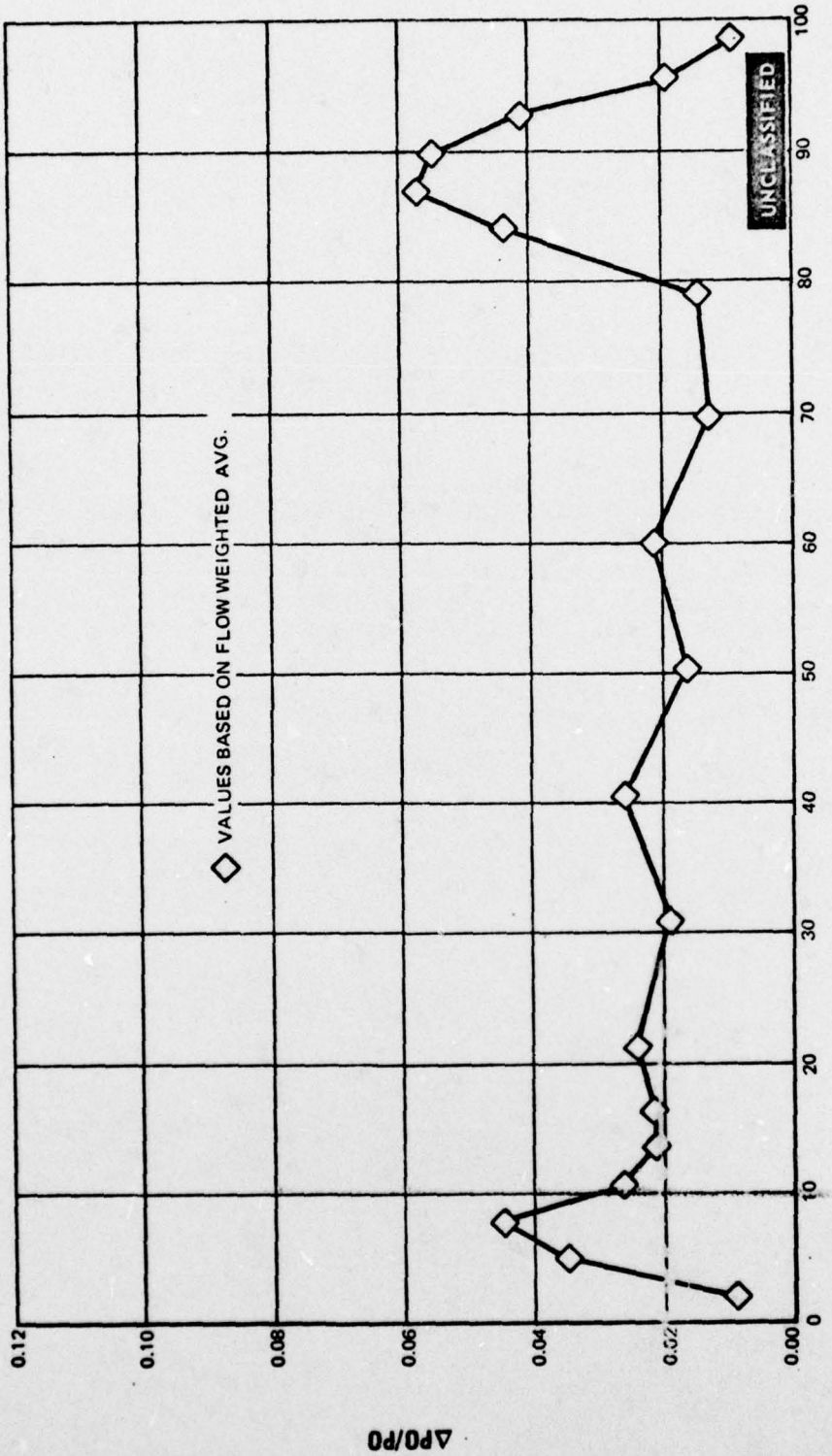

Figure 199 Spanwise Pressure Loss Distribution, Second Vane Recambering Design C at +10° Incidence. Midspan Exit Mach Number = 0.858

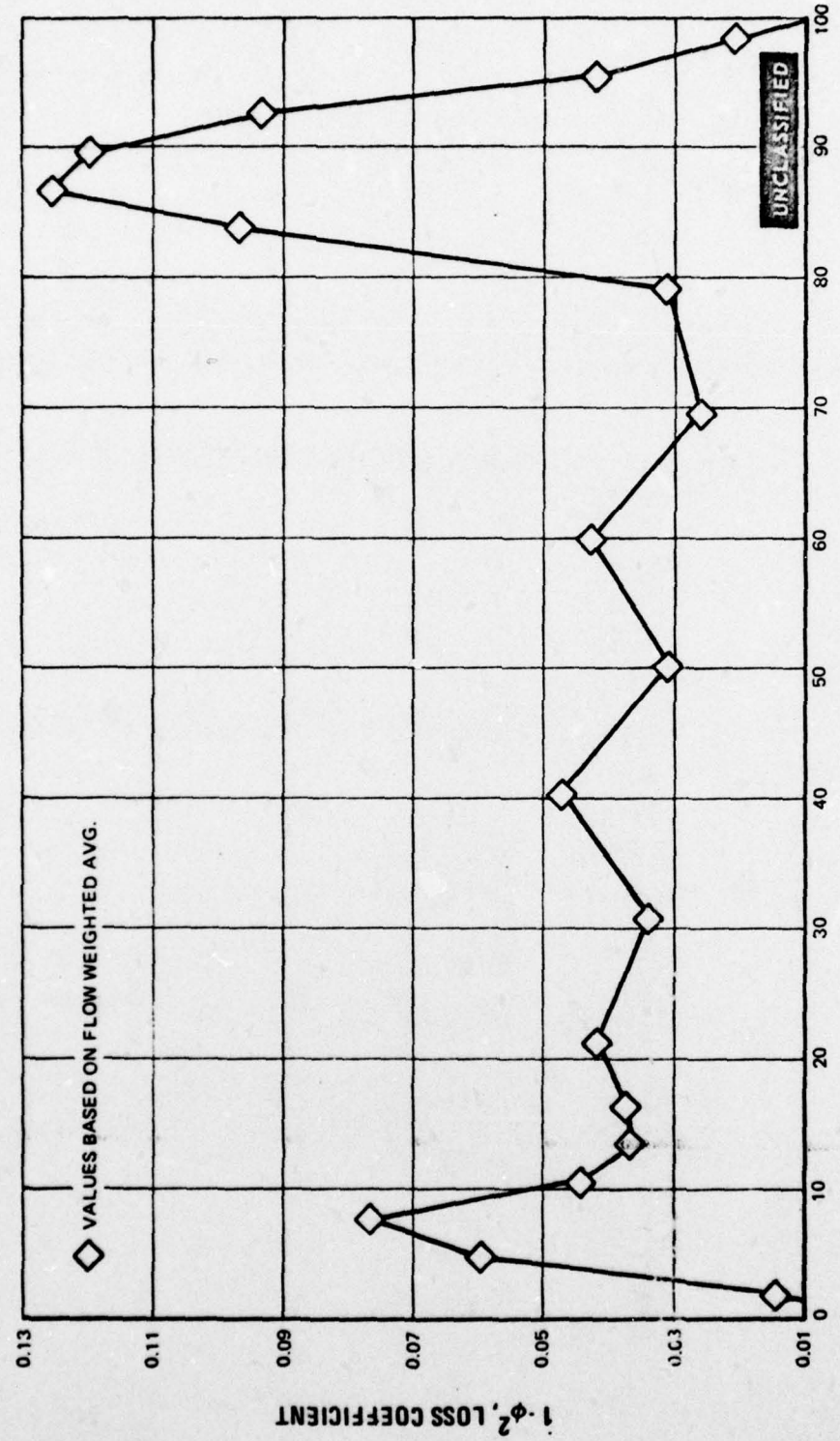

Figure 200 Spanwise Loss Coefficient Distribution, Second Vane Recambering Design C at +10° Incidence. Midspan Exit Mach Number = 0.858

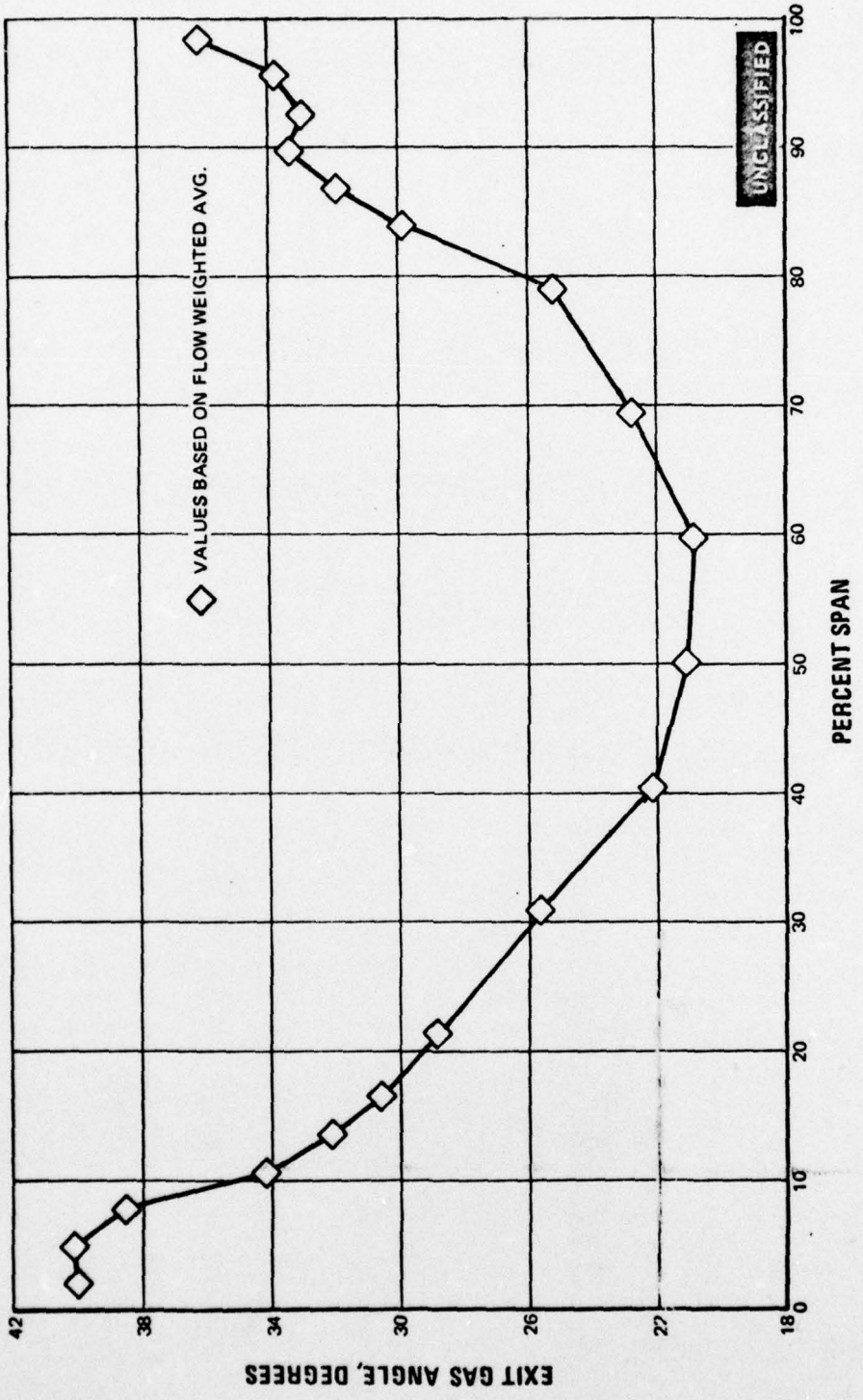

Figure 201 Spanwise Exit Gas Angle Distribution, Second Vane Recambering Design C at +10° Incidence. Midspan Exit Mach Number = 0.858

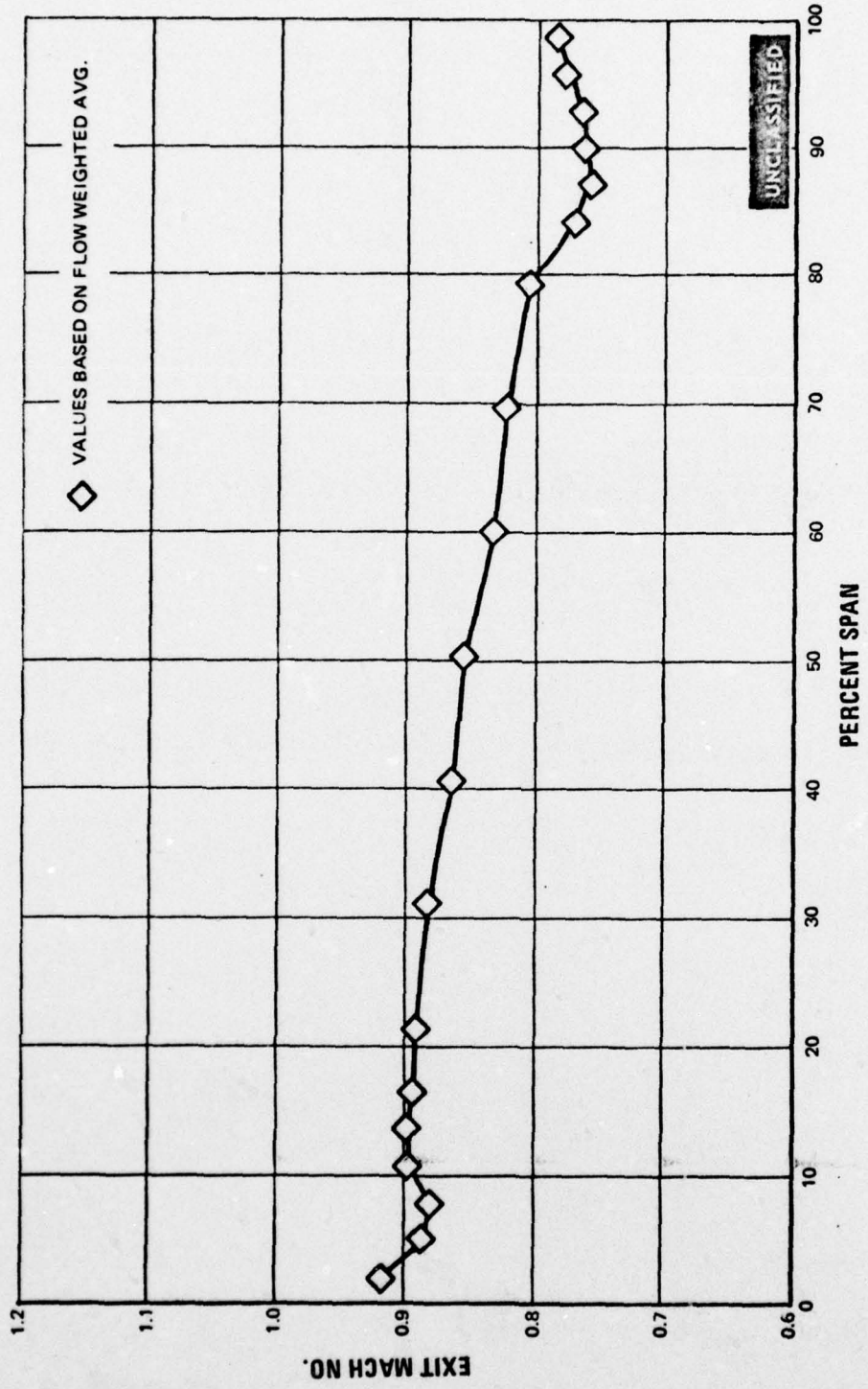

Figure 202 Spanwise Exit Mach Number Distribution, Second Vane Recambering Design C at +10° Incidence. Midspan Exit Mach Number = 0.858

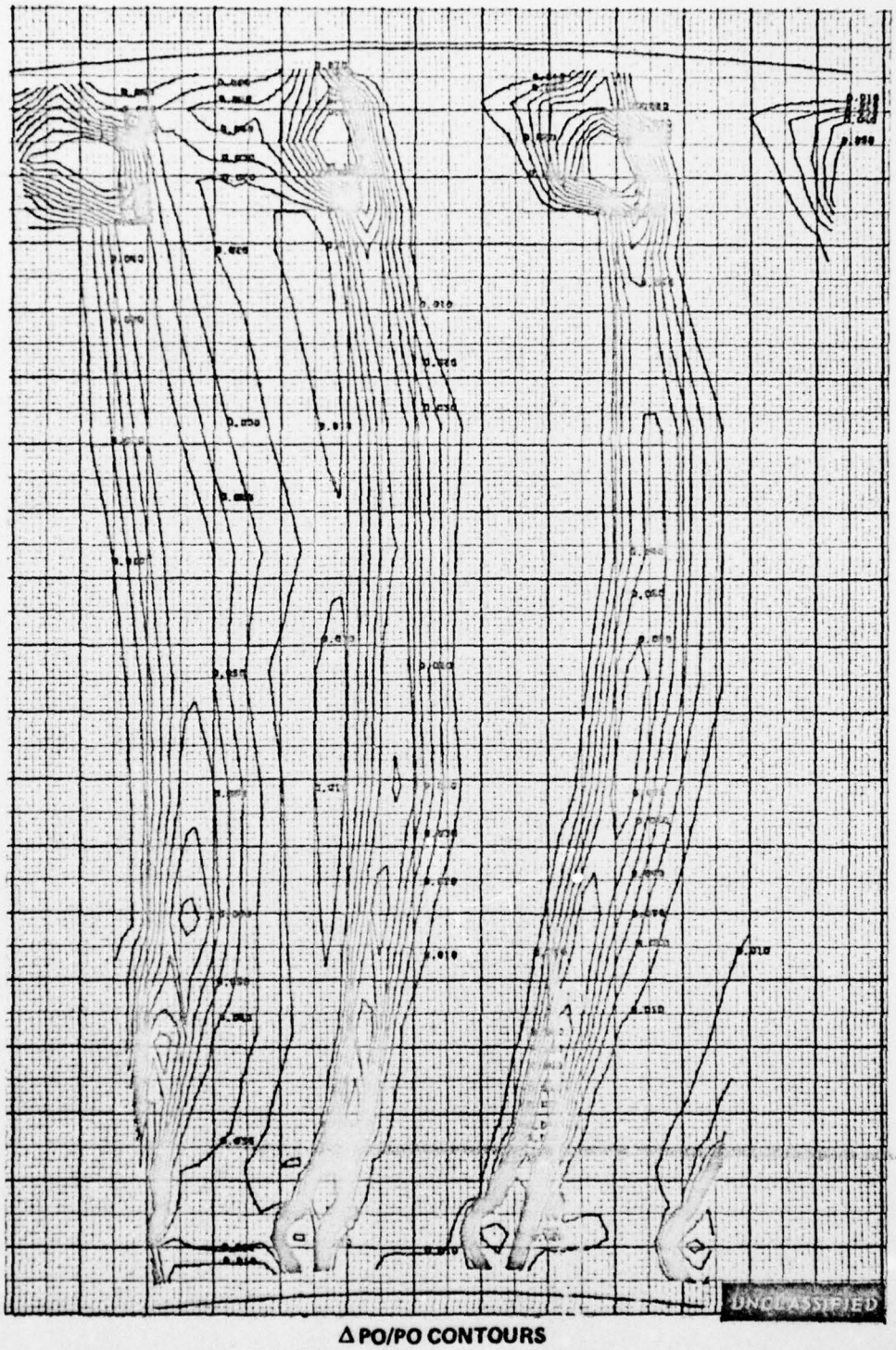

Figure 203 Bressure Loss Contours, Second Vane Recambering Design C at -6° Incidence. Three Flow Passages. Midspan Exit Mach Number = 0.879

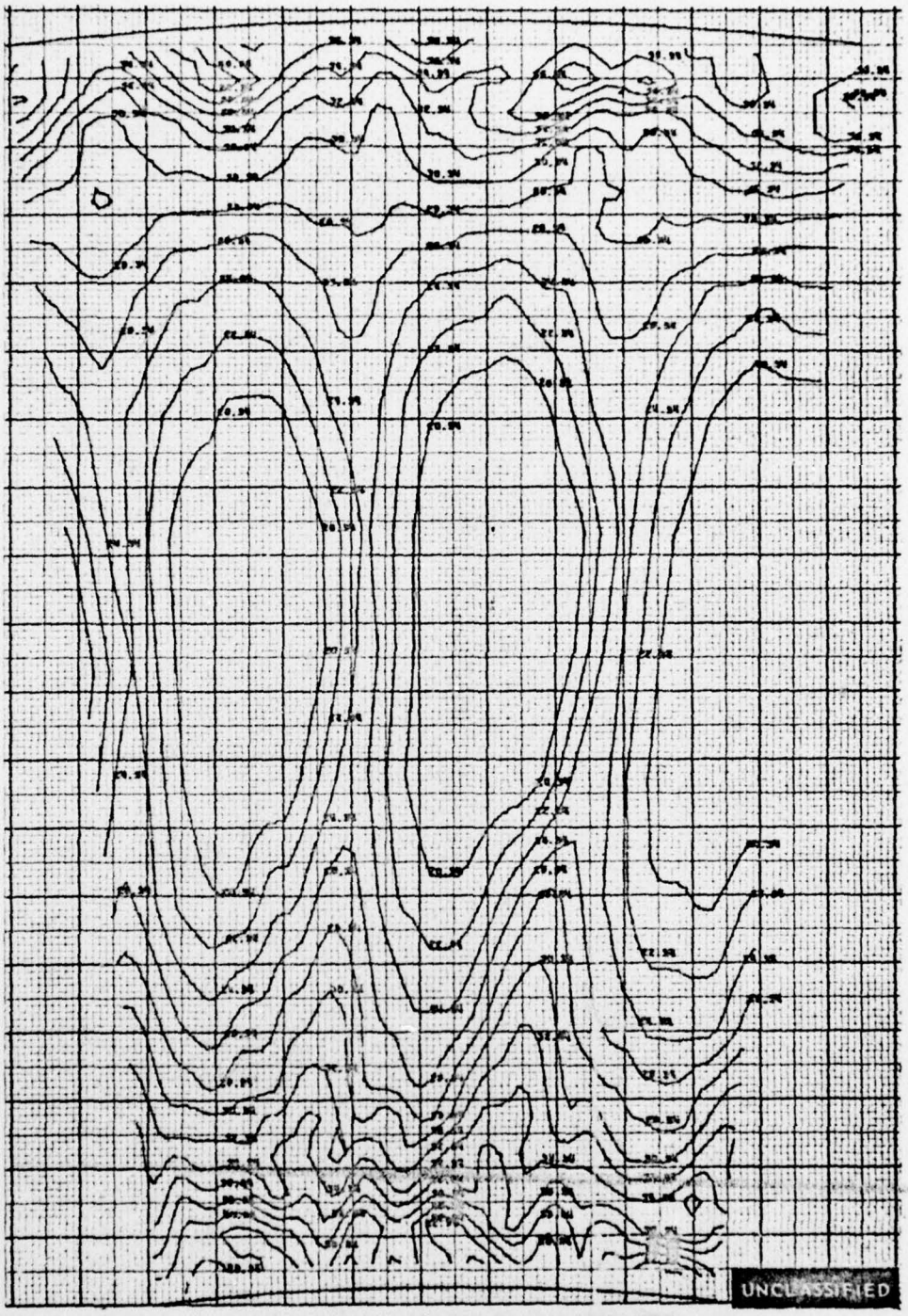

EXIT GAS ANGLE CONTOURS, DEGREES

Figure 204 Exit Gas Angle Contours, Second Vane Recambering Design C at -6° Incidence. Three Flow Passages. Midspan Exit Mach Number = 0.879

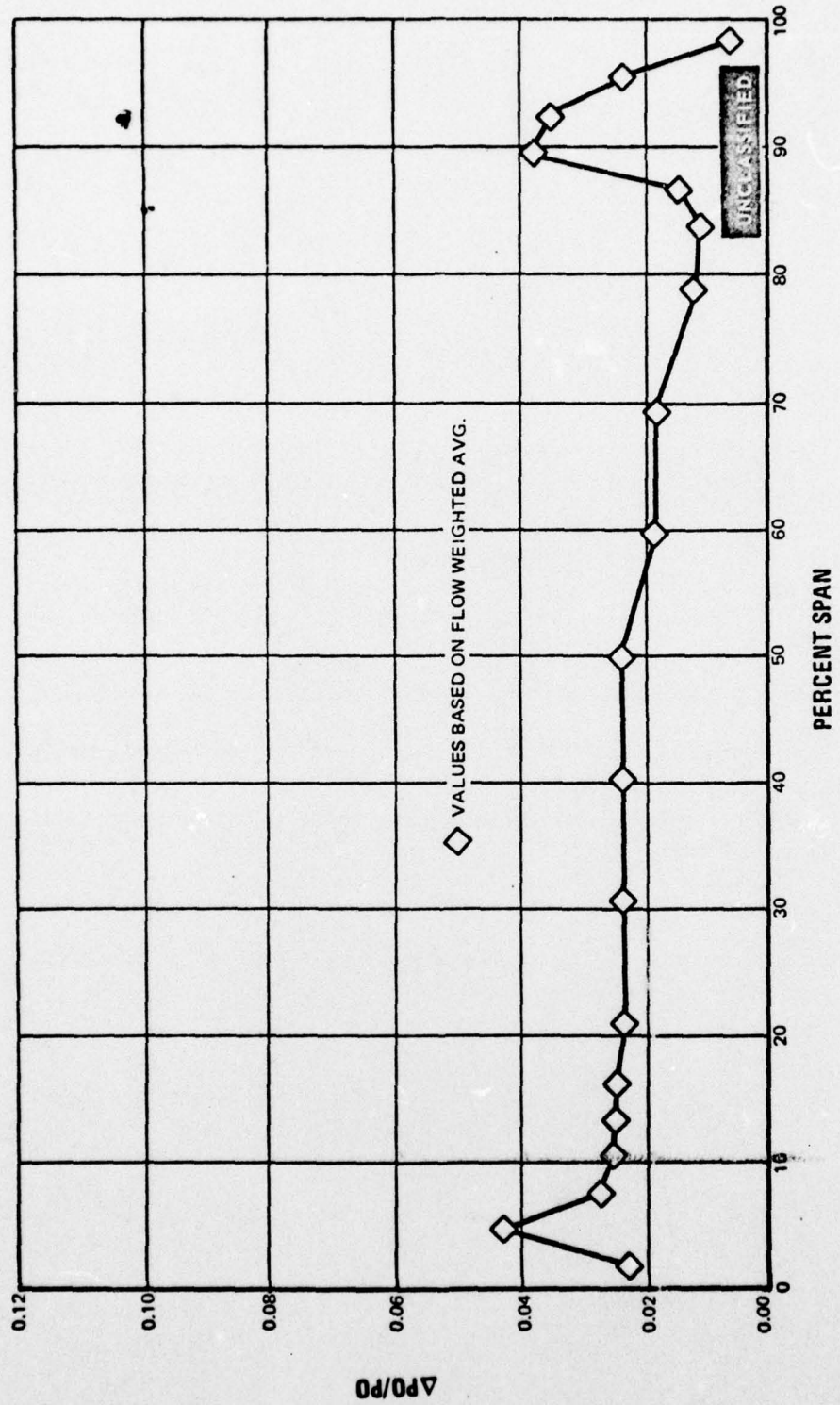

Figure 205 Spanwise Pressure Loss Distribution, Second Vane Recambering Design C at -6° Incidence. Midspan Exit Mach Number = 0.879

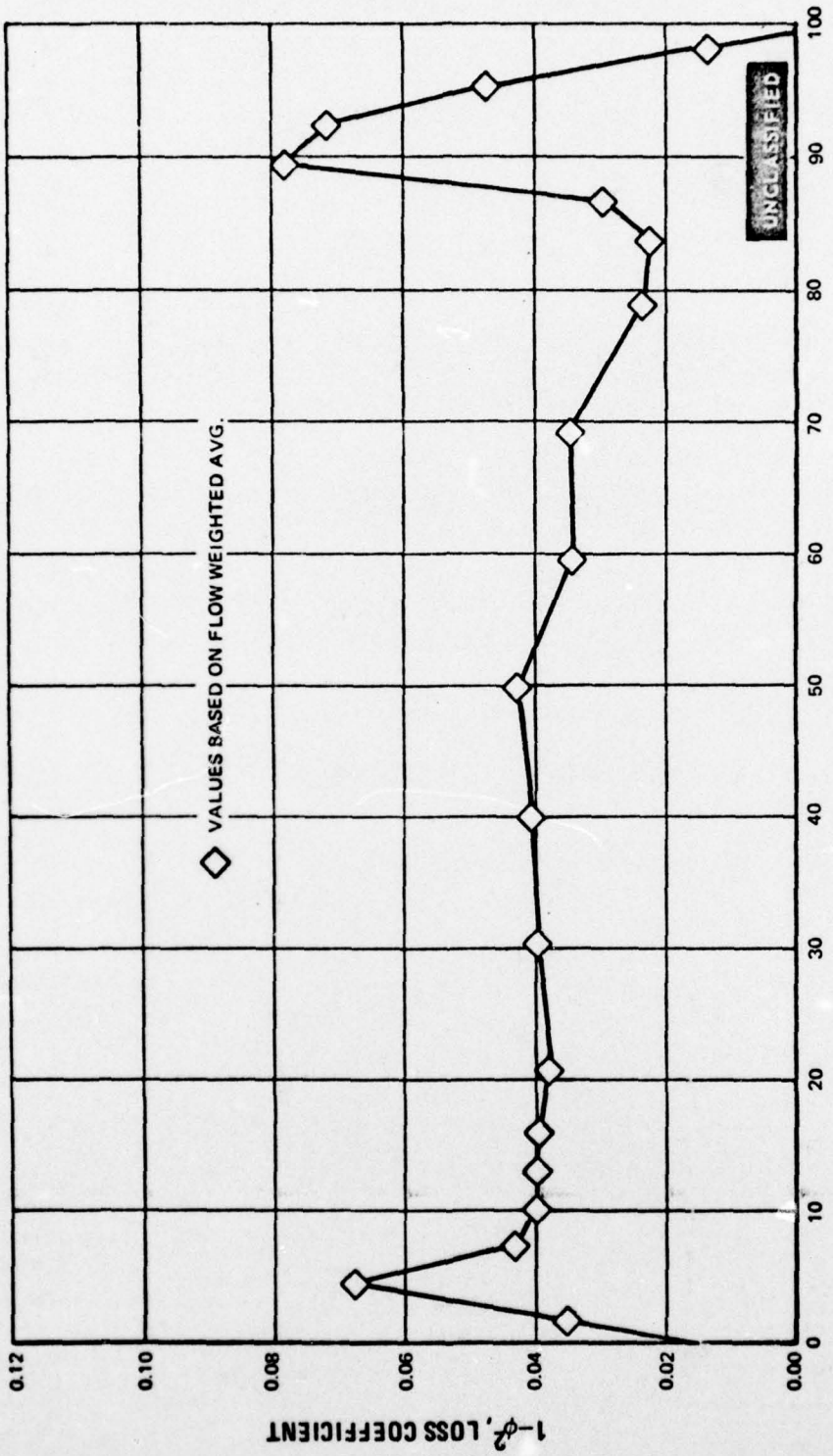

Figure 206 Spanwise Loss Coefficient Distribution, Second Vane Recambering Design C at -6° Incidence. Midspan Exit Mach Number = 0.879

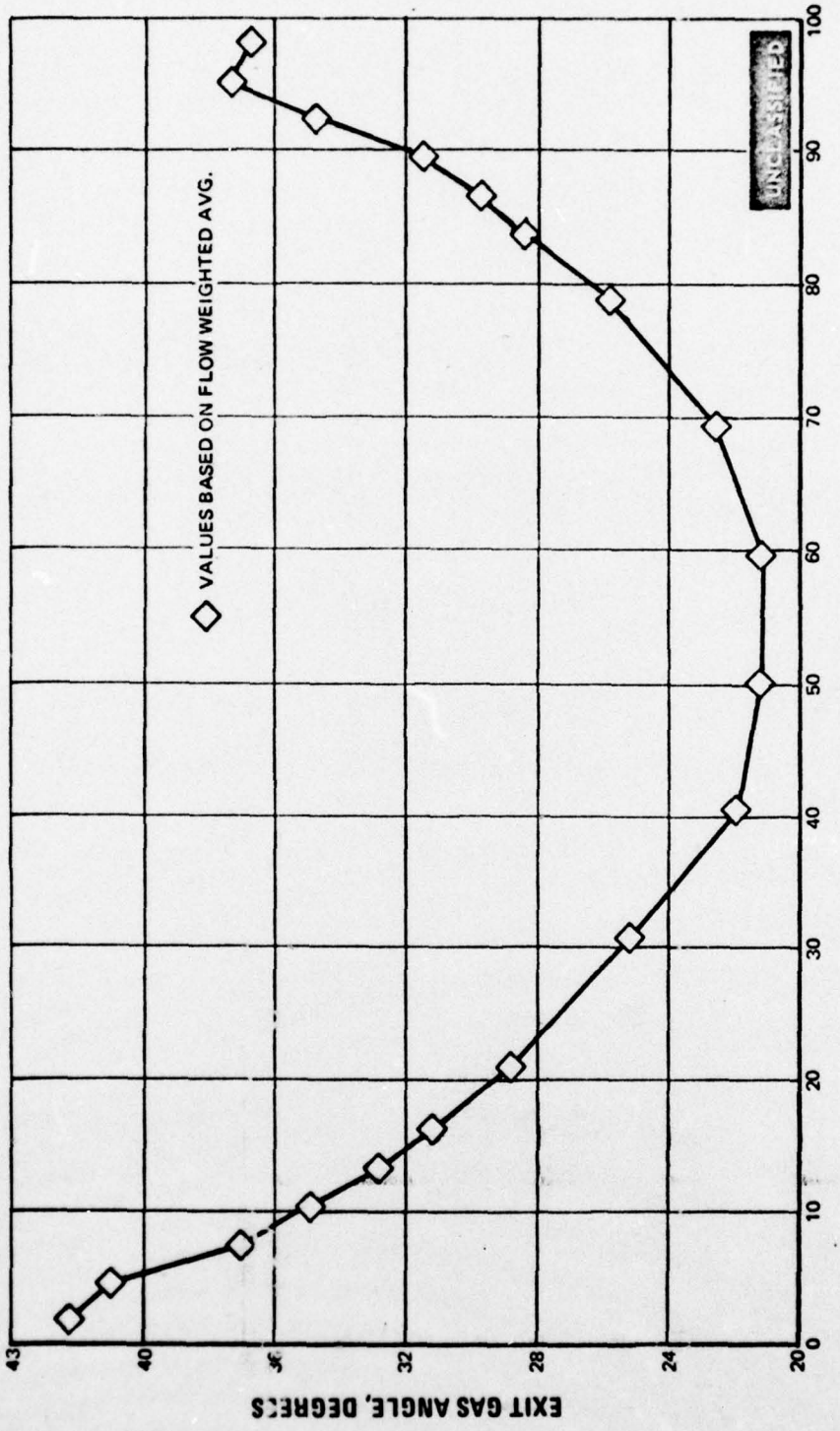

Figure 207 Spanwise Exit Gas Angle Distribution, Second Vane Recambering Design C at -6° Incidence. Midspan Exit Mach Number = 0.879

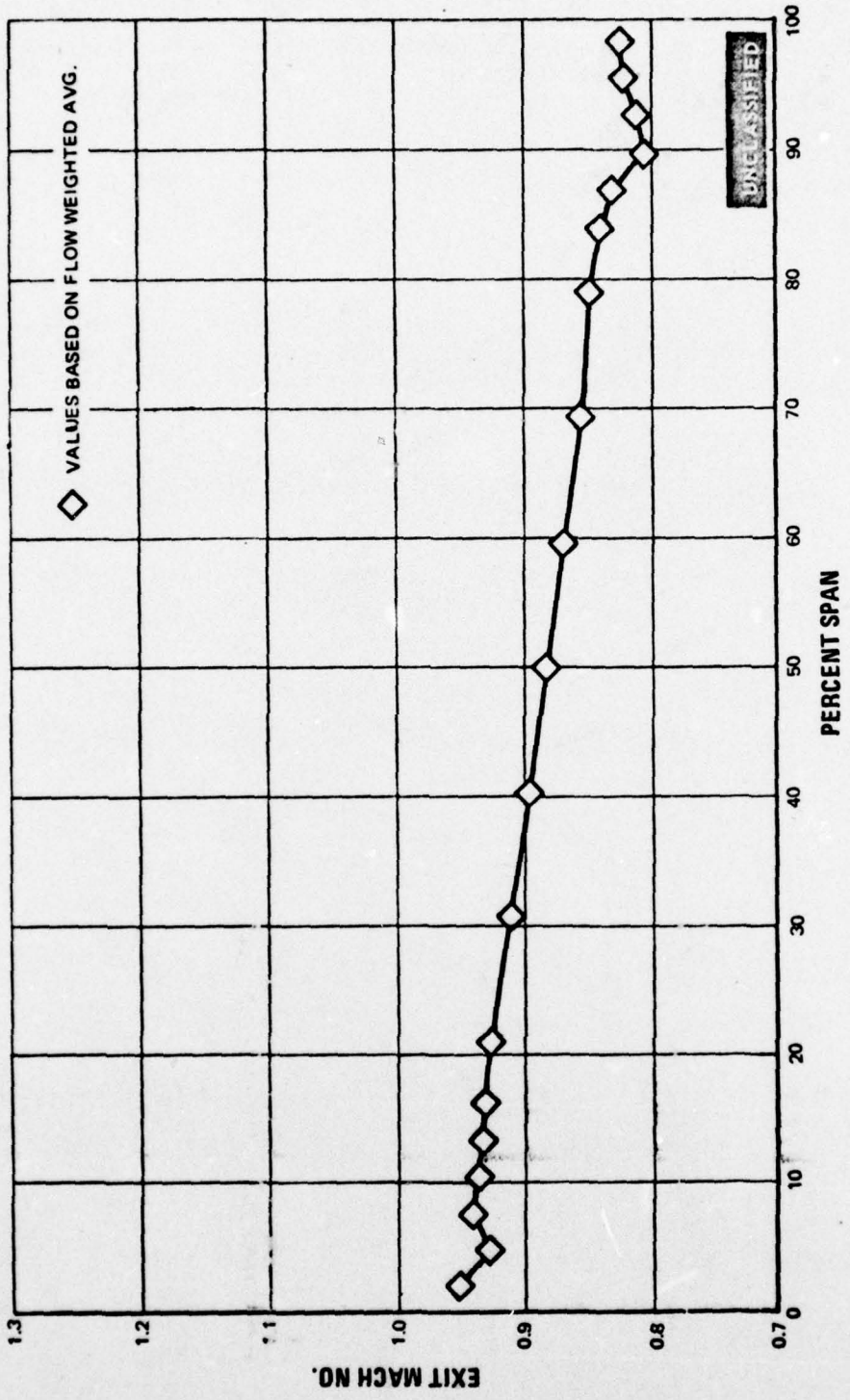

Figure 208 Spanwise Exit Mach Number Distribution, Second Vane Recambering Design C at -6° Incidence. Midspan Exit Mach Number = 0.879

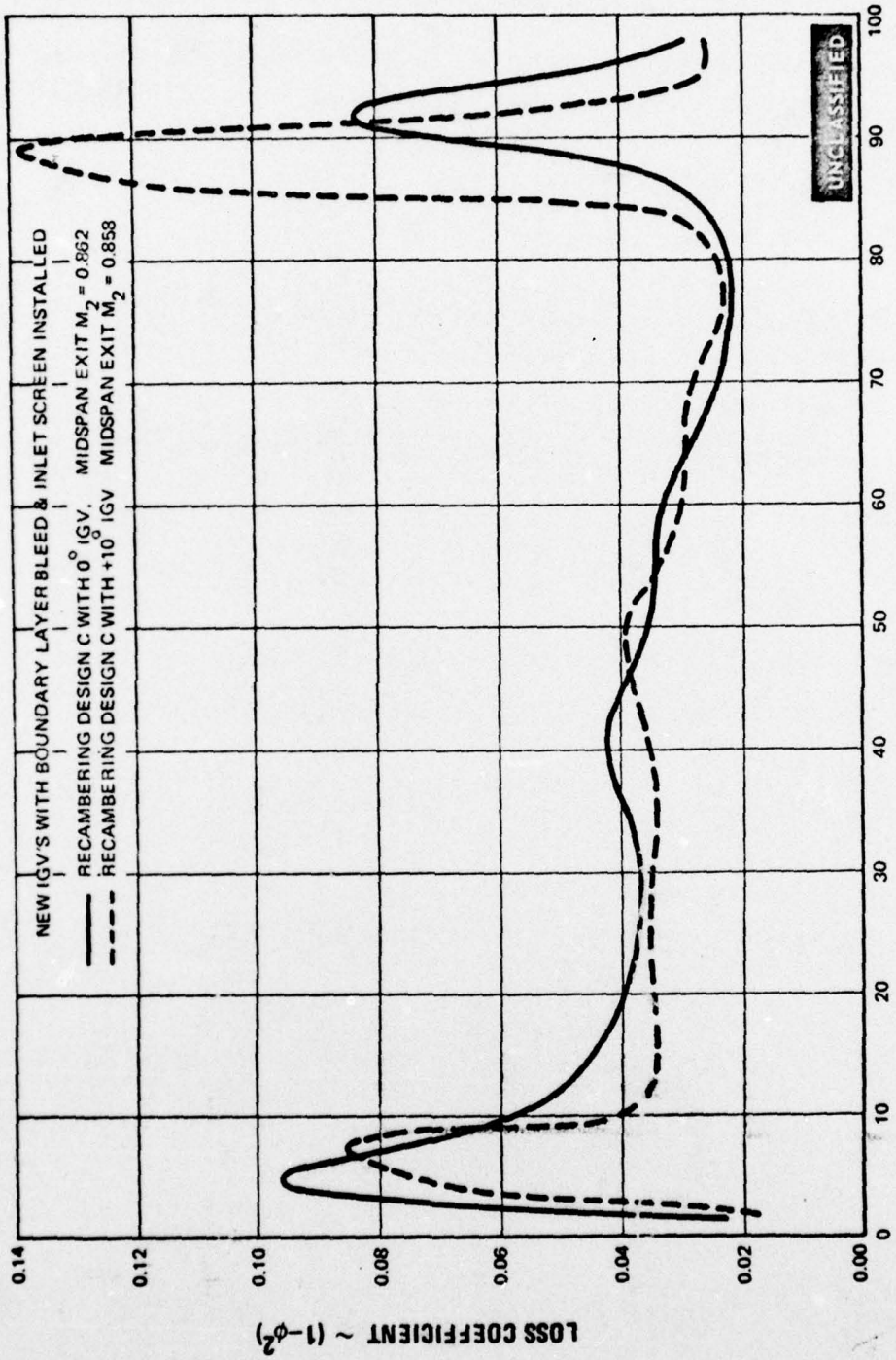

Figure 209 Comparison of Recambering Design C Airfoil Loss Coefficient Distribution at +10 Degrees Incidence With Zero Incidence Values

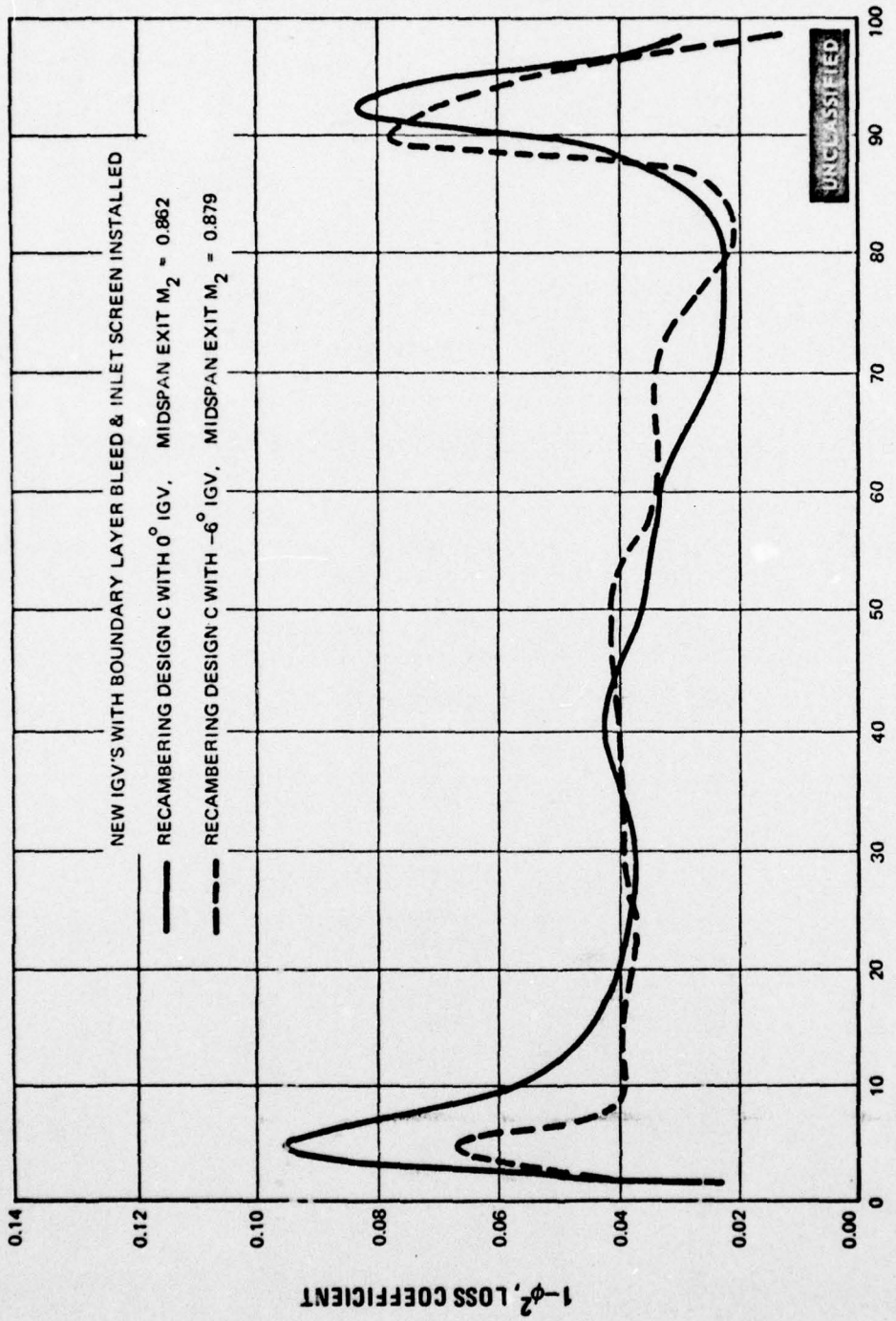

Figure 210 Comparison of Recambering Design C Airfoil Loss Coefficient Distribution at -6 Degrees Incidence With Zero Incidence Values

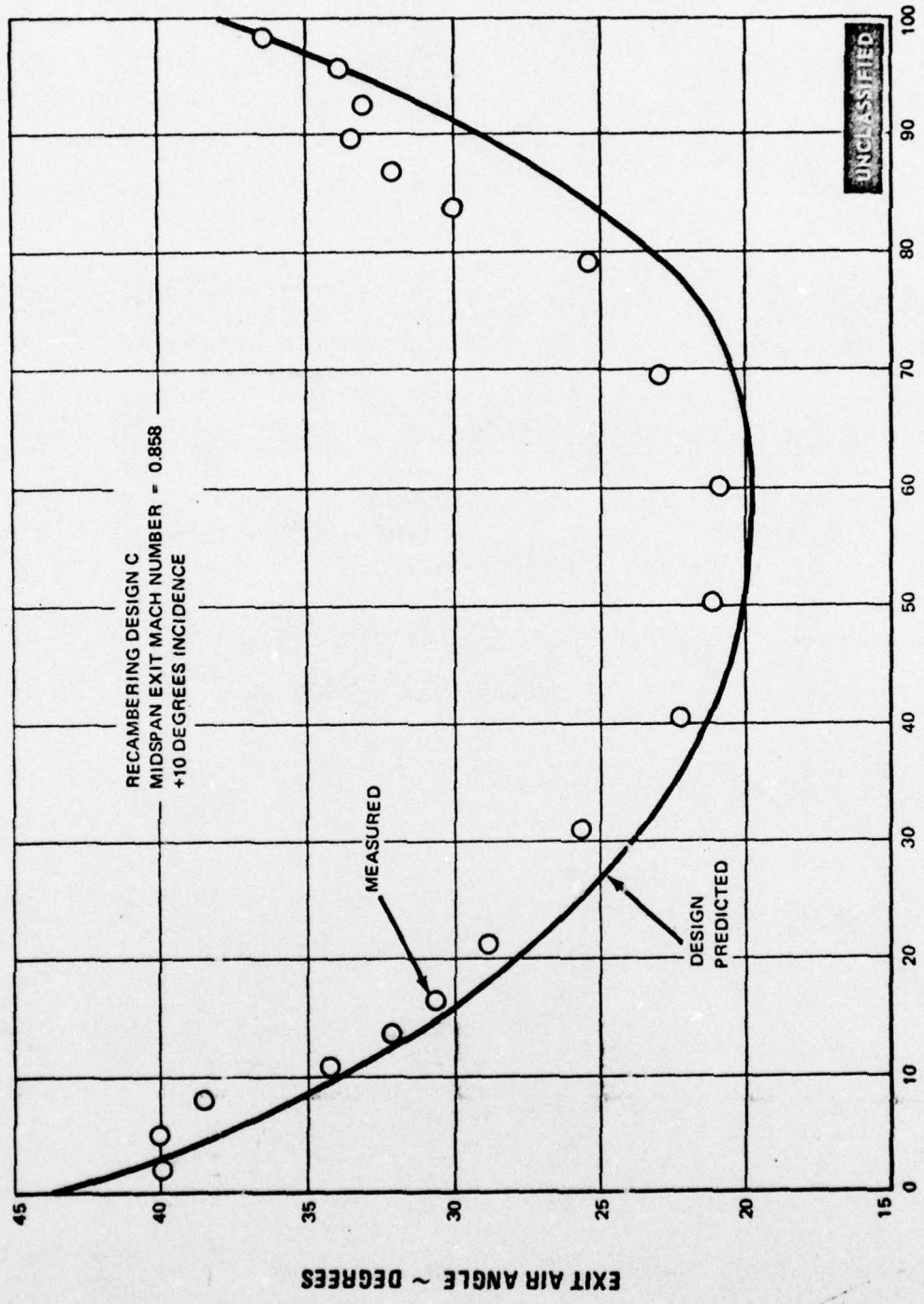

Figure 211 Comparison of Measured Exit Gas Angle With Predicted Design Values at +10 Degrees Incidence. Design C Airfoil at Midspan Exit Mach No. = 0.858

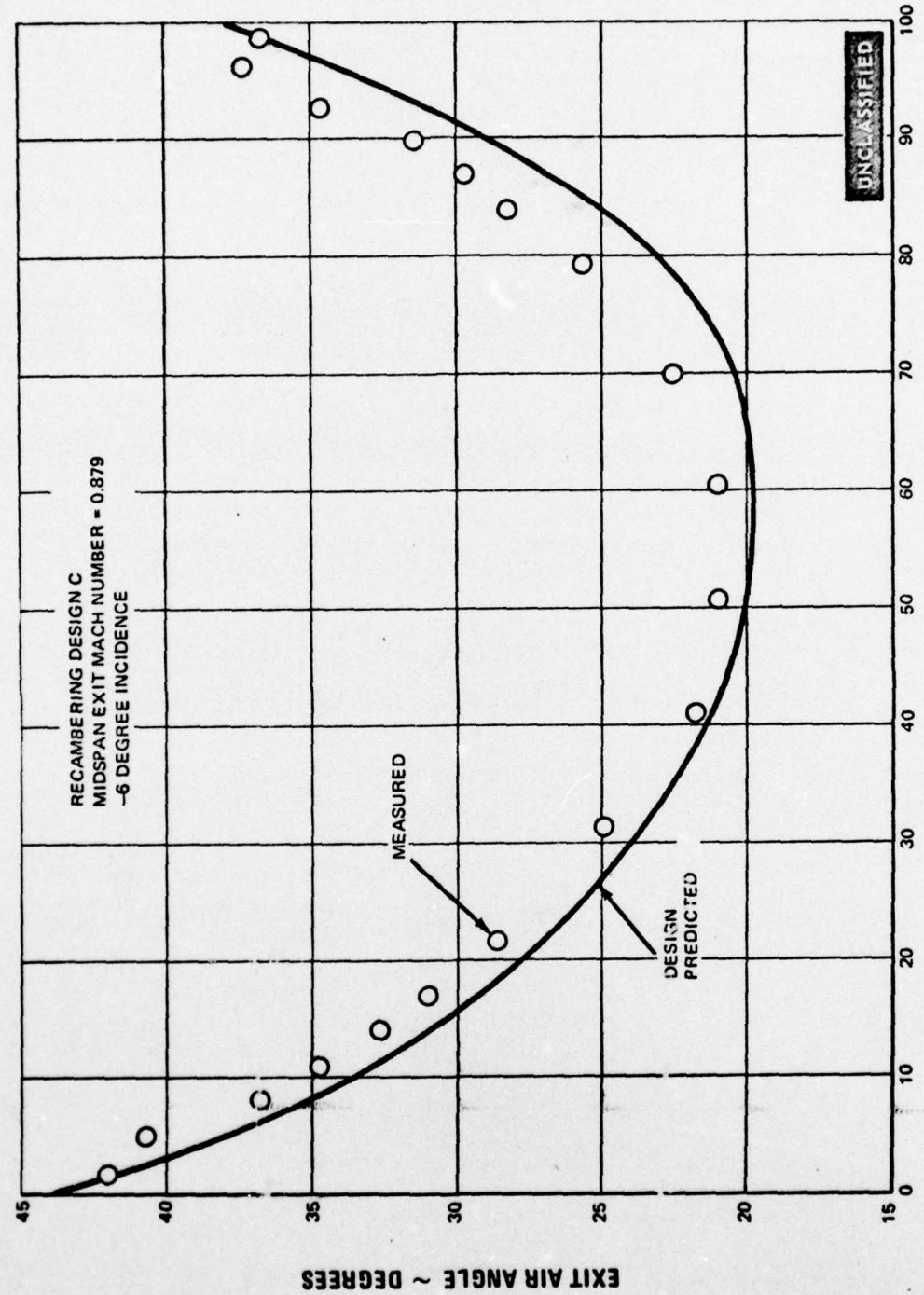

Figure 212 Comparison of Measured Exit Gas Angle With Predicted Design Values at -6 Degrees Incidence. Design C Airfoil at Midspan Exit Mach No. = 0.879

Figure 213 Oil and Graphite Flow Patterns, Second Vane Recambering Design C Airfoil at +10 Degrees Incidence. Midspan Exit Mach No. = 0.858 (FE95749)

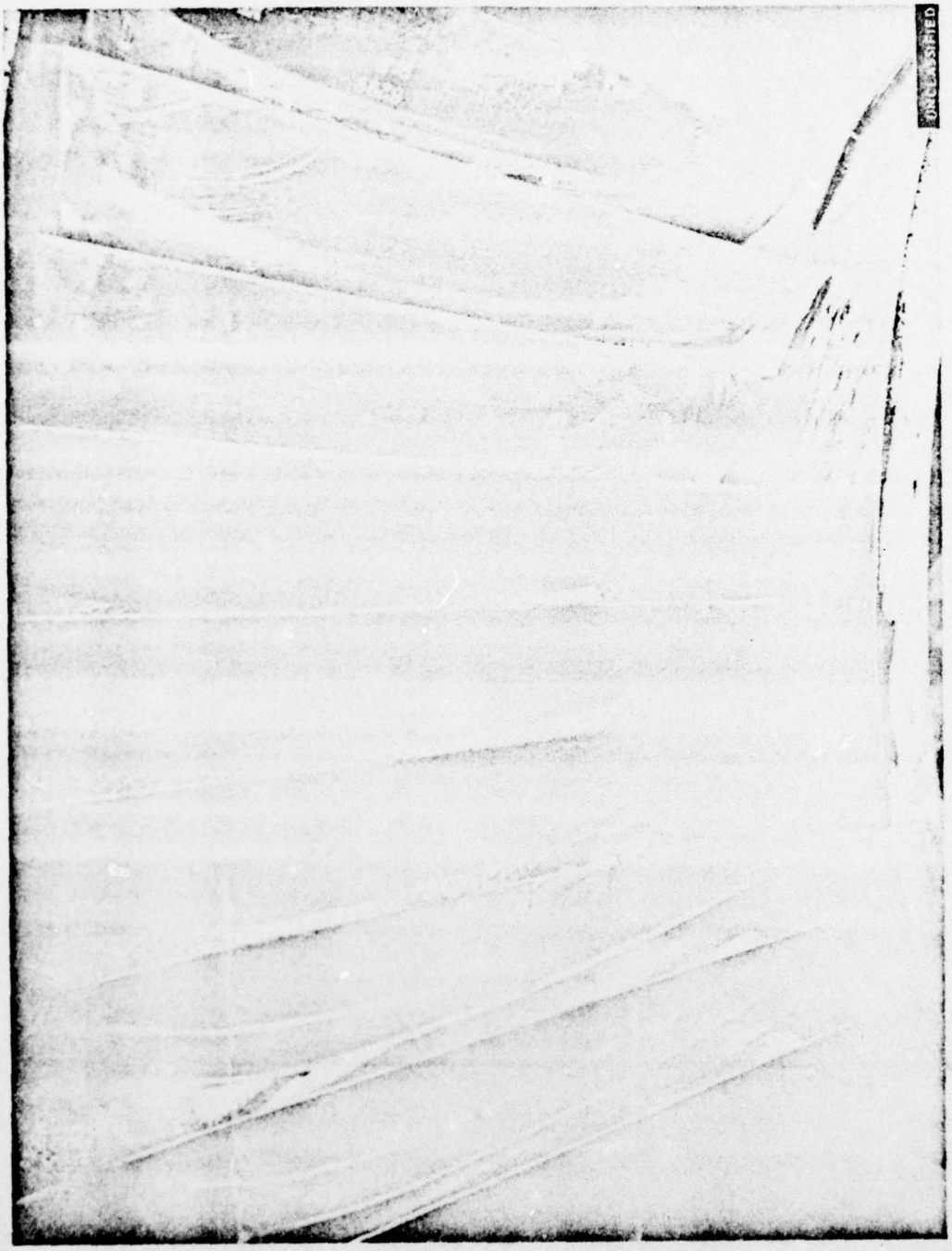

Figure 214 Oil and Graphite Flow Patterns, Second Vane Recambering Design C Airfoil at +10 Degrees Incidence. Midspan Exit Mach No. = 0.858 (FE95750)

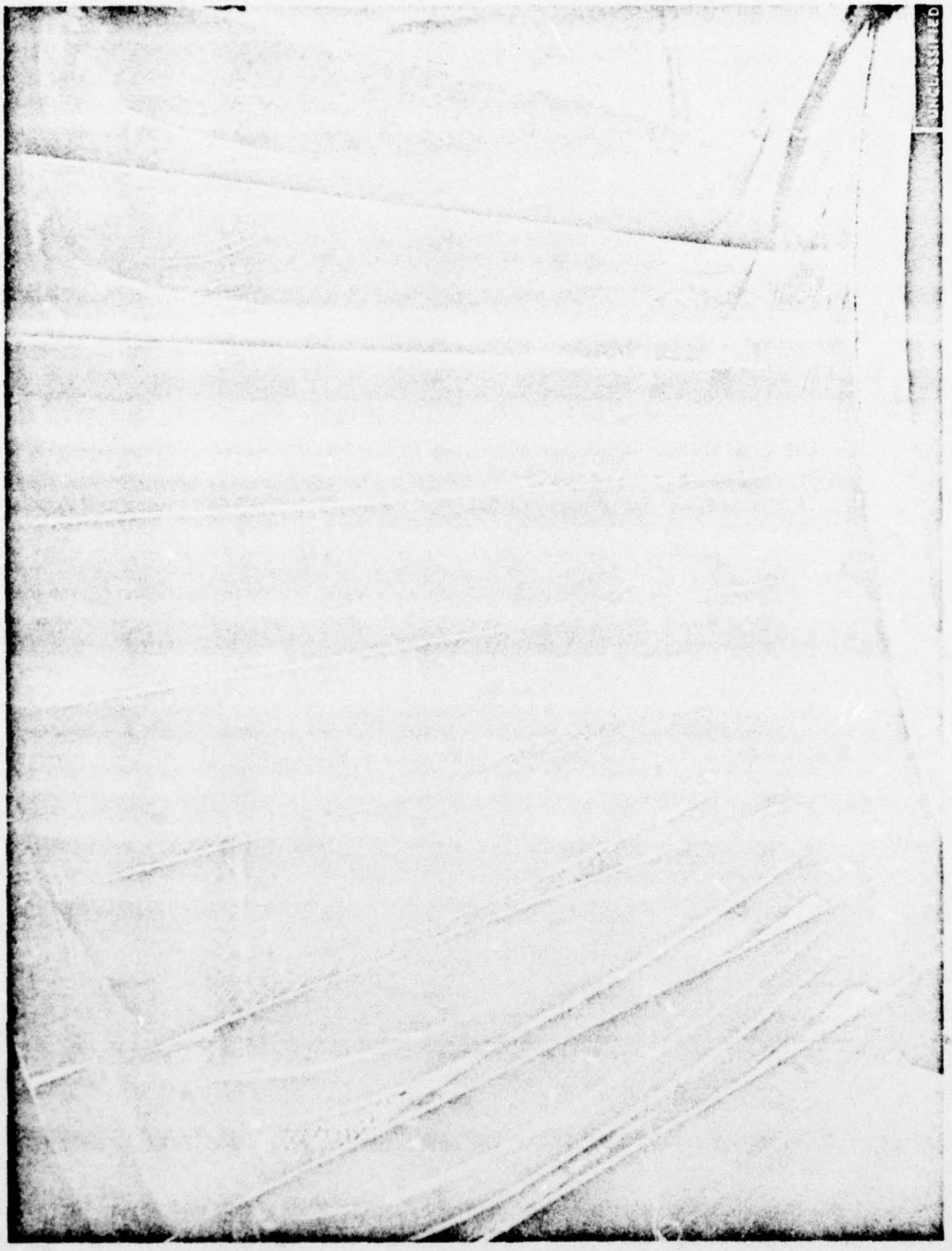

Figure 215 Oil and Graphite Flow Patterns, Second Vane Recambering Design C Airfoil at -6 Degrees Incidence. Midspan Exit Mach No. = 0.879 (FE95865)

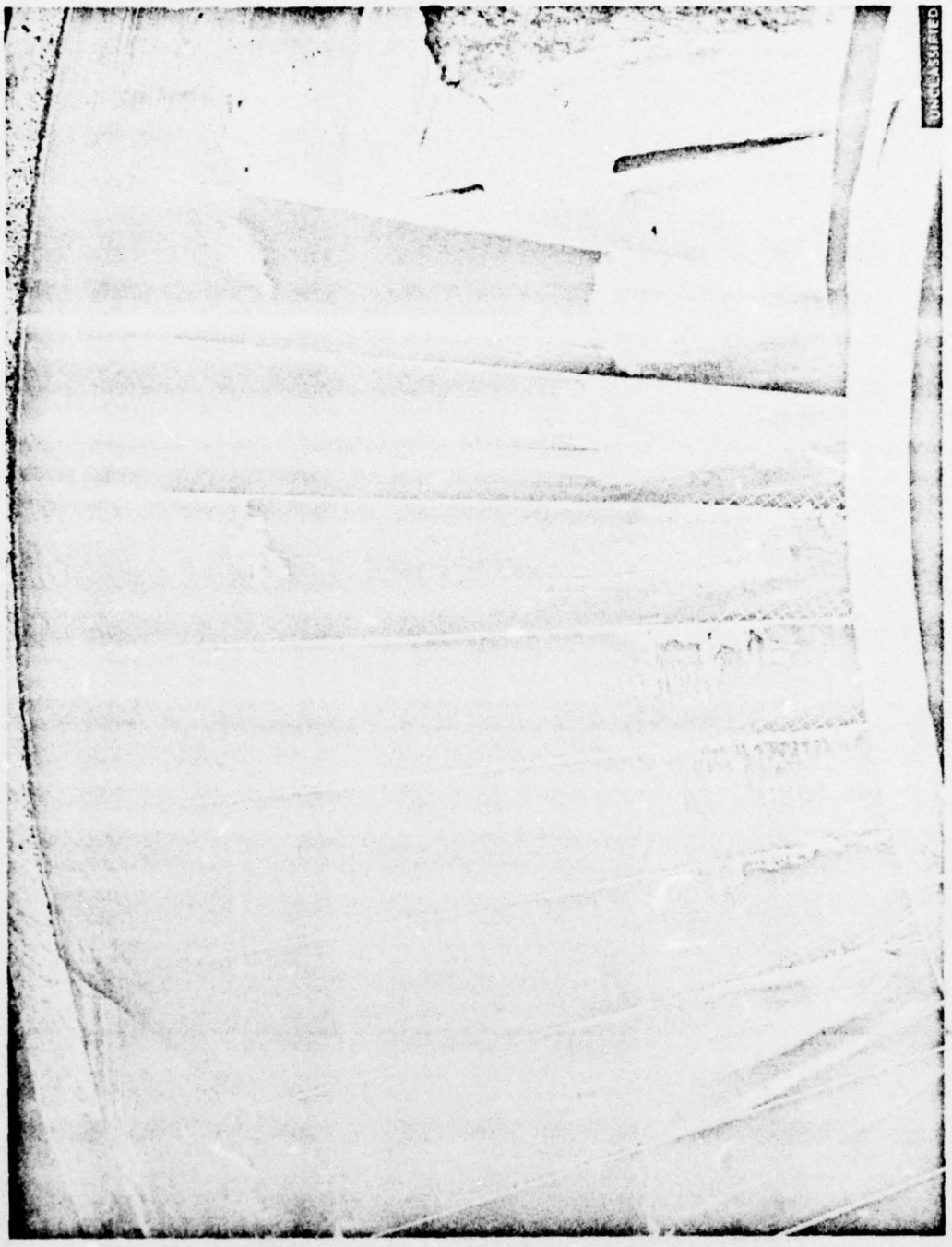

Figure 216 Oil and Graphite Flow Patterns, Second Vane Recambering Design C Airfoil at -6 Degrees Incidence. Midspan Exit Mach No. = 0.879 (PE95866)

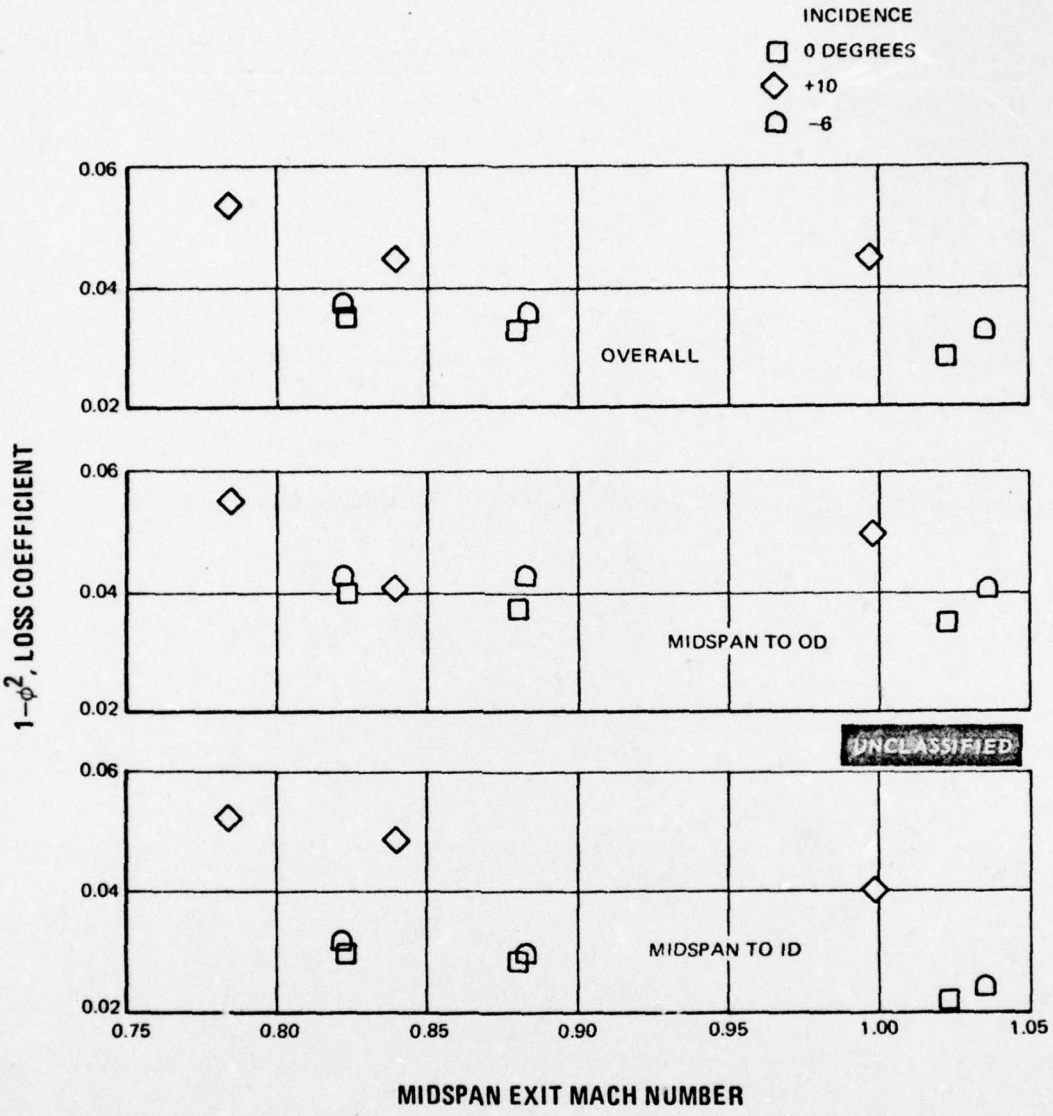

Figure 217 Effect of Mach Number on Loss for the First Recambered Airfoil at Various Incidence Angles

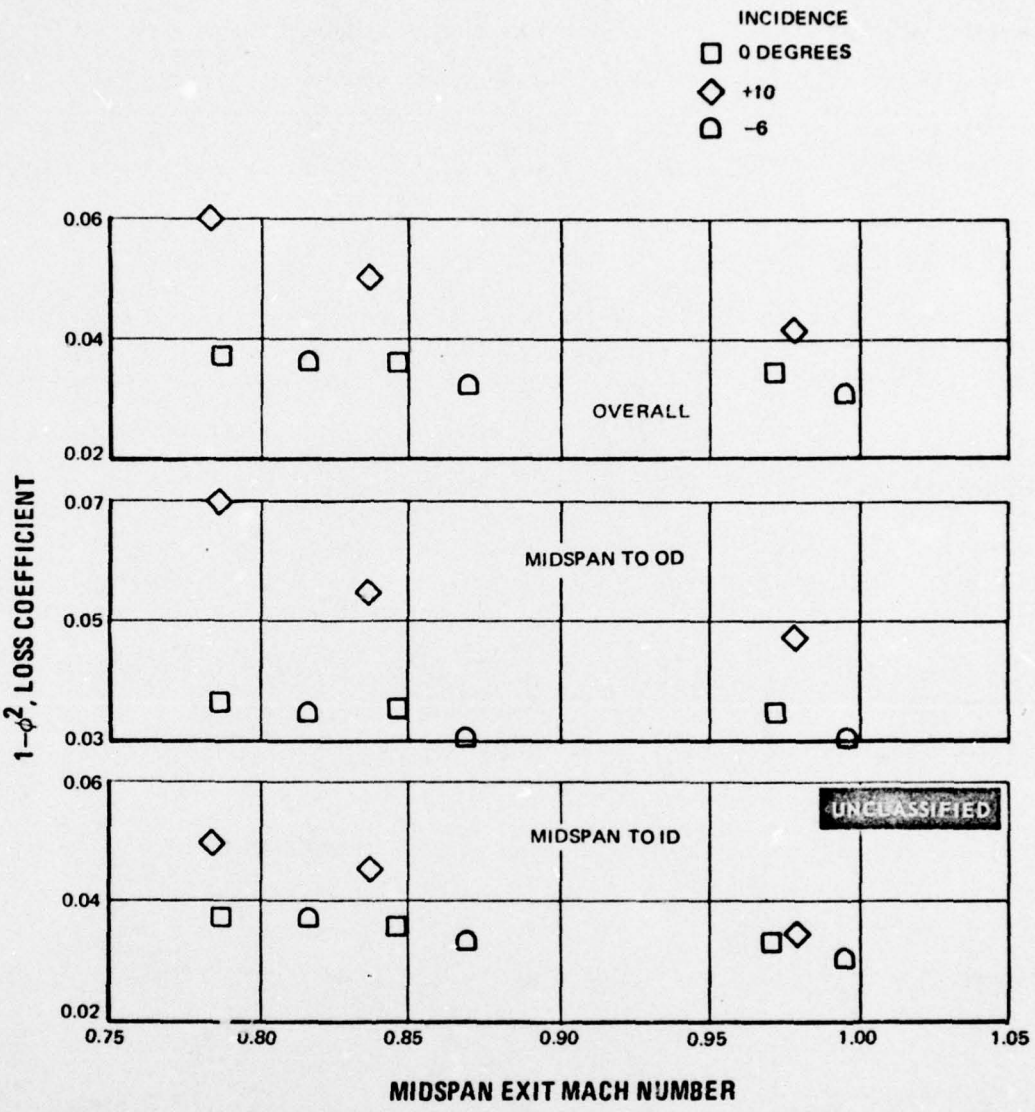

Figure 218 Effect of Mach Number on Loss for Recambering Design A at Various Incidence Angles

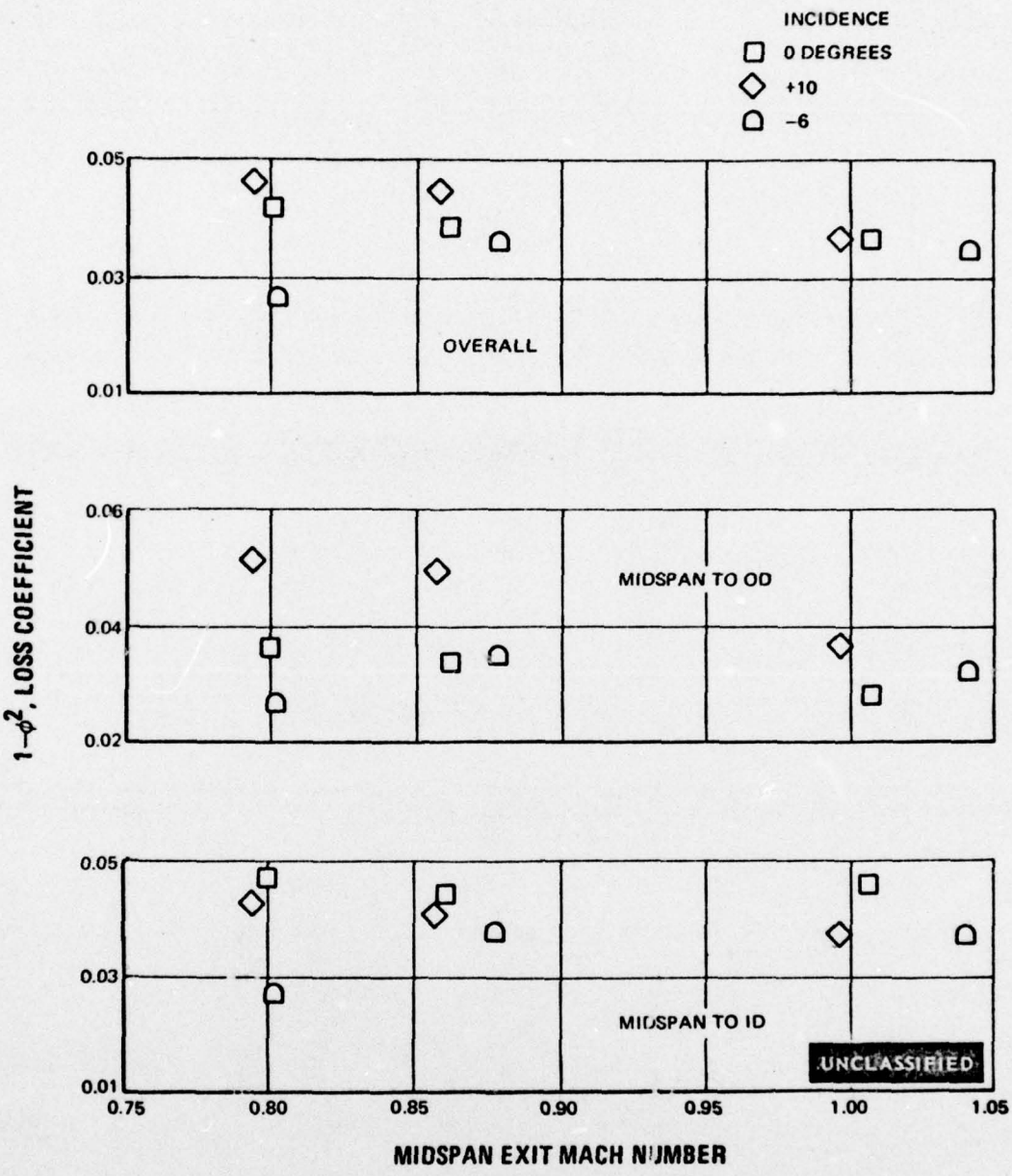

Figure 219 Effect of Mach Number on Loss for Recambering Design C at Various Incidence Angles

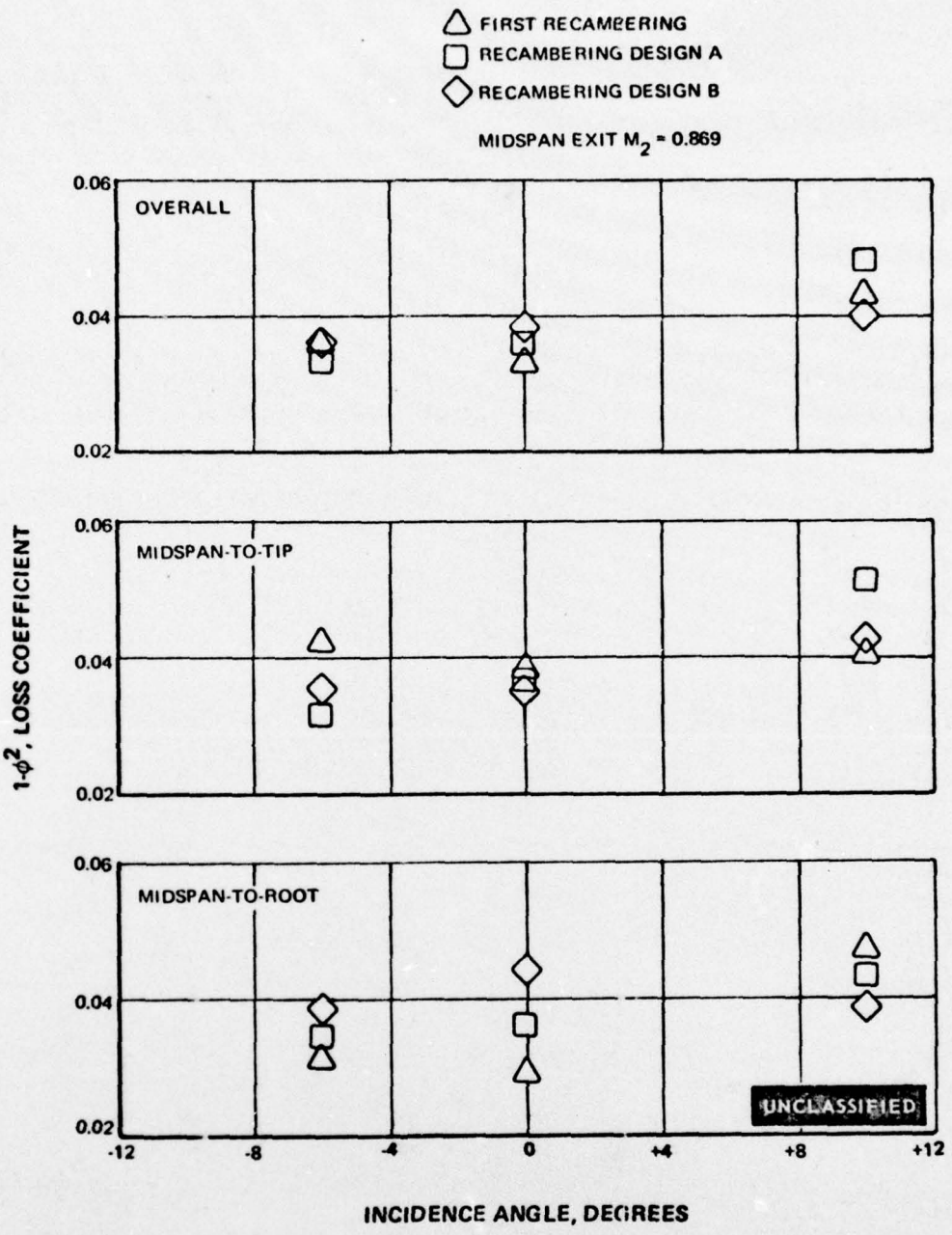

Figure 220 Effect of Incidence on Loss for the Various Recambered Second Vane Airfoils. Midspan Exit Mach Number = 0.869

5. SUMMARY

(U) The results of the off-design evaluation of the second vane baseline and recambered designs are summarized in Table XXXIII. The values shown in this table are those at the design midspan exit Mach number of 0.869 and were obtained by interpolation from Figures 217 through 219.

TABLE XXXIII

SECOND VANE RECAMBERING LOSS COEFFICIENTS
CORRECTED TO DESIGN POINT MACH NUMBER = 0.869

	Midspan-To-Root			Midspan-To-Tip			Overall		
Incidence, Degrees	+10	0	-6	+10	0	-6	+10	0	-6
Baseline	0.039	0.035	0.029	0.035	0.035	0.029	0.038	0.035	0.029
First Recambering	0.047	0.029	0.031	0.040	0.038	0.042	0.043	0.033	0.036
Recambering Design A	0.043	0.036	0.034	0.051	0.035	0.031	0.048	0.036	0.033
Recambering Design B	–	0.031	–	–	0.033	–	–	0.032	–
Recambering Design C	0.038	0.044	0.038	0.042	0.034	0.035	0.040	0.038	0.036

UNCLASSIFIED

(U) The following results are noted:

- For the baseline airfoil, the overall integrated loss level and the integrated loss coefficients at the end-wall regions have increased for +10 degrees incidence and decreased for -6 degrees incidence, compared to the zero incidence levels.
- For the first recambered airfoil, the overall integrated losses are higher for both the +10 degrees and -6 degrees incidence levels, compared to the zero incidence levels. At the +10 degrees incidence, the integrated losses are higher than the zero incidence condition at both the midspan and end-wall regions. At -6 degree incidence, the losses are relatively unchanged over the airfoil span except in the tip region, where the -6 degree incidence losses are significantly higher.

- For the airfoil with recambering design A, integrated losses were significantly higher at the +10 degrees incidence level than at zero incidence, and the losses at the -6 degrees incidence were essentially unchanged, compared to the zero incidence condition.

- For the airfoil with recambering design C, the overall integrated loss level was higher at +10 degrees incidence and lower at -6 degrees incidence, compared to zero incidence. In the root region, the losses at +10 degree incidence appeared to be slightly less than the zero incidence data. At -6 degrees incidence, the loss level is significantly below the zero incidence results near the root.

(U) The following conclusions are drawn from these results:

- The recambered airfoils generally showed an increase in loss coefficient with incidence (-6 to +10 degrees) which indicates that the airfoils are close to their optimum incidence

- None of the airfoils tested were sensitive to angle of attack, and the flow patterns of the airfoils did not change with incidence angle

- The tested airfoils did not show the transonic drag rise measured in the plane cascade evaluation (Section III). The difference may be due to the differences in the turbulence levels of the two test rigs, and the fact that the annular segment cascade permits the flow a greater latitude for radial readjustment

- The annular segment cascade is more representative of flow conditions in a turbine that the plane cascade. Therefore, the transonic drag rise indicated in the plane cascade is not expected in the turbine

- The characteristics of the evaluated airfoils verified the soundness of the current turbine design system

6. TEST PROCEDURE

(U) The test procedure employed during this Task was identical to that of the Task IIb baseline evaluation. This procedure was described in detail in Reference 3.

SECTION VII

DESIGN PROCEDURE MANUAL (TASK IIId)

1. RFP OBJECTIVE

(U) Prepare the turbine design procedure manual for the high work turbine.

2. TASK OBJECTIVE

(U) The purpose of this Task is to prepare the Turbine Design Procedure Manual. This manual will contain detailed information for each computer program listed in the Contract proposal. This information will contain the following: a flow diagram; a listing of all input and output items and their definitions; a list of definitions for each term used in the computer code; a write-up of the pertinent equations; a listing of the computer code in Fortran IV; a copy of the computer program decks in Fortran IV; any necessary test cases for deck check-out.

(U) The loss relations presently used will be modified, if necessary, based on the results of the two- and three-dimensional testing during Phases II and III.

3. STATUS

(U) The following decks constitute the proposal design procedure manual:

- Turbine Meanline Design Program
- Turbine Stage Off-Design Program
- Turbine Streamline Analysis Program
- Airfoil Boundary Layer Program
- Airfoil Pressure Distribution Program
- Turbine Airfoil Design and Section Properties Program
- Airfoil Curved Line Fairing Program
- Airfoil Straight Line Fairing Program

These decks have all been converted to Fortran IV, checked-out on IBM 7094, and delivered to the Air Force along with flow diagrams and test cases. This was done under Task IIe.

(U) Engineering write-up for the first four decks listed above has been completed. Those remaining will be prepared, and a complete set delivered to the Air Force as required by this Task. The above decks, with modifications based on recent test results, are presently being utilized to design the Demonstrator Turbine for Phase IV.

(The reverse of this page is blank)

TABLE VIII

SECOND VANE CASCADE AIRFOIL, RECAMBERING DESIGN A

Radius of FF Section = 7.5000 Axial Chord = 0.8320 Actual Chord = 0.8634
Pitch = 0.5890 No. of Foils = 80.00

Percent X	Foil X	Foil Y Suction	Foil Y (Circle)	Foil Y Pressure	Foil Y (Circle)
0.0	0.0	-0.2880	-0.2831	-0.2391	-0.2831
0.01	0.0083	-0.3016	-0.3016	-0.2479	-0.2682
0.02	0.0166	-0.3145	-0.3145	-0.2567	-0.2657
0.03	0.0250	-0.3269	-0.3269	-0.2655	-0.2673
0.04	0.0333	-0.3387	-0.3387	-0.2743	-0.2743
0.05	0.0416	-0.3500	-0.3500	-0.2825	-0.2825
0.10	0.0832	-0.3989	-0.3989	-0.3146	-0.3146
0.15	0.1248	-0.4368	-0.4368	-0.3353	-0.3353
0.20	0.1664	-0.4649	-0.4649	-0.3476	-0.3476
0.25	0.2080	-0.4843	-0.4843	-0.3531	-0.3531
0.30	0.2496	-0.4958	-0.4958	-0.3531	-0.3531
0.35	0.2912	-0.5001	-0.5001	-0.3482	-0.3482
0.40	0.3328	-0.4975	-0.4975	-0.3391	-0.3391
0.45	0.3744	-0.4886	-0.4886	-0.3262	-0.3262
0.50	0.4160	-0.4735	-0.4735	-0.3098	-0.3098
0.55	0.4576	-0.4526	-0.4526	-0.2901	-0.2901
0.60	0.4992	-0.4261	-0.4261	-0.2673	-0.2673
0.65	0.5408	-0.3939	-0.3939	-0.2416	-0.2416
0.70	0.5824	-0.3564	-0.3564	-0.2130	-0.2130
0.75	0.6240	-0.3134	-0.3134	-0.1817	-0.1817
0.80	0.6656	-0.2651	-0.2651	-0.1476	-0.1476
0.85	0.7072	-0.2111	-0.2111	-0.1109	-0.1109
0.90	0.7488	-0.1514	-0.1514	-0.0714	-0.0714
0.95	0.7904	-0.0854	-0.0854	-0.0291	-0.0291
0.98	0.8154	-0.0426	-0.0426	-0.0024	-0.0025
0.99	0.8237	-0.0277	-0.0277	0.0066	-0.0001
1.00	0.8320	-0.0125	-0.0100	0.0157	-0.0100

Foil L.E. Circle	X = 0.0175,	Y = -0.2831	R = 0.0175
Foil T.E. Circle	X = 0.8220,	Y = -0.0100,	R = 0.0100
Foil L.E. Tangency Pt. Suction	X = 0.0026,	Y = -0.2922	
Foil L.E. Tangency Pt. Pressure	X = 0.0302,	Y = -0.2711	
Foil T.E. Tangency Pt. Suction	X = 0.8308,	Y = -0.0148	
Foil T.E. Tangency Pt. Pressure	X = 0.8146,	Y = -0.0032	
Foil Nose Point	X = 0.0069,	Y = -0.2692	
Foil Tail Point	X = 0.8278,	Y = -0.0019	
Foil Area	= 0.1002		
Gaging	LAMBDA = 0.3310,	X = 0.9841,	Y = -0.3548
Gaging Angle	= 34.190		
Center of Gravity	X = 0.4132,	Y = -0.3347	
Radial Reference	X = 0.4132,	Y = -0.3347	
Inlet Angle	= 37.330,	DELTA BETA 1 = 12.000	
Exit Angle	= 35.574,	DELTA BETA 2 = 14.000	
Uncovered Turning	= 17.212		
Min. Moment of Inertia	= 0.00046481		
Max. Moment of Inertia	= 0.00476761		
Principal Axis Angle	= -22.819		
Pitch/Axial Chord	= 0.7080		
Pitch/Actual Chord	= 0.6823		

UNCLASSIFIED

TABLE IX

SECOND VANE CASCADE AIRFOIL, RECAMBERING DESIGN A

Radius of AA Section = 7.6500 Axial Chord = 0.8357 Actual Chord = 0.8739
Pitch = 0.6008 No. of Foils = 80.00

Percent X	Foil X	Foil Y Suction	Foil Y (Circle)	Foil Y Pressure	Foil Y (Circle)
0.0	-0.0083	-0.2987	-0.2937	-0.2494	-0.2937
0.01	0.0001	-0.3122	-0.3122	-0.2581	-0.2785
0.02	0.0085	-0.3251	-0.3251	-0.2667	-0.2758
0.03	0.0168	-0.3375	-0.3375	-0.2754	-0.2773
0.04	0.0252	-0.3493	-0.3493	-0.2840	-0.2840
0.05	0.0335	-0.3606	-0.3606	-0.2921	-0.2921
0.10	0.0753	-0.4101	-0.4101	-0.3250	-0.3250
0.15	0.1171	-0.4487	-0.4487	-0.3476	-0.3476
0.20	0.1589	-0.4776	-0.4776	-0.3620	-0.3620
0.25	0.2007	-0.4979	-0.4979	-0.3696	-0.3696
0.30	0.2425	-0.5102	-0.5102	-0.3712	-0.3712
0.35	0.2842	-0.5150	-0.5150	-0.3673	-0.3673
0.40	0.3260	-0.5128	-0.5128	-0.3585	-0.3585
0.45	0.3678	-0.5040	-0.5040	-0.3452	-0.3452
0.50	0.4096	-0.4888	-0.4888	-0.3277	-0.3277
0.55	0.4514	-0.4673	-0.4673	-0.3062	-0.3062
0.60	0.4932	-0.4399	-0.4399	-0.2812	-0.2812
0.65	0.5350	-0.4064	-0.4064	-0.2527	-0.2527
0.70	0.5767	-0.3671	-0.3671	-0.2211	-0.2211
0.75	0.6185	-0.3219	-0.3219	-0.1863	-0.1863
0.80	0.6603	-0.2708	-0.2708	-0.1487	-0.1487
0.85	0.7021	-0.2135	-0.2135	-0.1082	-0.1082
0.90	0.7439	-0.1497	-0.1497	-0.0650	-0.0650
0.95	0.7857	-0.0790	-0.0790	-0.0191	-0.0191
0.98	0.8107	-0.0328	-0.0328	0.0097	0.0095
0.99	0.8191	-0.0167	-0.0167	0.0194	0.0120
1.00	0.8275	-0.0003	0.0021	0.0292	0.0021

Foil L.E. Circle	X = 0.0096,	Y = -0.2937,	R = 0.0179
Foil T.E. Circle	X = 0.8175,	Y = 0.0021,	R = 0.0100
Foil L.E. Tangency Pt. Suction	X = -0.0056,	Y = -0.3030	
Foil L.E. Tangency Pt. Pressure	X = 0.0225,	Y = -0.2812	
Foil T.E. Tangency Pt. Suction	X = 0.8264,	Y = -0.0024	
Foil T.E. Tangency Pt. Pressure	X = 0.8099,	Y = 0.0086	
Foil Nose Point	X = -0.0013,	Y = -0.2795	
Foil Tail Point	X = 0.8230,	Y = 0.0104	
Foil Area	= 0.1008		
Gaging	LAMBDA = 0.3240,	X = 0.5788,	Y = -0.3650
Gaging Angle	= 32.635		
Center of Gravity	X = 0.4107,	Y = -0.3436	
Radial Reference	X = 0.4132,	Y = -0.3347	
Inlet Angle	= 37.732	DELTA BETA 1 = 12.494	
Exit Angle	= 33.834	DELTA BETA 2 = 13.772	
Uncovered Turning	= 17.541		
Min. Moment of Inertia	= 0.00051391		
Max. Moment of Inertia	= 0.00501637		
Principal Axis Angle	= -24.293		
Pitch/Axial Chord	= 0.7189		
Pitch/Actual Chord	= 0.6876		

UNCLASSIFIED

TABLE X

SECOND VANE CASCADE AIRFOIL, RECAMBERING DESIGN A

Radius of BB Section = 8.4863 Axial Chord = 0.8565 Actual Chord = 0.9485
Pitch = 0.6665 No. of Foils = 80.00

Percent X	Foil X	Foil Y Suction	Foil Y (Circle)	Foil Y Pressure	Foil Y (Circle)
0.0	-0.0543	-0.3745	-0.3683	-0.3252	-0.3683
0.01	-0.0458	-0.3869	-0.3869	-0.3324	-0.3519
0.02	-0.0372	-0.3989	-0.3989	-0.3397	-0.3485
0.03	-0.0286	-0.4105	-0.4105	-0.3469	-0.3492
0.04	-0.0201	-0.4217	-0.4217	-0.3542	-0.3542
0.05	-0.0115	-0.4325	-0.4325	-0.3613	-0.3613
0.10	0.0313	-0.4804	-0.4804	-0.3933	-0.3933
0.15	0.0741	-0.5190	-0.5190	-0.4191	-0.4191
0.20	0.1170	-0.5488	-0.5488	-0.4383	-0.4383
0.25	0.1598	-0.5701	-0.5701	-0.4504	-0.4504
0.30	0.2026	-0.5834	-0.5834	-0.4554	-0.4554
0.35	0.2454	-0.5888	-0.5888	-0.4531	-0.4531
0.40	0.2883	-0.5866	-0.5866	-0.4436	-0.4436
0.45	0.3311	-0.5767	-0.5767	-0.4270	-0.4270
0.50	0.3739	-0.5594	-0.5594	-0.4036	-0.4036
0.55	0.4167	-0.5346	-0.5346	-0.3738	-0.3738
0.60	0.4596	-0.5022	-0.5022	-0.3381	-0.3381
0.65	0.5024	-0.4621	-0.4621	-0.2970	-0.2970
0.70	0.5452	-0.4141	-0.4141	-0.2509	-0.2509
0.75	0.5880	-0.3580	-0.3580	-0.2004	-0.2004
0.80	0.6309	-0.2934	-0.2934	-0.1459	-0.1459
0.85	0.6737	-0.2197	-0.2197	-0.0878	-0.0878
0.90	0.7165	-0.1360	-0.1360	-0.0266	-0.0266
0.95	0.7593	-0.0409	-0.0409	0.0375	0.0375
0.98	0.7850	0.0226	0.0226	0.0771	0.0767
0.99	0.7936	0.0449	0.0449	0.0905	0.0796
1.00	0.8022	0.0679	0.0697	0.1038	0.0697

Foil L.E. Circle	X = -0.0343,	Y = -0.3683,	R = 0.0200
Foil T.E. Circle	X = 0.7922,	Y = 0.0697,	R = 0.0100
Foil L.E. Tangency Pt. Suction	X = -0.0508,	Y = -0.3796	
Foil L.E. Tangency Pt. Pressure	X = -0.0214,	Y = -0.3531	
Foil T.E. Tangency Pt. Suction	X = 0.8016,	Y = 0.0663	
Foil T.E. Tangency Pt. Pressure	X = 0.7838,	Y = 0.0751	
Foil Nose Point	X = -0.0477,	Y = -0.3535	
Foil Tail Point	X = 0.7966,	Y = 0.0787	
Foil Area	= 0.1073		
Gaging	LAMBDA = 0.2969,	X = 0.5531,	Y = -0.4044
Gaging Angle	= 26.460		
Center of Gravity	X = 0.3939,	Y = -0.3812	
Radial Reference	X = 0.4132,	Y = -0.3347	
Inlet Angle	= 42.100,	DELTA BETA 1 = 15.250	
Exit Angle	= 26.450,	DELTA BETA 2 = 12.500	
Uncovered Turning	= 18.492		
Min. Moment of Inertia	= 0.00073689		
Max. Moment of Inertia	= 0.00676781		
Principal Axis Angle	= -32.600		
Pitch/Axial Chord	= 0.7782		
Pitch/Actual Chord	= 0.7027		

UNCLASSIFIED

TABLE XI

SECOND VANE CASCADE AIRFOIL, RECAMBERING DESIGN A

Radius of CC Section = 9.4725 Axial Chord = 0.8810 Actual Chord = 1.0682
Pitch = 0.7440 No. of Foils = 80.00

Percent X	Foil X	Foil Y Suction	Foil Y (Circle)	Foil Y Pressure	Foil Y (Circle)
0.0	-0.1086	-0.4844	-0.4759	-0.4368	-0.4759
0.01	-0.0998	-0.4944	-0.4944	-0.4419	-0.4581
0.02	-0.0910	-0.5041	-0.5041	-0.4470	-0.4540
0.03	-0.0822	-0.5135	-0.5135	-0.4522	-0.4538
0.04	-0.0734	-0.5225	-0.5225	-0.4573	-0.4573
0.05	-0.0646	-0.5312	-0.5312	-0.4623	-0.4623
0.10	-0.0205	-0.5694	-0.5694	-0.4846	-0.4846
0.15	0.0235	-0.5994	-0.5994	-0.5019	-0.5019
0.20	0.0676	-0.6218	-0.6218	-0.5136	-0.5136
0.25	0.1116	-0.6366	-0.6366	-0.5191	-0.5191
0.30	0.1557	-0.6441	-0.6441	-0.5180	-0.5180
0.35	0.1997	-0.6445	-0.6445	-0.5099	-0.5099
0.40	0.2438	-0.6376	-0.6376	-0.4945	-0.4945
0.45	0.2878	-0.6235	-0.6235	-0.4716	-0.4716
0.50	0.3319	-0.6019	-0.6019	-0.4413	-0.4413
0.55	0.3759	-0.5727	-0.5727	-0.4037	-0.4037
0.60	0.4200	-0.5356	-0.5356	-0.3591	-0.3591
0.65	0.4640	-0.4899	-0.4899	-0.3080	-0.3080
0.70	0.5081	-0.4351	-0.4351	-0.2509	-0.2509
0.75	0.5521	-0.3703	-0.3703	-0.1882	-0.1882
0.80	0.5962	-0.2945	-0.2945	-0.1205	-0.1205
0.85	0.6402	-0.2063	-0.2063	-0.0484	-0.0484
0.90	0.6843	-0.1044	-0.1044	0.0276	0.0276
0.95	0.7283	0.0131	0.0131	0.1072	0.1072
0.98	0.7547	0.0917	0.0917	0.1564	0.1559
0.99	0.7635	0.1195	0.1195	0.1730	0.1593
1.00	0.7724	0.1479	0.1494	0.1895	0.1494

Foil L.E. Circle	X = -0.0861,	Y = -0.4759,	R = 0.0225
Foil T.E. Circle	X = 0.7624,	Y = 0.1494,	R = 0.0100
Foil L.E. Tangency Pt. Suction	X = -0.1031,	Y = -0.4908	
Foil L.E. Tangency Pt. Pressure	X = -0.0748,	Y = -0.4565	
Foil T.E. Tangency Pt. Suction	X = 0.7719,	Y = 0.1465	
Foil T.E. Tangency Pt. Pressure	X = 0.7535,	Y = 0.1541	
Foil Nose Point	X = -0.1035,	Y = -0.4616	
Foil Tail Point	X = 0.7662,	Y = 0.1587	
Foil Area	= 0.1178		
Gaging	LAMBDA = 0.2895,	X = 0.5185,	Y = -0.4207
Gaging Angle	= 22.900		
Center of Gravity	X = 0.3686,	Y = -0.3988	
Radial Reference	X = 0.4132,	Y = -0.3347	
Inlet Angle	= 50.500,	DELTA BETA 1 = 18.500	
Exit Angle	= 22.500,	DELTA BETA 2 = 11.900	
Uncovered Turning	= 18.394		
Min. Moment of Inertia	= 0.00078393		
Max. Moment of Inertia	= 0.00948326		
Principal Axis Angle	= -40.289		
Pitch/Axial Chord	= 0.8445		
Pitch/Actual Chord	= 0.6965		

UNCLASSIFIED

TABLE XII

SECOND VANE CASCADE AIRFOIL, RECAMBERING DESIGN A

Radius of DD Section = 10.4588 Axial Chord - 0.9055 Actual Chord = 1.1773
Pitch = 0.8214 No. of Foils - 80.00

Percent	Foil X	Foil Y Suction	Foil Y (Circle	Foil Y Pressure	Foil Y (Circle)
0.0	-0.1630	-0.5503	-0.5395	-0.5026	-0.5395
0.01	-0.1539	-0.5588	-0.5588	-0.5063	-0.5203
0.02	-0.1449	-0.5671	-0.5671	-0.5099	-0.5155
0.03	-0.1358	-0.5748	-0.5748	-0.5135	-0.5146
0.04	-0.1268	-0.5820	-0.5820	-0.5171	-0.5171
0.05	-0.1177	-0.5887	-0.5887	-0.5205	-0.5205
0.10	-0.0724	-0.6160	-0.6160	-0.5344	-0.5344
0.15	-0.0272	-0.6341	-0.6341	-0.5424	-0.5424
0.20	0.0181	-0.6443	-0.6443	-0.5442	-0.5442
0.25	0.0634	-0.6474	-0.6474	-0.5395	-0.5395
0.30	0.1087	-0.6440	-0.6440	-0.5280	-0.5280
0.35	0.1539	-0.6345	-0.6345	-0.5096	-0.5096
0.40	0.1992	-0.6188	-0.6188	-0.4843	-0.4843
0.45	0.2445	-0.5972	-0.5972	-0.4521	-0.4521
0.50	0.2898	-0.5694	-0.5694	-0.4132	-0.4132
0.55	0.3350	-0.5352	-0.5352	-0.3679	-0.3679
0.60	0.3803	-0.4940	-0.4940	-0.3164	-0.3164
0.65	0.4256	-0.4451	-0.4451	-0.2592	-0.2592
0.70	0.4709	-0.3871	-0.3871	-0.1965	-0.1965
0.75	0.5161	-0.3184	-0.3184	-0.1289	-0.1289
0.80	0.5614	-0.2367	-0.2367	-0.0567	-0.0567
0.85	0.6067	-0.1408	-0.1408	0.0197	0.0197
0.90	0.6520	-0.0305	-0.0305	0.0999	0.0999
0.95	0.6972	0.0929	0.0929	0.1835	0.1835
0.98	0.7244	0.1725	0.1725	0.2352	0.2350
0.99	0.7335	0.1998	0.1998	0.2526	0.2391
1.00	0.7425	0.2278	0.2291	0.2700	0.2291

Foil L.E. Circle	X = 0.1380	Y = -0.5395	R = 0.0250
Foil T.E. Circle	X = 0.7325	Y = -0.2291	R = 0.0100
Foil L.E. Tangency Pt. Suction	X = -0.1552	Y = -0.5577	
Foil L.E. Tengency Pt. Pressure	X = -0.1287	Y = -0.5163	
Foil T.E. Tangency Pt. Suction	X = 0.7420	Y = 0.2260	
Foil T.E. Tangency Pt. Pressure	X = 0.7237	Y = 0.2338	
Foil Nose Point	X = -0.1590	Y = -0.5260	
Foil Tail Point	X = 0.7364	Y = 0.2384	
Foil Area	= 0.1190		
Gaging	LAMBDA = 0.3223	X = 0.4546	Y = -0.3958
Gaging Angle	23.100		
Center of Gravity	X = 0.3340	Y = -0.3648	
Radial Reference	X = 0.4132	Y = -0.3347	
Inlet Angle	= 57.400	DELTA BETA 1 = 21.750	
Exit Angle	= 22.750	DELTA BETA 2 = 9.500	
Uncovered Turning	= 18.360		
Min. Moment of Inertia	= 0.00062268		
Max. Moment of Inertia	= 0.01144839		
Principal Axis Angle	= -44.141		
Pitch/Axial Chord	= 0.9072		
Pitch/Actual Chord	= 0.6977		

UNCLASSIFIED

TABLE XIII

SECOND VANE CASCADE AIRFOIL, RECAMBERING DESIGN A

Radius of EE Section = 10.8600 Axial Chord - 0.9155 Actual Chord - 1.2091
Pitch = 0.8529 No. of Foils = 80.00

Percent	Foil X	Foil Y Suction	Foil Y (Circle)	Foil Y Pressure	Foil Y (Circle)
0.0	-0.1851	-0.5548	-0.5431	-0.5068	-0.5431
0.01	-0.1759	-0.5630	-0.5630	-0.5100	-0.5233
0.02	-0.1668	-0.5708	-0.5708	-0.5130	-0.5183
0.03	-0.1576	-0.5782	-0.5782	-0.5161	-0.5172
0.04	-0.1485	-0.5850	-0.5850	-0.5192	-0.5192
0.05	-0.1393	-0.5914	-0.5914	-0.5222	-0.5222
0.10	-0.0935	-0.6166	-0.6166	-0.5323	-0.5323
0.15	-0.0478	-0.6322	-0.6322	-0.5356	-0.5356
0.20	-0.0020	-0.6395	-0.6395	-0.5320	-0.5320
0.25	0.0438	-0.6393	-0.6393	-0.5217	-0.5217
0.30	0.0896	-0.6321	-0.6321	-0.5048	-0.5048
0.35	0.1353	-0.6184	-0.6184	-0.4814	-0.4814
0.40	0.1811	-0.5983	-0.5983	-0.4516	-0.4516
0.45	0.2269	-0.5719	-0.5719	-0.4158	-0.4158
0.50	0.2727	-0.5393	-0.5393	-0.3739	-0.3739
0.55	0.3184	-0.5002	-0.5002	-0.3265	-0.3265
0.60	0.3642	-0.4544	-0.4544	-0.2739	-0.2739
0.65	0.4100	-0.4012	-0.4012	-0.2162	-0.2162
0.70	0.4558	-0.3397	-0.3397	-0.1538	-0.1538
0.75	0.5015	-0.2685	-0.2685	-0.0871	-0.0871
0.80	0.5473	-0.1858	-0.1858	-0.0164	-0.0164
0.85	0.5931	-0.0908	-0.0908	0.0581	0.0581
0.90	0.6388	0.0163	0.0163	0.1360	0.1360
0.95	0.6846	0.1339	0.1339	0.2172	0.2172
0.98	0.7121	0.2086	0.2086	0.2672	0.2671
0.99	0.7212	0.2341	0.2341	0.2841	0.2715
1.00	0.7304	0.2598	0.2616	0.3010	0.2616

Foil L.E. Circle	X = -0.1591	Y = -0.5431	R = 0.0260
Foil T.E. Circle	X = 0.7204	Y = 0.2616	R = 0.0100
Foil L. E. Tangency Pt. Suction	X = -0.1764	Y = -0.5625	
Foil L.E. Tangency Pt. Pressure	X = -0.1507	Y = -0.5185	
Foil T.E. Tangency Pt. Suction	X = 0.7298	Y = 0.2582	
Foil T.E. Tangency Pt. Pressure	X = 0.7116	Y = 0.2663	
Foil Nose Point	X = -0.1815	Y = -0.5300	
Foil Tail Point	X = 0.7245	Y = 0.2707	
Foil Area	= 0.1220		
Gaging	LAMBDA = 0.3519	X = 0.4306	Y = -0.3745
Gaging Angle	= 24.368		
Center of Gravity	X = 0.3059	Y = -0.3455	
Radial Reference	X = 0.4132	Y = -0.3347	
Inlet Angle	= 59.762	DELTA BETA 1 = 23.072	
Exit Angle	= 24.140	DELTA BETA 2 = 8.890	
Uncovered Turning	= 17.216		
Min. Moment of Inertia	= 0.00054959		
Max. Moment of Inertia	= 0.01220553		
Principal Axis Angle	= -44.918		
Pitch/Axial Chord	= 0.9317		
Pitch/Actual Chord	= 0.7054		

UNCLASSIFIED

TABLE XIV

SECOND VANE CASCADE AIRFOIL, RECAMBERING DESIGN A

Radius of HH Section = 11.4100 Axial Chord = 0.9291
Pitch = 0.8961 No. of Foils = 80.00 Actual Chord = 1.2378

Percent X	Foil X	Foil Y Suction	Foil Y (Circle)	Foil Y Pressure	Foil Y (Circle)
0.0	-0.2154	-0.5379	-0.5251	-0.4895	-0.5251
0.01	-0.2061	-0.5457	-0.5457	-0.4920	-0.5045
0.02	-0.1968	-0.5532	-0.5532	-0.4944	-0.4991
0.03	-0.1875	-0.5603	-0.5603	-0.4968	-0.4977
0.04	-0.1782	-0.5670	-0.5670	-0.4993	-0.4993
0.05	-0.1689	-0.5733	-0.5733	-0.5014	-0.5014
0.10	-0.1225	-0.5987	-0.5987	-0.5056	-0.5056
0.15	-0.0760	-0.6145	-0.6145	-0.5007	-0.5007
0.20	-0.0295	-0.6210	-0.6210	-0.4879	-0.4879
0.25	0.0169	-0.6187	-0.6187	-0.4683	-0.4683
0.30	0.0634	-0.6078	-0.6078	-0.4428	-0.4428
0.35	0.1098	-0.5887	-0.5887	-0.4117	-0.4117
0.40	0.1563	-0.5616	-0.5616	-0.3757	-0.3757
0.45	0.2027	-0.5269	-0.5269	-0.3352	-0.3352
0.50	0.2492	-0.4847	-0.4847	-0.2903	-0.2903
0.55	0.2956	-0.4353	-0.4353	-0.2416	-0.2416
0.60	0.3421	-0.3790	-0.3790	-0.1892	-0.1892
0.65	0.3886	-0.3158	-0.3158	-0.1334	-0.1334
0.70	0.4350	-0.2460	-0.2460	-0.0742	-0.0742
0.75	0.4815	-0.1696	-0.1696	-0.0119	-0.0119
0.80	0.5279	-0.0868	-0.0868	0.0533	0.0533
0.85	0.5744	0.0023	0.0023	0.1214	0.1214
0.90	0.6208	0.0974	0.0974	0.1923	0.1923
0.95	0.6673	0.1981	0.1981	0.2658	0.2658
0.98	0.6952	0.2610	0.2610	0.3112	0.3112
0.99	0.7045	0.2824	0.2824	0.3264	0.3160
1.00	0.7138	0.3039	0.3060	0.3417	0.3060

Foil L.E. Circle	X = -0.1880	Y = -0.5251	R = 0.0274
Foil T.E. Circle	X = 0.7038	Y = 0.3060	R = 0.0100
Foil L.E. Tangency Pt. Suction	X = -0.2055	Y = -0.5462	
Foil L. E. Tangency Pt. Pressure	X = -0.1809	Y = -0.4986	
Foil T. E. Tangency Pt. Suction	X = 0.7125	Y = 0.3021	
Foil T.E. Tangency Pt. Pressure	X = 0.6952	Y = 0.3112	
Foil Nose Point	X = -0.2123	Y = -0.5125	
Foil Nose Point	X = 0.7083	Y = 0.3149	
Foil Area	= 0.1311		
Gaging	LAMBDA = 0.4060	X = 0.3681	Y = -0.3444
Gaging Angle	= 26.937		
Center of Gravity	X = 0.2515	Y = -0.3179	
Radial Reference	X = 0.4132	Y = -0.3347	
Inlet Angle	= 62.722	DELTA BETA 1 = 34.885	
Exit Angle	= 27.322	DELTA BETA 2 = 8.053	
Uncovered Turning	= 12.843		
Min. Moment of Inertia	= 0.00047562		
Max. Moment of Inertia	= 0.01310568		
Principal Axis Angle	= -45.641		
Pitch/Axial Chord	= 0.9645		
Pitch/Actual Chord	= 0.7240		

UNCLASSIFIED

TABLE XV

SECOND VANE CASCADE AIRFOIL, RECAMBERING DESIGN A

Radius of GG Section - 11.4450 Axial Chord = 0.9300 Actual Chord = 1.2390
Pitch = 0.8989 No. of Foils = 80.00

Percent X	Foil X	Foil Y Suction	Foil Y (Circle)	Foil Y Pressure	Foil Y (Circle)
0.0	-0.2173	-0.5359	-0.5230	-0.4874	-0.5230
0.01	-0.2080	-0.5436	-0.5436	-0.4898	-0.5024
0.02	-0.1987	-0.5512	-0.5512	-0.4922	-0.4970
0.03	-0.1894	-0.5583	-0.5583	-0.4947	-0.4955
0.04	-0.1801	-0.5650	-0.5650	-0.4971	-0.4971
0.05	-0.1708	-0.5713	-0.5713	-0.4991	-0.4991
0.10	-0.1243	-0.5969	-0.5969	-0.5029	-0.5029
0.15	-0.0778	-0.6128	-0.6128	-0.4974	-0.4974
0.20	-0.0313	-0.6194	-0.6194	-0.4840	-0.4840
0.25	0.0152	-0.6170	-0.6170	-0.4638	-0.4638
0.30	0.0617	-0.6059	-0.6059	-0.4376	-0.4376
0.35	0.1082	-0.5865	-0.5865	-0.4060	-0.4060
0.40	0.1547	-0.5589	-0.5589	-0.3696	-0.3696
0.45	0.2012	-0.5236	-0.5236	-0.3288	-0.3288
0.50	0.2477	-0.4806	-0.4806	-0.2838	-0.2838
0.55	0.2942	-0.4305	-0.4305	-0.2351	-0.2351
0.60	0.3407	-0.3733	-0.3733	-0.1828	-0.1828
0.65	0.3872	-0.3094	-0.3094	-0.1271	-0.1271
0.70	0.4337	-0.2389	-0.2389	-0.0683	-0.0683
0.75	0.4802	-0.1621	-0.1621	-0.0064	-0.0064
0.80	0.5267	-0.0793	-0.0793	0.0583	0.0583
0.85	0.5732	0.0092	0.0092	0.1259	0.1259
0.90	0.6197	0.1032	0.1032	0.1961	0.1961
0.95	0.6662	0.2025	0.2025	0.2690	0.2690
0.98	0.6941	0.2645	0.2645	0.3139	0.3139
0.99	0.7034	0.2855	0.2855	0.3291	0.3188
1.00	0.7127	0.3067	0.3088	0.3442	0.3088

Foil L.E. Circle	X = -0.1898	Y = -0.5230	R = 0.0275
Foil T.E. Circle	X = 0.7027	Y = 0.3088	R = 0.0100
Foil L.E. Tangency Pt. Suction	X = -0.2073	Y = -0.5442	
Foil L.E. Tangency Pt. Pressure	X = -0.1829	Y = -0.4964	
Foil T.E. Tangency Pt. Suction	X = 0.7119	Y = 0.3048	
Foil T.E. Tangency Pt. Pressure	X = 0.6942	Y = 0.3141	
Foil Nose Point	X = -0.2143	Y = -0.5104	
Foil Tail Point	X = 0.7073	Y = 0.3177	
Foil Area	= 0.1319		
Gaging	LAMBDA = 0.4098	X = 0.3633	Y = -0.3431
Gaging Angle	= 27.119		
Center of Gravity	X = 0.2475	Y = -0.3161	
Radial Reference	X = 0.4132	Y = -0.3347	
Inlet Angle	= 62.900	DELTA BETA 1 = 25.000	
Exit Angle	= 27.574	DELTA BETA 2 = 8.000	
Uncovered Turning	= 12.470		
Min. Moment of Inertia	= 0.00047307		
Max. Moment of Inertia	= 0.01314440		
Principal Axis Angle	= -45.681		
Pitch/Axial Chord	= 0.9665		
Pitch/Actual Chord	= 0.7255		

UNCLASSIFIED

TABLE XVI

SECOND VANE CASCADE AIRFOIL, RECAMBERING DESIGN B

Radius of FF Section = 7.5000 Axial Chord = 0.8320
Pitch = 0.5890 No. of Foils = 80.00 Actual Chord = 0.8485

Percent X	Foil X	Foil Y Suction	Foil Y (Circle)	Foil Y Pressure	Foil Y (Circle)
0.0	0.0	-0.2402	-0.2346	-0.1842	-0.2346
0.01	0.0083	-0.2537	-0.2537	-0.1930	-0.2183
0.02	0.0166	-0.2665	-0.2665	-0.2018	-0.2148
0.03	0.0250	-0.2788	-0.2788	-0.2107	-0.2152
0.04	0.0333	-0.2904	-0.2904	-0.2195	-0.2196
0.05	0.0416	-0.3014	-0.3014	-0.2281	-0.2281
0.10	0.0832	-0.3489	-0.3489	-0.2640	-0.2640
0.15	0.1248	-0.3855	-0.3855	-0.2898	-0.2898
0.20	0.1664	-0.4129	-0.4129	-0.3076	-0.3076
0.25	0.2080	-0.4325	-0.4325	-0.3187	-0.3187
0.30	0.2496	-0.4449	-0.4449	-0.3241	-0.3241
0.35	0.2912	-0.4507	-0.4507	-0.3243	-0.3243
0.40	0.3328	-0.4504	-0.4504	-0.3200	-0.3200
0.45	0.3744	-0.4440	-0.4440	-0.3114	-0.3114
0.50	0.4160	-0.4318	-0.4318	-0.2988	-0.2988
0.55	0.4576	-0.4138	-0.4138	-0.2825	-0.2825
0.60	0.4992	-0.3898	-0.3898	-0.2627	-0.2627
0.65	0.5408	-0.3597	-0.3597	-0.2394	-0.2394
0.70	0.5824	-0.3231	-0.3231	-0.2128	-0.2128
0.75	0.6240	-0.2798	-0.2798	-0.1828	-0.1828
0.80	0.6656	-0.2310	-0.2310	-0.1496	-0.1496
0.85	0.7072	-0.1788	-0.1788	-0.1131	-0.1131
0.90	0.7488	-0.1246	-0.1246	-0.0733	-0.0733
0.95	0.7904	-0.0693	-0.0693	-0.0300	-0.0300
0.98	0.8154	-0.0357	-0.0357	-0.0024	-0.0025
0.99	0.8237	-0.0245	-0.0245	0.0070	-0.0001
1.00	0.8320	-0.0133	-0.0100	0.0164	-0.0100

Foil L. E. Circle	X = 0.0200	Y = -0.2346	R = 0.0200
Foil T. E. Circle	X = 0.8220	Y = -0.0100	R = 0.0100
Foil L. E. Tangency Pt. Suction	X = 0.0029	Y = -0.2450	
Foil L. E. Tangency Pt. Pressure	X = 0.0345	Y = -0.2208	
Foil T. E. Tangency Pt. Suction	X = 0.8300	Y = -0.0159	
Foil T. E. Tangency Pt. Pressure	X = 0.8145	Y = -0.0034	
Foil Nose Point	X = 0.0079	Y = -0.2187	
Foil Tail Point	X = 0.8283	Y = -0.0022	
Foil Area	0.0817		
Gaging	LAMBDA = 0.3552	X = 0.5738	Y = -0.3312
Gaging Angle	= 37.082		
Center of Gravity	X = 0.3924	Y = -0.3113	
Radial Reference	X = 0.3924	Y = -0.3113	
Inlet Angle	= 37.330	DELTA BETA 1 = 12.000	
Exit Angle	= 39.000	DELTA BETA 2 = 5.000	
Uncovered Turning	= 10.654		
Min. Moment of Inertia	= 0.00038949		
Max. Moment of Inertia	= 0.00367671		
Principal Axis Angle	= -17.113		
Pitch/Axial Chord	= 0.7080		
Pitch/Actual Chord	= 0.6942		

UNCLASSIFIED

TABLE XVII

SECOND VANE CASCADE AIRFOIL, RECAMBERING DESIGN B

Radius of AA Section = 7.6500 Axial Chord=0.8357 Actual Chord 0.8609
Pitch = 0.6008 No. of Foils=80.00

Percent X	Foil X	Foil Y Section	Foil Y (Circle)	Foil Y Pressure	Foil Y (Circle)
0.0	-0.0083	-0.2619	-0.2562	-0.2057	-0.2562
0.01	0.0001	-0.2754	-0.2754	-0.2144	-0.2397
0.02	0.0085	-0.2882	-0.2882	-0.2231	-0.2362
0.03	0.0168	-0.3003	-0.3003	-0.2317	-0.2364
0.04	0.0252	-0.3119	-0.3119	-0.2404	-0.2405
0.05	0.0335	-0.3228	-0.3228	-0.2488	-0.2488
0.10	0.0753	-0.3700	-0.3700	-0.2840	-0.2840
0.15	0.1171	-0.4063	-0.4063	-0.3090	-0.3090
0.20	0.1589	-0.4334	-0.4334	-0.3257	-0.3257
0.25	0.2007	-0.4526	-0.4526	-0.3355	-0.3355
0.30	0.2425	-0.4646	-0.4646	-0.3394	-0.3394
0.35	0.2842	-0.4702	-0.4702	-0.3381	-0.3381
0.40	0.3260	-0.4696	-0.4696	-0.3321	-0.3321
0.45	0.3678	-0.4630	-0.4630	-0.3219	-0.3219
0.50	0.4096	-0.4507	-0.4507	-0.3078	-0.3078
0.55	0.4514	-0.4325	-0.4325	-0.2900	-0.2900
0.60	0.4932	-0.4083	-0.4083	-0.2687	-0.2687
0.65	0.5350	-0.3777	-0.3777	-0.2440	-0.2440
0.70	0.5767	-0.3402	-0.3402	-0.2160	-0.2160
0.75	0.6185	-0.2951	-0.2951	-0.1844	-0.1844
0.80	0.6603	-0.2430	-0.2430	-0.1494	-0.1494
0.85	0.7021	-0.1859	-0.1859	-0.1105	-0.1105
0.90	0.7439	-0.1256	-0.1256	-0.0678	-0.0678
0.95	0.7857	-0.0636	-0.0636	-0.0207	-0.0207
0.98	0.8107	-0.0260	-0.0260	0.0098	0.0095
0.99	0.8191	-0.0135	-0.0135	0.0202	0.0120
1.00	0.8275	-0.0009	0.0021	0.0306	0.0021

Foil L.E. Circle	X=0.0121,	Y = -0.2562	R=0.0204
Foil T.E. Circle	X=0.8175	Y = 0.0021	R=0.0100
Foil L. E. Tangency Pt. Suction	X = -0.0052	Y = -0.2669	
Foil L. E. Tangency Pt. Pressure	X = 0.0268	Y = -0.2421	
Foil T. E. Tangency Pt. Suction	X = 0.8258	Y = -0.0035	
Foil T. E. Tangency Pt. Pressure	X = 0.8097	Y = 0.0084	
Foil Nose Point	X = -0.0004	Y = -0.2401	
Foil Tail Point	X = 0.8234	Y = 0.0102	
Foil Area	=0.0880		
Gaging	LAMBDA =0.3432	X=0.5720	Y = -0.3448
Gaging Angle	=34.829		
Center of Gravity	X=0.3938	Y = -0.3225	
Radial Reference	X=0.3924	Y = -0.3113	
Inlet Angle	=37.732	DELTA BETA 1 = 12.361	
Exit Angle	=36.513	DELTA BETA 2 = 5.120	
Uncovered Turning	=12.020		
Min. Moment of Inertia	=0.00043744		
Max. Moment of Inertia	=0.00408222		
Principal Axis Angle	= -19.374		
Pitch/Axial Chord	=0.7189		
Pitch/Actual Chord	=0.6979		

UNCLASSIFIED

TABLE XVIII

SECOND VANE CASCADE AIRFOIL, RECAMBERING DESIGN B

Radius of BB Section = 8.4863 Axial Chord = 0.8565 Actual Chord = 0.9463
Pitch = 0.6665 No. of Foils = 80.00

Percent X	Foil X	Foil Y Section	Foil Y (Circle)	Foil Y Pressure	Foil Y (Circle)
0.0	-0.0543	-0.3741	-0.3670	-0.3180	-0.3670
0.01	-0.0458	-0.3863	-0.3863	-0.3254	-0.3493
0.02	-0.0372	-0.3981	-0.3981	-0.3327	-0.3452
0.03	-0.0286	-0.4093	-0.4093	-0.3401	-0.3447
0.04	-0.0201	-0.4201	-0.4201	-0.3474	-0.3478
0.05	-0.0115	-0.4304	-0.4304	-0.3547	-0.3547
0.10	0.0313	-0.4756	-0.4756	-0.3853	-0.3853
0.15	0.0741	-0.6113	-0.5113	-0.4073	-0.4073
0.20	0.1170	-0.5385	-0.5385	-0.4216	-0.4216
0.25	0.1598	-0.5581	-0.5581	-0.4292	-0.4292
0.30	0.2026	-0.5704	-0.5704	-0.4305	-0.4305
0.35	0.2454	-0.5759	-0.5759	-0.4261	-0.4261
0.40	0.2883	-0.5747	-0.5747	-0.4162	-0.4162
0.45	0.3311	-0.5668	-0.5668	-0.4011	-0.4011
0.50	0.3739	-0.5520	-0.5520	-0.3809	-0.3809
0.55	0.4167	-0.5302	-0.5302	-0.3557	-0.3557
0.60	0.4596	-0.5008	-0.5008	-0.3256	-0.3256
0.65	0.5024	-0.4633	-0.4633	-0.2905	-0.2905
0.70	0.5452	-0.4166	-0.4166	-0.2504	-0.2504
0.75	0.5880	-0.3593	-0.3593	-0.2052	-0.2052
0.80	0.6309	-0.2904	-0.2904	-0.1546	-0.1546
0.85	0.6737	-0.2109	-0.2109	-0.0983	-0.0983
0.90	0.7165	-0.1231	-0.1231	-0.0360	-0.0360
0.95	0.7593	-0.0297	-0.0297	0.0328	0.0328
0.98	0.7850	0.0283	0.0283	0.0774	0.0767
0.99	0.7936	0.0479	0.0479	0.0927	0.0927
1.00	0.8022	0.0676	0.0697	0.1080	0.0697

Foil L. E. Circle	X = -0.0318	Y = -0.3670	R = 0.0225
Foil T. E. Circle	X = 0.7922	Y = 0.0697	R = 0.0100
Foil L. E. Tangency Pt. Suction	X = -0.0503	Y = -0.3799	
Foil L. E. Tangency Pt. Pressure	X = -0.0172	Y = -0.3499	
Foil T. E. Tangency Pt. Suction	X = 0.8013	Y = 0.0657	
Foil T. E. Tangency Pt. Pressure	X = 0.7834	Y = 0.0746	
Foil Nose Point	X = -0.0469	Y = -0.3503	
Foil Tail Point	X = 0.7966	Y = 0.0787	
Foil Area	= 0.1100		
Gaging	LAMBDA = 0.2953	X = 0.5532	Y = -0.4068
Gaging Angle	= 26.301		
Center of Gravity	X = 0.3802	Y = -0.3847	
Radial Reference	X = 0.3924	Y = -0.3113	
Inlet Angle	= 42.100	DELTA BETA 1 = 4.500	
Exit Angle	= 26.350	DELTA BETA 2 = 5.800	
Uncovered Turning	= 15.099		
Min. Moment of Inertia	= 0.00072721		
Max. Moment of Inertia	= 0.00627873		
Principal Axis Angle	= -30.144		
Pitch/Axial Chord	= 0.7782		
Pitch/Actual Chord	= 0.7043		

UNCLASSIFIED

TABLE XIX

SECOND VANE CASCADE AIRFOIL, RECAMBERING DESIGN B

Radius of CC Section = 9.4725 Axial Chord = 0.8810 Actual Chord = 1.0657
Pitch = 0.7440 No. of Foils = 80.00

Percent X	Foil X	Foil Y Suction	Foil Y (Circle)	Foil Y Pressure	Foil Y (Circle)
0.0	-0.1086	-0.4837	-0.4741	-0.4300	-0.4741
0.01	-0.0998	-0.4935	-0.4935	-0.4353	-0.4550
0.02	-0.0910	-0.5031	-0.5031	-0.4405	-0.4502
0.03	-0.0822	-0.5126	-0.5126	-0.4458	-0.4491
0.04	-0.0734	-0.5218	-0.5218	-0.4511	-0.4513
0.05	-0.0646	-0.5309	-0.5309	-0.4563	-0.4563
0.10	-0.0205	-0.5726	-0.5726	-0.4806	-0.4806
0.15	0.0235	-0.6084	-0.6084	-0.5012	-0.5012
0.20	0.0676	-0.6376	-0.6376	-0.5175	-0.5175
0.25	0.1116	-0.6599	-0.6599	-0.5290	-0.5290
0.30	0.1557	-0.6746	-0.6746	-0.5348	-0.5348
0.35	0.1997	-0.6812	-0.6812	-0.5342	-0.5342
0.40	0.2438	-0.6793	-0.6793	-0.5263	-0.5263
0.45	0.2878	-0.6682	-0.6682	-0.5106	-0.5106
0.50	0.3319	-0.6475	-0.6475	-0.4863	-0.4863
0.55	0.3759	-0.6168	-0.6168	-0.4532	-0.4532
0.60	0.4200	-0.5757	-0.5757	-0.4110	-0.4110
0.65	0.4640	-0.5238	-0.5238	-0.3600	-0.3600
0.70	0.5081	-0.4611	-0.4611	-0.3005	-0.3005
0.75	0.5521	-0.3872	-0.3872	-0.2332	-0.2332
0.80	0 5962	-0.3024	-0.3024	-0.1587	-0.1587
0.85	0.6402	-0.2065	-0.2065	-0.0778	-0.0778
0.90	0.6843	-0.0996	-0.0996	0.0087	0.0087
0.95	0.7283	0.0186	0.0186	0.1000	0.1000
0.98	0.7547	0.0948	0.0948	0.1568	0.1559
0.99	0.7635	0.1211	0.1211	0.1759	0.1593
1.00	0.7724	0.1478	0.1494	0.1951	0.1494

Foil L. E. Circle	X = -0.0836	Y = -0.4741	R = 0.0250
Foil T. E. Circle	X = 0.7624	Y = 0.1494	R = 0.0100
Foil L. E. Tangency Pt. Suction	X = -0.1023	Y = -0.4908	
Foil L. E. Tangency Pt. Pressure	X = -0.0708	Y = -0.4526	
Foil T. E. Tangency Pt Suction	X = 0.7719	Y = 0.1463	
Foil T. E. Tangency Pt. Pressure	X = 0.7533	Y = 0.1536	
Foil Nose Point	X = -0.1029	Y = -0.4582	
Foil Tail Point	X = 0.7660	Y = 0.1587	
Foil Area	= 0.1138		
Gaging	LAMBDA = 0.2763	X = 0.5189	Y = -0.4440
Gaging Angle	= 21.8000		
Center of Gravity	X = 0.3454	Y = -0.4429	
Radial Reference	X = 0.3924	Y = -0.3113	
Inlet Angle	= 50.500	DELTA BETA 1 = 17.250	
Exit Angle	= 21.400	DELTA BETA 2 = 6.500	
Uncovered Turning	= 13.718		
Min. Moment of Inertia	= 0.00099224		
Max. Moment of Inertia	= 0.00893008		
Principal Axis Angle	= -39.911		
Pitch/Axial Chord	= 0.8445		
Pitch/Actual Chord	= 0.6981		

UNCLASSIFIED

TABLE XX

SECOND VANE CASCADE AIRFOIL, RECAMBERING DESIGN B

Radius of DD Section = 10.4588 Axial Chord = 0.9055
Pitch = 0.8214 No. of Foils = 80.00 Actual Chord = 1.1746

Percent X	Foil X	Foil Y Suction	Foil Y (Circle)	Foil Y Pressure	Foil Y (Circle)
0.0	-0.1630	-0.5494	-0.5373	-0.4961	-0.5373
0.01	-0.1539	-0.5577	-0.5577	-0.4998	-0.5169
0.02	-0.1449	-0.5659	-0.5659	-0.5036	-0.5115
0.03	-0.1358	-0.5739	-0.5739	-0.5074	-0.5098
0.04	-0.1268	-0.5817	-0.5817	-0.5112	-0.5112
0.05	-0.1177	-0.5892	-0.5892	-0.5149	-0.5149
0.10	-0.0724	-0.6234	-0.6234	-0.5317	-0.5317
0.15	-0.0272	-0.6514	-0.6514	-0.5449	-0.5449
0.20	0.0181	-0.6726	-0.6726	-0.5538	-0.5538
0.25	0.0634	-0.6866	-0.6866	-0.5576	-0.5576
0.30	0.1087	-0.6928	-0.6928	-0.5555	-0.5555
0.35	0.1539	-0.6907	-0.6907	-0.5465	-0.5465
0.40	0.1992	-0.6799	-0.6799	-0.5296	-0.5296
0.45	0.2445	-0.6599	-0.6599	-0.5042	-0.5042
0.50	0.2898	-0.6303	-0.6303	-0.4698	-0.4698
0.55	0.3350	-0.5908	-0.5908	-0.4262	-0.4262
0.60	0.3803	-0.5411	-0.5411	-0.3737	-0.3737
0.65	0.4256	-0.4813	-0.4813	-0.3129	-0.3129
0.70	0.4709	-0.4111	-0.4111	-0.2446	-0.2446
0.75	0.5161	-0.3308	-0.3308	-0.1697	-0.1697
0.80	0.5614	-0.2403	-0.2403	-0.0891	-0.0891
0.85	0.6067	-0.1395	-0.1395	-0.0038	-0.0038
0.90	0.6520	-0.0282	-0.0282	0.0856	0.0856
0.95	0.6972	0.0940	0.0940	0.1783	0.1783
0.98	0.7244	0.1727	0.1727	0.2354	0.2350
0.99	0.7335	0.1999	0.1999	0.2545	0.2391
1.00	0.7425	0.2276	0.2291	0.2737	0.2291

Foil L. E. Circle	X = -0.1355	Y = -0.5373	R = 0.0275
Foil T. E. Circle	X = 0.7325	Y = 0.2291	R = 0.0100
Foil L. E. Tangency Pt. Suction	X = -0.1541	Y = -0.5575	
Foil L. E. Tangency Pt. Pressure	X = -0.1249	Y = -0.5119	
Foil T. E. Tangency Pt. Suction	X = 0.7420	Y = 0.2260	
Foil T. E. Tangency Pt. Pressure	X = 0.7235	Y = 0.2334	
Foil Nose Point	X = -0.1586	Y = -0.5225	
Foil Tail Point	X = 0.7362	Y = 0.2384	
Foil Area	0.1183		
Gaging	LAMBDA = 0.3077	X = 0.4621	Y = -0.4225
Gaging Angle	= 22.000		
Center of Gravity	X = 0.3085	Y = -0.4201	
Radial Reference	X = 0.3924	Y = -0.3113	
Inlet Angle	= 57.400	DELTA BETA 1 = 20.000	
Exit Angle	= 21.650	DELTA BETA 2 = 7.300	
Uncovered Turning	13.706		
Min. Moment of Inertia	= 0.00085047		
Max. Moment of Inertia	= 0.01156296		
Principal Axis Angle	= -44.723		
Pitch/Axial Chord	= 0.9072		
Pitch/Actual Chord	= 0.6993		

UNCLASSIFIED

TABLE XXI

SECOND VANE CASCADE AIRFOIL, RECAMBERING DESIGN B

Radius of EE Section = 10.8600 Axial Chord = 0.9155 Actual Chord= 1.2058
Pitch = 0.8529 No. of Foils = 80.00

Percent X	Foil X	Foil Y Suction	Foil Y (Circle)	Foil Y Pressure	Foil Y (Circle)
0.0	-0.1851	-0.5527	-0.5396	-0.4991	-0.5396
0.01	-0.1759	-0.5606	-0.5606	-0.5024	-0.5187
0.02	-0.1668	-0.5683	-0.5683	-0.5057	-0.5130
0.03	-0.1576	-0.5757	-0.5757	-0.5089	-0.5111
0.04	-0.1485	-0.5827	-0.5827	-0.5122	-0.5123
0.05	-0.1393	-0.5895	-0.5895	-0.5154	-0.5154
0.10	-0.0935	-0.6179	-0.6179	-0.5271	-0.5271
0.15	-0.0478	-0.6382	-0.6382	-0.5326	-0.5326
0.20	-0.0020	-0.6508	-0.6508	-0.5325	-0.5325
0.25	0.0438	-0.6557	-0.6557	-0.5268	-0.5268
0.30	0.0896	-0.6527	-0.6527	-0.5150	-0.5150
0.35	0.1353	-0.6419	-0.6419	-0.4971	-0.4971
0.40	0.1811	-0.6231	-0.6231	-0.4721	-0.4721
0.45	0.2269	-0.5960	-0.5960	-0.4402	-0.4402
0.50	0.2727	-0.5607	-0.5607	-0.4008	-0.4008
0.55	0.3184	-0.5169	-0.5169	-0.3540	-0.3540
0.60	0.3642	-0.4646	-0.4646	-0.3003	-0.3003
0.65	0.4100	-0.4037	-0.4037	-0.2402	-0.2402
0.70	0.4558	-0.3343	-0.3343	-0.1744	-0.1744
0.75	0.5015	-0.2566	-0.2566	-0.1037	-0.1037
0.80	0.5473	-0.1703	-0.1703	-0.0287	-0.0287
0.85	0.5931	-0.0757	-0.0757	0.0498	0.0498
0.90	0.6388	0.0274	0.0274	0.1315	0.1315
0.95	0.6846	0.1391	0.1391	0.2157	0.2157
0.98	0.7121	0.2104	0.2104	0.2673	0.2671
0.99	0.7212	0.2348	0.2348	0.2847	0.2715
1.00	0.7304	0.2597	0.2616	0.3020	0.2616

Foil L.E. Circle	X = -0.1566	Y = -0.5396	R = 0.0285
Foil T.E. Circle	X = 0.7204	Y = 0.2616	R = 0.0100
Foil L.E. Tangency Pt. Suction	X = -0.1752	Y = -0.5612	
Foil L.E. Tangency Pt. Pressure	X = -0.1469	Y = -0.5128	
Foil T.E. Tangency Pt. Suction	X = 0.7297	Y = 0.2580	
Foil T.E. Tangency Pt. Pressure	X = 0.7116	Y = 0.2663	
Foil Nose Point	X = -0.1812	Y = -0.5253	
Foil Tail Point	X = 0.7246	Y = 0.2707	
Foil Area	= 0.1167		
Gaging	LAMBDA = 0.3521	X = 0.4210	Y = -0.3877
Gaging Angle	= 24.380		
Center of Gravity	X = 0.2854	Y = -0.3740	
Radial Reference	X = 0.3924	Y = -0.3113	
Inlet Angle	= 59.762	DELTA BETA 1= 21.053	
Exit Angle	= 24.603	DELTA BETA 2 = 7.581	
Uncovered Turning	= 13.464		
Min. Moment of Inertia	= 0.00061387		
Max. Moment of Inertia	= 0.01185749		
Principal Axis Angle	= -45.026		
Pitch/Axial Chord	= 0.9317		
Pitch/Actual Chord	= 0.7074		

UNCLASSIFIED

TABLE XXII

SECOND VANE CASCADE AIRFOIL, RECAMBERING DESIGN B

Radius of HH Section = 11.4100 Axial Chord = 0.9291
Pitch = 0.8961 No. of Foils = 80.00 Actual Chord = 1.2317

Percent X	Foil X	Foil Y Suction	Foil Y (Circle)	Foil Y Pressure	Foil Y (Circle)
0.0	-0.2154	-0.5314	-0.5169	-0.4772	-0.5169
0.01	-0.2061	-0.5387	-0.5386	-0.4798	-0.4953
0.02	-0.1968	-0.5459	-0.5459	-0.4825	-0.4892
0.03	-0.1875	-0.5524	-0.5524	-0.4852	-0.4871
0.04	-0.1782	-0.5581	-0.5581	-0.4879	-0.4879
0.05	-0.1689	-0.5633	-0.5633	-0.4902	-0.4902
0.10	-0.1225	-0.5807	-0.5807	-0.4922	-0.4922
0.15	-0.0760	-0.5857	-0.5857	-0.4820	-0.4820
0.20	-0.0295	-0.5806	-0.5806	-0.4629	-0.4629
0.25	0.0169	-0.5670	-0.5670	-0.4371	-0.4371
0.30	0.0634	-0.5455	-0.5455	-0.4058	-0.4058
0.35	0.1098	-0.5173	-0.5173	-0.3700	-0.3700
0.40	0.1563	-0.4827	-0.4827	-0.3301	-0.3301
0.45	0.2027	-0.4423	-0.4423	-0.2869	-0.2869
0.50	0.2492	-0.3967	-0.3967	-0.2406	-0.2406
0.55	0.2956	-0.3459	-0.3459	-0.1914	-0.1914
0.60	0.3421	-0.2903	-0.2903	-0.1398	-0.1398
0.65	0.3886	-0.2300	-0.2300	-0.0860	-0.0860
0.70	0.4350	-0.1654	-0.1654	-0.0301	-0.0301
0.75	0.4815	-0.0966	-0.0966	0.0275	0.0275
0.80	0.5279	-0.0237	-0.0237	0.0868	0.0868
0.85	0.5744	0.0528	0.0528	0.1474	0.1474
0.90	0.6208	0.1330	0.1330	0.2095	0.2095
0.95	0.6673	0.2166	0.2166	0.2727	0.2727
0.98	0.6952	0.2684	0.2684	0.3112	0.3112
0.99	0.7045	0.2859	0.2859	0.3241	0.3160
1.00	0.7138	0.3035	0.3060	0.3370	0.3060

Foil L.E. Circle	X = -0.1855,	Y = -0.5169,	R = 0.0299
Foil T.E. Circle	X = 0.7038	Y = 0.3060,	R = 0.0100
Foil L.E. Tangency PT. Suction	X = -0.2041	Y = -0.5403	
Foil L.E. Tangency PT. Pressure	X = -0.1772	Y = -0.4882	
Foil T.E. Tangency PT. Suction	X = 0.7126	Y = 0.3013	
Foil T.E. Tangency PT. Pressure	X = 0.6957	Y = 0.3119	
Foil Nose Point	X = -0.2120	Y = -0.5032	
Foil Tail Point	X = 0.7091	Y = 0.3145	
Foil Area	= 0.1087		
Gaging	LAMBDA = 0.4598	X = 0.3379	Y = -0.2955
Gaging Angle	= 30.866		
Center of Gravity	X = 0.2041	Y = 0.2739	
Radial Reference	X = 0.3924	Y = -0.3113	
Inlet Angle	= 62.722	DELTA BETA 1 = 22.416	
Exit Angle	= 31.966	DELTA BETA 2 = 7.975	
Uncovered Turning	= 10.931		
Min. Moment of Inertia	= 0.00025003		
Max. Moment of Inertia	= 0.01117726		
Principal Axis Angle	= -44.941		
Pitch/Axial Chord	= 0.9645		
Pitch/Actual Chord	= 0.7276		

UNCLASSIFIED

TABLE XXIII

SECOND VANE CASCADE AIRFOIL, RECAMBERING DESIGN B

Radius of GG Section = 11.4450 Axial Chord = 0.9300
Pitch = 0.8989 No. of Foils = 80.00 Actual Chord = 1.2326

Percent X	Foil X	Foil Y Suction	Foil Y (Circle)	Foil Y Pressure	Foil Y (Circle)
0.0	-0.2173	-0.5289	-0.5144	-0.4747	-0.5144
0.01	-0.2080	-0.5363	-0.5361	-0.4774	-0.4927
0.02	-0.1987	-0.5434	-0.5434	-0.4800	-0.4867
0.03	-0.1894	-0.5498	-0.5498	-0.4826	-0.4845
0.04	-0.1801	-0.5555	-0.5555	-0.4853	-0.4853
0.05	-0.1708	-0.5606	-0.5606	-0.4876	-0.4876
0.10	-0.1243	-0.5770	-0.5770	-0.4889	-0.4889
0.15	-0.0778	-0.5810	-0.5810	-0.4774	-0.4774
0.20	-0.0313	-0.5746	-0.5746	-0.4569	-0.4569
0.25	0.0152	-0.5594	-0.5594	-0.4295	-0.4295
0.30	0.0617	-0.5366	-0.5366	-0.3967	-0.3967
0.35	0.1082	-0.5070	-0.5070	-0.3595	-0.3595
0.40	0.1547	-0.4713	-0.4713	-0.3186	-0.3186
0.45	0.2012	-0.4299	-0.4299	-0.2745	-0.2745
0.50	0.2477	-0.3835	-0.3835	-0.2277	-0.2277
0.55	0.2942	-0.3322	-0.3322	-0.1785	-0.1785
0.60	0.3407	-0.2763	-0.2763	-0.1272	-0.1272
0.65	0.3872	-0.2162	-0.2162	-0.0740	-0.0740
0.70	0.4337	-0.1521	-0.1521	-0.0190	-0.0190
0.75	0.4802	-0.0841	-0.0841	0.0375	0.0375
0.80	0.5267	-0.0124	-0.0124	0.0954	0.0954
0.85	0.5732	0.0626	0.0626	0.1546	0.1546
0.90	0.6197	0.1409	0.1409	0.2151	0.2151
0.95	0.6662	0.2222	0.2222	0.2766	0.2766
0.98	0.6941	0.2723	0.2723	0.3140	0.3140
0.99	0.7034	0.2892	0.2892	0.3266	0.3188
1.00	0.7127	0.3088	0.3088	0.3391	0.3088

Foil L. E. Circle	X = -0.1873	Y = -0.5144	R = 0.0100
Foil T. E. Circle	X = 0.7027	Y = 0.3088	
Foil L. E. Tangency Pt. Suction	X = -0.2059	Y = -0.5379	
Foil L. E. Tangency Pt. Pressure	X = -0.1791	Y = -0.4856	
Foil T. E. Tangency Pt. Suction	X = 0.7115	Y = 0.3041	
Foil T. E. Tangency Pt. Pressure	X = 0.6947	Y = 0.3148	
Foil Nose Point	X = -0.2140	Y = -0.5007	
Foil Tail Point	X = 0.7081	Y = 0.3173	
Foil Area	= 0.1079		
Gaging	LAMBDA = 0.4687	X = 0.3312	Y = 0.2881
Gaging Angle	= 31.430		
Center of Gravity	X = 0.2368	Y = -0.2683	
Radial Reference	X = 0.3924	Y = -0.3113	
Inlet Angle	= 62.900	DELTA BETA 1 = 22.500	
Exit Angle	= 32.570	DELTA BETA 2 = 8.000	
Uncovered Turning	= 10.575		
Min. Moment of Inertia	= 0.00023066		
Max. Moment of Inertia	= 0.01108872		
Principal Axis Angle	= 44.956		
Pitch/Axial Chord	= 0.9665		
Pitch/Actual Chord	= 0.7292		

UNCLASSIFIED

TABLE XXIV

SECOND VANE CASCADE AIRFOIL, RECAMBERING DESIGN C

Radius of FF Section = 7.5000 Axial Chord = 0.8320 Actual Chord = 0.8432
Pitch = 0.5890 No. of Foils = 80.00

Percent X	Foil X	Foil Y Suction	Foil Y (Circle)	Foil Y Pressure	Foil Y (Circle)
0.0	0.0	-0.2161	-0.2105	-0.1601	-0.2105
0.01	0.0083	-0.2296	-0.2296	-0.1690	-0.1943
0.02	0.0166	-0.2424	-0.2424	-0.1778	-0.1908
0.03	0.0250	-0.2545	-0.2545	-0.1866	-0.1911
0.04	0.0333	-0.2659	-0.2659	-0.1954	-0.1955
0.05	0.0416	-0.2767	-0.2767	-0.2038	-0.2038
0.10	0.0832	-0.3223	-0.3223	-0.2329	-0.2329
0.15	0.1248	-0.3563	-0.3563	-0.2494	-0.2494
0.20	0.1664	-0.3808	-0.3808	-0.2584	-0.2584
0.25	0.2080	-0.3972	-0.3972	-0.2622	-0.2622
0.30	0.2496	-0.4065	-0.4065	-0.2618	-0.2618
0.35	0.2912	-0.4094	-0.4094	-0.2580	-0.2580
0.40	0.3328	-0.4066	-0.4066	-0.2512	-0.2512
0.45	0.3744	-0.3983	-0.3983	-0.2419	-0.2419
0.50	0.4160	-0.3849	-0.3849	-0.2301	-0.2301
0.55	0.4576	-0.3665	-0.3665	-0.2160	-0.2160
0.60	0.4992	-0.3435	-0.3435	-0.1998	-0.1998
0.65	0.5408	-0.3158	-0.3158	-0.1814	-0.1814
0.70	0.5824	-0.2834	-0.2834	-0.1609	-0.1609
0.75	0.6240	-0.2466	-0.2466	-0.1382	-0.1382
0.80	0.6656	-0.2055	-0.2055	-0.1133	-0.1133
0.85	0.7072	-0.1609	-0.1609	-0.0860	-0.0860
0.90	0.7488	-0.1137	-0.1137	-0.0562	-0.0562
0.95	0.7904	-0.0644	-0.0644	-0.0236	-0.0236
0.98	0.8154	-0.0340	-0.0340	-0.0025	-0.0025
0.99	0.8237	-0.0238	-0.0238	0.0047	-0.0001
1.00	0.8320	-0.0135	-0.0100	0.0119	-0.0100

Foil L.E. Circle	X = 0.0200	Y = -0.2105	R = 0.0200
Foil T.E. Circle	X = 0.8220	Y = -0.0100	R = 0.0100
Foil L.E. Tangency Pt. Suction	X = 0.0029	Y = -0.2209	
Foil L.E. Tangency Pt. Pressure	X = 0.0345	Y = -0.1968	
Foil T.E. Tangency Pt. Suction	X = 0.8298	Y = -0.0163	
Foil T.E. Tangency Pt. Pressure	X = 0.8154	Y = -0.0025	
Foil Nose Point	X = 0.0079	Y = -0.1946	
Foil Tail Point	X = 0.8289	Y = -0.0028	
Foil Area	= 0.0931		
Gaging	LAMBDA = 0.3860	X = 0.5732	Y = -0.2910
Gaging Angle	= 40.940		
Center of Gravity	X = 0.3919	Y = -0.2691	
Radial Reference	X = 0.3919	Y = -0.2691	
Inlet Angle	= 37.330,	DELTA BETA 1 = 12.00	
Exit Angle	= 44.000	DELTA BETA 2 = 10.000	
Uncovered Turning	= 12.056		
Min. Moment of Inertia	= 0.00033518		
Max. Moment of Inertia	= 0.00401353		
Principal Axis Angle	= -16.359		
Pitch/Actual Chord	= 0.7080		
Pitch/Actual Chord	= 0.6988		

UNCLASSIFIED

TABLE XXV

SECOND VANE CASCADE AIRFOIL, RECAMBERING DESIGN C

Radius of AA Section = 7.6500 Axial Chord = 0.8357
Pitch = 0.6008 No. of Foils = 80.00 Actual Chord - 0.8529

Percent X	Foil X	Foil Y Suction	Foil Y (Circle)	Foil Y Pressure	Foil Y (Circle)
0.0	-0.0083	-0.2314	-0.2256	-0.1751	-0.2256
0.01	0.0001	-0.2448	-0.2448	-0.1838	-0.2092
0.02	0.0085	-0.2576	-0.2576	-0.1925	-0.2056
0.03	0.0168	-0.2697	-0.2697	-0.2011	-0.2058
0.04	0.0252	-0.2812	-0.2812	-0.2098	-0.2100
0.05	0.0335	-0.2921	-0.2921	-0.2181	-0.2181
0.10	0.0753	-0.3391	-0.3391	-0.2491	-0.2491
0.15	0.1171	-0.3750	-0.3750	-0.2692	-0.2692
0.20	0.1589	-0.4016	-0.4016	-0.2821	-0.2821
0.25	0.2007	-0.4202	-0.4202	-0.2894	-0.2894
0.30	0.2425	-0.4315	-0.4315	-0.2919	-0.2919
0.35	0.2842	-0.4363	-0.4363	-0.2901	-0.2901
0.40	0.3260	-0.4349	-0.4349	-0.2843	-0.2843
0.45	0.3678	-0.4278	-0.4278	-0.2748	-0.2748
0.50	0.4096	-0.4150	-0.4150	-0.2619	-0.2619
0.55	0.4514	-0.3968	-0.3968	-0.2458	-0.2458
0.60	0.4932	-0.3733	-0.3733	-0.2266	-0.2266
0.65	0.5350	-0.3443	-0.3443	-0.2047	-0.2047
0.70	0.5767	-0.3099	-0.3099	-0.1800	-0.1800
0.75	0.6185	-0.2698	-0.2698	-0.1526	-0.1526
0.80	0.6603	-0.2241	-0.2241	-0.1225	-0.1225
0.85	0.7021	-0.1735	-0.1735	-0.0896	-0.0896
0.90	0.7439	-0.1187	-0.1187	-0.0539	-0.0539
0.95	0.7857	-0.0609	-0.0609	-0.0152	-0.0152
0.98	0.8107	-0.0252	-0.0252	0.0096	0.0095
0.99	0.8191	-0.0132	-0.0132	0.0181	0.0120
1.00	0.8275	-0.0011	0.0021	0.0265	0.0021

Foil L. E. Circle	X = 0.0121	Y = -0.2256	R = 0.0204
Foil T. E. Circle	X = 0.8175	Y = 0.0021	R = 0.0100
Foil L. E. Tangency Pt. Suction	X = -0.0052	Y = -0.2363	
Foil L. E. Tangency Pt. Pressure	X = 0.0268	Y = -0.2115	
Foil T. E. Tangency Pt. Suction	X = 0.8256	Y = -0.0037	
Foil T. E. Tangency Pt. Pressure	X = 0.8104	Y = 0.0092	
Foil Nose Point	X = -0.0004	Y = -0.2095	
Foil Tail Point	X = 0.8239	Y = 0.0097	
Foil Area	= 0.0948		
Gaging	LAMBDA = 0.3659	X = 0.5704	Y = -0.3154
Gaging Angle	= 37.511		
Center of Gravity	X = 0.3932	Y = -0.2887	
Radial Reference	X = 0.3919	Y = -0.2691	
Inlet Angle	= 37.732	DELTA BETA 1 = 12.329	
Exit Angle	= 40.324	DELTA BETA 2 = 9.921	
Uncovered Turning	= 13.580		
Min. Moment of Inertia	= 0.00041249		
Max. Moment of Inertia	= 0.00430317		
Principal Axis Angle	= -17.910		
Pitch/Axial Chord	= 0.7189		
Pitch/Actual Chord	= 0.7044		

TABLE XXVI

SECOND VANE CASCADE AIRFOIL, RECAMBERING DESIGN C

Radius of BB Section = 8.4863 Axial Chord = 0.8565
Pitch = 0.6665 No. of Foils = 80.00 Actual Chord = 0.9216

Percent X	Foil X	Foil Y Suction	Foil Y (Circle)	Foil Y Pressure	Foil Y (Circle)
0.0	-0.0543	-0.3164	-0.3093	-0.2604	-0.3093
0.01	-0.0458	-0.3286	-0.3286	-0.2677	-0.2917
0.02	-0.0372	-0.3406	-0.3406	-0.2751	-0.2875
0.03	-0.0286	-0.3521	-0.3521	-0.2824	-0.2871
0.04	-0.0201	-0.3633	-0.3633	-0.2898	-0.2901
0.05	-0.0115	-0.3741	-0.3741	-0.2971	-0.2971
0.10	0.0313	-0.4232	-0.4232	-0.3311	-0.3311
0.15	0.0741	-0.4641	-0.4641	-0.3605	-0.3605
0.20	0.1170	-0.4972	-0.4972	-0.3847	-0.3847
0.25	0.1598	-0.5230	-0.5230	-0.4031	-0.4031
0.30	0.2026	-0.5416	-0.5416	-0.4155	-0.4155
0.35	0.2454	-0.5530	-0.5530	-0.4212	-0.4212
0.40	0.2883	-0.5573	-0.5573	-0.4199	-0.4199
0.45	0.3311	-0.5544	-0.5544	-0.4115	-0.4115
0.50	0.3739	-0.5442	-0.5442	-0.3957	-0.3957
0.55	0.4167	-0.5264	-0.5264	-0.3727	-0.3727
0.60	0.4596	-0.5006	-0.5006	-0.3425	-0.3425
0.65	0.5024	-0.4661	-0.4661	-0.3056	-0.3056
0.70	0.5452	-0.4224	-0.4224	-0.2622	-0.2622
0.75	0.5880	-0.3684	-0.3684	-0.2128	-0.2128
0.80	0.6309	-0.3030	-0.3030	-0.1579	-0.1579
0.85	0.6737	-0.2259	-0.2259	-0.0981	-0.0981
0.90	0.7165	-0.1374	-0.1374	-0.0338	-0.0338
0.95	0.7593	-0.0390	-0.0390	0.0346	0.0346
0.98	0.7850	0.0242	0.0242	0.0773	0.0767
0.99	0.7936	0.0459	0.0459	0.0917	0.0796
1.00	0.8022	0.0678	0.0697	0.1061	0.0697

Foil L.E. Circle	X = -0.0318	Y = -0.3093	R = 0.0225
Foil T.E. Circle	X = 0.7922	Y = 0.0697	R = 0.0100
Foil L. E. Tangency Pt. Suction	X = -0.0503	Y = -0.3222	
Foil L. E. Tangency Pt. Pressure	X = -0.0172	Y = -0.2923	
Foil T. E. Tangency Pt. Suction	X = 0.8015	Y = 0.0661	
Foil T. E. Tangency Pt. Pressure	X = 0.7836	Y = 0.0748	
Foil Nose Point	X = -0.0469	Y = -0.2926	
Foil Tail Point	X = 0.7965	Y = 0.0787	
Foil Area	= 0.1053		
Gaging	LAMBDA = 0.2911	X = 0.5594	Y = -0.4057
Gaging Angle	= 25.900		
Center of Gravity	X = 0.3893	Y = -0.3661	
Radial Reference	X = 0.3919	Y = -0.2691	
Inlet Angle	= 42.100	DELTA BETA 1 = 14.500	
Exit Angle	= 25.950	DELTA BETA 2 = 0.500	
Uncovered Turning	= 18.181		
Min. Moment of Inertia	= 0.00089655		
Max. Moment of Inertia	= 0.00611507		
Principal Axis Angle	= -27.285		
Pitch/Axial Chord	= 0.7782		
Pitch/Actual Chord	= 0.7232		

TABLE XXVII

SECOND VANE CASCADE AIRFOIL, RECAMBERING DESIGN C

Radius of CC Section = 9.4725 Axial Chord = 0.8810
Pitch = 0.7440 No. of Foils = 80.00 Actual Chord = 1.0247

Percent X	Foil X	Foil Y Suction	Foil Y (Circle)	Foil Y Pressure	Foil Y (Circle)
0.0	-0.1086	-0.4100	-0.4005	-0.3565	-0.4005
0.01	-0.0998	-0.4199	-0.4199	-0.3618	-0.3814
0.02	-0.0910	-0.4296	-0.4296	-0.3670	-0.3766
0.03	-0.0822	-0.4391	-0.4391	-0.3722	-0.3755
0.04	-0.0734	-0.4484	-0.4484	-0.3775	-0.3777
0.05	-0.0646	-0.4575	-0.4575	-0.3827	-0.3827
0.10	-0.0205	-0.5000	-0.5000	-0.4077	-0.4077
0.15	0.0235	-0.5371	-0.5371	-0.4305	-0.4305
0.20	0.0676	-0.5687	-0.5687	-0.4506	-0.4506
0.25	0.1116	-0.5943	-0.5943	-0.4674	-0.4674
0.30	0.1557	-0.6136	-0.6136	-0.4800	-0.4800
0.35	0.1997	-0.6263	-0.6263	-0.4876	-0.4876
0.40	0.2438	-0.6320	-0.6320	-0.4889	-0.4889
0.45	0.2878	-0.6301	-0.6301	-0.4828	-0.4828
0.50	0.3319	-0.6200	-0.6200	-0.4678	-0.4678
0.55	0.3759	-0.6011	-0.6011	-0.4428	-0.4428
0.60	0.4200	-0.5726	-0.5726	-0.4071	-0.4071
0.65	0.4640	-0.5335	-0.5335	-0.3605	-0.3605
0.70	0.5081	-0.4827	-0.4827	-0.3034	-0.3034
0.75	0.5521	-0.4187	-0.4187	-0.2368	-0.2368
0.80	0.5962	-0.3400	-0.3400	-0.1620	-0.1620
0.85	0.6402	-0.2448	-0.2448	-0.0801	-0.0801
0.90	0.6843	-0.1320	-0.1320	0.0074	0.0074
0.95	0.7283	-0.0010	-0.0010	0.0996	0.0996
0.98	0.7547	0.0863	0.0863	0.1568	0.1559
0.99	0.7635	0.1168	0.1168	0.1760	0.1593
1.00	0.7724	0.1480	0.1494	0.1953	0.1494

Foil L.E. Circle	X = -0.0836	Y = -0.4005	R = 0.0250
Foil T.E. Circle	X = 0.7624	Y = 0.1494	R = 0.0100
Foil L. E. Tangency Pt. Suction	X = -0.1023	Y = -0.4171	
Foil L. E. Tangency Pt. Pressure	X = -0.0709	Y = -0.3790	
Foil T. E. Tangency Pt. Suction	X = 0.7720	Y = 0.1467	
Foil T. E. Tangency Pt. Pressure	X = 0.7533	Y = 0.1536	
Foil Nose Point	X = -0.1029	Y = -0.3846	
Foil Tail Point	X = 0.7658	Y = 0.1588	
Foil Area	= 0.1192		
Gaging	LAMBDA = 0.2620	X = 0.5362	Y = -0.4434
Gaging Angle	= 20.620		
Center of Gravity	X = 0.3649	Y = -0.4037	
Radial Reference	X = 0.3919	Y = -0.2691	
Inlet Angle	= 50.500	DELTA BETA 1 = 17.500	
Exit Angle	= 20.100	DELTA BETA 2 = 9.000	
Uncovered Turning	= 18.178		
Min Moment of Inertia	= 0.00126226		
Max. Moment of Inertia	= .00876554		
Principal Axis Angle	= -35.891		
Pitch/Axial Chord	= 0.8445		
Pitch/Actual Chord	= 0.7261		

UNCLASSIFIED

TABLE XXVIII

SECOND VANE CASCADE AIRFOIL, RECAMBERING DESIGN C

Radius of DD Section = 10.4588 Axial Chord = 0.9055
Pitch = 0.8214 No. of Foils = 80.00 Actual Chord = 1.1187

Percent X	Foil X	Foil Y Suction	Foil Y (Circle)	Foil Y Pressure	Foil Y (Circle)
0.0	-0.1630	-0.4600	-0.4479	-0.4067	-0.4479
0.01	-0.1539	-0.4683	-0.4683	-0.4104	-0.4275
0.02	-0.1449	-0.4765	-0.4765	-0.4142	-0.4221
0.03	-0.1358	-0.4845	-0.4845	-0.4180	-0.4204
0.04	-0.1268	-0.4924	-0.4924	-0.4217	-0.4218
0.05	-0.1177	-0.5000	-0.5000	-0.4255	-0.4255
0.10	-0.0724	-0.5350	-0.5350	-0.4431	-0.4431
0.15	-0.0272	-0.5646	-0.5646	-0.4585	-0.4585
0.20	0.0181	-0.5886	-0.5886	-0.4711	-0.4711
0.25	0.0634	-0.6067	-0.6067	-0.4804	-0.4804
0.30	0.1087	-0.6187	-0.6187	-0.4854	-0.4854
0.35	0.1539	-0.6241	-0.6241	-0.4851	-0.4851
0.40	0.1992	-0.6225	-0.6225	-0.4785	-0.4785
0.45	0.2445	-0.5134	-0.6134	-0.4642	-0.4642
0.50	0.2898	-0.5963	-0.5963	-0.4409	-0.4409
0.55	0.3350	-0.5704	-0.5704	-0.4076	-0.4076
0.60	0.3803	-0.5349	-0.5349	-0.3639	-0.3639
0.65	0.4256	-0.4889	-0.4889	-0.3097	-0.3097
0.70	0.4709	-0.4311	-0.4311	-0.2459	-0.2459
0.75	0.5161	-0.3599	-0.3599	-0.1735	-0.1735
0.80	0.5614	-0.2738	-0.2738	-0.0938	-0.0938
0.85	0.6067	-0.1717	-0.1717	-0.0081	-0.0081
0.90	0.6520	-0.0535	-0.0535	0.0826	0.0826
0.95	0.6972	0.0801	0.0801	0.1771	0.1771
0.98	0.7244	0.1671	0.1671	0.2354	0.2350
0.99	0.7335	0.1971	0.1971	0.2550	0.2391
1.00	0.7425	0.2277	0.2291	0.2746	0.2291

Foil L.E. Circle	X = -0.1355	Y = -0.4479	R = 0.0275
Foil T.E. Circle	X = 0.7325	Y = 0.2291	R = 0.0100
Foil L.E. Tangency Pt. Suction	X = -0.1541	Y = -0.4681	
Foil L.E. Tangency Pt. Pressure	X = -0.1249	Y = -0.4225	
Foil T.E. Tangency Pt. Suction	X = 0.7421	Y = 0.2263	
Foil T.E. Tangency Pt. Pressure	X = 0.7234	Y = -0.2333	
Foil Nose Point	X = -0.1586	Y = -0.4331	
Foil Tail Point	X = 0.7360	Y = 0.2385	
Foil Area	= 0.1236		
Gaging	LAMBDA = 0.2969	X = 0.4789	Y = -0.4194
Gaging Angle	= 21.190		
Center of Gravity	X = 0.3240	Y = -0.3762	
Radial Reference	X = 0.3919	Y = -0.2691	
Inlet Angle	= 57.400	DELTA BETA 1 = 20.000	
Exit Angle	= 20.600	DELTA BETA 2 = 8.400	
Uncovered Turning	= 17.802		
Min. Moment of Inertia	= 0.00110931		
Max. Moment of Inertia	= 0.01076076		
Principal Axis Angle	= -40.470		
Pitch/Axial Chord	= 0.9072		
Pitch/Actual Chord	= 0.7343		

UNCLASSIFIED

TABLE XXIX

SECOND VANE CASCADE AIRFOIL, RECAMBERING DESIGN C

Radius of EE Section = 10.8600 Axial Chord = 0.9155 Actual Chord = 1.1438
Pitch = 0.8529 No. of Foils - 80.00

Percent X	Foil X	Foil Y Suction	Foil Y (Circle)	Foil Y Pressure	Foil Y (Circle)
0.0	-0.1851	-0.4552	-0.4422	-0.4016	-0.4422
0.01	-0.1759	-0.4631	-0.4631	-0.4049	-0.4212
0.02	-0.1668	-0.4709	-0.4709	-0.4082	-0.4155
0.03	-0.1576	-0.4783	-0.4783	-0.4114	-0.4137
0.04	-0.1485	-0.4854	-0.4854	-0.4147	-0.4148
0.05	-0.1393	-0.4923	-0.4923	-0.4180	-0.4180
0.10	-0.0935	-0.5219	-0.5219	-0.4315	-0.4315
0.15	-0.0478	-0.5442	-0.5442	-0.4406	-0.4406
0.20	-0.0020	-0.5598	-0.5598	-0.4452	-0.4452
0.25	0.0438	-0.5686	-0.5686	-0.4453	-0.4453
0.30	0.0896	-0.5708	-0.5708	-0.4405	-0.4405
0.35	0.1353	-0.5664	-0.5664	-0.4304	-0.4304
0.40	0.1811	-0.5554	-0.5554	-0.4144	-0.4144
0.45	0.2269	-0.5375	-0.5375	-0.3917	-0.3917
0.50	0.2727	-0.5123	-0.5123	-0.3619	-0.3619
0.55	0.3184	-0.4798	-0.4798	-0.3242	-0.3242
0.60	0.3642	-0.4392	-0.4392	-0.2784	-0.2784
0.65	0.4100	-0.3900	-0.3900	-0.2248	-0.2248
0.70	0.4558	-0.3312	-0.3312	-0.1640	-0.1640
0.75	0.5015	-0.2619	-0.2619	-0.0968	-0.0968
0.80	0.5473	-0.1809	-0.1809	-0.0244	-0.0244
0.85	0.5931	-0.0876	-0.0876	0.0525	0.0525
0.90	0.6388	0.0176	-0.0176	0.1329	0.1329
0.95	0.6846	0.1338	0.1338	0.2163	0.2163
0.98	0.7121	0.2083	0.2083	0.2674	0.2671
0.99	0.7212	0.2338	0.2338	0.2846	0.2715
1.00	0.7304	0.2597	0.2616	0.3018	0.2616

Foil L.E. Circle	X = -0.1566	Y = -0.4422	R = 0.0285
Foil T.E. Circle	X = 0.7204	Y = 0.2616	R = 0.0100
Foil L.E. Tangency Pt. Suction	X = -0.1752	Y = -0.4638	
Foil L.E. Tangency Pt. Pressure	X = -0.1469	Y = -0.4153	
Foil T.E. Tangency Pt. Suction	X = 0.7297	Y = 0.2580	
Foil T.E. Tangency Pt. Pressure	X = 0.7117	Y = 0.2664	
Foil Nose Point	X = -0.1812	Y = -0.4278	
Foil Tail Point	X = 0.7246	Y = 0.2706	
Foil Area	= 0.1167		
Gaging	LAMBDA = 0.3579	X = 0.4308	Y = -0.3645
Gaging Angle	= 24.910		
Center of Gravity	X = 0.2956	Y = -0.3218	
Radial Reference	X = 0.3919	Y = -0.2691	
Inlet Angle	= 59.762	DELTA BETA 1 = 21.993	
Exit Angle	= 25.141,	DELTA BETA 2 = 3.203	
Uncovered Turning	= 17.109		
Min. Moment of Inertia	= 0.00073264		
Max. Moment of Inertia	= 0.01057891		
Principal Axis Angle	= -40.621		
Pitch/Axial Chord	= 0.9317		
Pitch/Actual Chord	= 0.7457		

TABLE XXX

SECOND VANE CASCADE AIRFOIL, RECAMBERING DESIGN C

Radius of HH Section = 11.4100 Axial Chord = 0.9291
Pitch = 0.8961 No. of Foils = 80.00 Actual Chord = 1.1616

Percent X	Foil X	Foil Y Suction	Foil Y (Circle)	Foil Y Pressure	Foil Y (Circle)
0.0	-0.2154	-0.4210	-0.4066	-0.3668	-0.4066
0.01	-0.2061	-0.4282	-0.4282	-0.3695	-0.3849
0.02	-0.1968	-0.4355	-0.4355	-0.3722	-0.3789
0.03	-0.1875	-0.4421	-0.4421	-0.3748	-0.3767
0.04	-0.1782	-0.4480	-0.4480	-0.3775	-0.3776
0.05	-0.1689	-0.4535	-0.4535	-0.3800	-0.3800
0.10	-0.1225	-0.4725	-0.4725	-0.3859	-0.3859
0.15	-0.0760	-0.4796	-0.4796	-0.3817	-0.3817
0.20	-0.0295	-0.4767	-0.4767	-0.3686	-0.3686
0.25	0.0169	-0.4651	-0.4651	-0.3481	-0.3481
0.30	0.0634	-0.4459	-0.4459	-0.3215	-0.3215
0.35	0.1098	-0.4201	-0.4201	-0.2900	-0.2900
0.40	0.1563	-0.3884	-0.3884	-0.2545	-0.2545
0.45	0.2027	-0.3514	-0.3514	-0.2154	-0.2154
0.50	0.2492	-0.3095	-0.3095	-0.1737	-0.1737
0.55	0.2956	-0.2634	-0.2634	-0.1295	-0.1295
0.60	0.3421	-0.2133	-0.2133	-0.0833	-0.0833
0.65	0.3886	-0.1595	-0.1595	-0.0351	-0.0351
0.70	0.4350	-0.1021	-0.1021	0.0145	0.0145
0.75	0.4815	-0.0415	-0.0415	0.0655	0.0655
0.80	0.5279	0.0221	0.0221	0.1175	0.1175
0.85	0.5744	0.0887	0.0887	0.1705	0.1705
0.90	0.6208	0.1579	0.1579	0.2241	0.2241
0.95	0.6673	0.2295	0.2295	0.2785	0.2785
0.98	0.6952	0.2734	0.2734	0.3114	0.3114
0.99	0.7045	0.2882	0.2882	0.3224	0.3160
1.00	0.7138	0.3031	0.3060	0.3334	0.3060

Foil L. E. Circle	X = -0.1855	Y = -0.4066	R = 0.0299
Foil T. E. Circle	X = 0.7036	Y = 0.3060	R = 0.0100
Foil L. E. Tangency Pt. Suction	X = -0.2041	Y = -0.4300	
Foil L. E. Tangency Pt. Pressure	X = -0.1772	Y = -0.3778	
Foil T. E. Tangency Pt. Suction	X = 0.7122	Y = 0.3006	
Foil T. E. Tangency Pt. Pressure	X = 0.6962	Y = 0.3125	
Foil Nose Point	X = -0.2120	Y = -0.3929	
Foil Tail Point	X = 0.7097	Y = 0.3140	
Foil Area	= 0.0965		
Gaging	LAMBDA = 0.5111	X = 0.3212	Y = -0.2364
Gaging Angle	= 34.771		
Center of Gravity	X = 0.2328	Y = -0.2084	
Radial Reference	X = 0.3919	Y = -0.2694	
Inlet Angle	= 62.722	DELTA BETA 1 = 22.408	
Exit Angle	= 36.630	DELTA BETA 2 = 8.009	
Uncovered Turning	= 10.092		
Min. Moment of Inertia	= 0.00020983		
Max. Moment of Inertia	= 0.00895742		
Principal Axis Angle	= -40.993		
Pitch/Axial Chord	= 0.9645		
Pitch/Actual Chord	= 0.7715		

TABLE XXXI

SECOND VANE CASCADE AIRFOIL, RECAMBERING DESIGN C

Radius of GG Section = 11.4450 Axial Chord = 0.9300 Actual Chord = 1.1621
Pitch = 0.8989 *No. of Foils = 80.00*

Percent X	Foil X	Foil Y Suction	Foil Y (Circle)	Foil Y Pressure	Foil Y (Circle)
0.0	-0.2173	-0.4177	-0.4032	-0.3635	-0.4032
0.01	-0.2080	-0.4250	-0.4249	-0.3661	-0.3814
0.02	-0.1987	-0.4322	-0.4322	-0.3687	-0.3754
0.03	-0.1894	-0.4387	-0.4387	-0.3714	-0.3732
0.04	-0.1801	-0.4446	-0.4446	-0.3740	-0.3740
0.05	-0.1708	-0.4499	-0.4499	-0.3765	-0.3765
0.10	-0.1243	-0.4681	-0.4681	-0.3818	-0.3818
0.15	-0.0778	-0.4740	-0.4740	-0.3766	-0.3766
0.20	-0.0313	-0.4697	-0.4697	-0.3621	-0.3621
0.25	0.0152	-0.4565	-0.4565	-0.3399	-0.3399
0.30	0.0617	-0.4356	-0.4356	-0.3117	-0.3117
0.35	0.1082	-0.4081	-0.4081	-0.2785	-0.2785
0.40	0.1547	-0.3748	-0.3748	-0.2414	-0.2414
0.45	0.2012	-0.3363	-0.3363	-0.2012	-0.2012
0.50	0.2477	-0.2932	-0.2932	-0.1585	-0.1585
0.55	0.2942	-0.2460	-0.2460	-0.1139	-0.1139
0.60	0.3407	-0.1951	-0.1951	-0.0677	-0.0677
0.65	0.3872	-0.1410	-0.1410	-0.0201	-0.0201
0.70	0.4337	-0.0838	-0.0838	0.0285	0.0285
0.75	0.4802	-0.0241	-0.0241	0.0781	0.0781
0.80	0.5267	0.0381	0.0381	0.1284	0.1284
0.85	0.5732	0.1024	0.1024	0.1793	0.1793
0.90	0.6197	0.1685	0.1685	0.2309	0.2309
0.95	0.6662	0.2364	0.2364	0.2828	0.2828
0.98	0.6941	0.2779	0.2779	0.3142	0.3142
0.99	0.7034	0.2918	0.2918	0.3247	0.3188
1.00	0.7127	0.3058	0.3088	0.3352	0.3088

Foil L.E. Circle	X = -0.1873	Y = -0.4032	R = 0.0300
Foil T.E. Circle	X = 0.7027	Y = 0.3088	R = 0.0100
Foil L.E. Tangency Pt. Suction	X = -0.2059	Y = -0.4267	
Foil L.E. Tangency Pt. Pressure	X = -0.1791	Y = -0.3743	
Foil T.E. Tangency Pt. Suction	X = 0.7110	Y = 0.3033	
Foil T.E. Tangency Pt. Pressure	X = 0.6952	Y = 0.3155	
Foil Nose Point	X = -0.2140	Y = -0.3895	
Foil Tail Point	X = 0.7088	Y = 0.3168	
Foil Area	0.0947		
Gaging	LAMBDA = 0.5234	X = 0.3107	Y = -0.2283
Gaging Angle	35.610		
Center of Gravity	X = 0.2272	Y = -0.2003	
Radial Reference	X = 0.3919	Y = -0.2691	
Inlet Angle	= 62.900	DELTA BETA 1 = 22.500	
Exit Angle	= 30.570	DELTA BETA 2 = 8.000	
Uncovered Turning	= 9.150		
Min. Moment of Inertia	= 0.00018734		
Max. Moment of Inertia	= 0.00878485		
Principal Axis	= -41.099		
Pitch/Axial Chord	= 0.9665		
Pitch/Actual Chord	= 0.7735		

UNCLASSIFIED

REFERENCES

1. H. Welna, D. E. Dahlberg and W. H. Heiser; (Unclassified title) Investigation of a Highly Loaded Two-Stage Fan-Drive Turbine; Technical Report, AFAPL-TR-69-92 Volume 1; Pratt & Whitney Aircraft Division of United Aircraft Corporation; June 1968; Confidential.

2. H. Welna, D. E. Dahlberg and W. H. Heiser; (Unclassified title) Investigation of a Highly Loaded Two-Stage Fan-Drive Turbine; Technical Report AFAPL-TR-69-92 Volume 2; Pratt & Whitney Aircraft Division of United Aircraft Corporation; December 1968; Confidential.

3. H. Welna, D. E. Dahlberg and W. H. Heiser; (Unclassified title) Investigation of a Highly Loaded Two-Stage Fan-Drive Turbine; Technical Report AFAPL-TR-69-92 Volume 3; Pratt & Whitney Aircraft Division of United Aircraft Corporation; June 1969; Confidential.

4. H. Welna, D.E. Dahlberg, W.H. Heiser; (Unclassified title) Investigation of a Highly Loaded Two-Stage Fan-Drive Turbine; Technical Report AFAPL-TR-69-92, Volume IV; Pratt & Whitney Aircraft Division of United Aircraft Corporation; December 1969; Confidential.

Unclassified
Security Classification

DOCUMENT CONTROL DATA - R & D

(Security classification of title, body of abstract and indexing annotation must be entered when the overall report is classified)

1. ORIGINATING ACTIVITY (Corporate author)
Pratt & Whitney Aircraft Division
United Aircraft Corporation
East Hartford, Conn. 06108

2a. REPORT SECURITY CLASSIFICATION
~~Confidential~~ UNCLASSIFIED

2b. GROUP

3. REPORT TITLE
(U) Investigation of a highly loaded two-stage fan-drive turbine.
Volume V PHASE III BOUNDARY LAYER CONTROL OPTIMIZATION AND OFF-DESIGN EVALUATION.

4. DESCRIPTIVE NOTES (Type of report and inclusive dates)
Technical Report (January 1, 1970 - June 30, 1970)

5. AUTHOR(S) (First name, middle initial, last name)
Welna, Henry; Dahlberg, Donald E.; Heiser, William H.

6. REPORT DATE	7a. TOTAL NO. OF PAGES	7b. NO. OF REFS
June, 1970	262	4

8a. CONTRACT OR GRANT NO.	9a. ORIGINATOR'S REPORT NUMBER(S)
F33615-68-C-1208	
b. PROJECT NO. 3066	PWA 3967
c. Task No. 306606	9b. OTHER REPORT NO(S) (Any other numbers that may be assigned this report)
d.	AFAPL-TR-69-92, Volume V

10. DISTRIBUTION STATEMENT
Approved for public release; distribution unlimited

11. SUPPLEMENTARY NOTES	12. SPONSORING MILITARY ACTIVITY
	Air Force Aero Propulsion Laboratory Wright-Patterson AFB, Ohio 45433

13. ABSTRACT

(U) A comprehensive, four-phase, three-year program is in progress to investigate methods of improving the performance of fan-drive turbines. The goals of this program are to develop turbine design procedures and aerodynamic techniques for efficient, high work, low pressure turbines.

(U) The first phase effort of defining the preliminary turbine design has been completed and the results were reported (Reference 1). The second phase consisted of an experimental evaluation which included establishment of both two-dimensional loss levels and three-dimensional flow behavior for the baseline airfoils, and for airfoils utilizing various boundary layer control methods. The design of the baseline cascade packs was reported in Reference 2, and the annular cascade performance of the baseline airfoils was reported in Reference 3. The annular cascade results of the baseline airfoil boundary layer control methods were reported in Reference 4.

(U) The results of the plane-cascade, two-dimensional, baseline investigation, the decreased-solidity annular-cascade airfoil test results, and the Phase III boundary layer control optimization and off-design evaluation are presented in this report.

DD FORM 1 NOV 68 1473 REPLACES DD FORM 1473, 1 JAN 64, WHICH IS OBSOLETE FOR ARMY USE.

Unclassified
Security Classification

14. KEY WORDS	LINK A		LINK B		LINK C	
	ROLE	WT	ROLE	WT	ROLE	WT
Turbine Aerodynamic Design						
Boundary Layer Control Survey						